

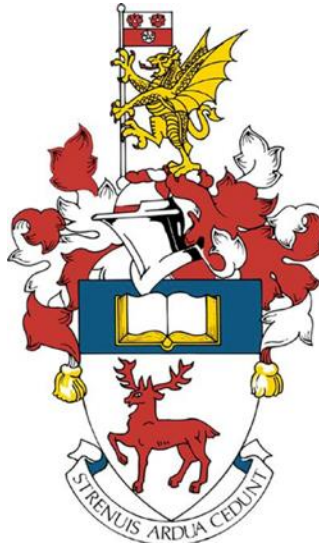
University of Southampton Research Repository

Copyright © and Moral Rights for this thesis and, where applicable, any accompanying data are retained by the author and/or other copyright owners. A copy can be downloaded for personal non-commercial research or study, without prior permission or charge. This thesis and the accompanying data cannot be reproduced or quoted extensively from without first obtaining permission in writing from the copyright holder/s. The content of the thesis and accompanying research data (where applicable) must not be changed in any way or sold commercially in any format or medium without the formal permission of the copyright holder/s.

When referring to this thesis and any accompanying data, full bibliographic details must be given, e.g.

Thesis: Author (Year of Submission) "Full thesis title", University of Southampton, name of the University Faculty or School or Department, PhD Thesis, pagination.

Data: Author (Year) Title. URI [dataset]



University of Southampton

Faculty of Engineering and the Physical Sciences

Institute of Sound and Vibration Research

Translational approaches to measurement and analysis of the cochlear implant-tissue interface

by

Alan Peter Sanderson

Thesis for the degree of Doctor of Philosophy

November 2019

Abstract

Cochlear implants (CI) are highly successful neuroprosthetic devices, which restore hearing function in children and adults with severe-profound hearing loss. Despite the great potential for improved communication and quality of life, a high degree of performance variability is observed across CI users over time. Clinical outcomes depend on complex interactions between many pre, peri and post-surgical factors. The present work focusses on the interface between the CI electrode array and the cochlea. The tissue response to CI surgery and long-term implantation is not fully understood. The CI-tissue interface is an attractive target for investigation because it can be interrogated using objective measures in humans and animal models.

Chapter 2 presents a case study of a migration related CI failure resulting in device explant and reimplantation. The extra-cochlea tissue, which had developed around the array during extrusion was analysed using immunohistochemistry. The study included a wider range of marker-specific antibodies than other published studies of the fibrotic sheath. Light microscopy imaging showed clear evidence of unresolved active inflammation alongside proliferating cells forming new tissue and blood vessels. This profile of wound-healing in human CI represents a novel finding among studies of similar design.

Chapter 3 presents a retrospective study of electrode impedance (EI) data from 221 CI users. Evidence suggests that EI can indicate the type and volume of newly developed tissue around the electrode array. The study describes EI trends over five years: greater EI levels in basal electrodes compared to apical, adults showed steady EI reduction in apical electrodes whereas children showed plateau or slight increase. A thresholding method allowed detection of cases exhibiting significant deviation from the sample median. 8% of adults and 5% of children exhibited significantly raised EI, often in mid and apical electrodes, which may be explained by localised fibrotic or bony tissue growth.

The case study and retrospective population study prompted research questions regarding underlying mechanisms. For example, is unresolved inflammation a common but under-reported feature of the CI wound healing response? Are the localised increases in EI associated with surgical micro-trauma? Such questions can be investigated using a non-human animal model. Chapter 4 presents method developments towards a mouse model of CI. Immunohistochemical staining was carried out alongside X-ray μ CT imaging to create a three-dimensional model of a C57BL/6 mouse cochlea. This combined approach, known as 3D X-ray histology, will provide high spatial resolution and cell-marker specificity for ongoing investigations of the CI-tissue interface.

Mouse models greatly benefit from genetic tractability and well established immune challenge paradigms. They allow controlled investigation of factors that influence human CI outcomes such as specific hearing loss aetiology. The statistical approach to data processing applied in Chapter 3 could be used to improve monitoring of the CI-tissue interface with minimal cost and could guide prophylactic anti-inflammatory treatment. Clinical decision making will be enhanced by knowledge of the cochlear wound healing response gained from current and future work using the mouse model and explanted human fibrotic tissue.

Table of Contents

| | |
|--|--------------|
| Table of Contents | i |
| Table of Tables | ix |
| Table of Figures | xi |
| Accompanying Material | xiii |
| Research Thesis: Declaration of Authorship | xv |
| Research Contribution | xvii |
| Acknowledgements | xix |
| Contributors | xxi |
| Abbreviations | xxiii |
| Chapter 1 Cochlear implant performance is influenced by the cochlear implant-tissue interface | 25 |
| 1.1 Hearing loss and technological approaches to rehabilitation | 25 |
| 1.1.1 Anatomy and physiology of hearing | 25 |
| 1.1.2 Pathophysiology of hearing loss..... | 30 |
| 1.1.3 Burden of severe hearing loss..... | 32 |
| 1.1.4 Aids and prosthetics of hearing | 33 |
| 1.1.5 Cochlear implants..... | 34 |
| 1.1.6 Cochlear implant processing and stimulation..... | 35 |
| 1.1.7 Cochlear implant surgery | 38 |
| 1.1.8 Cochlear implant candidacy | 39 |
| 1.2 Cochlear implant performance | 40 |
| 1.2.1 Measuring cochlear implant performance | 40 |
| 1.2.2 Pre-implant factors influencing performance variability..... | 41 |
| 1.2.3 Surgical factors influencing performance variability | 43 |
| 1.2.4 Application of steroids in cochlear implant surgery | 45 |
| 1.2.5 Electrode array factors influencing performance variability | 46 |
| 1.2.6 Cochlear implant adverse events..... | 47 |
| 1.3 Cochlear implantation provokes a tissue response | 48 |
| 1.3.1 Investigations of the tissue response to cochlear implantation | 48 |

Table of Contents

| | | |
|------------------|---|-----------|
| 1.3.2 | Methodological comparisons from Table 1-1..... | 65 |
| 1.3.3 | Studies of the tissue response and performance outcomes | 66 |
| 1.4 | Three approaches to measuring the tissue response to cochlear implantation..... | 69 |
| 1.4.1 | Histochemical analysis of human fibrotic tissue from an explanted CI..... | 71 |
| 1.4.2 | Retrospective analysis of telemetry data from adult and paediatric CI users | 71 |
| 1.4.3 | Development of a mouse model of the tissue response to CI | 72 |
| Chapter 2 | Rapid performance deterioration and explant associated with cellular indicators of unresolved inflammation | 73 |
| 2.1 | Introduction | 73 |
| 2.1.1 | Explant following soft failure presents an opportunity for histochemical tissue analysis..... | 73 |
| 2.1.2 | Soft failure following electrode migration..... | 73 |
| 2.1.3 | The generic wound-healing response to non-CI biodevices..... | 75 |
| 2.1.4 | Similarities and differences between the cochlea and other tissues..... | 77 |
| 2.1.5 | The cellular and molecular response to cochlear implants..... | 78 |
| 2.1.6 | Case details | 79 |
| 2.2 | Research aims and questions..... | 80 |
| 2.3 | Method | 82 |
| 2.3.1 | Management of the explanted device and tissue | 82 |
| 2.3.2 | Tissue embedding | 82 |
| 2.3.3 | Tissue sectioning | 83 |
| 2.3.4 | Histochemical staining | 84 |
| 2.3.5 | Immunohistochemical staining..... | 84 |
| 2.3.6 | Image acquisition and processing..... | 86 |
| 2.4 | Results..... | 87 |
| 2.4.1 | Clinical evidence of physical migration of the electrode array | 87 |
| 2.4.2 | Fibrotic tissue removed from the explanted array shows spatially variable organisation | 89 |
| 2.4.3 | Immunohistochemical evidence of active inflammation | 91 |
| 2.4.4 | Immunohistochemical evidence of cellular proliferation and angiogenesis... | 92 |

| | | |
|------------------|--|------------|
| 2.5 | Discussion | 94 |
| 2.5.1 | This case study presents new findings compared to post-mortem studies | 94 |
| 2.5.2 | Confirmed electrode migration associated with cellular indicators of simultaneous chronic inflammation and proliferation | 94 |
| 2.5.3 | Novel findings of cell-specific immunohistochemical stains of tissue from an explanted CI..... | 95 |
| 2.5.4 | Evidence for the mechanism of electrode migration | 96 |
| 2.5.5 | Cellular markers of inflammation and proliferation in an animal model | 97 |
| 2.5.6 | Silicone Breast implants provide useful insights into the wound healing response to bioimplants..... | 98 |
| 2.5.7 | Future development of methods for analysing tissue from explanted CIs | 98 |
| Chapter 3 | Early detection of abnormal electrode impedance in a large sample of Med-El cochlear implant users | 101 |
| 3.1 | Introduction..... | 101 |
| 3.1.1 | Clinical monitoring of the CI tissue interface | 101 |
| 3.1.2 | An overview of electrode impedance telemetry | 101 |
| 3.1.3 | Electrode impedance development over time | 102 |
| 3.1.4 | Electrode impedance as a biomarker of tissue change | 103 |
| 3.1.5 | Clinical management of electrode status | 104 |
| 3.1.6 | Research aim and questions | 104 |
| 3.2 | Methods | 106 |
| 3.2.1 | Statement of ethics | 106 |
| 3.2.2 | Participants..... | 106 |
| 3.2.3 | Electrode characteristics | 106 |
| 3.2.4 | Electrode impedance data acquisition..... | 106 |
| 3.2.5 | Electrode impedance data management..... | 108 |
| 3.2.6 | Deactivated electrode data filtering | 108 |
| 3.2.7 | Electrode numbers were corrected for extra-cochlea position..... | 108 |
| 3.2.8 | Statistical analysis..... | 109 |
| 3.3 | Results | 111 |
| 3.3.1 | Distribution of electrode impedance data varies with electrode | 111 |

Table of Contents

| | | |
|------------------|--|------------|
| 3.3.2 | Deactivation rate depends on electrode position | 112 |
| 3.3.3 | Clinical reasons for deactivation vary with electrode and age category..... | 113 |
| 3.3.4 | Long-term impedance trends vary with electrode position | 113 |
| 3.3.5 | Differences in adult and paediatric long-term impedance trends | 114 |
| 3.3.6 | Fourteen adult cases were identified with statistically high electrode impedance levels | 115 |
| 3.3.7 | Three paediatric cases were identified with statistically high electrode impedance levels | 116 |
| 3.4 | Discussion..... | 118 |
| 3.4.1 | Summary of main findings | 118 |
| 3.4.2 | Electrode impedance changes associated with tissue development | 118 |
| 3.4.3 | A novel method for early detection of increased electrode impedance | 120 |
| 3.4.4 | Discretely localised electrode impedance increase may indicate insertion trauma..... | 121 |
| 3.4.5 | Electro-chemical changes at the electrode surface may be reflected in electrode impedance | 121 |
| 3.4.6 | Electrode impedance as an objective guide to electrode deactivation | 122 |
| 3.4.7 | Future work..... | 123 |
| 3.4.7.1 | Proposed benefits of measuring impedance sub-components..... | 123 |
| 3.4.8 | Conclusion..... | 125 |
| Chapter 4 | A mouse model of the cochlear wound healing response and resulting CI- tissue interface | 127 |
| 4.1 | Translation from a mouse model to human CI users | 127 |
| 4.1.1 | Selection of mouse as the model species for cochlear implantation | 127 |
| 4.1.2 | The mouse model of CI is viable and shows development opportunity | 128 |
| 4.1.3 | Research aim and goals | 129 |
| 4.2 | Methods..... | 131 |
| 4.2.1 | Workflow overview..... | 131 |
| 4.2.2 | Subjects..... | 131 |
| 4.2.3 | Mouse cochlea dissection..... | 131 |
| 4.2.4 | Tissue processing | 133 |

| | | |
|------------------|--|------------|
| 4.3 | Histology and Immunohistochemistry methods..... | 133 |
| 4.3.1 | Sectioning mouse cochlea tissue | 133 |
| 4.3.2 | Immunohistochemical and histochemical staining..... | 134 |
| 4.3.3 | Image acquisition and processing | 134 |
| 4.4 | Computed tomography methods..... | 134 |
| 4.4.1 | Pilot X-ray μ CT investigation | 134 |
| 4.4.2 | Synchrotron X-ray μ CT investigation | 135 |
| 4.4.3 | Synchrotron X-ray μ CT scanning | 137 |
| 4.4.4 | Image file details | 137 |
| 4.4.5 | Image processing and feature extraction | 137 |
| 4.4.6 | Feature segmentation | 140 |
| 4.5 | Results | 142 |
| 4.5.1 | The mouse cochlea scalae were modelled by rendering the manually edited slices | 142 |
| 4.5.2 | Development of 3D X-ray histology of the mouse cochlea..... | 142 |
| 4.6 | Discussion..... | 145 |
| 4.6.1 | Technical outcomes from histological and X-ray μ CT analysis of the C57BL/6 mouse cochlea..... | 145 |
| 4.6.2 | Short-term planned application for the CI mouse model..... | 145 |
| 4.6.3 | The protocol for dissection of the mouse cochlea was refined with experience | 146 |
| 4.6.4 | Future methodological planning for the mouse cochlea tissue processing .. | 146 |
| Chapter 5 | Discussion | 149 |
| 5.1 | Summary of outcomes | 149 |
| 5.2 | The challenge of unpredictable and highly variable CI performance | 151 |
| 5.3 | The challenge of monitoring the CI-tissue interface..... | 151 |
| 5.3.1 | A novel and widely applicable method for filtering potential ‘problem’ cases | 152 |
| 5.3.2 | Clinical impedance telemetry findings can be explored in a mouse model .. | 152 |

Table of Contents

| | | |
|-----------------------|---|-----|
| 5.3.3 | Wider applications of the automated analysis of electrode impedance data | 152 |
| 5.4 | Experimental investigation of individual differences and their effect on CI performance | 153 |
| 5.4.1 | Experimental approach to modelling human CI in a mouse model | 153 |
| 5.5 | Improving outcomes for existing CI users | 155 |
| 5.5.1 | Anti-inflammatory intervention to modulate cochlear wound healing | 155 |
| 5.6 | Conclusion..... | 156 |
| Appendix A 159 | | |
| A.1 | Appendix A1 | 159 |
| A.2 | Appendix A2 | 160 |
| A.3 | Appendix A3 | 161 |
| A.4 | Appendix A4 | 163 |
| A.5 | Appendix A5 | 165 |
| Appendix B 169 | | |
| B.1 | Appendix B1 | 169 |
| B.2 | Appendix B2 | 177 |
| B.3 | Appendix B3 | 181 |
| B.4 | Appendix B4 | 187 |
| B.5 | Appendix B5 | 191 |
| B.6 | Appendix B6 | 200 |
| B.7 | Appendix B7 | 205 |
| B.8 | Appendix B8 | 221 |
| Appendix C 229 | | |
| C.1 | Appendix C1 | 229 |
| C.2 | Appendix C2 | 233 |
| C.3 | Appendix C3 | 236 |
| C.4 | Appendix C4 | 239 |
| C.5 | Appendix C5 | 240 |
| C.6 | Appendix C6 | 245 |

Appendix D 246

D.1 Appendix D1246

D.2 Appendix D2247

D.3 Appendix D3250

List of References..... 251

Table of Tables

| | |
|---|------------|
| Table 1-1: Literature review of investigations of the cochlear wound healing response following implantation | 51 |
| Table 2-1: Immunohistochemical reagents and methods used in staining the human fibrotic tissue..... | 85 |
| Table 4-1: Processing details for cochleae included in X-ray SRμCT session | 136 |

Table of Figures

| | |
|---|-----|
| Figure 1-1: Cross sectional schematic of the ear and major components of the cochlear implant | 35 |
| Figure 1-2: The CI electrode sits in close proximity to sensory and immunogenic tissues within the cochlea | 38 |
| Figure 1-3: Performance measures from the present case study (SW) compared to other retrospective studies of performance and cochlea histology..... | 68 |
| Figure 2-1: The wound healing response to surgically implanted devices; characterised using non-CI bioimplants..... | 77 |
| Figure 2-2: Full insertion demonstrated by X-ray images captured following implantation surgery | 80 |
| Figure 2-3: Fibrotic tissue attached to the surgically explanted electrode array | 82 |
| Figure 2-4: Fibrotic tissue isolated from the array prior to preparation for histology | 83 |
| Figure 2-5: Tissue sections from four regions along the array..... | 84 |
| Figure 2-6: Clinical measures indicate electrode array migration and decrement of speech recognition score over time | 88 |
| Figure 2-7: Density and organisation of cells was variable within and across regions | 89 |
| Figure 2-8: Variation in cell-types and protein expression observed..... | 90 |
| Figure 2-9: Organisation of the collagen differed across the tissue..... | 91 |
| Figure 2-10: Cells and cytokines characteristic of an inflammatory response were observed throughout the tissue..... | 92 |
| Figure 2-11: Cellular markers associated with cell proliferation were observed throughout the tissue..... | 93 |
| Figure 3-1: Electrode impedance shows short and long-term evolution which is influenced by stimulation | 103 |
| Figure 3-2: Electrode voltage is influenced by the physical attributes of the electrode and surrounding environment..... | 107 |

Table of Figures

Figure 3-3: Electrode number was corrected to account for extra-cochlear electrodes 109

Figure 3-4: Electrode impedance (k Ω) measured over 5 years from implantation 111

Figure 3-5: Electrode deactivation was most common in basal electrodes, especially in adults 112

Figure 3-6: Reasons for deactivation were proportionally different for adults and children 113

Figure 3-7: Mean EI for each electrode, over 5 years, for adults and children 114

Figure 3-8: The 5-year trend of EI evolution for each electrode was different in adults and children 115

Figure 3-9: Two individual adult cases showing EI at active electrodes only 116

Figure 3-10: Two individual paediatric cases showing EI at active electrodes only 117

Figure 3-11: The physical properties of the interface between electrode and tissue can be modelled by a resistor-capacitor circuit 124

Figure 4-1: Workflow for mouse cochlea tissue processing, testing and analysis 131

Figure 4-2: The cochlea was dissected from the mouse skull after tissue fixation 133

Figure 4-3: X-ray μ CT Image reconstruction of a C57 mouse cochlea 135

Figure 4-4: Dissected cochlea tissue preparations in sealed containers for scanning 136

Figure 4-5: Workflow for X-ray μ CT image processing using Image-J software 138

Figure 4-6: Image processing steps to extract a binary mask of the cochlea scalae in preparation for 3D reconstruction 139

Figure 4-7: Steps taken to manually edit and segment X-ray μ CT image slices 141

Figure 4-8: A 3D reconstruction of the scalae of the mouse cochlea was created using Avizo 142

Figure 4-9: Proposed spatial alignment of X-ray μ CT data and histology light microscopy imaging. 144

Figure 5-1: Cochlea health can be influenced by pathogens and immune mediators from distal parts of the body 154

Figure 5-2: Conceptual timeline of bio-marker fluctuations in the human body that may affect cochlea health 155

Accompanying Material

Data supporting the study in Chapter 3 are openly available from the University of Southampton repository at <https://doi.org/10.5258/SOTON/D1636>

Research Thesis: Declaration of Authorship

Print name: **Alan Peter Sanderson**

Title of thesis: **Translational approaches to measurement and analysis of the cochlear implant-tissue interface**

I declare that this thesis and the work presented in it are my own and has been generated by me as the result of my own original research.

I confirm that:

1. This work was done wholly or mainly while in candidature for a research degree at this University;
2. Where any part of this thesis has previously been submitted for a degree or any other qualification at this University or any other institution, this has been clearly stated;
3. Where I have consulted the published work of others, this is always clearly attributed;
4. Where I have quoted from the work of others, the source is always given. With the exception of such quotations, this thesis is entirely my own work;
5. I have acknowledged all main sources of help;
6. Where the thesis is based on work done by myself jointly with others, I have made clear exactly what was done by others and what I have contributed myself;
7. Parts of this work have been published as: "Exploiting Routine Clinical Measures to Inform Strategies for Better Hearing Performance in Cochlear Implant Users" Sanderson et al, 2019. Published in the journal *Frontiers in Neuroscience*

Signature:

Date: 29/11/2019

Research Contribution

| Title | Format | Place | Date |
|--|--|--|----------------|
| Investigation of fibrotic tissue from an explanted CI array following migration-related failure | National Conference Talk | British Cochlear Implant Group Annual Conference, Southampton Solent University | April-2019 |
| Exploiting Routine Clinical Measures to Inform Strategies for Better Hearing Performance in Cochlear Implant Users | Published peer reviewed research article (Appendix B7, page 205) | Frontiers in Neuroscience | January-2019 |
| Clinical and Laboratory Approaches to Assessing the Cochlear Implant-Tissue Interface | Meeting Seminar Talk | Meeting to establish collaboration for multi-centre study, Addenbrookes Hospital Cambridge | January-2019 |
| The immense benefits of cochlear implants are not enjoyed by everyone. What can we learn from immune reactions in the ear? | 10 Minute Public Talk (Appendix D3, page 250) | Three-minute thesis competition, University of Southampton | May-2018 |
| Cochlear Implant Electrode Impedance: A biomarker of localised tissue changes | Poster Presentation | OverHear Workshop: Evotion 'Big Data Supporting Public Hearing Health Policies', University College London | September-2017 |
| Electrode impedance: Defining the norm | Meeting Seminar Talk | Annual cochlear performance meeting, University College London | July-2017 |
| Cochlear implant electrode impedance: A potential biomarker for clinical outcomes? | Poster Presentation | British Academy of Audiology Annual Conference, Glasgow | November-2016 |
| Cochlear implant electrode impedance: A retrospective study of MED-EL CI users | Meeting Seminar Talk | Annual cochlear performance meeting, University College London | July-2016 |

Acknowledgements

I dedicate this thesis to the memory of my parents, Peter and Susan Sanderson who passed away during the studentship. I thank my brother Dale James Sanderson for supporting me through these challenging years, and for caring for our family dog Molly.

I thank my supervisors Professor Carl Verschuur and Dr Tracey Newman who supported me academically and personally throughout the PhD project.

This studentship was funded by Engineering and Physical Sciences Research Council (EPSRC). I am grateful for the provision of funding and resources to carry out this research. The affiliation of this research with EPSRC has been acknowledged in conference talks, posters and also in a published peer reviewed journal article (see Research Contribution).

I am forever grateful to the inhabitants of 8 Horder Close: Pete Johnson, Bhavik Barochia, Chris Tomsett, Ben Shaw, Dan Noel and especially my close friend Connor Maltby who kept a roof over my head while I worked on this research.

I am equally grateful to Jo Bailey who saved me from the Southern Rail industrial strikes by welcoming me into her home for several months while I worked on this research.

I offer my sincerest thanks to the Hill family: James, Emma, Ava and Blake (and now Ella) who supported me when there was no option but to knuckle down to work between daily visits to Preston Royal Infirmary.

This research and my enjoyment of it would not have been the same without my friend and colleague Kate Hough. I thank her for being a caring friend and a motivating science buddy.

I thank my Mother and Father in-law Barbara and Tony Mulhern who provided me with a quiet office and supplied a steady flow of tea and homemade soup.

Finally, and most importantly, I thank my wife Laura May Sanderson. She cared for our baby daughter Erica while I worked seven days a week to complete this research and earn a living. She has been the most reliable element of my life throughout a surprisingly turbulent five years. I can't say enough here to prove my gratitude.

Contributors

Dr Edward Rogers contributed to **Chapter 4** in the writing of the Matlab code (**Appendix B5 and B6, page 191**) used to process and analyse data, and generate **Figure 3-4 - Figure 3-10**.

Katie Hough carried out the immunohistochemical stains for cellular markers of inflammation and proliferation shown in **Figure 2-10** and **Figure 2-11**. She contributed to the conceptual development of the mouse model in **Chapter 4** through several meetings, and conversations. She plays an ongoing role in the development of the project with The University of Southampton and Oticon Medical.

Dr Lucy Anderson provided training in mouse dissection and CI surgery at University College London. She contributed to the conceptual development of the mouse model in **Chapter 4** through several conversations. She plays a continued roll in the development of the project in collaboration with The University of Southampton and Oticon Medical.

The artist **Jody Clark** contributed to training on the software Adobe Illustrator and provided artistic guidance. He applied shading detail to **Figure 1-1 and Figure 1-2** using Adobe Photoshop.

Dr Mary Grasmeder contributed the clinical data and preliminary figure idea for **Figure 2-6**. As a clinician working with the patient SW, she has played a significant role in discussions regarding the case study paper which was in preparation for submission to journal at the time of writing.

Dr Shmma Quraishie contributed practical advice and guidance on laboratory assays used in **Chapter 2** and **Chapter 4**.

Dr Orestis Katsamenis carried out the μ CT scans shown in **Section 4.4.1** and **Section 4.4.3**. He provided significant contributions to the development of the μ CT X-ray scanning component of this research through several conversations.

Dr Susan Wilson, Jenny Norman and Jon Ward of University of Southampton Histochemistry Research Unit provided training and practical advice on tissue processing, sectioning and histological staining used in **Chapter 2** and **Chapter 4**.

Dr David Chatelet of University of Southampton Biomedical Imaging Unit provided training for Avizo and Image-J software to allow creation of the 3D model of the mouse cochlea. He adapted an early version of the feature extraction process to create the macro shown in **Appendix C2 (page 233)**.

Contributors

Kathryn Brookes, a visiting Nuffield student, contributed to the 3D mouse cochlea model (**Figure 4-8**) by manually editing the majority of the 1300 slices following the process shown in **Figure 4-7**.

Sarie Cross of The University of Southampton, Auditory Implant Service contributed to problem solving during analysis of clinical data in **Chapter 3**

Mr William Hellier contributed to the improvement of data analysis in **Chapter 3** by scrutinising the methods as an examiner at the PhD transfer viva. This conversation led to the development of the technique shown in **Figure 3-3** which and led to publication in a peer reviewed journal (**Appendix B7 page 205**)

Abbreviations

AB – Arthur Boothroyd
 ABC – Avidin Biotin Complex
 ABI – Auditory Brainstem Implant
 AC – Auditory Cortex
 ACE – Advanced Combinatorial Encoder
 APES – 3-Aminopropyltriethoxysilane
 α -SMA – Alpha Smooth Muscle Actin
 BAHA – Bone Anchored Hearing Aid
 BKB – Bamford-Kowal-Bench
 BM – Basilar Membrane
 CI – Cochlear Implant
 CIS – Continuous Interleaved Sampling
 CMV – Cytomegalovirus
 CNS – Central Nervous System
 CSF – Cerebrospinal Fluid
 CT – Computed Tomography
 DPX – Dibutylphthalate Polystyrene Xylene
 EAS – Electro Acoustic Stimulation
 ECM – Extracellular matrix
 EDS – Energy-Dispersive X-ray Spectroscopy
 EDTA – Ethylenediaminetetraacetic acid
 EI – Electrode Impedance
 FBGC – Foreign Body Giant Cell
 FBR – Foreign Body Response
 FFT – Fast Fourier Transform
 FSP – Fine Structure Processing
 H&E – Haematoxylin and Eosin
 HRU – Histochemistry Research Unit
 IC – Inferior Colliculus
 IHC – Inner Hair Cells
 LL – Lateral Lemniscus
 LW – Lateral wall
 M – Macrophage
 MAUDE – Manufacturer and User Facility Device Experience
 MGB – Medial Geniculate Body
 MH – Modiolar hugging
 MSB – Martius/Scarlet/Blue
 NF2 - Neurofibromatosis Type 2
 NRT – Nerve Response Telemetry
 OCT – Optimum Cutting Temperature
 OHC – Outer Hair Cell
 PBS – Phosphate buffered saline
 PCR – Polymerase Chain Reaction
 PDMS – Polydimethylsiloxane
 Pt – Platinum
 PTA – Pure Tone Audiometry
 PVM/M – Perivascular Melanocyte-like Macrophage
 ROS – Reactive Oxygen Species
 RW – Round Window
 SEI – Statistically High Electrode Impedance Level

Chapter 1

SEM – Scanning Electron Microscopy
SNHL – Sensori-Neural Hearing Loss
SGH – Southampton General Hospital
SGN – Spiral Ganglion Neurones
SiN – Speech in Noise
SL – Spiral Ligament
SM – Scala Media
SOC – Superior Olivary Complex
SOP – Standard Operating Procedure
SPEAK – Spectral Peak Coding
ST – Scala Tympani
SV – Stria Vascularis
SVes – Scala Vestibuli
SR μ CT – Synchrotron radiation-based μ CT
TB – Temporal Bone
UCL – University College London
UoM – University of Melbourne
USAIS – University of Southampton Auditory Implant Service
VEGF – Vascular Endothelial Growth Factor
WRS – Word Recognition Score
XFM – X-ray Fluorescence Microscopy

Chapter 1 Cochlear implant performance is influenced by the cochlear implant-tissue interface

1.1 Hearing loss and technological approaches to rehabilitation

1.1.1 Anatomy and physiology of hearing

Hearing is the perception of sound following sensory detection of vibrations of the air. Depending on the species of animal and nature of the sound source the perception will have specific ecological salience. Generally, hearing provides access to information in sound signals to reduce uncertainty about the local environment. In the case of humans, the most important sound signals are speech, environmental sounds and music. The subjective experience of these sounds is profoundly important for human well-being. Sound waves propagate as vibrations through the air from a source to the listener. The air molecules are pushed and pulled according to the intensity and frequency of the sound source. The vibration propagates along the length of the listener's ear canal and causes a displacement of the eardrum or tympanic membrane (TM) (Figure 1-1). A different displacement occurs at the right and left TM depending on the location of the sound source relative to the listener's head. The displacement of the left and right TM carries level and timing information that are used by the brain to identify the position of the source.

The next stage of the ear, behind the TM, is the middle ear (Figure 1-1). This is an air-filled space, which communicates with the upper part of the throat, the nasopharynx, via the Eustachian tube. This allows ventilation of the middle ear to maintain an air pressure equilibrium with the outer ear. The middle ear space is lined with ciliated, secretory and non-secretory epithelial cells. The cells and secretions of mucous create the mucosa which is very similar to the lining of the respiratory tract.

The TM is acoustically coupled to the cochlea by the ossicles, which allows sound energy to be transferred from the air to the fluids inside the cochlea. The ossicles comprise three small bones: the malleus, incus and stapes. The malleus is connected to the centre of the TM and allows transfer of sound energy through the incus and ultimately to the stapes. The footplate of the stapes terminates onto the oval window of the cochlea, a membrane that seals the cochlea but allows vibrations to transfer to the cochlear fluid and therefore the sensory apparatus within.

The cochlea (Figure 1-1), the vestibule and the semi-circular canals make up the inner ear. These sensory organs allow detection of sound, linear acceleration and angular head movements

Chapter 1

respectively. They develop quite early in gestation from the same precursor tissue to form the bony labyrinth and the membranous labyrinth. These inner ear structures are embedded within the temporal bone of the skull. The membranous labyrinth is encased within the bony labyrinth; it comprises all of the cells and tissues responsible for sensory transduction and homeostasis of the inner ear.

The bony and membranous labyrinths of the cochlea are organised as a spiral of two and a half turns. There is considerable variability between cochleae of different individuals but the average length, measured along the lateral wall is 42mm (Erixon et al, 2009). The internal length and shape of the cochlea is adapted to allow accurate transduction of sound frequency, intensity and phase information. Figure 1-2 shows a cross sectional schematic representation of the cochlea. The membranous tissues create the segmentation of three chambers or scalae: the scala tympani (ST), the scala media (SM) and scala vestibuli (SVes). The ST and SVes are filled with perilymph, which has a similar composition to cerebrospinal fluid (CSF) with high sodium and low potassium levels. The SM is filled with endolymph, which is derived from perilymph and has low sodium and high potassium. The high concentration of potassium in endolymph is maintained through the function of the stria vascularis (SV) (Figure 1-2 blue). The SV is composed of three distinct layers, which allow the fluid in the middle and on each side to be separated. The lateral side which contacts the spiral ligament (SL) is made up of basal cells sealed together with tight junctions. Perilymph bathes the outer edge of the basal cells around the fibrocytes of the SL. The central layer of the SV is lined with intermediate cells and blood vessels. The medial layer of the SV is made up of marginal cells, which are sealed together by tight junctions. The medial aspect of the SV contacts the endolymph of the scala media (SM). Each cell layer of the SV contains ATP driven ion pumps which transport sodium and potassium to establish the aforementioned compositions of endolymph and perilymph. The ionic differentials between perilymph and endolymph are essential contributors to the endo-cochlear potential. This is a voltage that exists across the hair cells (Figure 1-2 orange and red) to drive the flow of charged ions to allow the depolarisation, hyperpolarisation and recovery of the membrane potential.

Inner hair cells (IHC) are a specialised type of epithelial cell with stereocilia on their apical surface. Stereocilia are hair-like projections that give hair cells their name. There are between 30 and 300 per cell, depending on the position and type of cell. Each stereocilium is connected to its neighbour by filamentous proteins called a tip-links, which has the primary function of opening ion channels in response to pressure changes induced by sound. Deflection of stereocilia in one direction opens cation selective channels, whereas deflection in the opposite direction closes the channels. Upon opening of the channels, potassium, which is in relatively high concentration in the endolymph, diffuses down an electro-chemical gradient into the hair cell resulting in

depolarisation. This in turn triggers voltage gated calcium channels. In inner hair cells the influx of calcium ions causes the release of the neurotransmitter glutamate which binds receptors on myelinated fast-conducting fibres of the auditory nerve. The binding of glutamate at the post-synaptic terminal leads to generation of action potentials which propagate along the auditory nerve. Ultimately, the role of the IHC is transduction, to convert mechanical displacement of the basilar membrane into nerve impulses in the auditory nerve. The vast majority, ~90%, of auditory nerve fibres are fast-conducting fibres that innervate IHCs. It is generally understood that the main route of signal transduction and transmission is from IHCs through fast fibres of the auditory nerve.

Outer hair cells (OHC) are also innervated by afferent fibres of the auditory nerve, albeit non-myelinated slow conducting fibres. These make up only 10% of the total auditory nerve fibres. Their role is less well understood than fast-conducting fibres, although this is a dynamic area of research producing regular novel insights (Zhang & Coate, 2016). There are roughly three times more OHCs (~12000) than IHCs (~3500) in the human cochlea. The primary role of OHCs is the active process known as the cochlear amplifier, which affords the cochlea impressive sensitivity to sounds of low intensity and also refined frequency selectivity. These features are attributable to the OHCs contractile properties. Depolarization of the cell, due to potassium influx following stereocilia displacement, causes contraction of the intracellular protein prestin. Prestin is associated with the OHCs plasma membrane; its contraction shortens the cell and changes the membrane stiffness. Modulation of these properties by the cell membrane potential gives OHCs the ability to steer the dynamics of the basilar membrane, which is central to normal hearing function.

In addition to the ascending nerve fibre afferents, the hair cells also have efferent nerve fibre connections which descend from the brain stem. Efferent fibres of the auditory nerve fibres synapse with the OHCs directly. Through this connection the nervous system can regulate the membrane potential of the OHC to suppress their action. This may be protective in limiting the negative effects of intense sound exposure and also allows selective filtering of unwanted noise, especially considering this system operates binaurally (Ciuman, 2010). The efferent modulation of IHCs is achieved through a synapse onto the afferent post-synaptic terminal, which envelops the majority of the IHC cell body. The cells are sealed side-by-side with supporting cells (Figure 1-2 light grey) so the endolymph at the apical surface does not mix with the perilymph which surrounds the basal part of the cells. Inner hair cells (Figure 1-2 red) are densely innervated by the afferent peripheral projections of the auditory nerve whose axons extend to the cochlear nucleus, the first of several brain nuclei of the auditory pathway.

Chapter 1

The auditory nerve is a branch of the vestibulocochlear nerve, which is the eighth cranial nerve. The vestibular nerve branches away from the auditory nerve in the internal auditory canal. It then sub-divides to innervate the semi-circular canals and the otolith organs of the vestibular system. The cell bodies of auditory neurons cluster together in a spiral channel around the modiolus to form the spiral ganglion; hence the name spiral ganglion neurons (SGN). Although the myelinated and non-myelinated neurons have different structure and role, they both bundle together as the auditory nerve. From the ganglion of cell bodies, the central axon projects into the brainstem to terminate at the cochlear nucleus.

The auditory nerve forms a synapse with the central nervous system (CNS) at the cochlear nucleus (CN) in the brainstem. There are a range of different neuronal cell types in the cochlear nucleus, organised into distinct regions. The neurons from the auditory nerve split into bundles that innervate these separate regions. Although the regions constitute different cell types and organisations, each area maintains tonotopic organisation, so frequency information is maintained throughout the auditory pathway. From the cochlear nucleus, secondary nerve fibres project to the superior olivary complex (SOC) in the medulla, which is the first contralateral synapse. The auditory system uses these connections to make interaural comparisons, which provide binaural benefits such as sound source localisation. From there, the auditory pathway extends into the midbrain where the nerve fibres form synapses in the lateral lemniscus (LL). Next is the inferior colliculus (IC), the medial geniculate body (MGB) in the thalamus and the auditory cortex (AC). The cell organisation within and between these nuclei is highly complex and includes many ipsilateral and contralateral connections. In addition to the ascending auditory pathway, there are also descending or efferent projections. For example, the olivocochlear system is a routing of efferent connections from the SOC to the ipsilateral and contralateral cochleae. These neurons are bundled within the audiovestibular nerve and innervate the OHCs to allow real-time modulation of their responses to incoming acoustic signals.

Auditory processing occurs at every stage of the auditory system including the cochlea. The initial frequency and amplitude processing occur during signal transduction in the Organ of Corti. At every stage thereafter the signal is parsed and derived to code information that is salient to human listening perception. This processing allows basic acoustic features to be represented throughout the auditory pathway in parallel with other derived information such as amplitude and frequency change, onset and offset, interaural level and timing differences. At the highest level of the pathway, the auditory cortex and associated areas, gross speech features like formant shifts are represented. The auditory system is clearly adapted for coding the aspects of speech, music and environmental sound that are ecologically most useful and important. In the latter stages of auditory processing, the acoustic features are mapped onto memories of a language

lexicon so that understanding can occur. Evidence from functional magnetic resonance imaging (fMRI) and electro-encephalogram (EEG) show that this involves multiple cortical regions, including non-auditory areas such as the frontal cortex. The organisation and function of the auditory system makes the most of the redundancy of the speech signal. Speech perception can occur even in cases where the input is distorted or partially masked; a feature that can be exploited by hearing aid and prosthetic implant technologies.

The cochlea and vestibular organs receive blood supply from the labyrinthine artery, which is routed through the internal auditory canal alongside the vestibulocochlear nerve. There is some natural variability in the origin of the labyrinthine artery; in most people it branches from the anterior inferior anterior cerebellar artery but in a small number of people it branches from the basilar artery. Although the cochlea is considered part of the peripheral nervous system, the blood supply originates in the central nervous system (CNS). At the point where the labyrinthine artery exits the internal auditory canal it divides into the vestibular artery and common cochlear artery. The main portion of cochlear artery routes through the modiolus as the spiral modiolar artery. A separate subdivision of the cochlear artery, the vestibulocochlear artery, branches off to supply the basal turn of the cochlea as well as proximal parts of the vestibular end-organ. Venous blood is drained through the modiolus via the spiral modiolar vein. Unlike the labyrinthine artery, there is no vein routed through the internal auditory meatus with the nerve. There are several routes of venous blood drainage from the cochlea: directly into the inferior petrosal sinus or internal jugular vein or through the vein of the cochlea or vestibular aqueducts (Mei et al, 2018).

The main vascular network in the cochlea is found in the SL and SV. The interface between the blood and intracochlear fluids is the blood-labyrinthine-barrier, which is similar in structure and function to the blood-brain-barrier. The SV is a highly vascularised structure which is specialised for mediating the ionic composition, in particular potassium levels, within endolymph of the SM. Capillaries originating from the spiral modiolar artery and vestibulocochlear artery project through the middle region of the SV, the intra-strial space. This middle region of the SV is populated with two cell types: intermediate cells, which are melanocytes and perivascular melanocyte-like macrophages (PVM/Ms) that actively pump potassium into the intra-strial space, an essential step in establishing the endo-cochlear potential. They have characteristic markers of both melanocytes and macrophages and have been shown to regulate the integrity of the intra-strial fluid-blood barrier (Zhang et al, 2012). They do this through chemical signalling to the endothelial cells and pericytes which make up capillary walls (Nyberg et al, 2019). Intermediate cells connect to basal cells via gap junctions which allow ions to flow. Basal cells are bathed in perilymph which flows through the extra-cellular space between cells (mainly fibrocytes) of the SL.

Chapter 1

The SV is the main supply of oxygen and nutrients to the cochlea. Oxygen supply to the key functional units of the cochlea such as the Organ of Corti is delivered by diffusion through the perilymph, although the capillaries of the basilar membrane are also likely to provide some vascular support (Misrahy et al, 1960; Nomura, 1977).

1.1.2 Pathophysiology of hearing loss

A disturbance or abnormality of the hearing pathway described above can result in a hearing loss with significant functional impact on the individual. Generally, hearing loss is characterised by the site of the lesion or abnormality. Pathology or damage of the outer and/or middle ear cause conductive hearing loss. This type of hearing loss is characterised by reduced conduction of the sound pressure through the ear canal, the tympanic membrane, the ossicles and oval window of the cochlea. Pathologies of the cochlea and/or neural pathway cause sensori-neural hearing loss. This is a broad category comprising any impediment to transduction of the mechanical vibration into neural signals or transmission of those signals through the nuclei of the auditory pathway. A lesion at any stage between the cochlea and the AC can cause a sensori-neural hearing loss, which can make diagnosis and prediction of treatment outcomes difficult. It is possible for a hearing loss to be mixed, where the deficit is attributable to both conductive and sensori-neural components. However, the vast majority of significant permanent hearing losses are sensori-neural in nature.

There are two main subtypes of sensori-neural hearing loss: acquired and inherited, which have equal incidence rates. Two thirds of inherited hearing loss are classified as non-syndromic. Depending on the nature of the gene mutation and its chromosomal position, non-syndromic hearing loss can show different inheritance patterns. The majority (~75-80%) are autosomal recessive which means a defective gene must be inherited from both mother and father in order to manifest a hearing loss. Around 20% follow autosomal dominant inheritance where a single mutant gene will give rise to a hearing loss. Approximately 5% of non-syndromic hearing loss is inherited through the sex chromosomes or the mitochondria which are passed from the maternal egg. The most common cause of hereditary non-syndromic hearing loss is mutation of the gene GJB2, which encodes the gap junction beta 2 protein, known as connexin-26 (Smith & Hildebrand, 1998). This type of hearing loss shows a recessive pattern of inheritance, where a mutation must be present in both copies (maternal and paternal) of GJB2 for the hearing loss to manifest. Connexin-26 gap junctions are expressed in cells throughout the body. In the cochlea they are abundant in the Organ of Corti and the SV, creating an ionic connection between cells. They play an important role in the diffusion of potassium to create and maintain the endo-cochlear

potential. Dysfunctional connexin-26 hinders cochlear homeostasis and ultimately causes significant non-progressive sensori-neural hearing loss (Wingard & Zhao, 2015).

The remaining third of inherited hearing losses are syndromic, where the hearing loss presents as part of a collection of typical comorbidities. For example, Waardenburg's syndrome is characterised by abnormalities of pigment of skin, hair and eyes, as well as varying degrees of sensori-neural hearing loss. This is caused by mutations in specific genes involved with development and function of pigment producing cells, melanocytes. This cell type is an important component of the SV. The malfunction of these cells, known as intermediate cells in the context of the SV compromises cochlear homeostasis. This results in a disturbance of the endo-cochlear potential has a direct effect on the transduction capabilities of the sensory hair cells and ultimately results in a moderate to profound hearing loss. Another example of syndromic hearing loss is Usher's syndrome, which manifests as sensori-neural hearing loss, vestibular dysfunction and vision loss through retinitis pigmentosa. The severity of symptoms depends on the category of Usher's: type I, II or III, which each involve different gene mutations. The proteins associated with these genes form multi-protein complexes which are important for hair-bundle formation in sensory hair cells in the cochlea and vestibular organs. In the mutated form, the genes encode proteins with poor function, which ultimately leads to loss of hair cells (Mathur & Yang, 2015).

Acquired hearing loss can affect people at any age, including before birth. It may be caused by noise trauma, ototoxic drugs such as platinum based chemotherapy, head trauma, asphyxia, long-term otitis media in infancy, viral or bacterial infection, auto-immune conditions and aging. Each of these hearing loss aetiologies are associated with damage of the structures of the ear and/or auditory brain. Depending on their specific pathophysiology, the damage might be present at the tissue, cellular or sub-cellular level. The wide range of pathophysiological mechanisms of damage highlights the vulnerability of hearing function. A key reason for this is the fine homeostatic regulation of cochlea as an essential feature of its function and its poor capacity for regeneration following significant insult. Noise induced hearing loss is primarily caused by damage to hair cells and their stereocilia bundles (Kurabi et al, 2017), although changes in the SV (Hirose & Liberman, 2003) and synapses of auditory nerve fibres have been reported (Bullen et al, 2019). High intensity sounds cause extreme displacement of the basilar membrane which can breach the barrier between endolymph and perilymph with detrimental effects on the endo-cochlear potential. However, most noise induced damage occurs below the threshold of physical trauma and, rather, is biochemically mediated. The mechanisms of cell damage include reactive oxygen species (ROS), apoptosis, which is also known as programmed cell death and inflammation (Kurabi et al, 2017). It has become clear, mainly from studies of animal models that noise exposure is associated with the production of pro-inflammatory signalling molecules known as cytokines

Chapter 1

(Fujioka et al, 2006). Noise exposure of sufficient intensity and duration can ultimately lead to loss of hair cells, which reduces the transduction function of the Organ of Corti. Other aetiologies of acquired hearing loss can produce similar damage to the Organ of Corti and the same functional impact of deafness. For example, viral infections can directly damage the cochlea or create damage indirectly through strong induction of an inflammatory response. One of the most common causes of congenitally acquired hearing loss is cytomegalovirus (CMV), which can induce severe bilateral sensori-neural hearing loss. Different viruses interact with the host tissue in specific ways depending on their particular structure, mode of infection and replication. For example, CMV is a double stranded enveloped DNA virus whereas measles is a single stranded enveloped RNA virus. Both can cause significant damage to the cochlea, but CMV does this through host inflammation whereas measles causes direct damage to cells of the Organ of Corti (Cohen et al, 2014). Measles has also been found to be present in the stapes footplates of individuals with hearing loss caused by otosclerosis (Karosi et al, 2005).

There is some complex interaction between inherited and acquired hearing loss where genetic factors interact with environmental factors over time to give rise to progressive hearing loss. Our knowledge of the contributions and interactions of hereditary and acquired components of progressive hearing loss is a new area of scientific research. The ultimate aim of research in this area is to understand and predict predisposing risks posed by an individual's genetic profile (Cherny et al, 2020).

1.1.3 Burden of severe hearing loss

Human health, well-being and prosperity depends on communication. Although the transfer of information between individuals is multi-modal and multi-sensory, hearing is uniquely important for verbal communication. Recent evidence highlights the importance of hearing to cognition, risk of dementia (Livingston et al, 2017; Liu & Lee, 2019) and isolation leading to depression (Mener et al, 2013). The communication barrier created by hearing impairment can be highly debilitating for individuals but also costly to them, and society. The estimated yearly burden of reduced quality of life is £26bn, the estimated loss of earnings in £4bn, the estimated cost of increased GP visits is £76m and the estimated cost of increased social care is £60m (Archbold et al, 2014). The impact of hearing loss on an individual depends on several factors. The age of onset of hearing loss can have a significant impact on language development. Pre-lingual deafness can cause significant auditory deprivation if not treated before the first few years of life. Post-lingual deafness presents significant challenges for receptive language but is usually associated with normally developed expressive language. Depending on the effectiveness of treatment of pre-lingual deafness with a hearing prosthesis such as hearing aids, the neurological maladaptation following auditory

deprivation can have severely detrimental effects on auditory processing. This means that the clinical outcomes for patients who were deafened pre or post-lingually can be significantly different.

1.1.4 Aids and prosthetics of hearing

A range of electronic devices can be used to treat hearing loss, depending of the type and severity. The most common type of device is the acoustic hearing aid, which allows auditory rehabilitation by delivering an amplified acoustic signal to the ear canal. There are several different styles of hearing aid designed to meet different requirements. For example, a person with a severe hearing loss can be fitted with a power hearing aid that is tightly coupled to the ear canal to allow the sound pressure to be delivered to the middle ear and onward to the basilar membrane. A person with a mild to moderate hearing loss can be fitted with a low-power device which directs the acoustic signal into the ear canal via an open-fitting so the person can hear a combination of amplified and natural sound. Hearing aids are a highly effective way to overcome a range of hearing loss; however, because they deliver an acoustic signal through the air of the ear canal their success is dependent on middle ear transfer and transduction in the Organ of Corti by IHCs. In the cases of significant conductive hearing loss where the middle ear transfer is poor, a bone anchored hearing aid (BAHA) may be most appropriate. Rather than acoustic transfer via the ear canal, BAHAs bypass the outer and middle ear by coupling directly to the temporal bone through a surgically implanted abutment. The collection and processing of sound by the BAHA is very similar to acoustic hearing aids. The delivery of the vibration via fixed mechanical coupling is the key difference and relies on a different style of output transducer. An important benefit of BAHA is that it can provide amplification without any need for an ear-level device or ear mould, which means that conditions such as microtia and chronic middle ear effusion are not contraindicated.

Middle ear implants allow transfer of vibration to the cochlea via direct coupling of a floating mass transducer onto the ossicles or oval window membrane. The collection and processing of the acoustic sound is performed by a processor positioned on the outside of the head, held in place by a subcutaneous magnet. Once processed to meet the amplification requirements of the user, the signal is sent to the implanted receiver via transcutaneous induction coil. The receiver is connected to the floating mass transducer in the middle ear via a flexible cable, through which the processed audio signal is delivered. Middle ear implants have similar fitting criteria to BAHA, except, because they are fully implanted, they are suited to cases of impaired wound healing or where BAHA abutment may be at risk of infection.

Chapter 1

Some types of hearing loss cannot be treated using the device discussed above due to the nature of the cochlea and and/or auditory nerve pathophysiology. For example, neurofibromatosis type 2 (NF2) is a condition characterised by bilateral Schwannoma of the audiovestibular nerve. The function of the nerve is destroyed either through persistent Schwannoma growth or the surgery used to remove the tumours. In such cases, the neural connection between the cochlea and second order neurons of the auditory pathway are severed. An auditory brainstem implant (ABI) can be used in such cases to electrically stimulate the second order neurons, which synapse with the auditory neurons in the CN. The ABI consists of externally worn components and surgically implanted internal components. A device is worn on or behind the ear which houses the microphone system and speech processor. The processor is connected to a transmitter coil, which is held by a magnet over the receiver implanted under the skin. This creates a transcutaneous connection between the external and internal components, through which signals can be transferred by electromagnetic induction. The ABI has the important benefit of providing hearing function in cases where all other devices fail to meet the challenge presented by the pathophysiology (Wong et al, 2019).

1.1.5 Cochlear implants

The most common implantable hearing prosthesis is the cochlear implant (CI). This device allows some hearing function to be restored through direct stimulation of the first-order neurons of the auditory nerve. This is achieved using a thin flexible electrode array inserted into the ST of the cochlea. The standard components of a cochlear implant are shown in Figure 1-1. The acoustic signal is captured by microphones, which are housed within the speech processor unit worn on the pinna. Like the ABI, the CI uses a transcutaneous connection between the processor and implanted receiver-stimulator. A magnet holds the transmitter coil over the implanted receiver coil. Electrical current flow in the transmitter induces a current in the receiver under the skin. This signal carries the acoustic information of speech, music or environmental sound encoded by the speech processor. The receiver stimulator unit is hermetically sealed, usually within a titanium case wrapped with medical grade silicone. The electrode array is connected to the receiver stimulator by a lead wire. These parts are also sealed by a silicone carrier. The most commonly used material is polydimethylsiloxane (PDMS) which is known to be biocompatible but not fully inert. The array consists of platinum electrode contacts and flexible PDMS. Each platinum contact is connected to the receiver-stimulator by iridium coated platinum wires. The CI electrode occupies the ST within the cochlea and delivers controlled pulses of electrical current to stimulate the auditory nerve resulting in sound perception.

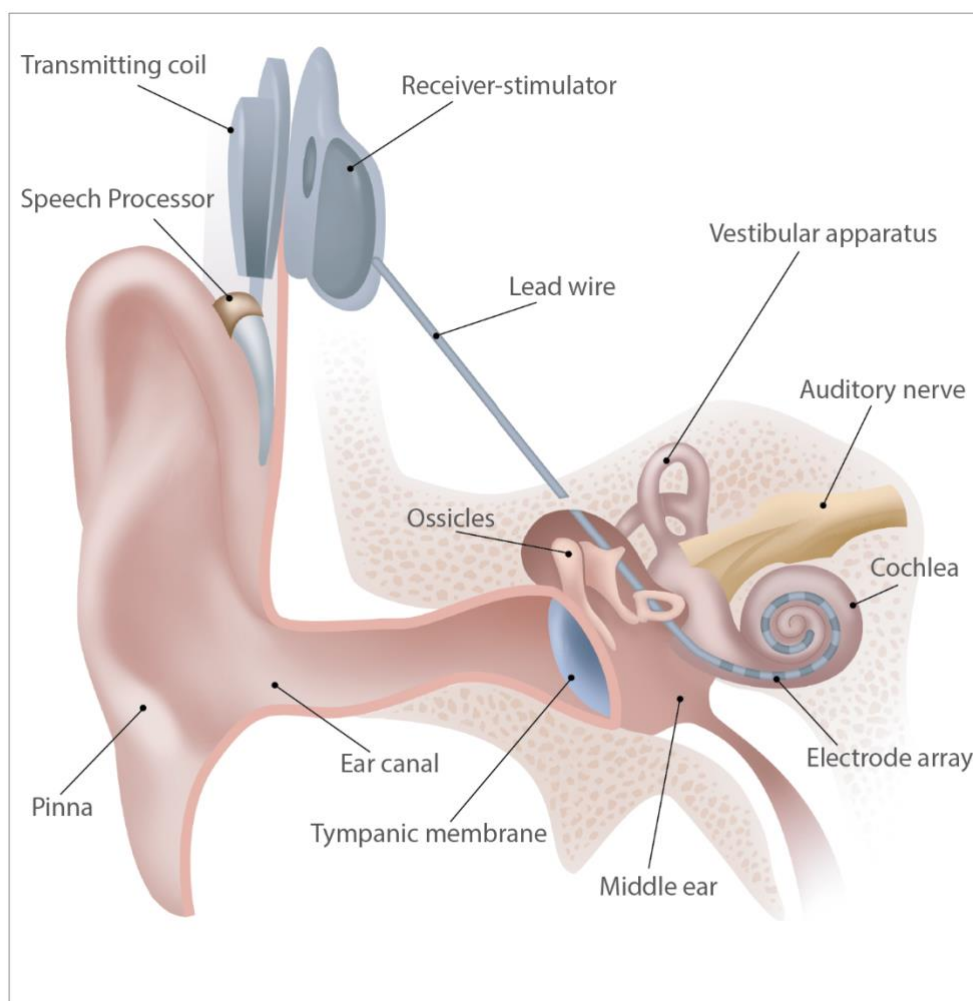


Figure 1-1: Cross sectional schematic of the ear and major components of the cochlear implant

1.1.6 Cochlear implant processing and stimulation

Cochlear implants allow people with severe/profound hearing impairment to perceive sounds, which would otherwise be inaudible, through direct electrical stimulation of the auditory nerve. To achieve this, the components of the CI shown in Figure 1-1 transform sound waves into a coded electrical signal which is delivered to the CNS via the auditory nerve. In this way, the cochlear implant takes advantage of the electrophysiological properties of the nervous system discovered by Luigi Galvani in the 1770s, that electrical current from an external source triggers a cascade of electrical current through neurons to convey information.

The main manufacturers of CIs supplying the UK at this time are MED-EL, Advanced Bionics, Cochlear, and Oticon Medical. The devices offered by these companies differ with respect to the design of the processor and electrode array, and the signal processing strategy; however, the broad steps towards translating the acoustic signal to pulses of electrical current that evoke

Chapter 1

neural activity in the auditory nerve are standard across manufacturers. The first step of CI processing is transduction of sound pressure fluctuations into an electrical signal by the microphones. There are usually two microphones to allow spatially focussed sensitivity to reduce unwanted noise. The signal is resampled into digital data by the analogue-digital converter. The digital signal is processed to enhance the representation of soft sounds and compress that of loud sounds. The signal is split into separate frequency bands. The temporal envelope is extracted from each frequency band using digital filters and a Fast Fourier Transform (FFT). This envelope signal carries the intensity fluctuation information for each frequency band. This is used to modulate the amplitude of pulse trains delivered by the receiver stimulator to the electrode array. The pulse rate (number of pulses per second) and pulse width (duration of one phase of each pulse) are set to achieve the desired stimulation of the auditory nerve. The loudness contribution of each pulse depends on the charge delivered during each phase (current level x pulse width). These parameters can be adjusted in the clinic to set the 'threshold of hearing sensation' and 'most comfortable' levels. Modern CI systems avoid durations shorter than ~10 ms due to the high peak current required to generate useable charge.

The most common CI speech processing strategies are Continuous Interleaved Sampling (CIS), Advanced Combinational Encoder (ACE) and Spectral Peak Coding (SPEAK). In the CIS processing strategy, pulse trains of a fixed rate are delivered in a sequence from one channel to the next in a predefined order. This approach avoids channel interactions by delivering stimulation at each channel in isolation. The ACE and SPEAK processing strategies select channels for stimulation based on the dominant frequency band i.e. the extracted envelopes with the greatest intensity. This has the benefit of producing a more accurate spectral representation of the speech. The pulse rate of ACE (>1000 pps) is much higher than SPEAK (250 pps). This is a basic description of the main strategies and there are several modern modifications developed and implemented by manufacturers. One example is the Fine Structure Processing (FSP) strategy applied in MED-EL devices, which varies pulse rate to match the low frequency filter bands so fine structure pitch cues can be conveyed.

Stimulation of the SGNs requires a physical interface between the electrode array and the biological tissue of the cochlea. Positioning of the electrode array within the ST minimises the distance between the active electrodes and the SGN cell bodies and peripheral projections innervating IHCs. Contemporary CI devices utilise multi-electrode arrays which allow spatially distributed stimulation along the length of the cochlea to take advantage of the tonotopic organisation of spiral ganglion neurones. Figure 1-2 shows a schematic representation of the spatial relationship between the electrode array and the peripheral projections of the SGNs.

Depending on the design of the array and positioning during surgery the array may sit on the medial wall near the SGN cell bodies (open grey circle) or at the lateral wall (closed grey circle).

The electrical charge is delivered as bi-phasic square wave current pulses. Cochlear implant receiver stimulators provide a constant current source, where a predefined current level is maintained by modulation of the source voltage. The bi-phasic pulse is charge balanced to ensure direct current, which is damaging to tissue, is minimised. Cochlear implant receiver stimulators regulate charge density (current x pulse width x electrode surface area) levels to achieve the desired loudness perception while minimising electro-chemical changes to the tissue, cochlear fluids and electrode. By stimulating the SGNs, the CI can overcome the pathophysiological barrier of damage in the Organ of Corti, the SV, and supporting tissues. Therefore, the CI is an appropriate and often highly effective treatment option for severe sensori-neural hearing loss of inherited and acquired aetiologies.

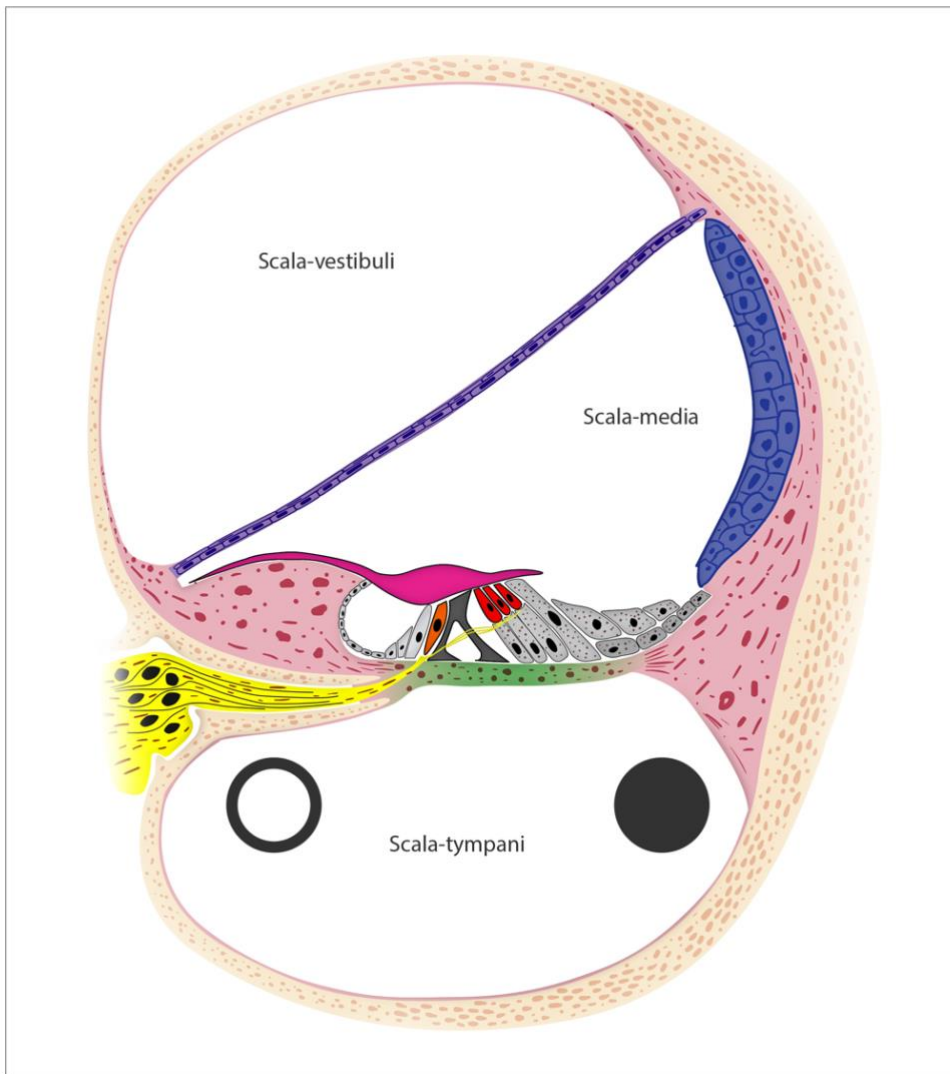


Figure 1-2: The CI electrode sits in close proximity to sensory and immunogenic tissues within the cochlea

Grey open circle: Electrode array positioned at medial wall. Grey closed circle: Electrode array positioned at lateral wall. Yellow: The SGN and peripheral neuronal projections. Orange: Inner hair cell. Red: Outer hair cells. Light grey: Other cells including Deiter’s cells, Hensen’s cells, Boettcher’s cells, and Claudius’ cells. Dark grey: Pillar cells making up the tunnel of Corti. Green: Basilar membrane. Purple: Reisner’s membrane. Blue: Stria vascularis. Pink: Limbus and spiral ligament on medial and lateral wall respectively.

1.1.7 Cochlear implant surgery

In the majority of cases the CI electrode array is inserted into the cochlea by either by cochleostomy or the round window approach. The cochleostomy technique is performed by drilling through the cochlear promontory using a 1-1.5 mm diamond burr. This is done carefully to reveal the soft inner lining of the bony labyrinth, the periosteum. The periosteum is opened with

a pick before the electrode array is inserted. Surgeons avoid contamination of the cochlea with blood and bone dust where possible due to their pro-inflammatory and pro-proliferative effect on the intracochlear tissues. The round window approach avoids drilling with the aim of minimising trauma to intracochlear structures. The equivalent sound pressure level of drilling can be up to 130dB (James et al, 2005). The electrode is inserted through the round window membrane and the array itself seals the opening; sometimes with additional muscle or periosteum as packing (Mangus et al, 2012).

1.1.8 Cochlear implant candidacy

Since their commercial introduction in the late 1980s CIs have allowed people with severe to profound hearing impairments to access speech so they can communicate verbally. This can have a transformational impact on the user's life with regard to development, education, relationships and employment. Children and adults of almost any age, with acquired or congenital hearing impairment can be implanted. In the UK, new-born babies are screened for hearing impairment using otoacoustic emissions and auditory brainstem response testing. Early detection of significant hearing loss increases the chance that a child can be implanted at an early age and benefit maximally from a CI. Older individuals diagnosed with severe to profound hearing loss by pure tone audiometry and speech audiometry would also be potential candidates for implantation. The decision to implant in the UK is guided by the National Institute for Health and Care Excellence (NICE) evidence-based CI guidelines. An individual may be a candidate for CI if they cannot hear pure tones softer than 80 dB HL at two or more of the following frequencies: 500 Hz, 1,000 Hz, 2,000 Hz, 3,000 Hz and 4,000 Hz. Adults should be implanted unilaterally when acoustic hearing aids do not provide adequate benefit. Children should be implanted bilaterally when acoustic hearing aids do not provide adequate benefit. Hearing aid performance is deemed adequate when individuals can score 50% or greater on Arthur Boothroyd (AB) words test. For young children, the AB words test is not appropriate so they should be assessed on their speech, language and listening skills, taking into account expected milestones for the age and cognitive level. The cost-benefit aspect of CI candidacy is highly important. Therefore, it is recommended by NICE that individuals are assessed by a multidisciplinary team to consider their functional communication ability as broadly as possible. Also, devices and services should be selected based on lowest cost when all other factors are equal (NICE, 2019).

1.2 Cochlear implant performance

1.2.1 Measuring cochlear implant performance

Many CI users are able to achieve 100% speech recognition when listening in quiet and some patients can also discriminate speech in background noise (Wilson & Dorman, 2008). Despite the success of CIs, high levels of performance are not guaranteed. In some cases, performance can be below optimum on measures such as speech recognition, speech discrimination in noise and subjective reports of sound quality and non-auditory sensations. The term performance in the context of CI is quite broad and can be ambiguous. It commonly refers to a user's score on a clinical speech recognition test such as Bamford-Kowal-Bench (BKB) sentences or AB words tests. It can also refer to psychoacoustic measures such as sound source localisation. At the broadest level, performance is a collection of measures and descriptors including the user's self-report of sound quality (Balkany et al, 2005). Part of the challenge of improving CI hearing performance is the lack of defined outcome measures. Our concept of performance and expectations for attainment will vary for different patient groups. For example, children and adults are at different stages of development, may have different hearing loss aetiologies and have different communication needs. Patients with acquired or inherited hearing impairment, or different age of deafness onset are likely to have different outcomes.

Studies of CI clinical outcomes are limited in terms of sample size and group heterogeneity. The power of cross-study comparisons could be improved by standardising the methods of measurement of CI performance (Bruce et al, 2015). Schaefer et al, (2017) found a wide range of hearing and speech perception outcomes being used in publications from 2015 in the journal Cochlear Implants International. The specific tools used to make the measurements, as well as the timing of tests were highly variable. Studies also covered other outcomes such as 'complications of surgery' and 'auditory perceptions' which highlights the wide range of non-standardised measures being used. The type of measure used can profoundly affect the conclusion of a study. For example, CI users often perform well on sentence tests where context and redundancy of information are greatest. However, performance can be highly variable between individuals and some CI users experience much poorer outcomes than expected (Wilson and Dorman, 2008).

There is a lack of prospective randomised controlled trials (RCT) in CI research because of relatively low numbers of CI users and the high degree of sample heterogeneity. A study aiming to test the benefit of CI tuning based on regular neuroimaging to monitor neural plasticity was recently registered. This trial has an RCT design aiming to mitigate the biases present in the common retrospective studies of CI performance (Lambriks et al, 2020).

1.2.2 Pre-implant factors influencing performance variability

Cochlear implant performance is influenced by a multitude of factors acting at all levels from cognitive processing down to cellular inflammatory responses in the cochlea. Several studies have investigated the association of these factors with performance measures such as word recognition scores. (Lazard et al, 2012) analysed clinical data from 2251 post-lingually deafened adults across several international CI services. Of the pre-implant factors investigated, they found that hearing threshold levels in the better ear, hearing aid use and duration of moderate hearing loss contributed significantly to speech scores. Duration of deafness has been shown to have a strong effect on CI auditory performance of post-lingually deafened adults in other studies (Blamey et al, 1996; Leung et al, 2005). A study including 17 post-lingually deafened adults found that duration of profound deafness was the main predictor of performance on a BKB sentence test (Green et al, 2007).

The vast majority of studies of CI auditory performance include adult participants only. Investigation of auditory performance in children is more difficult because the tools of measurement tend to be language based. There are, however, a growing number of studies presenting evidence of auditory performance in implanted children (Cosetti & Waltzman, 2012). For example, (Gaurav et al, 2020) used 'categories of auditory performance' and 'meaningful auditory integration scale' to compare children below and above the age of five. These tools are administered by a trained clinician who categorises each child based on their auditory behaviours. The study showed that the younger age group exhibited a greater improvement following one year of CI use than the older children.

A study of factors influencing CI performance outcomes showed that age was significant in two forms; age of onset of severe-to-profound hearing impairment and age of implantation (Blamey et al, 2012). Age has been shown to negatively correlate with speech recognition score in adult CI users (Holden et al, 2016). Pre-implant speech performance is a reliable predictor of post-implant outcomes. A study of 312 adult CI users measured speech performance on a monosyllabic word perception test before and after implantation. They found that higher pre-implant scores reliably predicted higher post-implant scores. The post-implant score was improved in 96% of cases suggesting that the integrity and preparedness of the speech processing apparatus of the CNS is critical to CI performance (Hoppe et al, 2019). Rousset (2017) showed that CI users who exclusively use verbal communication had better speech scores than those who also use sign language. This highlights the importance of higher-level auditory processing, which is primed by

Chapter 1

auditory processing during verbal communication, especially in the critical period of language acquisition. A study of cognitive predictors of speech recognition showed that CI users with greater capacity for working memory scored better on speech-in-noise (SiN) tests. The SiN score was correlated with duration of deafness, further supporting the findings of earlier studies that identified the importance of this factor (Kaandorp et al, 2017).

Our knowledge and understanding of factors influencing speech performance are limited. Published research findings only account for a small amount of the observed variance (Blamey et al., 2012). Despite approximately 25 years of research into performance with modern CI devices, there has been little progress in accounting for more than about 20% of the observed variance in outcome measures (Lazard et al, 2012). Future developments in our understanding of neural plasticity in the auditory system, cognition, auditory training and the critical period for language development may guide the development of more sensitive measurement tools (Cosetti & Waltzman, 2012).

Another important focus for future research development is the biology the CI-tissue interface, especially in aetiologies that directly impact the cochlea. Evidence shows that performance is maximised when implantation is performed soon after diagnosis before excessive cochlear ossification (Philippon et al, 2010). In a study of 'the spiral ganglion hypothesis' it was shown that mutant genes expressed in the spiral ganglion are associated with poorer CI outcomes than genes expressed in other compartments of the cochlea (Eppsteiner et al, 2012). A meta-analysis showed that children with GJB2 hearing loss had better CI outcomes than those with acquired hearing loss, but not significantly different from those with non-GJB2 inherited hearing loss. It seems that different aetiological profiles are indeed associated with performance outcome. For example, Rajput et al, (2003) showed that children with syndromic hearing loss, as well as those with reports of vestibular disorders had lower speech improvement scores at 4 and 5 years than children with non-syndromic hearing loss following cochlear implantation.

Cochlear implant outcomes are generally poorer in pre-lingually deafened individuals compared to post-lingually deafened individuals (Dawson et al, 1992). Normal language acquisition appears to require that the nervous system is primed through auditory stimulation during a critical period from the age of 2 until puberty (KrashenI, 1967). Evidence for this is shown in a PET scan study demonstrating different activation patterns in the auditory cortex of pre-lingually and post-lingually deafened CI users. The significant functional differences between these groups has a neuro-developmental basis, which is significantly affected by auditory deprivation during the critical period of language acquisition. This highlights the paramount importance of effective treatment of severe hearing loss at the earliest possible opportunity using hearing aids or implant.

Duration of deafness essentially describes the magnitude of the auditory deprivation effect, which is “a systematic decrease (over time) in auditory performance associated with the reduced availability of acoustic cues” (Arlinger et al, 1996). The evidence from psychoacoustic and physiological investigations indicates plastic changes in central auditory pathways (Munro, 2008). These effects manifest as slow deviations in auditory performance following onset of deafness. Although the cause of the hearing loss and subsequent effects of auditory deprivation occur along different timescales and have distinct underlying mechanisms, they both show a high degree of individual variability, which depends on an individual’s unique profile of intrinsic (genetic and epigenetic) and extrinsic (environmental and lifestyle) factors. Understanding aetiology at the fundamental level of biological complexity is necessary if prediction and monitoring of hearing performance are to be improved along with treatment interventions for poor outcomes. This research need is a central theme in the work presented here.

1.2.3 Surgical factors influencing performance variability

One of the most important considerations in CI surgery is the post-implant health of the cochlea. Preservation of residual hearing is a key indicator of cochlea function and has been shown to predict CI speech-discrimination-in-noise performance (Gifford et al, 2013). Atraumatic techniques known as ‘soft surgery’ are used to minimise damage in the apical regions of the cochlea to preserve natural hearing. The main causes of damage, which are mitigated by soft-surgery are mechanical trauma during electrode insertion e.g. fracture of osseous spiral lamina, shock waves in perilymph during electrode insertion, acoustic trauma due to drilling, loss of perilymph, potential bacterial infection and secondary intracochlear fibrous tissue formation (Miranda et al, 2014). The approach was first introduced by Lehnhardt (1993) who acknowledged the potentially traumatic impact of electrode implantation and proposed surgical methods that promote hearing preservation.

Most CI electrode array insertion is performed by either cochleostomy or round window insertion. Electrode array insertion via a drilled cochleostomy is a common technique, which has a key benefit of being adaptable for the individual patient and their specific cochlear anatomy. For example, in patients with a tight turn from the hook region of the basal turn, a carefully located cochleostomy can allow direct atraumatic insertion (Addams-Williams et al, 2011). One potential drawback of the drilled cochleostomy is the risk of noise and/or vibration induced damage, which has been revealed in post-mortem histological investigation of implanted cochleae (Richard et al, 2012). Another potential risk of the procedure is contamination of the cochlea with blood and bone dust, which is thought to cause damage through inflammation and osteogenesis (Friedland & Runge-Samuelson, 2009). Round window insertion is therefore considered to be least traumatic

Chapter 1

to intracochlear structures. Evidence from CT imaging study of electrode placement showed that round window insertion produced closer proximity of electrode contacts to the modiolus and therefore SGNs (Jiam, 2016). There is some evidence that the round window approach produces better hearing preservation outcomes than cochleostomy. However, studies of this comparison often have low participant numbers and aetiologically heterogeneous samples, so interpretation should be carried out with caution (Snels et al, 2019). A metaanalysis including 16 studies with a total of 170 patients found no evidence that one particular surgical approach yields significantly different results to another with regard to hearing preservation (Havenith et al, 2013). These studies highlight the absence of clear evidence that either surgical approach affords better hearing preservation outcomes. Despite evidence that the different methods may have an effect on the tissue response of the cochlea, the difference does not necessarily extend to auditory performance outcomes. One possible reason for the lack of evidence is the fact that studies so far have been retrospective and therefore not controlled. A prospective clinical study was registered in 2015 to look at electrode placement using X-ray computed tomography (CT) and speech performance following either round window or cochleostomy approach. The study was terminated in 2019 due to low interest in enrolment (Carlson, 2015).

Electrode insertion can disturb intra-cochlear structures and cause damage, which results in loss of residual hearing. This deleterious effect has been investigated through post-mortem histology and categorised into degrees of damage; Grade 0: no observable trauma, Grade 1: elevation of the basilar membrane, Grade 2: rupture of basilar membrane, Grade 3: translocation of electrode array into SVs, and Grade 4: severe trauma such as fracture of the osseous spiral lamina or modiolus or tear of SV (see Table 1) (Eshraghi et al, 2003). The level of trauma resulting from array insertion is likely to be the product of many interacting factors. The speed of insertion of the electrode array through the cochleostomy is an important factor because higher speeds result in greater intra-cochlear fluid pressure (Todt et al, 2014). The dimensions of the cochlea vary significantly between people. The height of the cochlea and the width of the lumen of the cochlear duct can be reduced in the case of sensori-neural hearing loss, although the length varies significantly irrespective of hearing loss level. Considering this variability in cochlea size, electrode array selection and insertion technique could be personalised in future to minimise trauma (Pelliccia et al, 2014).

The main indicator of atraumatic insertion is minimal loss of residual hearing. A study of several surgical factors in 82 children (1 to 9 years) and 73 adults (16 to 79 years) showed the only subgroup with significant preservation were children with genetic hearing loss. No other significant correlations were observed although the authors note the small sub-group sizes as a limitation (Zanetti et al, 2015). Another study of hearing preservation in a mixed group of children

and adults observed a high success rate of 92% hearing preservation, when using the (Balkany et al, 2006) method of preservation classification. They also showed that pre-implantation thresholds had no effect on the degree of preservation. Most surgeons in the study employed cochleostomy approach (Gautschi-Mills et al, 2019). There is a high degree of variability in study methods and approaches to analysis, which is problematic for cross-study comparisons. A standard for defining hearing preservation has been proposed to improve the reliability of such comparisons between CI centres (Skarzynski et al, 2013).

1.2.4 Application of steroids in cochlear implant surgery

Several studies have investigated the effect of steroid treatments on the intra-cochlear tissue response. For example, a recent study investigated the effect of electrode insertion depth and pre-surgery intra-venous steroids in 48 guinea pigs. They showed that deep insertions caused greatest intra-cochlear trauma and volume of fibrotic tissue growth, but this was reduced by steroid administration prior to surgery (Lo et al, 2017). A study using steroid eluting electrodes in guinea pigs showed significantly reduced intra-cochlear fibrosis which correlated with reduced electrode impedance (EI) levels. The authors note that EI, which reflects the ease of electrical current flow between electrodes, may be a surrogate measure of tissue development inside the cochlea (Scheper et al, 2017). Another study from the same research group demonstrated that steroid elution into the cochlea has a protective effect on SGNs (Wilk et al, 2016). The route of steroid application; systemic or topical can affect the outcome of the treatment. A study looking at hearing preservation after CI in a guinea pig model showed that topical application at the round window protected residual hearing. They found that the duration of application to give the desired result could be reduced if the concentration was increased from 2% to 20% (Chang et al, 2009). These findings are supported by a recent study comparing systemic, intratympanic and intracochlear application methods. Residual hearing was better preserved in the locally administered conditions (Lyu et al, 2018).

In a human study where the cochlea was perfused with the steroid triamcinolone, long-term EI levels were significantly lower in the treatment group compared to controls. The effect was still significant when measured 12 months after implantation. The authors speculate that the single dose of steroids may have reduced the initial inflammatory response which modulates the long-term behaviour of the developing fibrosis (De Ceulaer et al, 2003). This study supports the findings of (Scheper et al, 2017), providing support for the Guinea pig model. Other clinical studies of intra-operative steroids show high variability in methods of delivery, dose and duration, and as a result the findings are quite variable. One study assessed the efficacy of post-operative systemic steroids and found no significant difference between the steroid and control group (Tanamai et al,

2018). There is no clear consensus on the effectiveness of steroid treatment for improving CI outcomes in humans (Kuthubutheen et al, 2016).

1.2.5 Electrode array factors influencing performance variability

There are a range of different CI electrode arrays. Those manufactured by Cochlear range in length from 15.5mm to 25mm, MED-EL from 15mm to 31.5mm, Advanced Bionics 18.5mm to 20mm and Oticon Medical from 25mm to 26mm. The length of the basal turn is roughly 20mm. Depending on the desired tonotopic alignment of the array to the SGNs, a longer or shorter array may be selected. The manufacturers apply their own rationales to electrode design; Advanced Bionics arrays are relatively short and therefore designed to span the basal turn of the cochlea. MED-EL offer 10 array options, with the longest extending into the apical turn of the cochlea i.e. 31.5mm (Dhanasingh & Jolly, 2017). Electrode array types fall into three categories; straight lateral wall (LW) (Figure 1-2 Closed grey circle), pre-curved modiolar hugging (MH) (Figure 1-2 Open grey circle) and mid-scalar, which is designed to sit centrally in the scala tympani and is often considered to be a MH style. In selecting an appropriate electrode for a given individual patient, surgeons and clinicians aim to maximise tonotopic coverage and minimise distance between electrodes and SGNs while avoiding trauma to the fragile intra-cochlear structures. Modiolar hugging electrodes are designed to curve towards the modiolus and reduce the distance to the SGNs. This increases their effectiveness in stimulating the auditory nerve; however, their pre-curved shape limits their maximum insertion depth and increases the chance of translocation into the SVes. For this reason, LW electrode arrays are generally considered to be closest to the ideal electrode array (Dhanasingh & Jolly, 2017), and evidence suggests LW arrays give better hearing preservation outcomes (Snels et al, 2019). However, these electrode arrays may be more prone to partial extrusion (Rader et al, 2016). Ishai et al, (2017) demonstrated an asymmetry in growth of the fibrotic sheath around MH arrays with half-band electrode contacts compared to straight LW array with full-band electrode contacts. The ongoing medial force of MH electrode arrays along with the asymmetrical charge delivery seems to be associated with greater medial fibrosis. However, the long-term clinical outcome of these differences is unclear; the authors found no significant difference in speech performance between the two groups. The needs and constraints of an individual such as cochlear anatomy or abnormality, post-meningitis ossification and audiological needs may require an electrode array to be shorter than an average LW array.

The number of electrode contacts on an electrode array varies between manufacturer. MED-EL arrays have 12 electrode contacts, Cochlear arrays have 22 and Advanced Bionics have 16. Evidence shows that speech perception improves with increasing electrode number from 1 up to 10 beyond which, the performance level plateaus (Perreau et al, 2010). A key reason for the

plateau and a limiting factor of CI performance in general is size and number ratio between electrode contacts and a single neuron in the spiral ganglion. The target of stimulation, the SGNs are roughly a thousand times smaller than the electrode contacts and there are roughly a thousand times more SGNs than electrodes. This means that charge delivery spans a wide area of the tonotopic area of the cochlea, which limits the resolution of the pitch cue from place coding (Zeng, 2017).

Electrode array positioning and orientation can influence CI performance outcomes. A study using CT scanning alongside phoneme speech testing showed that poorer outcomes were associated with deeper electrode insertion and translocation of the array from the ST into the SVes. The authors suggest that the deleterious effects of poor electrode placement could be reduced by improved selection of cochleostomy site and insertion depth regulation, which would improve average speech performance levels (Finley & Skinner, 2009). Decisions to select particular electrode array types and implant by particular surgical methods requires knowledge of the individual patient's anatomy (Timm et al, 2018). This approach could be extended to other bio-measures such as genetics in the future when we understand more about the relationship between biology, hearing loss aetiology and hearing performance outcomes.

1.2.6 Cochlear implant adverse events

A small proportion of CI cases where poor performance leads to failure require revision surgery and are classified as adverse events (Chung, 2010). These have a significant cost in terms of patient well-being and economic losses for service providers and CI manufacturers. Adverse events fall into three categories; hardware failure (e.g. malfunction of the implanted device), medical failure (e.g. excessive trauma to the cochlea during implantation) or soft failure. Soft failure is associated with reports of undesirable symptoms such as reduced performance in speech recognition, poor sound quality, vertigo and/or somatic sensations. The current working definition of soft failure is indicated by a broad assessment battery that allows hardware and medical failures to be ruled out (Balkany et al, 2005). This leaves patients that present with a complex, non-uniform profile of symptoms. A study of the adverse events entered into the Manufacturer and User Facility Device Experience (MAUDE) database between 2000 and 2010 showed that the proportion of complex failures such as 'idiopathic gradual performance decrement' increased whereas hardware failures such as 'confirmed spontaneous device malfunction' decreased. This suggests that improvements in design and manufacture are reducing hardware complications, which results in a proportional increase in complex soft failures (Causon et al, 2013). A study of CI outcomes in a sample of 500 cases found a soft failure rate of 6%. Examples included electrode shifting and performance decrement (Venail et al, 2008). A

Chapter 1

retrospective review from 1979 to 2008 included approximately 1500 CI users and found 113 failures, 14 of which were soft failure (12.4%). The authors of this study speculate that immune derangement may be a common factor because 4 cases had a previous diagnosis of meningitis and 2 cases had history of asthma (Chung et al, 2010). A review of clinical outcomes of 487 CI users showed 4 individual cases of soft failure, 7 hardware failures and 9 medical failures (Sorrentino et al, 2009). Two case reports describe underperformance, extrusion and implant failure as a result of an increased inflammatory or proliferative (fibrotic) response to the electrode array (Nadol et al, 2008; Neilan et al, 2012). Examples of CI soft failure seem to highlight this importance of biocompatibility of electrode arrays with the cochlea and surrounding tissue.

1.3 Cochlear implantation provokes a tissue response

1.3.1 Investigations of the tissue response to cochlear implantation

Table 1-1 shows a summary of published studies of the human tissue response to CI. The studies span 30 years and document a wide range of methodologies and findings. They are all post-mortem investigations, often using tissue from an archive. A central question in this area of research has been the relationship between the implant factors such as surgery and the outcomes in terms of audiological performance and biological tissue response. The association of the tissue response and performance has also been investigated. Kawano (1998) showed that new bone formation around individual electrodes was correlated positively with psychoacoustic threshold and negatively with dynamic range. A study of 12 temporal bones from CI users implanted by cochleostomy showed fibrotic tissue and new bone growth in all cases. The volume of tissue correlated with damage to the lateral wall, but not with word recognition score (WRS) or SGN count (Li et al, 2007). Kamakura & Nadol (2016) found that the volume of new bone correlated negatively with WRS. The variability and contradictions in these studies may be due to the methodological differences between them. For example, Li et al (2007) showed no correlation between volume of new tissue whereas Kamakura & Nadol (2016) showed a negative correlation between volume and WRS. They both included a wide range of aetiologies and device types which increases the heterogeneity in the sample. (Li et al, 2007) notes that the lack of observed association between tissue and WRS could be either a true indication of a negative result or a reflection of the low sample size. The wide variability in CI performance creates a challenge for researchers aiming to recruit a sufficient large and standardised sample to achieve external validity.

The volume and type of newly formed intra-cochlear tissue can be affected by the surgical method of electrode insertion; cochleostomy, round window enlargement or direct round

window insertion. The former two, which involve drilling and cause a greater degree of cochlear damage, volume of fibrous and bony tissue than direct round window insertion. The differences between conditions is only observed in the basal regions of the cochlea near the site of implant insertion (Richard et al, 2012). This evidence argues for minimally traumatic surgical techniques to reduce the proliferative tissue response, although the studies linking this response to performance are limited in number and scope. Our understanding of the response and its many different profiles remains incomplete. However, there is evidence that disturbance to particular structures within the cochlea provokes a strong wound healing response. Damage to the basilar membrane, osseous spiral lamina and lateral wall are associated with higher volumes of new tissue growth, as is the translocation of the array into the SM and SVs (Kamakura & Nadol, 2016). A post-mortem analysis of seven temporal bones showed new bone and fibrosis universally and, in some cases, extending the whole length of array and beyond. Volume of fibrotic tissue and bone was greatest in cases where the electrode had rolled-over at the tip causing significant damage to the basilar membrane and lateral wall (Somdas et al, 2007).

Some of the studies shown in table 1-1 included quantification of the SGNs and their peripheral projections from Rosenthal's canal. One study showed that degree of damage to the main structures including spiral ligament, hair cells and SV was not associated with performance but SGN count was correlated positively with WRS (Fayad & Linthicum, 2006). There is evidence that relatively few SGNs are sufficient for sentence recognition of >80% (Gassner et al, 2005). Fayad and Linthicum (2009) performed post-mortem analysis of 10 temporal bones. They showed a significant negative correlation between volume of new tissue in the basal turn and SGN survival. The same authors demonstrated that SGNs are quite robust; a complete loss of hair cells and supporting cells is not associated with proportional SGN loss. They conclude that poor CI performance following prolonged deafness is not due to ongoing degeneration of SGNs (Linthicum & Fayad, 2009).

Clark (2014) performed a post-mortem analysis of tissue following long term CI use in a single user who had been implanted with a prototype CI in 1978, CI22 in 1983 and CI24 in 1998. The latter two arrays both remained in cochlea together, i.e. CI22 was not fully explanted. Histological analysis showed fibroblasts around the lead-wire and adherent to the magnet and surrounding capsule. There was an 85-90% SGN reduction. Both arrays were surrounded by 40-60um thick fibrous connective tissue with active fibroblasts and some heterotopic bone. Microscopy showed dark particulate material thought to be platinum within macrophages. The electrode surfaces showed signs of corrosion and energy-dispersive (EDS) spectroscopy showed peaks for platinum bound to oxygen, sodium, potassium, and calcium. This study provides a rich insight into the

Chapter 1

material and cellular changes around the electrode, although it might be considered an outlier case taking into account the long history of multiple electrodes.

Another post-mortem analysis of temporal bones included 28 cochleae from 21 donors. This is a relatively large sample although it included a range of ages (57 to 92 years), aetiologies (including Meniere's, acoustic neuroma and temporal bone fracture) and devices (mostly Cochlear but some Advanced Bionics devices). In one of the cases they noted "many eosinophils with bilobed nuclei and cytoplasm filled with large red refractile granules can be recognized". Previous studies have not reported eosinophil infiltration, which may indicate a Type-1 hyper-sensitivity mediated by Ig-E. A granulomatous reaction was very common (17/28 cases). Eosinophil infiltrate was observed in 7 cases and lymphocyte infiltration in 25 cases. Using their scoring system, the base showed a significantly greater inflammatory reaction; as indicated by more FBGCs, lymphocytes and eosinophils. All but one showed FBGC formation (Seyyedi & Nadol Jr, 2014).

This evidence taken together with that from other implanted biodevices suggests that FBGC formation is a common, if not normal reaction. The fact that some cases of device failure are also referred to as foreign body reactions (Xin et al, 2015; Lim et al, 2011; O'Leary et al, 2013) can complicate the overall picture. Although FBGCs are observed in cases of frank allergic reactions associated with complete failure, they are also seen in most histological analyses of patients where no device failure occurred. It seems that the ambiguity arises from the overlapping terminology of 'foreign body'. All foreign body allergic reactions involve FBGCs but not vice versa. The FBR can be variable in its type and severity, depending on the material, surgical factors and the individual (Christo et al, 2015)

Table 1-1: Literature review of investigations of the cochlear wound healing response following implantation

RW = Round window, SEM = Scanning electron microscopy, SGN = Spiral ganglion neurones, EDTA = Ethylenediaminetetraacetic acid, H&E = Haematoxylin and eosin, PTA = Pure tone audiometry, TB = Temporal bone, SV = Stria vascularis, BM = Basilar membrane, WRS = Word recognition score, PCR = Polymerase chain reaction, FBR = Foreign body reaction, FBGC = Foreign body giant cell, EDS = Energy-dispersive X-ray spectroscopy, M = Macrophage, Pt = Platinum, ST = Scala tympani, SM = Scala media, SVes = Scala vestibuli, AB = Advanced bionics, SL = spiral ligament, UoM = University of Melbourne, XFM = X-ray fluorescence microscopy

| Author | Number | Age (life duration) | Age at implant | Implant duration | Aetiology | Device | Surgery | Aim | Method | Finding |
|----------------------|--------|---------------------|----------------|------------------|------------------|---------------------|------------|--|--|--|
| (Clark et al., 1988) | 1 | 59 | 57 | 2 years | Meningitis at 15 | Cochlear Nucleus 22 | RW drilled | Assess safety of CI procedures. 1) Histological analysis. 2) SEM analysis of electrode surface. 3) Histological analysis of auditory brain. Limitation that control ear shows significant changes due to meningitis. | Placed in 10% formalin fix for transport. 24 hrs later, cochleae infused with cold 2%: 10% glutaraldehyde-formaldehyde solution. Submerged for 12hrs. X-rays taken. Decalcified using EDTA. Stapes removed and apex pierced to facilitate infiltration of Spurr's resin (highly penetrative embedding medium). Sectioned at 2µm. Stained with toluidine blue (for nuclei and general sharpening) and H&E for light microscopy. | Cochlea histology findings: Extra-cochlear electrode showed mesothelial lining surrounded by mature fibrous with some areas of macrophages, plasma cells and occasional lymphocytes. Intra-cochlear electrode showed that lymphocytes and plasma cells had not extended into the cochlea. Electrode lined with mesothelial cells with some fibrinoid material and occasional giant cells. Sheath 0.05 mm thick. Areas of bone formation with 12 mm from RW. Bone was trabeculated with loose fibrous tissue in the spaces. |

Chapter 1

| Author | Number | Age (life duration) | Age at implant | Implant duration | Aetiology | Device | Surgery | Aim | Method | Finding |
|----------------------|--------|----------------------------|----------------------------|--|---|---------------------|-----------------------|--|---|--|
| (Nadol et al, 1994) | 1 | 62 | 62 | 10 weeks (no stimulation) | IV gentamycin therapy | Richards Ineraid | Not stated (assume C) | To compare tissue changes and SGN number between implanted and non-implanted ears | Temporal bones formalin fixed. EDTA decalcification. Araldite embedded. Microtome sectioned (35 µm) with tungsten carbide blade for 3D reconstruction. Selected sections were remounted, and glass knife sectioned (5 µm) and toluidine blue stained for microscopy. SGN density calculation. | Significant disruption of basilar membrane, spiral ligament, SV and Reisner's membrane in basal turn of implanted ear only. SGN count significantly reduced for both implanted and non. |
| (Kawano et al, 1998) | 5 | 74 59 76 20 64 | 71 57 68 19 59 | 3 years 2 years 8 years 1 year 5 years | Unknown Meningitis 40 Otosclerosis 20s Juvenile arthritis Mastoidectomy | Cochlear Nucleus 22 | Cochleostomy | Correlate the psychophysical threshold, comfortable level and dynamic range with spiral ganglion cell survival, presence of fibrous tissue and/or new bone, and distance between the centres of the electrode bands and Rosenthal's canal. | Assume arrays were removed before tissue archived. 3D reconstructions. EDTA, Celloidin embedded, sectioned at 20-30 µm, Selected sections every 100-135 µm stained with H&E. Electrode array position taken from post-op X-ray overlaid onto digital model. One exception embedded in Spurr's resin and sectioned at 2 µm. This case from (Clark et al, 1988) | Threshold levels correlated with presence of newly formed intra-cochlear tissue, especially bone. Distance from electrode contacts to modiolus increased with level of fibrous tissue. SGN count was negatively correlated with level of fibrous tissue. |

| Author | Number | Age (life duration) | Age at implant | Implant duration | Aetiology | Device | Surgery | Aim | Method | Finding |
|-----------------------|--------|---------------------|----------------|------------------|-----------------------------------|---------------------|--------------|--|--|---|
| (Gassner et al, 2005) | 1 | 84 | 77 | 7 | Progressive SNHL unknown cause | Cochlear Nucleus 22 | Cochleostomy | Assess the relationship between audiological performance pre and post implant and histological analysis of the cochlea and SGNs. | Audiological measures acquired in clinic at 6 and 60 months. Pre-op and post-op PTA and speech (sentence). Fixed 10% formalin, EDTA, Celloidin embedded. Sectioned at 25 μm . Every 10 th section H&E stained. SGN quantification performed using Schuknecht (1993) 2D model method. | Small number of surviving SGNs. No hair cells. Bone around entry blocking cochlear duct. Fibrous sheath around electrode sheath. Degeneration of organ of corti and spiral ganglion. This was true for control also, albeit to a slightly lesser extent. Significant difference in speech performance between HA < CI. Sentences >80% with CI only or binaural. |

Chapter 1

| | | | | | | | | | | |
|---------------------------|--|-----------------------------|---------------|---------------------------|--|---|--------------|---|--|---|
| (Fayad & Linthicum, 2006) | 14 TBs from 13 patients (8 had non-implanted contralateral for comparison) | Mean 68.6 (range 41.9-87.1) | All >40 years | 12-year mean (1-40 range) | 8 unknown, 3 hereditary, 1 otosclerosis, 1 Meniere's | 11 Nucleus 22. 1 Nucleus 24. 1 Ineraid. 1 Clarion. | Cochleostomy | To determine the relationship of surviving neural elements to auditory function in multichannel cochlear implant temporal bones | Performance measured as word and sentence scores. 6 and 12 month and most recent where available. Some had data missing so highest score used in analysis. Performance ranked: Poor, fair, good, excel. Fixed in formalin for 1 month then electrodes removed. EDTA decalcified, celloidin embedded. 20 µm sections, stained with H&E. SGN % relative to expected num. Peripheral process % relative to osseous spiral lamina thickness. Spiral ligament % of normal compared to total. SV % remaining compared to distance from spiral prominence to Reisner's membrane. HCs done by counting in modiolar and perimodiolar sections. All done in basal, mid and apical cochlear regions. Counts (cells with nuclei only) done using every tenth grid section. Used Schuknecht (1993) 2D model method. | Some SGN survival in all TBs even though hair cells and peripheral processes are absent. Performance unrelated to % remaining normal structures (eg spiral ligament, SV, hair cells, and spiral ganglion cells). SGN count in segments III and IV negatively correlated with word score. No difference in SGN count implanted vs non-implanted TB except Segment 1 where implanted < non. |
|---------------------------|--|-----------------------------|---------------|---------------------------|--|---|--------------|---|--|---|

| Author | Number | Age (life duration) | Age at implant | Implant duration | Aetiology | Device | Surgery | Aim | Method | Finding |
|---|----------------------|---------------------|----------------|------------------|--|--|--------------|---|--|--|
| (Li et al, 2007) includes 7 TBs from (Somdas et al, 2007) | 12 patients (12 TBs) | Mean 76 (64 – 94) | Mean 67 | Mean 9 | Genetic, Meniere's, Acoustic neuroma, Otosclerosis, Immune mediated, Ototoxicity. Several unknown. Excluded Meniere's. | 1 Nucleus contour, 1 Nucleus 24, 7 Nucleus 22, 2 Ineraid, 1 Clarion. | Cochleostomy | Evaluate new bone and fibrous tissue after CI | Excluded patients with bone/fibrosis related aetiology (although included otosclerosis). Performance measured as word scores at the latest available clinical session. All >30 at age of implant. Fixed 10% formalin, some had array removed, EDTA. Array in-situ = embedded in Araldite. Array removed = embedded in celloidin. Every 10 th section was mounted. Celloidin slides were H&E stained, Araldite slides were toluidine blue. 2D (Schuknecht, 1993)(for counting cells) and 3D (for calculating volume) reconstruction. | New bone and fibrous tissue all 12. Sig. correlation between damage to lateral wall and volume of tissue. Vol of tissue did not correlate with WRS or SGC count. |

Chapter 1

| Author | Number | Age (life duration) | Age at implant | Implant duration | Aetiology | Device | Surgery | Aim | Method | Finding |
|----------------------|--------|---------------------|-----------------------------|----------------------------|---|--|--------------|--|--|--|
| (Somdas et al, 2007) | 7 TBs | Mean 56 | Mean 63.3 (Range: 30-76) | Mean: 7.3 (Range: 1-17) | Mix: Genetic, Meniere's, Acoustic trauma, Otosclerosis, immune mediated and unknown | Nucleus Contour, Nucleus 24, Nucleus 22, Clarion, Ineraid. | Cochleostomy | Analyse new bone and fibrous tissue in implanted cochlea | Fixed in formalin, decalcified in EDTA. Electrodes left in-situ, fixed in osmium tetroxide, dehydrated in graded alcohols, exchanged with propylene oxide, embedded in araldite. Axial (horizontal) sections 20 µm. As described by Nadol 1994. Both 2D and 3D reconstruction (latter using Amira). Digital images taken at x1.25 under light microscope | New bone and fibrous in all 7 cases, particularly at cochleostomy site. Tissue extends to various lengths (mostly basal and apical but 2 just basal) along array, sometimes beyond (2 cases). Bone and fibrous tissue evident in SV in cases where BM pierced, or electrode inserted into SV. Lower surgical trauma gave lowest amount of new tissue. Most tissue seen in case where electrode folded back on itself. Trend of more new bone in cases of longer CI duration. 1 case does not follow pattern (low duration/ high bone) although this case had 2 surgeries so maybe more trauma. |

| Author | Number | Age (life duration) | Age at implant | Implant duration | Aetiology | Device | Surgery | Aim | Method | Finding |
|---------------------|--|--|-------------------------|-------------------------------------|---------------------------------------|--|--------------|---|---|---|
| (Nadol et al, 2008) | 1 post soft failure- Bilateral CI. 8 other cases | Case: 71 years. Others: Years 80 years | Case:58 Others: Mean 72 | Case: 13 years Others: Mean 8 years | Case: Probable genetic cause. Others: | Case: Nucleus 22 Others: 1 Clarion, 1 Nucleus 24, 6 Nucleus 22 | Cochleostomy | Compare tissue correlates of soft failure to several control cases. | Performance measured as detailed and frequent threshold and comfort levels. Sentence scores given for R ear at 8 and 12 months. Formalin fixed, CT scan, EDTA decalcified, Celloidin embedded, sectioned 20 µm, every 10 th section H&E stained for 2D reconstruction. PCR and mycobacteria histology. | Delayed hypersensitivity reaction most likely. Occurred bilaterally. FBGC and monocytes in most of the 8 other cases. Difficult to distinguish the mechanistic differences between standard FBR and this failure showing strong necrosis. Assays negative for mycobacteria. |

Chapter 1

| Author | Number | Age (life duration) | Age at implant | Implant duration | Aetiology | Device | Surgery | Aim | Method | Finding |
|---------------------|---------------------|---------------------|----------------------------|----------------------------|----------------|---|--|---|---|--|
| (Fayad et al, 2009) | 10 TBs (8 patients) | Not documented | Mean 69 (range: 48.3-83.8) | Mean 6yrs (range 0.9-12.9) | Not documented | 7 Nucleus 22 1 Nucleus 24 1 Ineraid 1 House single | 3 Coch 2 Coch revision 4 RW 1 RW revision | Relate new bone and fibrosis to survival of neural elements (extend 2006 study) | Same 3D software reconstruction as Li 2007 and Somdas, 2007. EDTA 8-12 months, celloidin processing then 20 µm sections, every 10 th section H&E stained. Segmentation according to Otte et al 1978. Analysed as segments but also as basal vs apical. For SGN count: slides containing cells were selected. Only count cells with nucleus. Used ocular mounted grid x200 mag. Corrections for 10 th section and double counting (cells at section boundary). % survival relative to normal 25000 in base and 10000 in apex. 3D recon used Amira software. Images taken at x10 mag and scale added using photoshop. Label tool used to discriminate anatomical detail manually. | No sig relationship between duration of implant and amount of new tissue. Sig relationship between new tissue and survival of neural elements only in segment I. New tissue mainly in seg I & II. Little to none in seg III. None in IV. High degree of variation across analysed bones. Sig negative correlation SGN count and total new tissue in seg I (non sig trend for same thing in other segs). Base vs Apex showed almost all of new tissue formation in former. No HCs or peripheral projections survived in basal. No sig difference in total tissue between RW and cochleostomy. |

| Author | Number | Age (life duration) | Age at implant | Implant duration | Aetiology | Device | Surgery | Aim | Method | Finding |
|-----------------------|--------------------------------------|---------------------|----------------|------------------|---|---|-----------------------|--|---|--|
| (Richard et al, 2012) | 12 TBs (5 cochleostomy, 4 ERW, 3 RW) | Mean 76 | 67 (52 – 84) | 9 (<1 – 25) | Excluded meningitis to avoid confound of earlier osteogenesis | 5x nucleus 22 5x House/3M 2x House Urban | Cochleostomy, ERW, RW | Compare cochleostomy, round window enlargement and RW. | Fixed in formalin for 1-month, decalcified EDTA several months, alcohol dehydration then into celloidin. Cleared with cedar wood oil. Stained with H&E. 20 µm sections mounted. Amira 3D software reconstruction. | RW fibrosis was areolar whereas RWE and cochleostomy was dense fibrosis or bone. RWE had sig more bone than others. Overall RWE > Cochleostomy > RW. Stats limited by heterogenous mixture of devices and surgeries. Low N. Single electrode devices used in RW cases- now obsolete. |

Chapter 1

| | | | | | | | | | | |
|---------------------|---|----|--|----|--|--|--|--|---|---|
| (Clark et al, 2014) | 1 | 76 | Initial implant 46 years old. Left cochlea implanted with prototype CI in 1978, CI-22 in 1983 and CI-24 in 1998. | 30 | head injury which led to a left occipital extradural haematoma requiring a craniectomy | University of Melbourne prototype, Nucleus CI 22, Nucleus 24 | Cochleostomy in the region of the round window | Analyse TB of first patient to receive multichannel CI | <p>Left prototype CI in 1978, CI-22 in 1983 and CI-24 in 1998. 6 electrode bands left at CI22 explant. CI-24 electrode inserted alongside.</p> <p>X-rays during life. X-ray micro CT post-mortem.</p> <p>TBs in 10% neutral buffered formalin. EDTA, celloidin embedded, axially sectioned at 20µm. Sections of interest were also stained with Gomori's trichrome and Luxol Fast Blue. 3D reconstruction using Amira.</p> <p>Tissue containing CI-22 bands reprocessed-stained using H&E and Trichrome. Treated with picric acid to exclude formalin pigment, stained with Perl's stain, excluding haemosiderin as the cause of dark particulate material around the electrode sheaths. Bands were then extracted and tissue re-processed (H&E etc).</p> <p>SEM with EDS with particulate analysis</p> | <p>Fibroblasts observed along the cord from array to receiver and also adherent to magnet and in surrounding capsule. 85-90% reduction in SGNs.</p> <p>Both CI-22 and CI-24 electrodes were surrounded by 'fibrous connective tissue sheath' 40-60um thick. Also, active fibroblasts and some small regions of heterotopic bone. Also, dark particulates within macrophages, thought to be pt. Surface of electrode contacts show signs of corrosion. EDS indicates peaks for Pt bound to O_{1s}, O_{2s}, (oxidation) Na, K, Ca</p> |
|---------------------|---|----|--|----|--|--|--|--|---|---|

| Author | Number | Age (life duration) | Age at implant | Implant duration | Aetiology | Device | Surgery | Aim | Method | Finding |
|----------------------------|--------------------|---------------------|----------------|------------------|---|------------------------|--------------|---|---|--|
| (Nadol et al, 2014) | 7 TBs (5 patients) | 75 (71 – 91) | 61 (47 – 81) | 14 (10 – 21) | Mix: Skull fracture, familial HL, Menieres, | Nucleus 22 and 24 | Cochleostomy | Characterise cellular response and any particulates from metal. | Same as Nadol 2008. Then specific antibody process for B-cell lymphocytes (CD20), T-cell lymphocytes (CD3) and macrophages (CD68). Also, EDS-SEM for metal particulates | B-lymphocytes and T-cells in the fibrous sheath. FBGCs (CD68+) at interface between fibrous sheath and electrode track. Macrophages (CD68+) found in the sheath containing particulates. Analysis shows particulates in M are Pt. SEM shows pitting on electrode surface. |
| (Seyyedi & Nadol Jr, 2014) | 28 TBs (21 pts) | 78 (57 – 92) | 67 (48 – 82) | 11 (1 – 23) | Mixed incl. Meniere's, AN, fracture | Most nucleus. Some AB. | Cochleostomy | Characterise tissue response | Fixed in 10% formalin, decalcified in EDTA, Electrode removed, Celloidin embedded. Sectioned at 20 µm. Every 5 th slide stained with H&E. 2D reconstruction Schuknecht segmenting system used. Matlab used to calculate lengths of cochlear duct, Rosenthal's canal and array insertion. Tissue response assessed (for fibrosis, bone and various cells types) at cochleostomy, midway along array and tip of array. Each variable scored using a severity grading system. | 27 TBs show granulomatous reaction, Eosinophil infiltrate in 7 tb, inflammation significantly stronger in basal turn. True for cellular response and new bone/fibrosis development. Overall, the cellular response is more pronounced than previously thought. 25% show evidence of Type-I allergic reaction. No correlation between amount of tissue development and duration of implant. |

Chapter 1

| Author | Number | Age (life duration) | Age at implant | Implant duration | Aetiology | Device | Surgery | Aim | Method | Finding |
|--------------------------|---|---------------------|----------------|------------------|---|-----------------------------|--------------|--|--|--|
| (Kamakura & Nadol, 2016) | 17 TBs (Assume 17 patients. Not stated) | 82 (57 – 96) | 72 (47 – 91) | 11 | Genetic, Presbycusis, Mondini deformity, Otosclerosis, Otitis media, Sudden idiopathic, Meniere's | Mix: Nucleus and AB devices | Not reported | Evaluate new bone and fibrous tissue and assess correlation with WRS | Excluded aetiologies involving neo-osteogenesis. Performance measured as the last-available CNC word score. (average score: 40%, average age of test: 79) Fixed in 10% formalin, Decalcified in EDTA, Electrode array removed. Embedded in celloidin. Sectioned at 20 µm. Every 10 th slide stained with H&E. 2D reconstruction using Schuknecht segmenting method. 3D reconstruction using Somdas 2007 method Amira. Calculations of volumes as % to correct for individual variability. | New bone and fibrosis in all cases. Not always in scala M and V. WRS +ve correlation with SGC count and –ve correlation with new bone and length of electrode in SM, SVes and SL. WRS –ve correlation with volume of new bone in ST, SM and SVes, cochlea. (but not correlated with fibrosis) Amount of bone in SM/Ves correlated with BM damage, the total of the lateral cochlear wall and osseous spiral lamina and the total damage score. Length of electrode in SM/Ves and SL correlates with damage BM, lateral wall. |

| Author | Number | Age (life duration) | Age at implant | Implant duration | Aetiology | Device | Surgery | Aim | Method | Finding |
|----------------------|---------------|---------------------|---|------------------|---|---|--|---|---|--|
| (Spiers et al, 2016) | 1 | 76 | Initial implant 46 years old. Left cochlea implanted with prototype CI in 1978, CI-22 in 1983 and CI-24 in 1998. Same case as (Clark et al, 2014) | 30 | head injury which led to a left occipital extradural haematoma requiring a craniectomy | University of Melbourne prototype, Nucleus CI 22, Nucleus 24 | Cochleostomy in the region of the round window | Assess particulate material in the fibrous capsule. | Tissue processing as (Clark et al, 2014) Alternate slice used for X-ray fluorescence microscopy (XFM, Synchrotron X-ray source) or stained with Masson's trichrome. | 100µm sheath around UoM and CI 22, 40-60 µm sheath around CI 24. Osteoid material around CI 24. Dark particulate matter in sheath around UoM and CI 22. Identified as Platinum. Platinum has infiltrated the spiral ligament |
| (Ishai et al, 2017) | 7 TBs (6 Pts) | 82 (64 – 94) | 72 (56 – 86) | 10 (2 – 24) | Progressive sensori-neural, sudden sensori-neural, Genetic, Meniere's, Acoustic trauma. | x3 AB Clarion CII (perimodiolar array, half band) x4 AB HR90K (perimodiolar array, half band), x4 Nucleus 22 (straight array, banded), x1 Nucleus 24 (straight array, banded) | Cochleostomy and round window insertion | Investigate patterns of fibrous tissue around different array types to determine cause. Test correlation between thickness and performance. | EDTA, Celloidin embedded, 20µm sections, H&E stain of every 10 th slide, imaged using light microscopy, reconstructed using Schuknecht technique | No correlation between surgery type and sheath thickness. AB showed thickest sheath medially. Nucleus showed equal thickness. Medial sheath sig thicker in AB than nucleus. BM displacement and OSL fracture much more common in AB than Nucleus |

1.3.2 Methodological comparisons from Table 1-1

Table 1-1 presents a chronological overview of several studies from 1988 to 2017. One of the challenges of extracting themes from these studies is the variability within and between them. They range from single case to larger group studies, with the latter type including a heterogeneous mix of patients, hearing loss aetiologies, age at implant, duration of and CI devices. The majority of the group studies are retrospective analyses of archival temporal bone tissue, which prevents any real-time clinical decision making at the time of performance fluctuation. A common limitation of such studies is the generalisability of the findings when they are based on low sample size (Richard et al, 2012). Even in a case of a relatively large sample, like (Seyyedi & Nadol Jr, 2014), which included 28 temporal bones from 21 donors, the data is too sparse to reach normal distribution to allow parametric analysis. A common technique for parsing the findings down to manageable quantitative data is counting of cells such as HCs and SGNs. This means that the data validity will depend on the thoroughness of the tissue processing and analysis procedures. Many of the studies use an elegant method of reconstructing imaged sections of the cochlea tissue in 2 dimensions, which provides useful standardisation across studies (Schuknecht, 1953). Several of the studies in table 1-1 were carried by or in collaboration with Joseph Nadol at Harvard University, who has refined techniques of temporal bone analysis over the course of many years. One particular study introduced a grading system to categorise tissue trauma following cochlear implantation and demonstrated general mastery over methods of cochlear tissue analysis (Seyyedi & Nadol Jr, 2014).

The methods used to process tissue samples are mostly standard across studies shown in Table 1-1; Tissue fixation was performed using 10% buffered formalin, decalcification in ethylenediaminetetraacetic acid (EDTA), embedded in celloidin and sectioned using a microtome at 20 μm . The majority of studies used haematoxylin and eosin (H&E) to stain the tissue sections to be viewed under light microscopy. This combination of stains predominantly highlights cell nuclei, extracellular matrix and cytoplasm. Although it is the most commonly used histological stain and widely considered the gold standard in pathology diagnoses it provides no molecular or cellular specificity. The method used by (Nadol et al, 2008) was extended to include immunohistochemical techniques of staining using antibodies for B-cell and T-cell lymphocytes and macrophages (Nadol et al, 2014). Another development in methods is the introduction of 3-dimensional reconstruction of the cochlea using specialist software, Amira. (Somdas et al, 2007)(Fayad et al, 2009) both employ 3-dimensional modelling in addition to the traditional 2-dimensional method (Schuknecht, 1953). The combined approach allows cell counting and volume calculations, although the latter is somewhat inferred because the input images are taken

Chapter 1

every 10th slide for efficiency (Kamakura & Nadol, 2016). Imaging techniques such as μ CT and cone-beam CT are now available and allow 3-dimensional modelling of the implanted cochlea with better spatial resolution than scanned slides. This technique has been demonstrated in one of the post-mortem studies listed in Table 1-1 (Clark et al, 2014). The missing link in these methods is the correlation of spatial coordinates of specific cells from histological slides and μ CT. This is a new technology developed at The University of Southampton; it allows non-destructive high-resolution imaging of embedded tissue samples before they are sectioned and immunostained in a standard histological workflow (Katsamenis et al, 2019).

The studies discussed here are post-mortem histological investigations of cochleae from donated temporal bones. The method involves decalcification of the bone, embedding of the tissue, sectioning into thin sections before staining and visualisation using light microscopy and software reconstruction. The limitation of such studies is that they reveal the state of intra-cochlear tissue at the end of life after many years of CI use. The question remains, what is the real-time dynamic of the electrode-tissue interface in living CI users? The vast majority of histology studies discussed here used archival temporal bone tissue. Any detailed ongoing clinical measurements from patients during life were limited due to the retrospective design of the studies. By widening the scope of clinical measurement and improving the resolution of the recorded clinical data we will increase the chance of mapping the temporal dynamics of performance onto any tissue analysis, post-mortem or otherwise.

Two of the studies investigated tissue response in cases where there had been soft failure: (Nadol et al, 2008) and (Neilan et al, 2012). In both cases, the failure was found to be associated with granuloma.

1.3.3 Studies of the tissue response and performance outcomes

CI performance is not accurately defined. At the broadest level, performance is a collection of measures and descriptors including the user's self-report of sound quality (Balkany et al, 2005). Studies reviewed by (Schaefer et al, 2017) found a wide range of hearing and speech perception outcomes being used in publications from 2015. The specific tools used to make the measurements, as well as the timing of tests were administered were highly variable. It is important to be mindful of the fluctuating nature of performance, especially when considering cases which reach failure in the future. Better understanding the of interdependence of hearing performance and the CI tissue response requires standardised clinical data capture paired with histochemical tissue analysis where possible. Figure 1-3 shows clinical measures of CI performance from post-mortem studies of temporal bones from CI users. The findings of the

tissue analyses are presented in Table 1-1. Due to the retrospective design of the studies, the clinical data is sparse with little standardisation across them. The figure highlights the wide range of different clinical measures included in the different studies. This creates a challenge for cross-study comparisons or determining a consensus. In cases where an arrow symbol is used, the study included the last available clinical data before death. This means that measures were captured at vastly different time points for each individual included in the calculation of the mean result. Overall the table highlights sparsity and lack of reliable measures of CI performance in studies of the CI-tissue interface. This research need is the focus of the present study, which combines a rich dataset of impedance telemetry, with histochemical and immunohistochemical tissue analysis.

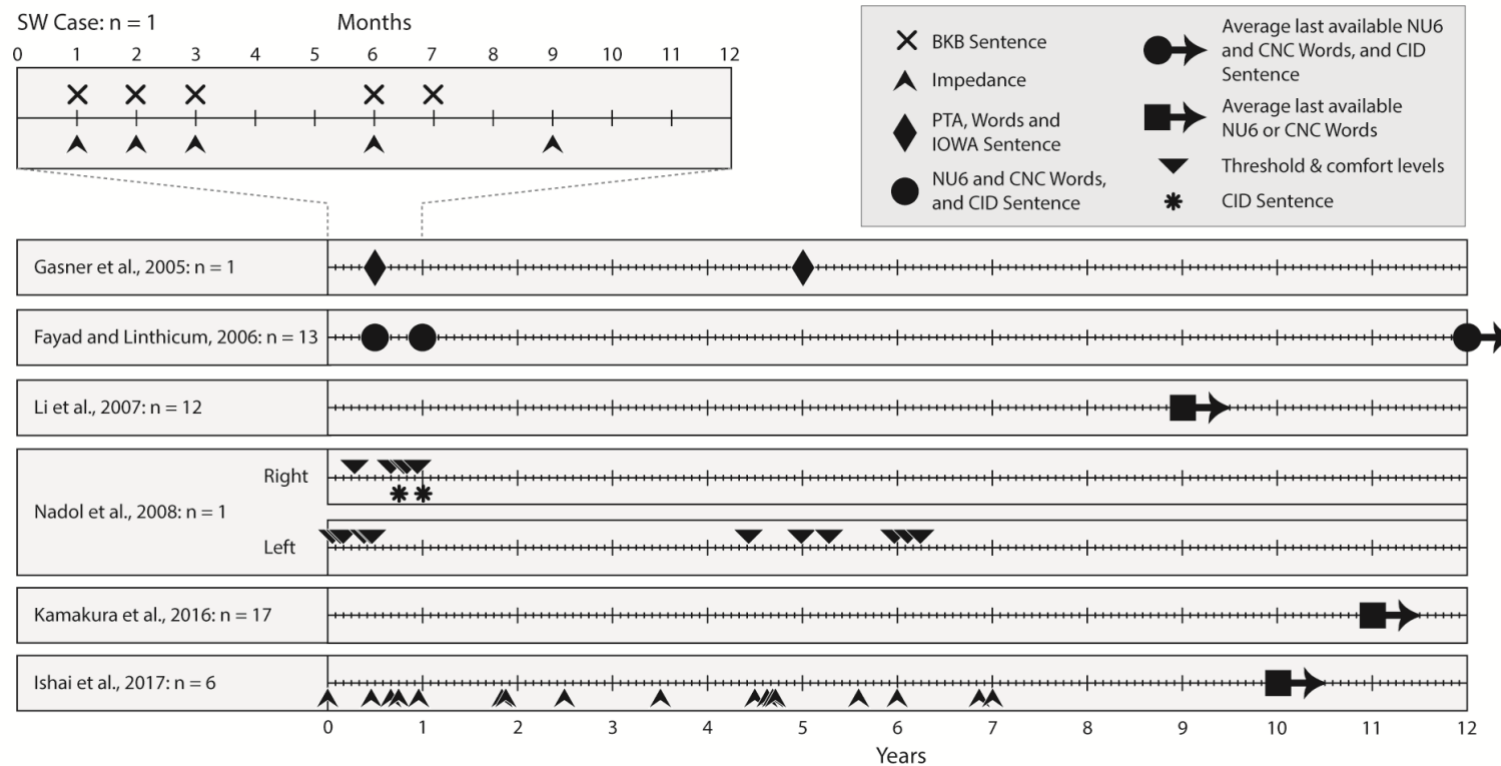


Figure 1-3: Performance measures from the present case study (SW) compared to other retrospective studies of performance and cochlea histology

Studies are a mixture of case study (n =1) and group study (n = 6 – 17). The experimental detail of the studies is shown in Table 1-1. The key shows the wide variation in clinical measures used in the studies. In cases where the symbol indicates “average last available” score (symbols with an arrow), the value may represent significantly different time points depending on the individual user’s age and CI duration. Top-left panel presents the clinical data captured in the present case (Patient SW). This shows the BKB test and EI measure spanning the first year.

1.4 Three approaches to measuring the tissue response to cochlear implantation

Severe to profound sensori-neural hearing loss can be caused by a range of different inherited or acquired conditions with distinct underlying pathophysiology. Whether the locus of dysfunction is the SV, hair cells, synapses or gap junctions expressed throughout the cochlea, the outcome is a loss of transduction of the acoustic signal into electrical impulses in the auditory nerve. By stimulating the auditory nerve directly, the CI can bypass the loss of function to allow deaf individuals access to verbal communication, music and environmental sound. The CI is widely considered the most successful neuro-prosthesis; many users are able to achieve 100% scores on word recognition tests. However, not all users experience optimal auditory performance. Investigation the complex factors that influence performance is an active area of research including clinical and laboratory studies, computer modelling and animal studies.

Pre-implant factors, which have been shown to influence performance are hearing threshold levels in the better ear, duration of deafness, use of hearing aids. It is thought that neuroplastic changes due to auditory deprivation affect auditory processing to reduce auditory performance with a CI. Age has also been shown to a factor. Although the effect is not linear across an individual's life, being implanted at a younger age is generally associated with better outcomes. The most extreme example of this is individuals who are deafened pre-lingually i.e. new-borns with congenital hearing loss; it is imperative that they receive auditory rehabilitation using hearing aids and/or implantable hearing devices as early as possible. Auditory performance is affected by cognitive factors and pre-implant hearing ability. For example, an individual with a favourable score on speech testing when listening acoustically, is more likely to have optimal performance with the CI. Finally, there is some evidence that specific aetiologies are associated with better CI performance. Sensori-neural hearing loss caused by mutations in the gene for connexin 26 have better outcomes than other hearing aetiologies, especially those associated with syndromes.

Surgical factors have also been shown to influence CI performance outcomes. It desirable to preserve low frequency hearing threshold levels because acoustic hearing can be utilised electro-acoustic stimulation and also because preserved hearing reflects cochlear health. Damage to specific cochlear structures such as the osseous spiral lamina following electrode insertion can lead to excessive fibrosis and ossification and is generally associated with poorer long-term performance outcomes. Atraumatic methods known as 'soft surgery' are now applied to minimise such occurrences. Insertion of the electrode via the round window rather than through a drilled

Chapter 1

cochleostomy has been shown to result in lower levels of tissue growth. However, there is no clear evidence that the difference is reflected in performance outcomes. In fact, in some cases where the round window is obscured, a drilled cochleostomy is necessary for accurate positioning of the array into the scala-tympani. Existing studies are retrospective and have heterogeneous sample groups. Prospective RCT studies are needed to better control sources of variation measure the actual effect of insertion method. Application of steroids is also part of the soft surgery approach and can reduce intracochlear fibrosis and EI. This approach is proven to be effective in animal studies and there is some suggestion of long-term effect in humans eg EI. However, studies show no evidence of long-term improvement in auditory performance with a CI.

The physical characteristics of the electrode array may also influence performance outcomes. They are available in a range lengths, thicknesses, stiffness and number of electrode contacts. Studies comparing them show no significant difference although each type may be better suited to an individual's anatomy. Curved MH arrays have the benefit of positioning the electrodes nearer the SGNs, but they exhibit a slightly higher rate of translocation into the SM and SVes than LW arrays. LW arrays seem to be associated with lower levels of intra-cochlear trauma although they exhibit higher rates of extrusion. There is no clear evidence that one design is better than the other. Prospective RCT studies are needed to investigate the difference more carefully than existing retrospective comparisons.

The pre-implant, surgical and electrode array factors discussed here can influence CI performance but only account for about 20% of individual variability. Further investigations are needed at each level of the auditory pathway from cochlea to the higher CNS to understand more about variability in CI performance. The CI-tissue interface in the cochlea has been shown to vary across patients in post-mortem studies. As shown in Figure 1-3, the existing studies of the relationship between the interface and performance outcomes leave a gap for further investigation. New research findings could direct interventions such as optimisation of stimulation strategy and guide the use of anti-inflammatory drugs. Characterisation of the molecular and cellular mechanisms of the wound-healing response to CI will facilitate efforts to understand performance variability and reduce the incidence of poor performance and soft failure.

This thesis presents three approaches to measuring and analysing aspects of the CI-tissue interface which translate from basic research to clinical application. The work was carried out between the University of Southampton faculty of Medicine and the University of Southampton Auditory implant Service (USAIS).

1.4.1 Histochemical analysis of human fibrotic tissue from an explanted CI

The current understanding of the tissue response following cochlear implantation is taken from post-mortem studies. A planned CI explant procedure presented an opportunity to investigate the tissue developing around the electrode array in a patient experiencing migration related failure. Histochemical analysis of the fibrotic tissue from this single case formed the basis of the observational study. Based on knowledge gained from the studies outlined in Table 1-1, the following research questions were asked.

1. What is the overall composition and organisation of the tissue?

The clinical measurements and X-ray CT imaging showed rapid electrode array migration. In order to investigate the cellular causes or correlates of the migration, the following research questions were asked.

2. Is the composition and organisation spatially variable?
3. Do the cell types, phenotypes and ECM structure indicate the functional status of the tissue?

1.4.2 Retrospective analysis of telemetry data from adult and paediatric CI users

The effectiveness of the CI is dependent on electrical stimulation of the auditory nerve. Any barrier to the flow of current will reduce the effective charge at the SGN. This represents one of the major bottlenecks in the CI signal path. The above studies highlight the main factors influencing the CI-tissue interface. Previous studies show that fibrotic tissue and new bone act like an electrical resistor at the CI-tissue interface. Attempts to increase current flow to improve the subjective sound percept can have the detrimental effect of current spread across channels, which reduces subjective pitch resolution (Arenberg Bierer, 2010). Chapter 3 presents a clinical study of EI in a large sample of adult and paediatric CI users.

There is currently a lack of clinical tools for monitoring of the CI interface. Although EI is a candidate, there are no published population statistics to guide clinicians in interpreting a given case. Evidence suggests that EI magnitude reflects intra-cochlear tissue type and volume; however very little focus has been placed on fluctuations in the mid and apical portion of the cochlea where a vigorous fibrotic and FBR response is thought to be rare. To address these gaps in knowledge, the following research questions were asked.

1. What is the distribution and long-term temporal trend of EI change for basal and apical electrodes?

Chapter 1

2. How many individuals exhibit significantly raised impedance levels?
3. Of these, how many were identified with raised impedance at electrodes away from the base?

A further aim was to apply the findings to clinical decision making to improve patient management. For example, clinicians make case-by-case decisions to deactivate electrodes, adapt stimulation strategies and, in a few published cases, treat with steroids. It is necessary to describe the current clinical decisions around deactivation before any EI informed recommendations can be made. To address this, the following research questions were asked.

4. What is the rate of deactivation for each electrode for adults and children?
5. For each deactivation decision, what are the recorded reasons?

1.4.3 Development of a mouse model of the tissue response to CI

Chapter 4 aims to triangulate between the EI measure (Chapter 3) and the immune mediated tissue response (Chapter 2). This is approached using a mouse model which allows implantation and electrical stimulation akin to human CI, with the additional benefits of experimental manipulation of genetics and environment followed by time-point specific tissue analysis.

This study includes the histological analysis of the mouse inner ear alongside the physical modelling using μ CT imaging; a new technology known as 3D X-ray histology. This chapter forms the basis of a versatile animal model for CI that aims to meet the following aims.

1. Controlled genetic and environmental variables to model human condition (Treatments/Independent variables).
2. Impedance telemetry measurement following chronic stimulation to verify human data (Measurements/dependent variables).
3. Acquire and spatially align X-ray μ CT and immunohistochemical light microscopy (Measurements/dependent variables).

Chapter 2 Rapid performance deterioration and explant associated with cellular indicators of unresolved inflammation

2.1 Introduction

2.1.1 Explant following soft failure presents an opportunity for histochemical tissue analysis

Individual variability in cochlear implant (CI) performance presents a significant challenge to healthcare professionals and patients. Factors influencing CI performance include hardware, surgical factors, psychological factors such as cognition and biological factors such as hearing loss aetiology and the inflammatory tissue response to implantation. The contribution of the cochlea tissue response to performance outcomes is poorly understood; any improvement in our knowledge in this area will aid development of methods for pre-implant prediction and post-implant monitoring. The case study presented in this chapter includes clinical measures spanning 10 months between implantation and explant-reimplantation surgery. The results collected in the clinic provide evidence of progressive migration of the electrode array over this period. Histological analysis was performed on the tissue developing around the extruded array. The findings provide insight into the fibrotic and foreign body response to a CI device that was explanted from a living patient. To our knowledge this represents the first case of histological analysis of human tissue associated with an explanted CI from a living patient.

2.1.2 Soft failure following electrode migration

Despite careful array insertion, positioning and securing of the lead wire to hold the array in place, migration of the electrode can still occur, resulting in performance decline. Migration has been shown to be the second most common reason for re-implantation (Connell et al, 2008). Migration of the CI electrode array has been demonstrated in several cases causing disruption of the electrode-tissue interface with an impact on pitch perception and speech recognition. A study of 35 CI users using CT scan analysis to measure migration distance found a small but significant shift in 10 patients. Interestingly they showed small migrations in individuals with no subjective indications of performance change, suggesting that migrations of this magnitude may not be an exception to the norm (Van Der Marel et al, 2012). Another another study used cone-beam CT to

Chapter 2

image the cochleae of patients with systematic increase in impedance levels and/or non-auditory stimulation at basal electrodes. They found 12 out of 18 cases exhibited significant electrode migration, suggesting that electrode migration should be considered when EI levels increase or non-auditory sensations develop (Dietz et al, 2016). A retrospective study including 358 CIs (278 users implanted either unilaterally or bilaterally) assessed a battery of measures that might indicate migration, including perceptual measures and x-ray imaging. Results showed 10 cases out of 358 (2.8%). Average speech perception score in these cases had dropped from 75% to 62%, but recovered in the 8 individuals who underwent revision surgery (Rader et al, 2016). In both of the latter studies, the confirmed cases of migration were exclusively straight lateral wall electrode arrays. This suggests that the physical properties of array itself can cause migration. It has been noted that this type of migration is most likely to occur in the first hours or days before the fibrotic response creates adhesion around the device (Van Der Marel et al, 2012).

Other pathological causes of migration have been observed, for example, that associated with cholesterol granuloma in the middle ear/mastoid space. The authors suggest possible causes of the migration including, intra-cochlear factors such as fibrosis and extra-cochlea factors such as scarring at the round window (Di Laora et al, 2019). Another cause of electrode migration driven by immunological factors is silicone allergy. This is a rare but well documented condition. A review of CIs from 1991 to 2004 in USA showed 3 confirmed cases of array migration with dermatologically confirmed silicone allergy. In all three cases the authors report delayed migration occurring several months after implantation. They postulate a delayed onset type IV hypersensitivity reaction to explain the immunological mechanism (Kunda et al, 2006).

The literature suggests several mechanisms of electrode array migration. There may be mechanical electrode factors which cause passive migration as well as biological factors which actively extrude the array from the cochlear. A better understanding of the functional interactions between the device and the wound-healing response is needed for improved personalised device choice and monitoring of performance. Currently, the main tool for measuring the array position is X-ray imaging. Although this technique has been highly successful in providing positional information, it does not provide insight into the biological status of the developing tissue.

The evidence discussed here raises interesting questions about the mechanisms of electrode array migration. This phenomenon is not fully understood and may have many overlapping drivers. We must consider the synergy between the implanted material and the cellular response of the recipient. There may be mechanical electrode factors which cause passive migration as well as biological factors which actively extrude the array from the cochlear. Chapter 2 of this thesis presents a case study of a single migration related CI failure. Detailed histological analysis was

performed on the tissue, which had developed on the extra cochlear portion of the electrode array. The cellular details of the tissue are described with a view to highlighting the biological correlates of migration related failure.

2.1.3 The generic wound-healing response to non-CI biodevices

Figure 2-1 shows the basic stages of the tissue response following bio-implantation. The immediate response following implant surgery is acute inflammation (Figure 2-1 Red); an innate immune response characterised by exudation of fluid and plasma proteins into the locality from the blood and infiltration of neutrophils. Activated neutrophils have a degradative function, which normally allows the break-down and removal of pathogens by secretion of proteolytic enzymes and reactive oxygen species (ROS) (Christo et al, 2015). Prior to formation of the fibrotic capsule or foreign body giant cell formation, proteins such as fibrin are adsorbed onto the implanted biomaterial. This begins immediately and is ongoing as a dynamic process. The initially adsorbed proteins such as albumin, can be displaced by other proteins with higher affinity for the biomaterial such as fibrinogen; the Vroman effect. This stage of the wound-healing response establishes the biochemical basis for cell adhesion. The adsorbed proteins form a provisional matrix that attracts and enables macrophages to adhere via integrins. These cell surface receptors are heterodimers which have binding specificity for different molecules that facilitate cell-cell fusion and cell-biomaterial adhesion. Integrin binding can also induce intra-cellular signalling cascades that switch macrophage phenotype. Therefore, the proteins laid down in the provisional matrix have strong potential to modulate the ongoing behaviour of the cellular response to the implant.

With ongoing presence of the implanted device, the cellular response transitions into the chronic inflammatory phase which lasts no longer than 7 days (Figure 2-1 Blue). It is characterised by the presence of macrophages and lymphocytes. Some cells, often referred to as classically activated, secrete proinflammatory cytokines such as IL-1 β which inhibit proliferation of granulation tissue. Other cells show an alternative phenotype associated with allergic responses, parasite elimination and remodelling of the extra-cellular matrix. The regulation of this balance of phenotypes, which controls the functional status of the fibrotic sheath, is not fully understood. It has mainly been investigated in in-vitro studies (Anderson et al, 2008); none with a focus on CI devices in media analogous to perilymph.

When switched towards proliferation, macrophages show upregulation of integrins and mannose receptors which promote fusion and adhesion to the provisional matrix. The protein fibronectin is secreted to attract fibroblasts, which secrete collagen to lay down the nascent extra-cellular

Chapter 2

matrix. The majority of neutrophils begin to enter apoptosis at this stage of the response. The first signs of new vasculature can be observed in the proliferative stage of the tissue response (Figure 2-1 Yellow). The final phase of the tissue response is tissue-remodelling where the fibrotic sheath reaches a stable and mature state. The key features of this stage are reduced cellularity, tight linear organisation of collagen molecules. Both fibroblasts and myofibroblasts are observed at this stage. Myofibroblast cells are able to secrete collagen and play a role in organising the structure of the ECM (Rolfe, 2011). Although the developmental origin of myofibroblasts is complex and highly tissue-specific, it seems clear that macrophages play a central role (Mesure et al, 2010).

At the tissue remodelling stage (Figure 2-1 Green), the fibrotic sheath can be observed as a separate layer to the FBGCs lining the implanted material. These cells create a barrier between the material and local areas of fibrotic sheath. This component of the tissue response is known as the foreign body reaction (FBR), and is defined as an acute sterile innate immune inflammatory reaction, which occurs in parallel to vascularisation and tissue remodelling (Christo et al, 2015). The FBR has been observed in other implants including Ventriculoperitoneal shunts (Snow & Kossovsky, 1989) and breast implants (Kamel et al, 2001). There are very few human studies of CI to verify the cellular and molecular signalling processes detailed in Figure 2-1.

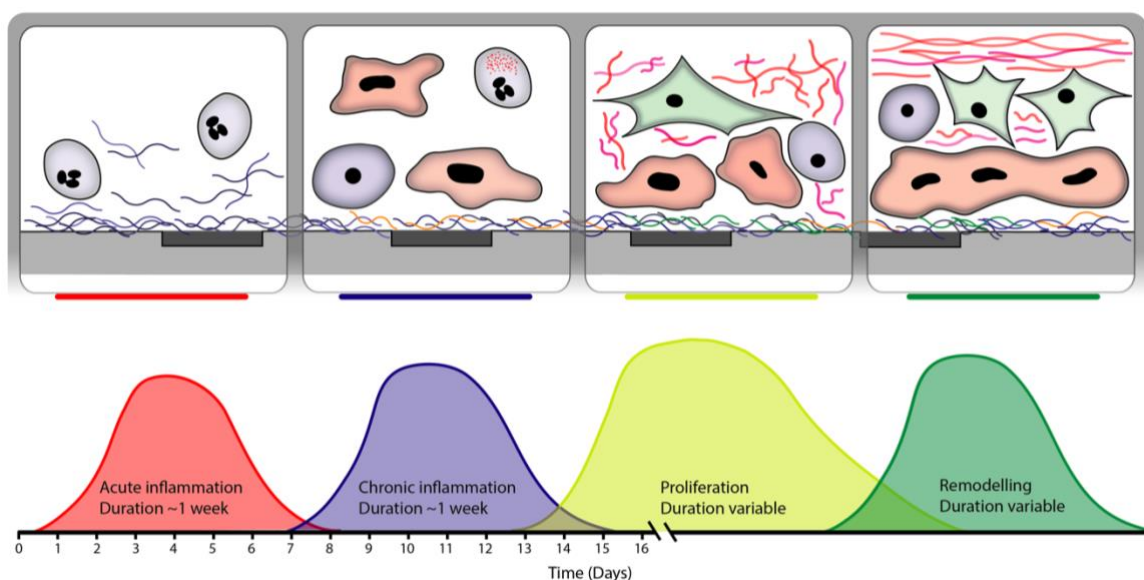


Figure 2-1: **The wound healing response to surgically implanted devices; characterised using non-CI bioimplants**

Red: Acute Inflammation is characterised by fluid exudation (swelling), adsorption of free floating proteins such as albumin on the implanted material and the infiltration of neutrophils.

Blue: Chronic inflammation is characterised by exchange of the initially adsorbed protein with those of high mass and affinity for the implanted material (Vroman effect), infiltration of white blood cells including eosinophils, B and T lymphocytes and macrophages.

Yellow: Proliferation is characterised by formation of granulation tissue, macrophage adhesion, neutrophil apoptosis, emergence of fibroblasts (infiltration and phenotypic switching), collagen secretion and formation of new blood vessels.

Green: Remodelling is characterised by formation of a mature fibrotic sheath, macrophage fusion to form FBGCs, presence of both fibroblasts and myofibroblast and collagen being reorganised (Christo et al, 2015; Anderson et al, 2008)

2.1.4 Similarities and differences between the cochlea and other tissues

The tissue response depends on the physicochemical properties of the implant such as shape, size, surface chemistry, morphology and porosity (Morais et al, 2010). The tissue specificity of the response is central to any investigation of a bioimplant. The small molecules, proteins, resident and circulating immune cells and their respective phenotypes will synergise to produce a unique response in a given tissue within an individual. The intra-cochlea fluid environment isolated from systemic blood circulation by the blood-labyrinth barrier, which consists of endothelial cells in the stria microvasculature, tight junctions, pericytes, basement membrane, and perivascular resident

macrophage-like melanocytes (PVM/Ms) within the SV. The tissue reaction in the cochlea may be different from other parts of the body, although the cochlea wound healing response is not fully elucidated. Although the cochlea is not immune privileged, it probably has lower immune reactivity than other compartments of the body because of the blood-labyrinthine barrier. The composition of perilymph is compositionally similar to CSF rather than blood plasma. The homeostasis of the cochlea is maintained by the SV. Although there is evidence of resident macrophages in the cochlea (Okano et al, 2008), the opportunity for infiltration of circulating immune cells is limited by the SV and the cochlear duct. Surgical opening of the cochlea by cochleostomy provides an opening for infiltration of molecules and cells which may promote immune reactivity more akin to other body compartments. Although the generic wound healing response described in Figure 2-1 is a useful guide to the events occurring in the cochlea following implantation, further specific investigations are needed to characterise cochlear immunity and inflammation.

2.1.5 The cellular and molecular response to cochlear implants

Using both *in vivo* and *in vitro* animal models of cochlear implantation, Bas et al investigated the biological mechanisms responsible for the stages of the wound healing process that occur in the cochlea following insertion of an electrode analogue. They showed upregulation of various genes including Vascular Endothelial Growth Factor (VEGF α) which is associated with angiogenesis following electrode insertion. They demonstrated positive immunostaining for cytokines IL-1 β (pro-inflammatory) and Arg1 (anti-inflammatory) indicated the presence of macrophages with polarised phenotypes that overlapped in the wound site in the weeks following implantation; providing evidence for both inflammation and proliferation. There was significantly more collagen deposition in the fibrous tissue from implanted animals compared to controls. There was positive staining for myofibroblasts and collagen type 1A, which were absent in the control animals (Bas et al, 2015). Myofibroblasts differentiate from fibroblasts during the proliferative phase of wound healing. They are collagen depositing cells that have contractile properties which allow for wound contraction seen during the development of granulation tissue; the tissue type that is the hallmark of healing inflammation (Micallef et al, 2012).

The human cochlear wound healing response has been described in less detail than the above animal model study. Post-mortem investigations of temporal bones donated by CI users describe the fibrotic sheath and new bone formation (osteogenesis), which is often more pronounced at the basal regions of the cochlea near the cochleostomy (Clark et al, 1988; Kawano et al, 1998; Gassner et al, 2005; Li et al, 2007; Somdas et al, 2007; Kamakura & Nadol, 2016). Evidence from 28 human temporal bones revealed a characteristic cellular immune response consisting of

foreign body giant cell reaction (96% of cases) and a lymphocytic infiltrate (89% of cases) (Seyyedi & Nadol Jr, 2014). The cellular profile of intra-cochlear fibrosis was further characterised which indicated the presence of both B- and T-cell lymphocytes, as well as macrophages and foreign body giant cells containing platinum inclusions (Nadol et al, 2014). There is some agreement between studies suggesting that this pattern of tissue change, especially in the basal turn of the cochlea is the norm following CI. However, our understanding of the cellular response and molecular signalling in the CI wound-healing response is incomplete. The post-mortem investigations which form the basis of our understanding of the wound-healing response describe the tissue status at the end of life and may not reflect the day-to-day fluctuations in the fibrotic sheath that may coincide with performance fluctuations. By combining detailed histochemical and immunohistochemical tissue analysis with a relatively rich dataset of clinical findings, this study extends our knowledge of the wound healing response, fibrosis and FBR provoked by CI.

2.1.6 Case details

The case study included a single adult female who was implanted with a Cochlear Nucleus CI 522 CI. The surgeon reported a full insertion (Figure 2-2) via the round window. However, basal electrodes 1 and 2 showed maximal impedance (open circuit) at the device activation session and therefore were not stimulated. Over the course of ten months, basal electrodes were sequentially deactivated because of non-auditory sensations, poor loudness growth and ultimately maximal/unrecordably high impedance levels. Electrode impedance levels at basal electrodes followed a systematic pattern of increase to maximal, followed by reduction after deactivation (Figure 2-6). The same pattern spread from the basal-most electrodes to electrode 7 at the 9-month review session. This pattern, taken together with subjective reports of non-auditory stimulation for basal electrodes was taken as strong evidence for progression electrode migration. There was also a continuous reduction in word recognition score across the 10 months. X-ray images were acquired and judged by the surgeon to confirm significant migration of the electrode array. None of the individual images were clear enough to illustrate the migration and therefore were not included here. Consequently, the decision was made at ten months to remove the device and re-implant a new device: Nucleus CI 512. At the explant-reimplantation surgery, the surgeon reported a mechanical resistance to array removal and observed five extra-cochlear electrodes. The new electrode array was inserted via a drilled cochleostomy, with all electrode contacts reported as successfully positioned inside the cochlea. Manufacturer integrity testing of the original Nucleus CI 522 confirmed that the failure was not attributable to the device, thus confirming soft failure. The patient has a long-standing diagnosis of rheumatoid arthritis, which is controlled using Methotrexate.

Chapter 2

An X-ray scan was performed shortly after the initial implantation. Figure 2-2a shows the electrode contacts within the cochlea. The electrode contact positions are highlighted using black dots in Figure 2-2b.

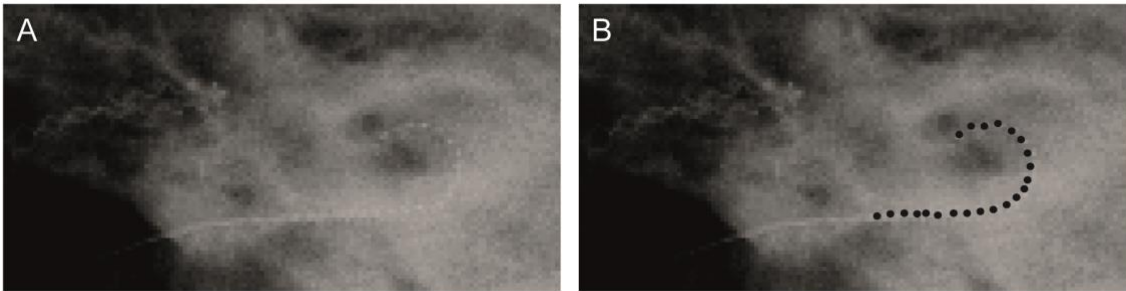


Figure 2-2: **Full insertion demonstrated by X-ray images captured following implantation surgery**
A) Raw X-ray radiograph image showing electrode array curving round inside the cochlea. B) Image edited to highlight the positions of the electrode contacts. The surgeon's notes report full insertion.

2.2 Research aims and questions

More research needs to be carried out to better understand what mechanisms drive the biological responses to CIs that cause poor performance and soft failure. This chapter presents a unique investigation of the tissue composition and cellular profile of the fibrotic sheath that had formed around the array, over the course of ten months, as the device migrated out of the cochlea. The study not only provides some information about the biological correlates of a one-off failure but adds to the general description of CI wound healing in humans.

The current understanding of the tissue response following cochlear implantation is taken from post-mortem studies. There is a lack of knowledge of the wound healing response in living patients. In order to investigate the tissue directly, a study was carried out to perform histochemical analysis of fibrotic tissue from an explanted electrode array following migration related failure. The following research questions were asked.

1. What is the overall composition and organisation of the tissue?

The clinical measurements and surgeons report confirmed progressive significant electrode array migration. In order to investigate the cellular composition and functional properties of the tissue the following research questions were asked.

2. Is the composition and organisation spatially variable?

3. Do the cell types, phenotypes and ECM structure indicate the functional status of the tissue?

2.3 Method

2.3.1 Management of the explanted device and tissue

The electrode array and attached tissue was surgically explanted and immediately placed in formalin solution for tissue fixation. The tissue was then transferred to 70% ethanol solution and stored at 4 °C. Figure 2-3 shows the tissue connected to the array in a petri dish.

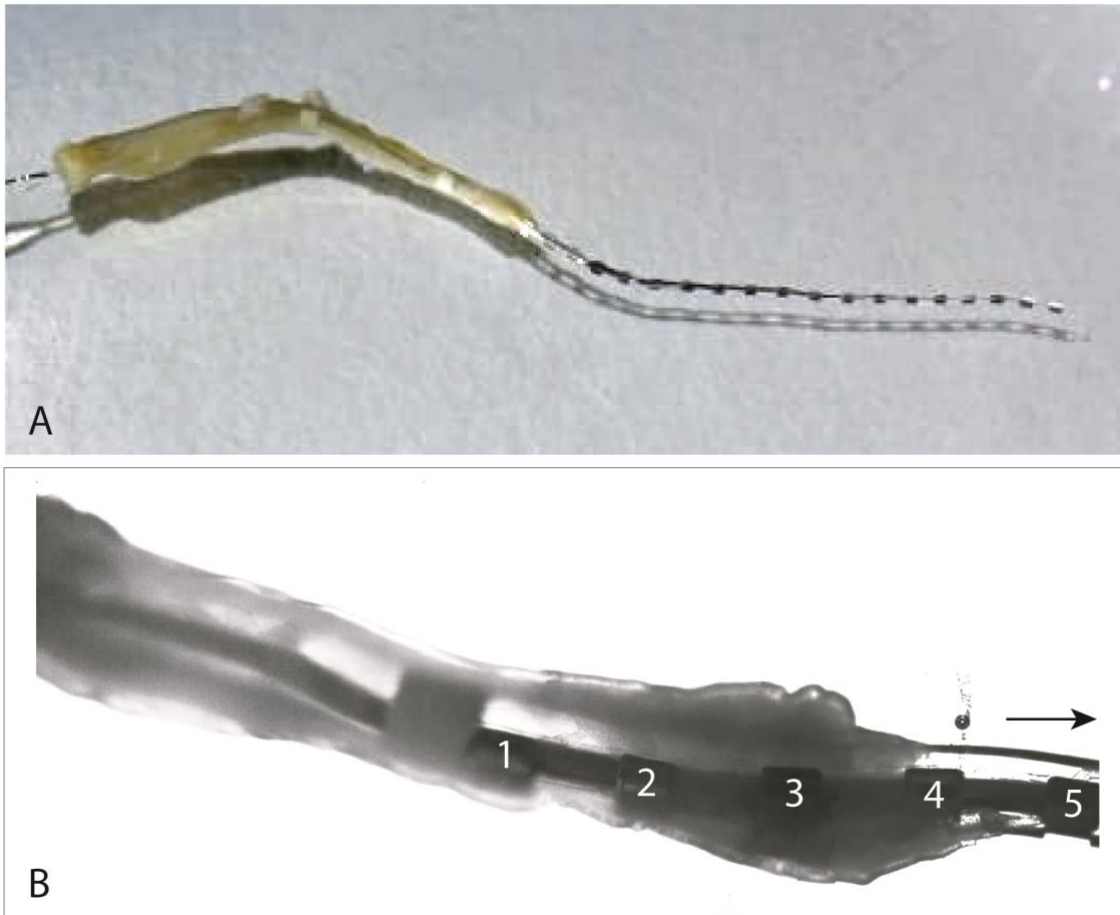


Figure 2-3: **Fibrotic tissue attached to the surgically explanted electrode array**

Photographs show A) Full length of electrode array showing fibrotic tissue enveloping the basal portion of the array and extending onto lead wire. B) High magnification image with increased brightness showing 4 electrodes enveloped by fibrotic tissue. Electrode number 1 is the most basal electrode. Arrow indicates direction of the array tip.

2.3.2 Tissue embedding

The tissue enveloped the basal portion of the electrode array. **Error! Reference source not found.** shows the basal four electrodes covered by a tubular sleeve of fibrotic tissue of roughly even thickness around the array. The fibrotic sheath was removed from the electrode array in one

piece after making a single incision along its length. Figure 2-4 a shows the isolated tissue following removal from the array. The tissue sample was then cryo-protected using 30% sucrose solution (48 hours). The embedding procedure was carried out according to the standard operating procedure (SOP) in Appendix A1 (page 159). The tissue was then covered with optimum cutting temperature (OCT) cryomatrix to allow infiltration into the void left by the array. The specimen was then transferred into an aluminium foil well containing ~25ml of OCT cryomatrix. The well, containing the tissue was frozen by submerging the foil well into isopentane cooled to -80 °C using dry ice (solid carbon dioxide).

2.3.3 Tissue sectioning

The frozen tissue was cryo-sectioned at Southampton General Hospital Histochemistry Research Unit using a Leica CM 1850 UV cryostat. Tissue sectioning was carried out following the SOP in Appendix A2 (page 160). The tissue was sectioned at 10 μm with the knife blade at 5°. Cryostat temperature was -20°C. Sectioned tissue was mounted on glass 3-Aminopropyltriethoxysilane (APES) coated slides; 3 sections per slide. Slides were left to dry at room temperature for 1 hour before being stored at -20 °C.

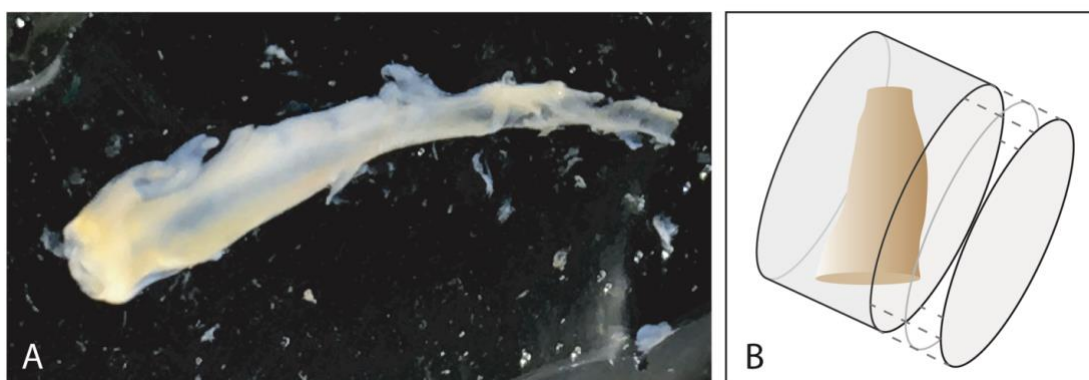


Figure 2-4: **Fibrotic tissue isolated from the array prior to preparation for histology**

A) Photograph of the isolated tissue in a petri dish. B) Schematic representation of the tissue cryo-embedded in OCT matrix. The basal-most portion of the tissue was tilted toward the cutting face, which is indicated by the sectioned disk to the right.

The tissue was tilted within the OCT block as shown in Figure 2-4b. The angle of the cutting plane is shown in blue dashed lines in Figure 2-5. The tissue was split roughly into four regions to give a view of the organisation in steps from the lead wire, towards the round window (R1 to R4).

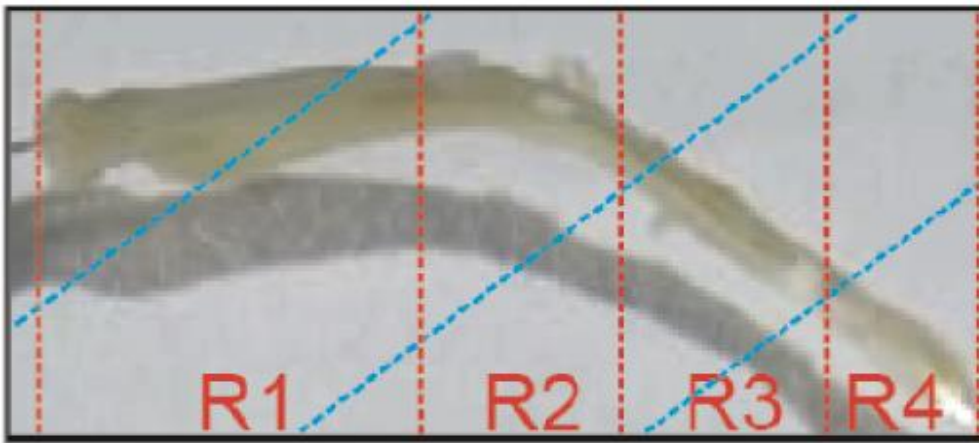


Figure 2-5: **Tissue sections from four regions along the array**

R1 = lead wire (furthest from round window), R2 = lead wire to array, R3 and R4 = electrode contacts as shown in Figure 2-4b. Blue dashed lines indicate the cutting plane.

2.3.4 Histochemical staining

Tissue sections were stained using haematoxylin and eosin (H&E) using the SOP shown in Appendix A3 (page 161). Haematoxylin is a basic dye which binds to DNA molecules when in complex with metal ions such as aluminium. This allows the nucleus to be labelled blue/purple. Eosin is an acidic dye which binds to molecules in the cytoplasm and extra-cellular space. This allows cells to be visualised as pink. This common staining technique was performed to allow a detailed view of the cellularity and overall organisation of the tissue under light microscopy.

Slides were stained using martius/scarlet/blue (MSB) trichrome stain, following the SOP shown in Appendix A4 (page 163). This staining protocol was chosen to allow visualisation of connective tissue but also has the benefit of differentiating various proteins and cell types involved in inflammation. Haematoxylin was used to stain cell nuclei. Next, the tissue was stained using martius yellow, crystal ponceau and aniline blue. The MSB series of stains allows visualisation of erythrocytes in yellow, collagen in blue, fibrin in red and cell nuclei in blue/black.

Following staining with H&E or MSB trichrome, the tissue was dehydrated through ethanol steps and cleared using xylene. Glass cover slips were sealed over the tissue using dibutylphthalate polystyrene xylene (DPX) mountant and dried overnight at room temperature.

2.3.5 Immunohistochemical staining

Slides were selected from each of the four tissue regions. Immunohistochemical staining was carried out according to the SOP shown in Appendix A5 (page 165). Methodological details are shown in Table 2-1.

Table 2-1: Immunohistochemical reagents and methods used in staining the human fibrotic tissue

| Target cell/tissue | Antibody | Manufacturer | Host species | Dilution | Antigen Retrieval | Blocking agent | Secondary antibody | DAB time |
|---|-----------------------------|--|--------------|----------|--|--|--|----------|
| Macrophage | CD68 Monoclonal | Abcam (ab783) | Mouse | 1:100 | Hot citrate buffer 5 mins, cool 5 mins | Normal goat serum 1.5% in PBS | Goat anti-mouse 1:1000 (BA-9200) | 2-4 min |
| Macrophage | CD163 | Abcam (ab182422) | Rabbit | 1:250 | Hot citrate buffer 5 mins, cool 5 mins | Normal goat serum 1.5% in PBS | Goat anti-rabbit 1:200 | 2-4 min |
| Dividing cells (proliferation) | Ki-67 Polyclonal | Abcam (ab15580) | Rabbit | 1:600 | Hot citrate buffer 5 mins, cool 5 mins | Normal goat serum in 0.01% TX100 0.25% BSA | Goat -anti Rabbit 1:200 in 0.01% TX100 0.25% BSA | 3 min |
| Blood vessels, myofibroblasts | α -SMA Monoclonal | Sigma | Mouse | 1:50,000 | Hot citrate buffer 5 mins, cool 5 mins | Normal goat serum 1.5% | Goat -anti mouse 1:200 in 0.01% TX100 0.25% BSA | 1.5 min |
| T-Lymphocytes | CD3 | Dako | Rabbit | 1:200 | Hot citrate buffer 3 mins, cool 5 mins, hear 3 min, cool 5 min | Normal goat serum 1.5% | Goat anti-rabbit 1:200 | 2 min |
| Pro-inflammatory cytokine IL-1 β | IL-1 β | Peprotech | Rabbit | 1:50 | Hot citrate buffer 3 mins, cool 5 mins, hear 3 min, cool 5 min | Normal goat serum 20% | Goat anti-rabbit 1:200 | 1 min |
| Vasculogenesis | VEGF-R2 | Cell signalling Technology (55B11) | Rabbit | 1:600 | EDTA with tween microwave until boiling then place slides in and leave 15 min | Normal goat serum 5% | Goat anti-rabbit 1:200 in TBS Tween | 6.5 min |

2.3.6 Image acquisition and processing

The stained tissue was viewed using bright-field light microscopy. Images were captured using Q-imaging Q-Capture software via a Q-Imaging 2000R digital camera connected to a Nikon Eclipse E4000 microscope and Nikon HB-101004F light source. Various magnifications were achieved using 4x, 10x, 20x, 40x and 100x objectives. Brightness and contrast of the images were adjusted using Image-J software.

2.4 Results

2.4.1 Clinical evidence of physical migration of the electrode array

The patient SW reported reduced sound quality and speech recognition at the three-month review appointment. Figure 2-6 shows data captured at clinical sessions over the 10-month period of CI use before explant-reimplantation. The study was a retrospective design, so the data presented represent both clinical finding and also decisions made by the clinicians in USAIS. The reasons given for deactivation were either maximal EI levels (open circuit) shown in the CI programming software or electrode stimulation produced subjective non-auditory sensation.

The clinical findings suggest at stepwise migration of the electrode array. Figure 2-6a shows electrode status and hearing performance tested using the BKB sentence test. At the device activation appointment (time point 0) 20 electrodes were active and 2, most basal electrodes, were open circuit, meaning that the impedance at those electrodes was too high for current to flow. The surgeon's report stated that full electrode array insertion was achieved. Figure 2-2 is a post-implantation X-ray image showing complete, or near-complete insertion of the electrode array. At the next clinical session (1 month), the number of open circuit electrodes had increased to three, again the most basal electrode positions. The adjacent three electrodes had been deactivated at the session. Figure 2-6a shows an increase over time of the number of electrodes either open circuit or deactivated. At the nine-month review appointment 13 of the 22 electrodes were either deactivated or open circuit. The systematic pattern of change in electrode status is also reflected in the speech performance results. There was significant decline in the BKB sentence score between 3 and 6 months, for both CI-alone and CI-plus-hearing aid hybrid. At 6 months, the BKB score had fallen to below 40% and half of the electrodes were either deactivated or open circuit. At six months the hybrid speech performance was almost 80%, what fell to 50% by seven months, which is probably mostly attributable to the hearing aid.

Figure 2-6b shows the electrical impedance measurement results for the 8 most basal electrodes. The systematic pattern impedance change across the basal electrodes is further evidence of migration. At the activation appointment the two most basal electrodes showed extremely high impedance levels i.e. open circuit. One month later, electrode two remained high but electrode one had reduced. At the two-month review appointment the impedance peak has shifted to electrode four, while impedance levels at electrodes 3, 2 and 1 had decreased. This pattern continued, with a peak seen at electrodes 5, 6 and 7 at the 3-month, 6-month and 7-month appointments respectively. As the impedance peak shifts away from the base, electrodes previously showing raised impedance recovered to lower levels. This temporal pattern of impedance change is

Chapter 2

consistent with active electrodes changing positions so the current path to the reference electrode is varying in its conductive properties. This is strong evidence of the electrode array physically migrating out of the cochlea.

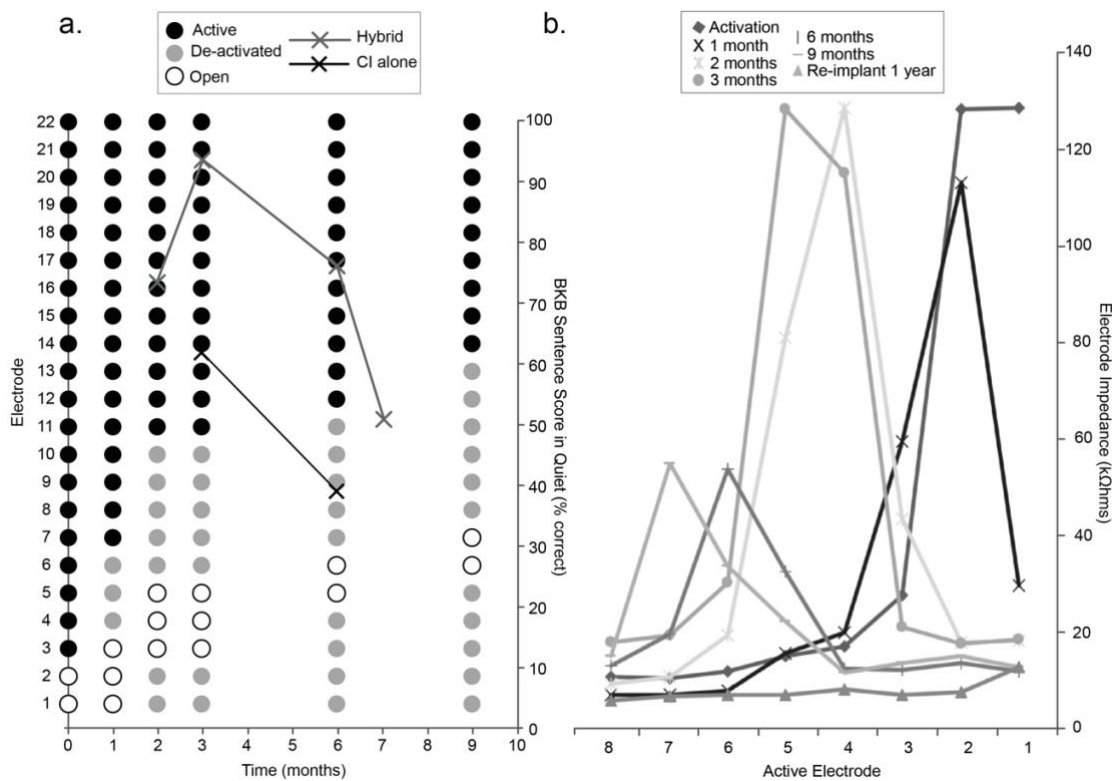


Figure 2-6: Clinical measures indicate electrode array migration and decrement of speech recognition score over time

Measures were acquired across the 10-month period of CI use before explant-reimplantation surgery. A) Electrode status shown by circles and speech recognition (BKB sentence test) shown as crosses. B) EI level for the basal 8 electrodes.

2.4.2 Fibrotic tissue removed from the explanted array shows spatially variable organisation

The aim of this research project was to investigate the organisation and cellular constituents of the fibrotic tissue that had developed around the newly extruded portion of the electrode array. In order to answer the first research question regarding the organisation of the fibrotic tissue, histological analysis was performed on four regions of the tissue as shown in Figure 2-5. The tissue sections shown in Figure 2-7 are examples from the regions: A) nearest the lead wire to D) nearest the array tip. The tissue sleeve was thicker in region 1 and thinned towards region 4, which is shown in Figure 2-3.

The images shown in Figure 2-7 were taken by light microscopy and show a graded increase in cellularity from Figure 2-7a (region 1) to Figure 2-7d (region 4) towards the round window. Within regions, there are sub-areas of variable cell density and cellular organisation. There are clearly strata of different cell densities from the central lumen or electrode track, out towards the external edge of the tissue.

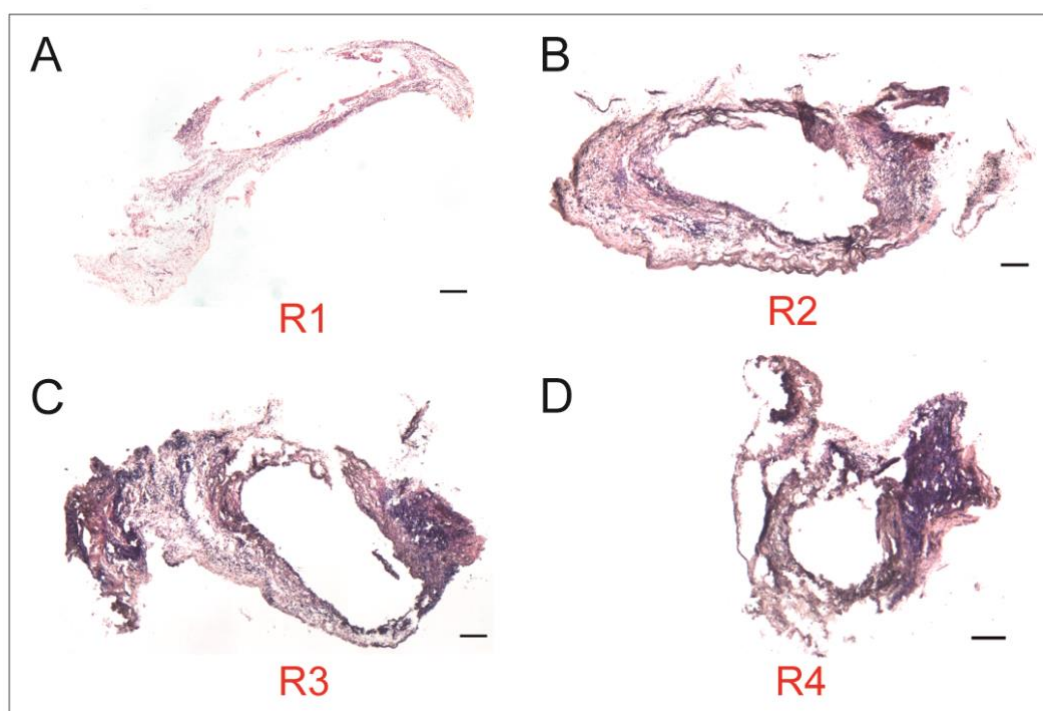


Figure 2-7: **Density and organisation of cells was variable within and across regions**

Tissue sections stained with H&E to visualise cell nuclei (blue/purple) and membranes and cytoplasm (hues of pink) from regions 1 to 4. A) Region 1, furthest from the round window niche at the time of explant. This section of the array is assumed to have migrated from the cochlea

Chapter 2

first. B) Region 2. C) Region 3. D) Region 4, nearest to the round window niche at the time of explant. This section of the array is assumed to have been extruded from the cochlea last. Scale bar = 200 μm

In addition to the gross spatial variability, there were a wide range of cell types and densities across the tissue. Figure 2-8 shows examples of an area of sparse cellularity (Figure 2-8a), layered strata of cells that were organised around the electrode track across the length of the tissue sample (Figure 2-8b) and highly dense areas of cells with red clusters of fibrin protein (Figure 2-8c). Figure 2-8 also shows stained eosinophils (Figure 2-8d) and neutrophils (Figure 2-8e) highlighted by black arrows, which suggest an ongoing process of active inflammation. Figure 2-8f shows an example of a multi-nucleated giant cell, which is evidence of the FBR. There was no obvious trend for specific cells in any given region; they were distributed across the tissue. However, the areas of densely packed cells and clusters of fibrin protein were most prevalent near the round window.

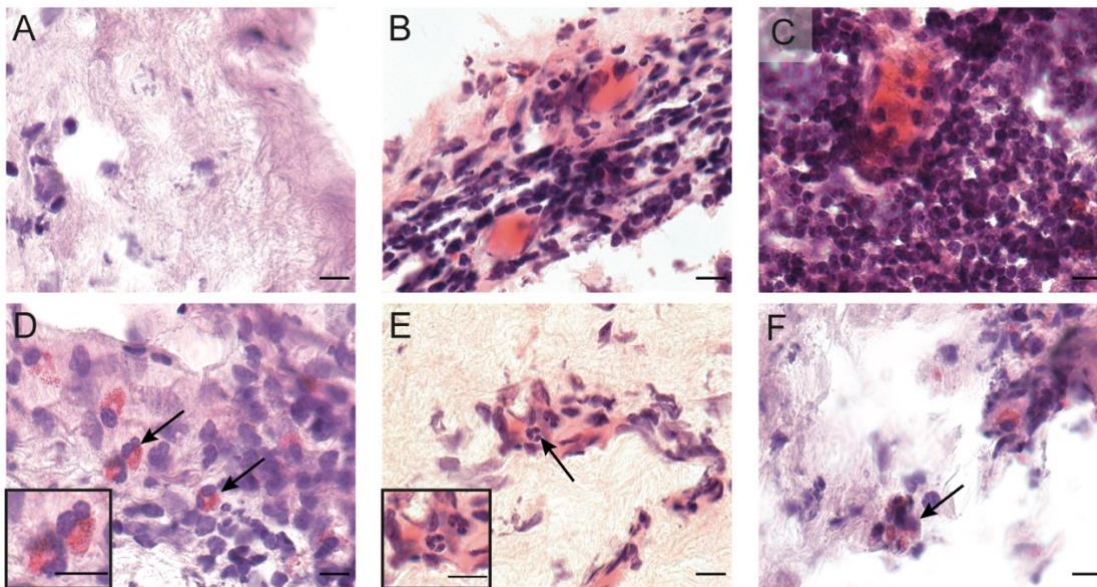


Figure 2-8: **Variation in cell-types and protein expression observed**

High magnification light microscopy images of tissue sections stained using H&E. A) Area of loose collagen in the region furthest from the round window. B) Example of cells organised in layers or strata from the electrode track. C) Area of high-density cells near the round window. D) Examples of eosinophils, which were distributed throughout the tissue, stained red and highlighted by arrows. E) Examples of neutrophils stained light pink by eosin and displaying multi-lobed nuclei. F) Example of a polynucleated foreign body giant cell. Scale bar = 10 μm

Histochemical staining using MSB trichrome allowed a detailed view of the collagen organisation (Figure 2-9). The results show heterogeneous collagen organisation across the tissue sample. The general pattern was for densely layered collagen fibres proximal to the electrode track and tending to be more prevalent in the region near the round window. The loose collagen fibres were most common on the outer layer of the tissue, especially furthest from the round window. Areas of dense collagen were observed to be more cellular than the loose collagenous areas, which were sparsely cellular.

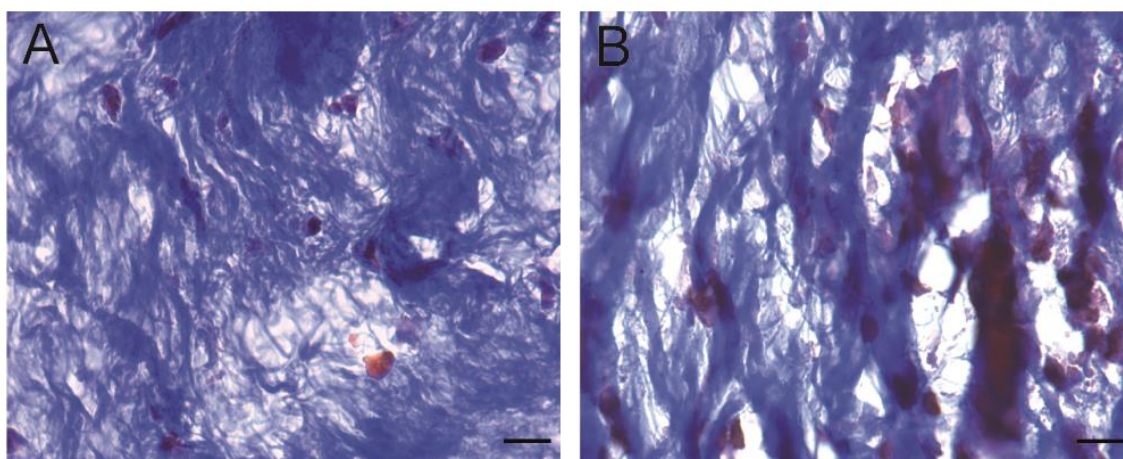


Figure 2-9: **Organisation of the collagen differed across the tissue**

A) An example of loose collagen fibres observed in areas distal to the electrode track. B) An example of dense layers of collagen fibres observed more proximal to the electrode track.

2.4.3 Immunohistochemical evidence of active inflammation

The final research question of this project addressed the cellular composition of the fibrotic tissue removed from the explanted array, and specifically, whether this indicated functional status. Tissue development around bioimplants follows three stages with defining cellular features. Inflammation is the first stage of the reaction and has been shown to last approximately two weeks. An assay for markers of inflammation was performed to further the findings of H&E staining. Antibodies to detect macrophages (CD68 and CD163), T cells (CD3) and the pro-inflammatory cytokine (IL-1 β) were used.

Figure 2-10a shows CD68 positive cells on the edge of the tissue in close proximity to the electrode track. Figure 2-10b shows positive staining for the cytokine IL-1 β providing evidence for inflammatory signalling between cells. A second macrophage population, CD163 was observed; in lower number and generally distributed around the perimeter of the tissue section (Figure 2-10c).

Clusters of T cells were observed in the region of the sample near the round window, toward the outer layer of the tissue (Figure 2-10d).

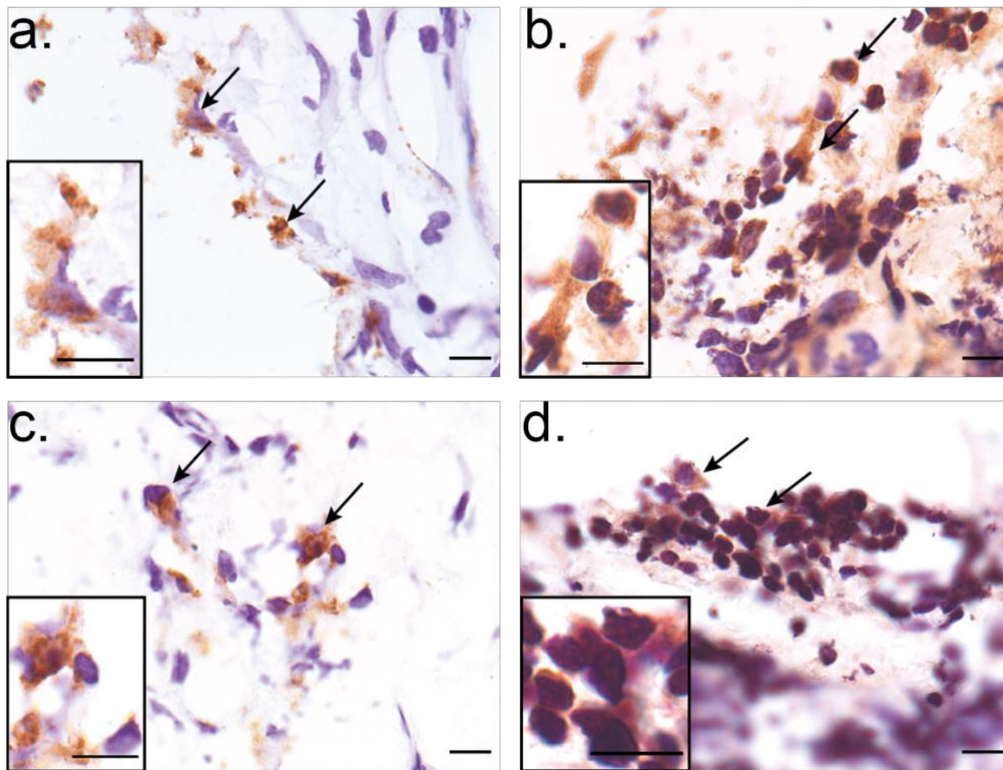


Figure 2-10: Cells and cytokines characteristic of an inflammatory response were observed throughout the tissue

Light microscopy images of tissue sections immuno-stained using four specific antibodies. A) CD68 marker for macrophages (IL-6 sensitive). B) IL-1 β pro-inflammatory cytokine. C) CD163 marker for macrophages (IL-10 sensitive). D) CD3 marker for T-lymphocytes. Chromogen: DAB in all cases. Scale bar 10 μ m.

2.4.4 Immunohistochemical evidence of cellular proliferation and angiogenesis

The second stage of the tissue response to bioimplants is proliferation, where cell number increase, extra cellular matrix is laid down and blood vessels begin to develop.

Immunohistochemical stains using markers of proliferation were performed on tissue sections from the four tissue regions. Figure 2-11a shows positive staining for the proliferation marker Ki-67. Most of the Ki-67 positive cells were observed in regions of low cell density and high ECM. This marker indicates cells that are preparing or in the process of dividing. Examples of such cells are likely to be endothelial cells which proliferate and organise to form the internal lining of blood

vessels. Figure 2-11b shows staining for VEGF-R2 expression indicating the presence of proliferating blood vessels. VEGF-R2 was primarily observed in the outer layer of the tissue, distal to the electrode array surface and clustered in one area. An example of a cross-sectioned blood vessel is highlighted in the zoomed window to the bottom left. Figure 2-11c and d show cells positively stained with α -SMA highlighting the presence of developing smooth muscle lining blood vessels and myofibroblasts respectively. The former is clearly identifiable based on the tubular form of the structures. The myofibroblasts, which play an essential role in collagen deposition and remodelling were observed to be organised linearly.

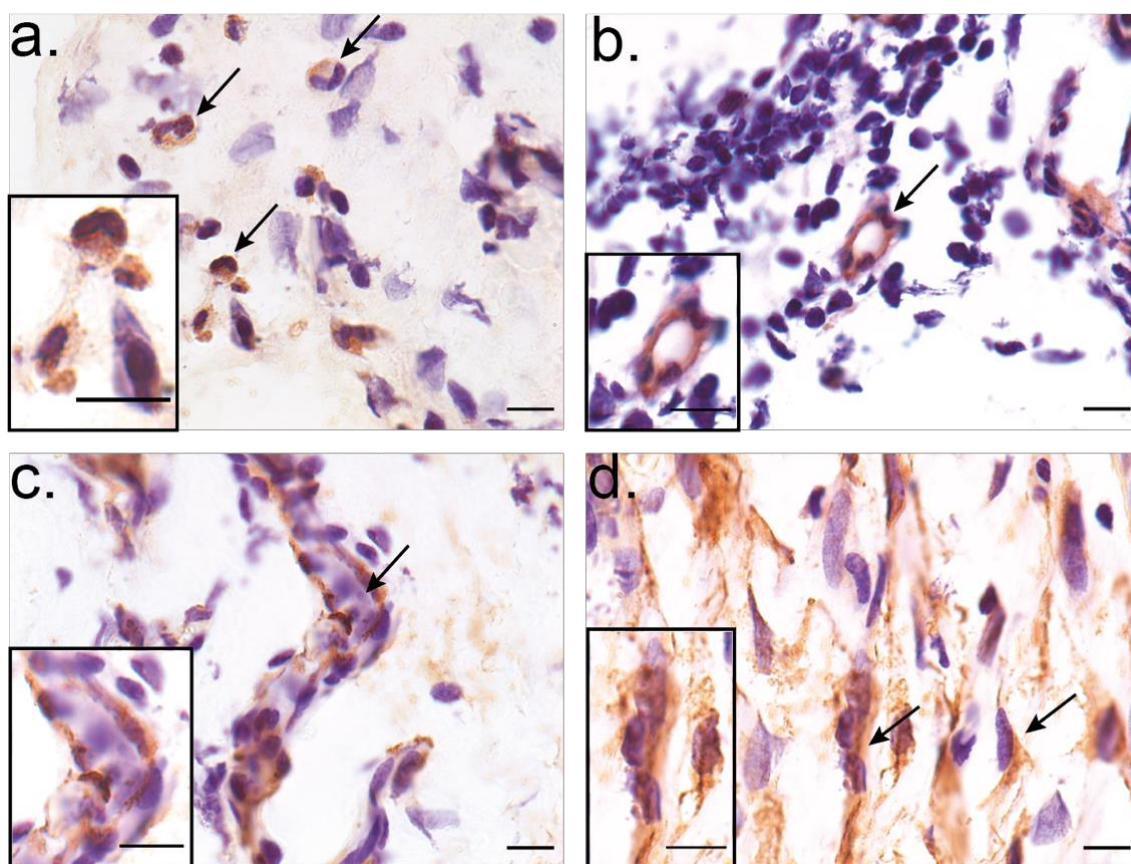


Figure 2-11: **Cellular markers associated with cell proliferation were observed throughout the tissue**

Light microscopy images of tissue sections immuno-stained using three specific antibodies. A) Ki-67 marker of dividing i.e. proliferating cells. B) VEGF-R2 marker for developing blood vessels i.e. angiogenesis. C) α -SMA marker showing blood vessel endothelium and D) α -SMA marker showing myofibroblasts. Positively stained cells indicated by black arrows. Scale bar 10 μ m.

2.5 Discussion

2.5.1 This case study presents new findings compared to post-mortem studies

Several studies have described the gross tissue reaction in post-mortem investigations. Relatively few have focussed on the details of the molecular and cellular reaction to CI (Table 1-1). The temporal dynamics of the FBR and fibrotic response to CI is only partially characterised, especially in cases of spontaneous idiopathic performance decline. This chapter presents a case study of a CI explant following electrode array migration associated with significant performance decline. The study design was observational and opportunistic; as clinicians became aware of the performance decline, a group decision was made, with patient consent, to capture regular clinical measurements and sample the explanted tissue for histological analysis. Therefore, the results of histological analysis represent a single point in time. The same is true for the previous studies shown in Figure 1-3, except they all involved post-mortem analyses soft tissue most often from archival tissue. They are therefore purely retrospective and didn't have the opportunity to make clinical decisions during a significant decline in performance in the same way as the present study. The main difference between this study and previous temporal bone investigations is that here, the tissue sample was taken from the extruded (extracochlear) portion of the explanted array.

Three research questions were addressed

1. What is the overall composition and organisation of the tissue?
2. Is the composition and organisation spatially variable?
3. Do the cell types, phenotypes and ECM structure indicate the functional status of the tissue?

These questions address unknowns at two levels of enquiry. Firstly, to investigate the tissue correlates of migration related CI failure in order to better understand the causal mechanisms. Secondly, to take steps towards an improved understanding of the immune mediated tissue response to cochlear implantation.

2.5.2 Confirmed electrode migration associated with cellular indicators of simultaneous chronic inflammation and proliferation

The impedance telemetry measurements were consistent with rapid and continuous electrode extrusion over a period of 10 months, which was confirmed by x-ray imaging. The migration and ultimate failure of the device prompted questions about the type and characteristics of the tissue on the electrode array. The research aim was to produce a detailed description of the cellular and

molecular profile of the tissue. This elucidates details of the human CI tissue response that have not previously been shown following migration related failure. Specifically, this investigation demonstrated that cells associated with different stages of wound healing; inflammation, proliferation and maturation, were present simultaneously. Specific cell types which indicate ongoing, active inflammation were present. This finding is interesting considering the electrode was explanted at 10 months, by which time the acute and chronic inflammatory phases should have resolved. The cellular profile of the tissue was highly heterogeneous, containing localised areas of inflammatory and proliferative cells and varying densities and formations of ECM. This suggests highly localised chemical signalling to control the phenotype of cells in specific areas. Although there was evidence of tissue maturation, mainly dense collagen fibres, the overall picture was one of regions of recently active inflammation and proliferation. Because of the novelty of the method applied here i.e. tissue explant analysis in a living patient, there are no direct comparisons in the literature. The one published case of tissue from this section of the electrode array shows similar stratification of the tissue relative to the array but less overall heterogeneity. This study also has a more basic method soft tissue analysis, using H & E, which does not afford the cellular specificity presented here (Clark et al, 1988). The findings of the cellular and molecular analysis do not elucidate the mechanism that drove the migration.

2.5.3 Novel findings of cell-specific immunohistochemical stains of tissue from an explanted CI

Immuno-histochemical staining using anti-CD68 showed individual macrophages distributed throughout the tissue. Some of these cells were observed aggregated together as foreign body giant cells. As discussed in Chapter 1, giant cells are formed as part of the FBR to implanted biomaterials. Previous investigations have found giant cells to be a common constituent of the CI fibrotic sheath.

Several pieces of evidence indicate active inflammation in the explanted tissue. Eosinophils were identified in the H&E stain, sparsely distributed throughout each of the four regions. These cells are granulocytes which release a range of molecules involved with mediation of allergic reactions. The H&E stain also revealed a small number of neutrophils, identified by their multi-lobed nuclei. These cells are also granulocytes and contribute to the initial inflammatory phase of the innate immune response. The MSB trichrome/H&E stain revealed several large clusters of fibrin protein. Fibrin is one the first molecules to accumulate at the site of any wound or implant. It is a keystone component of the provisional matrix and presents pro-inflammatory and chemoattractant signals to local white blood cells. A stain with anti-IL-1 β served as a confirmatory indicator of active inflammation. This protein is a cytokine which promotes inflammation, proliferation and

Chapter 2

apoptosis. It is released by activated macrophages. Therefore, positive staining gives functional information about the macrophages -which makes it a useful marker of inflammation in clinical diagnostics.

Further immunohistochemical stains were performed using markers for molecules involved with cellular proliferation. Ki-67 is a protein that is strictly associated with cell division; it increases in concentration in the cell nucleus during cell division but is absent in resting cells. It is therefore a useful marker of cell proliferation in clinical diagnostic cases such as tumour growth. In the present case, positive staining for Ki-67 was observed associated with nuclei counterstained with haematoxylin. The clinical findings show that Region 4 of the tissue covers a portion of the array that emerged from the cochlea only a few weeks before explant surgery. The histochemical findings show that recently extruded CI electrode array is associated with rapidly developing fibrotic tissue. Based on the evidence presented in Table 1-1, it is likely that this fibrotic sheath is continuous with the intra-cochlea fibrotic sheath. Two antibodies which indicate the development of blood vessels were used to stain the tissue. The VEGF receptor 2 protein (VEGF-R2) is expressed by endothelial cells. Positive staining of this molecule combined with the visual identification of tube-like structures is clear evidence of angiogenesis. VEGF signalling to mediate angiogenesis is driven by fibroblasts (Kendall & Feghali-Bostwick, 2014). Cells positively stained with α -SMA were also observed organised into vessel structures indicating the formation of the smooth muscle containing endothelium of blood vessels.

None of the studies discussed in Chapter 1, which describe the basic composition of the fibrotic sheath in human CI users report evidence of angiogenesis. This finding is likely to be the norm for developing fibrosis, at least outside the cochlea, and likely unrelated to the device migration. However, the finding represents a novel observation and adds a valuable new piece of the CI wound healing picture.

The MSB trichrome stain allowed clear visualisation of the collagen deposition. The organisation of collagen fibres was different across the tissue and likely indicates different developmental and function status i.e. how mature the ECM is and what role it is playing. Figure 2-9a shows loose connective tissue, which has been described before as flexible, well vascularised with low tensile strength. Figure 2-9b shows dense connective tissue, which has been described before as inflexible, minimally vascularised with high fibre alignment.

2.5.4 Evidence for the mechanism of electrode migration

The third research question in this study asked whether the identification of specific cells indicates the functional identity of the tissue. One interesting observation was the presence of

myofibroblasts which are α -SMA positive. Myofibroblasts differentiate from fibroblasts during the proliferative phase of wound healing. They are collagen depositing cells that have contractile properties which allow for wound contraction seen during the development of granulation tissue; the tissue type that is the hallmark of healing inflammation (Micallef et al, 2012). Although the presence of myofibroblasts was confirmed, along with densely organised collagen fibres, which can indicate wound contraction, there is insufficient evidence to conclude that wound contraction contributed to the extrusion of the electrode array over 10 months. Previous investigations of CI revision surgery following device failure show that electrode migration is most common with straight LW arrays (Rader et al, 2016). There is evidence from in-vitro experiments that applied tensile forces can skew fibroblast phenotype toward myofibroblast (Kollmannsberger et al, 2018). From this perspective, the presence of myofibroblasts may be an indicator of tensile forces associated with electrode migration. Further histochemical analysis of explanted extra-cochlear fibrotic sheaths will be required to test this hypothesis.

2.5.5 Cellular markers of inflammation and proliferation in an animal model

The present findings are supportive of a recent study of the CI wound healing mechanism in mouse and rat models. Using both in vivo and in vitro models of cochlear implantation, Bas et al investigated the biological mechanisms responsible for the stages of the wound healing process that occur in the cochlea upon insertion of an electrode analogue. In vitro analysis revealed increased leukocyte recruitment into the cochlea following insertion of the nylon filament demonstrating the early inflammatory response. Upregulation of genes involved in the recruitment of leukocytes to the wound site (Ccl3, Ccl2), proliferation (Pdgfb) and the promotion of angiogenesis (VEGFa) was observed in cochlear tissues following electrode insertion. Immunostaining for cytokines IL-1 β (pro-inflammatory) and Arg1 (anti-inflammatory) indicated the presence of macrophages with polarised phenotypes that overlapped in the wound site in the weeks following implantation; providing evidence for both inflammatory and proliferative stages. Histological staining of tissue harvested 30 days after implantation showed significantly more collagen deposition in the fibrous tissue that formed in implanted animals compared to controls. This was accompanied by positive staining for myofibroblasts and collagen type 1A, which were absent in the control animals (Bas et al, 2015).

2.5.6 Silicone Breast implants provide useful insights into the wound healing response to bioimplants

One particularly informative area has been breast implants. One study looked at breast implants that were removed because of symptoms such as pain allow detailed histological analysis. This study showed a low grade non-specific inflammatory response in all of the explanted capsules. The tissue response was characterised by CD68 positive histiocytes, some foreign body giant cells, and sparse variably distributed lymphocytes. X-ray analysis also showed calcification around the explanted capsule that was not associated with inflammatory cell participation (Kamel et al, 2001). These findings match the general consensus discussed above; namely a parallel fibrotic and foreign body response. It seems that bioimplants provoke the fusion of macrophages into FBGCs and also the stepwise development of a fibrotic sheath or capsule with monocyte derived cells embedded within extra-cellular matrix. A notable difference observed in breast implant observations is the occurrence of capsular contracture. This phenomenon is associated with implant failure and seems to be controlled by myofibroblasts which reorganise collagen fibres in the extracellular matrix and also exert significant contractile forces around the implant (Bui et al, 2015). The complex development and regulation of the fibrotic sheath over short and longer time frames is not fully understood.

2.5.7 Future development of methods for analysing tissue from explanted CIs

In order to validate the present findings, it would be desirable to repeat the investigation using newly explanted tissue. At the time of writing, a second sample has been collected from surgical explant, fixed and stored, ready for analysis. Lessons from each stage of procedure will be applied to the new protocols. For example, the orientation of the tissue in embedding media will be controlled more rigorously to improve translation of the from tissue (before sectioning) to the analysed images in the digital domain.

In addition to the discoveries made through this tissue analysis, two highly valuable assets have been created. Firstly, a multi-disciplinary working group involving academics, clinicians and a surgeon has been established. This collaborative group has proven itself to be effective carrying out the various steps of this research project and producing a scientific report, which was being prepared for submission to a peer reviewed journal at the time of writing. The group itself, as well as the culture around it will continue to address the challenges of CI performance using clinical and laboratory techniques. The second asset is the transferability of the laboratory techniques employed. Many of the cell types investigated in this human tissue e.g. macrophages, lymphocytes and myofibroblasts are also central to the immune-mediated tissue response to

implants in the mouse. The laboratory assays and imaging techniques can be transferred directly to the ongoing mouse project described in Chapter 4.

Chapter 3 Early detection of abnormal electrode impedance in a large sample of Med-El cochlear implant users

3.1 Introduction

3.1.1 Clinical monitoring of the CI tissue interface

Cochlear implantation provokes an immune mediated tissue reaction, involving FBR and fibrosis (Table 1-1). In the majority of cases, this tissue state remains stable over time, although in some instances there is tissue hypertrophy, or allergic type reactions which can lead to device failure. Lim et al. (2011) found that pathological FBR requiring revision surgery are rare. However, evidence from post-mortem temporal bones suggests that the characteristic indicators of FBR such as foreign body giant cells are more common than expected (Nadol et al, 2014; Seyyedi & Nadol Jr, 2014). This post-mortem evidence suggests that there may be a continuum of tissue type from sustainable mature fibrotic sheath to chronically inflamed and over proliferative. This includes bone growth, or osteogenesis which is a common complication following implantation (Somdas et al, 2007). Osteogenesis has been shown to significantly reduce speech discrimination scores, (Kamakura & Nadol 2016) and reduce subjective dynamic range of loudness (Kawano et al, 1998). The wide variability in tissue type and volume observed in post-mortem studies can be partially attributed to specific aspects of surgical trauma and electrode design, although these factors explain only a small percentage of variability. There are currently no validated clinical tools for monitoring changes in tissue status around the CI electrode array. Early indicators of the transition from a healthy short-lived tissue response to a chronic or abnormal response will help us to understand the process and select appropriate interventions to reduce the risk of device failure.

3.1.2 An overview of electrode impedance telemetry

A readily-available, non-invasive, clinical measure from a CI is EI telemetry (Hughes et al, 2001). Electrode impedance describes the ease with which electrical current flows through and between implanted electrodes. The CI stimulator delivers a current pulse that flows through the platinum electrodes of the CI and into the ionic environment of the cochlear tissue. This pulse must be calibrated so that it delivers sufficient charge to stimulate the SGN, without damaging the tissue.

High EI means the implant must produce a higher voltage to maintain the delivered charge. This has two undesirable effects: it drains the battery of the device faster and spreads the excitation across more SGNs which reduces pitch resolution. In general, low EI makes it more likely that an implant performs well. Electrode impedance is determined by delivering a low-level current pulse through the relevant electrode inputs on the CI and measuring the resulting voltage across the associated electrodes. It can be performed quickly in the clinic using a hardware interface that connects the implant to a computer via a transcutaneous link. In the clinic, EI telemetry is primarily used as an electrode integrity test. Open or short circuit faults (very high or very low impedances respectively) can easily be diagnosed, which is useful to clinicians in deciding whether a given electrode should be activated. These faults are relatively common: Carlson et al (2010) showed a 9% chance of either at least one open- or short-circuit fault in an implanted device.

3.1.3 Electrode impedance development over time

Electrode impedance develops over time according to changes in the macro and microscopic environment around the electrode array. Following surgical implantation of the CI electrode array the tissue undergoes some acute changes that are attributed to the early stages of the immune mediated tissue response (Shepherd et al, 1994). Figure 3-1 shows this change from A to B; EI increases between implantation and the date of activation (Saunders et al, 2002; Busby et al, 2002). The reduction shown in Figure 3-1 B to C describes the significant reduction in EI following commencement of electrical stimulation which reaches a plateau over 1-3 months (Jia et al, 2011; Henkin et al, 2006; Hughes et al, 2001). Evidence suggests that this reduction can be attributed to molecular processes occurring at the electrode surface, namely changes in the proteins adsorbed onto the platinum (Newbold et al, 2010) and an increase in effective electrode surface area that results from the hydride coating of the platinum during electrical stimulation (Rose & Robblee, 1990; Brummer & Turner, 1977). After the initial stimulation induced reduction, EI remains at a stable plateau in actively stimulated electrodes for several months (Henkin et al, 2006; Henkin et al, 2003). The dashed line in Figure 3-1 describes how deactivated electrodes show a slow increase over time (Dorman et al, 1992; Hughes et al, 2001). Vargas et al (2012) verified this pattern; they observed that average EI decreased within the first month of stimulation before steadily increasing and plateauing around four months.

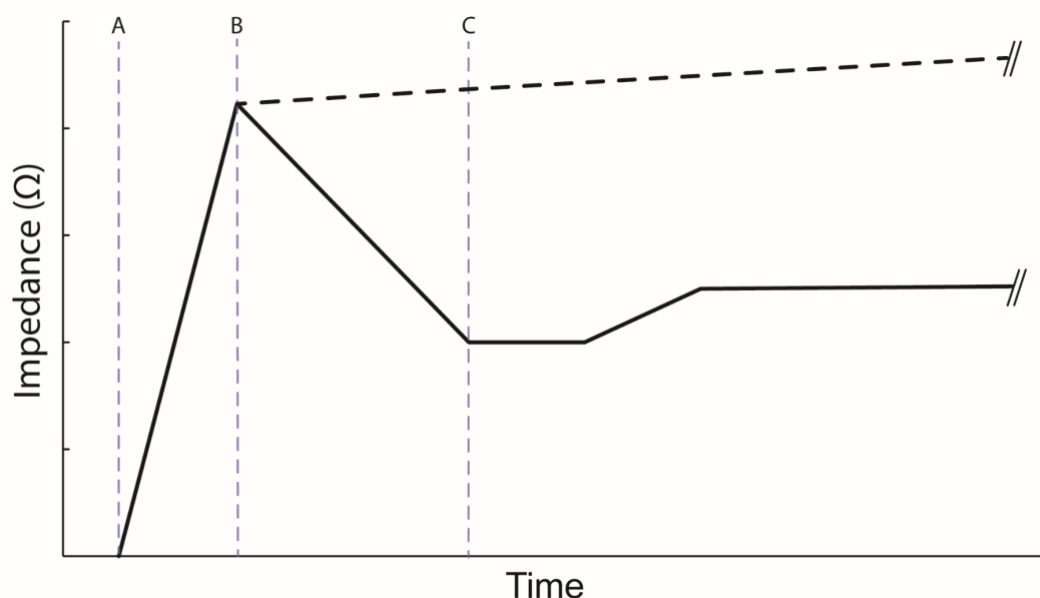


Figure 3-1: **Electrode impedance shows short and long-term evolution which is influenced by stimulation**

Schematic description of average EI development over time following implantation. Three time-points are indicated: A) Implant surgery. B) Device activation point. C) Stabilised impedance level following stimulation-induced reduction. Dashed line represents impedance behaviour at deactivated (non-stimulated) electrodes.

3.1.4 Electrode impedance as a biomarker of tissue change

Despite its primary role as an integrity check, EI can provide insight into the tissue around the implant. The volume and composition of bulk tissue surrounding the implanted electrode array influences EI significantly (Tykocinski et al, 2001). Clark (2003) recommends that EI levels should be monitored routinely as an indicator of cochlear tissue changes such as fibrosis and electrode surface roughening. In a study of chronic high-rate stimulation using cats, Xu et al. (1997) demonstrated that levels of fibrosis and presence of inflammatory cells were greatest in the cochleae that exhibited the greatest EI levels. Clark et al (1995) found that EI was significantly correlated with the amount of tissue around the electrode contacts and cases where inflammatory cells were found in the tissue showed particularly high levels of EI. Electrodes that exhibit high impedance levels are associated with raised thresholds of auditory sensation and reduced dynamic range (Busby et al, 2002) which can be associated with poorer performance outcomes (Wolfe et al, 2013). Electrode impedance increase and/or fluctuation are recognised as clinical indicators of soft-failure (Balkany et al, 2005). The onset of sudden changes in EI over time are correlated with marked loss of residual hearing in CI users (Choi et al, 2017).

Chapter 3

Considering the potential value of monitoring and interpreting EI fluctuations, there is a surprising lack of consensus on clinical utility of impedance telemetry. A number of authors have shown greater EI levels in the basal region of the cochlea compared to more apical locations. Jia (2011) analysed EI from 20 adult CI users and found higher levels at the basal position after three months that were maintained for the 36-month study duration. The pattern of raised EI at basal electrodes has been observed in other clinical CI studies (Busby et al, 2002; Hughes et al, 2001; Leone et al, 2017) and supports the temporal bone histology studies showing greater tissue growth in this region (Table 1-1). To date there is no published evidence of a clinical platform for systematic analysis of EI to produce normative models, against which individuals can be compared. The work presented here proposes such a model; a tool to allow individuals with statistically raised impedance levels to be identified early.

3.1.5 Clinical management of electrode status

There is currently no published or clinically available tool to guide interpretation of EI fluctuation. Available telemetry systems can automatically indicate excessively low or high levels to indicate gross electrode faults. However, lower level perturbations of EI associated with early stages of abnormal tissue response or electrode migration would not be identified. Electrode impedance data are displayed in single-patient view; the magnitude is displayed per electrode, which can obscure the view of time as a variable. The study detailed in this chapter presents EI data over 5 years using a method than allows time to be viewed along a traditional X axis. Moreover, the method allows for individuals to be viewed within the complete sample, to allow comparison. Organising the data in this fashion allows for population statistics to be used to explore the distribution and highlight outliers that would not be detected using existing systems. Clinical data review, like that proposed here, incurs a negligible burden on the CI user and minimal cost in both money and time.

3.1.6 Research aim and questions

As discussed in Chapter 1, there is a need to improve monitoring and understanding of the wide variance of CI performance outcomes and improve implant longevity. Evidence shows that the volume and type of tissue at the CI interface can influence performance outcomes. The broad aim of the present research project is to improve clinical methods for monitoring the interface. Although EI is a known and recommended candidate for this purpose, there are no published guides or software tools to aid clinicians in interpreting a given case.

A retrospective investigation of clinical data from USAIS was performed. Data were tested against a statistical threshold to identify individuals with raised impedance; those outside the main distribution but below the manufacturer's 'high impedance' warning level. Such cases are particularly interesting because no mechanism has been proposed for localised tissue proliferation away from the site of array insertion i.e. cochleostomy. This information could be used as early detection of unwanted tissue responses or electrode migration, which may adversely affect longer-term performance.

To address these gaps in knowledge, the following research questions were asked.

1. What is the distribution and long-term temporal trend of EI change for basal and apical electrodes?
2. How many individuals exhibit significantly raised impedance levels?
3. Of these, how many were identified with raised impedance at electrodes away from the base?

A further aim was to apply the findings to clinical decision making to improve patient management. For example, clinicians make case-by-case decisions to deactivate electrodes, adapt stimulation strategies and, in a few published cases, treat with steroids. It is necessary to describe the current clinical decisions around deactivation before any EI informed recommendations can be made. To address this, the following research questions were asked.

4. What is the rate of deactivation for each electrode for adults and children?
5. For each deactivation decision, what are the recorded reasons?

3.2 Methods

3.2.1 Statement of ethics

This study was carried out in accordance with the recommendations of the University of Southampton Ethics Committee (UEC) and Faculty of Engineering and the Environment Ethics Committee (FEC). The protocol (page 169). was approved by the FEC (Appendix B2, page 177). All subjects gave written informed consent in accordance with the Declaration of Helsinki [UEC Ethics ID: 17430]. Consent forms in Appendix B3 (page 181) and Appendix B4 (page 187).

3.2.2 Participants

The study included 172 adult (176 adult ears) and 47 children (74 ears). Mean adult age-at-implant was 58 years (18-91) and mean child age-at-implant was 4.5 years (1-17). Age-at-implant was calculated using the difference between 'patient age' and 'date of surgery'. The patients included were implanted using either cochleostomy (approximately one third) or round window insertion (approximately two thirds). Data were collected from two sources within the University of Southampton Auditory Implant Service (USAIS); the clinical software database MED-EL Maestro and the local patient database.

3.2.3 Electrode characteristics

Study participants had previously received MED-EL Standard (n=131), Flex-28 (96), Flex-24 (7), Flex-Soft (2), or Form24 (1) CI arrays. These are relatively long arrays enabling EI measures to be taken at a wide range of physical positions in the cochlea. For example, the Standard array has an active stimulation range of 26.4 mm, which is equivalent to two turns of the cochlea or an insertion angle of 720°. The other common array included in the study, Flex-28, is shorter with an active stimulation range of 23.1 mm. This creates some variability in the electrode positioning across the dataset which is not corrected. Each array carries 12 electrodes, each of which has either one or two exposed electrical contacts, depending on the array model. The effective electrode surface area for these MED-EL electrodes is 0.13-0.14 mm².

3.2.4 Electrode impedance data acquisition

The main study aims were to describe the trends of EI in a large sample and highlight individuals who deviate from this. A single manufacturer and limited number of arrays were chosen to minimise the hardware variability with a view to focusing primarily on the soft or biological mechanisms for impedance evolution. Importantly, the method of voltage acquisition and

impedance calculation varies significantly between manufacturers. The method used by the MED-EL telemetry system is shown in Figure 3-2. The change in EI can be separated into two components; access resistance and polarization impedance. The latter reflects the physical properties of the electrode surface and is therefore affected by protein adsorption, surface area increase and localised ionic changes (Tykocinski et al, 2005; Newbold et al, 2010). The stimulation-induced EI reduction, which occurs rapidly following device activation, is dominated by this component (Newbold et al, 2014). Access resistance is known to reflect the bulk material around the electrode such as fluid, cells and tissue and is likely to change over longer time scales. Clinically available impedance telemetry does not allow the two components to be measured separately; however, using the MED-EL system allows both impedance components to be captured. Therefore, changes occurring over different time scales give some indication of the relative contribution of the two components. The impedance measurement is performed using monopolar, low-amplitude bi-phasic current pulses, similar to those used for stimulation via the device. Total impedance (Z_t) can be calculated using total voltage which is measured at the end of the current pulse. Total impedance comprises the developing polarization component (Z_p) and the access resistance component (R_a). Electrode impedance is calculated as: $Z_t = V_t/I$

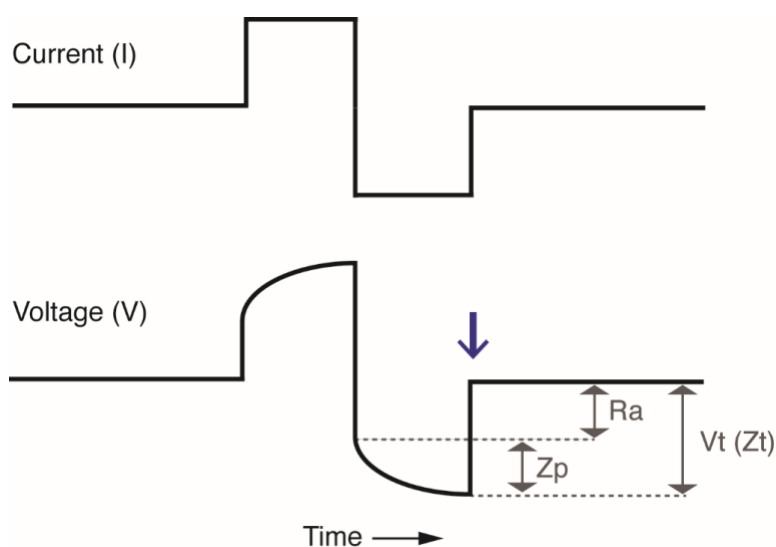


Figure 3-2: **Electrode voltage is influenced by the physical attributes of the electrode and surrounding environment**

Input current and resulting voltage across active and reference electrode during monopolar impedance measurement. The blue arrow indicates the measurement time. V_t , Total voltage; Z_t , Total impedance; Z_p , Polarization impedance; R_a , Access resistance.

3.2.5 Electrode impedance data management

Data were exported from MED-EL Maestro in Microsoft Access format. A custom database query was then used to return anonymised individual patients with their age at implant, implanted ear, date of birth, electrode activation status, electrode specific EI and corresponding date stamp. The difference between the date of implant and date stamp for each EI measurement was used to normalise data to a zero date (day zero is date of implantation) for each patient. Subsequent EI measurements were split according to the 12 individual electrodes and then averaged into 3-month time bins. All query results were exported in Microsoft spreadsheet format. Mathworks Matlab (R2018a) was used to read data from excel spreadsheets and plot figures 2, 3, 4, 5, 6, 7 and 8. Matlab code for processing and plotting EI data is shown in Appendix B5 (page 191). Matlab code for processing and plotting the reasons for electrode deactivation data is shown in Appendix B6 (page 200).

3.2.6 Deactivated electrode data filtering

It is very common for CI users to have electrodes deactivated by clinicians. As discussed, several studies show an increasing EI in the absence of electrical stimulation. Therefore, to minimise the effect of this upward bias on the analysis, only data from actively stimulating electrodes (black dots in Figure 3-4) were included in analyses from Figure 3-5 onwards; deactivated electrodes (red dots in Figure 3-4) were automatically removed from the analysis using a custom Matlab script shown in Appendix B5 (page 191).

3.2.7 Electrode numbers were corrected for extra-cochlea position

The electrode array is sometimes incompletely inserted due to anatomical constraints, which results extra-cochlear electrode contacts. In these cases, electrode number was corrected to allow meaningful comparison of electrode positions between patients. Surgical records were interrogated to determine presence/number of extra-cochlear electrodes. The following correction was applied: correct electrode number = [original electrode number + number of extra cochlear electrodes; maximum of 12]. Figure 3-3 shows how this results in new electrode numbers being assigned to intra-cochlear electrodes. This does not allow for an estimation of insertion depth, but it does enable analysis of electrodes from 'most basal' onwards. This correction is applied to all data in Figure 3-4, Figure 3-5, Figure 3-7, Figure 3-8, Figure 3-9, Figure 3-10. The correction is not applied to Figure 3-6 (analysis of reasons for deactivation) as it would mask extra-cochlear deactivations.

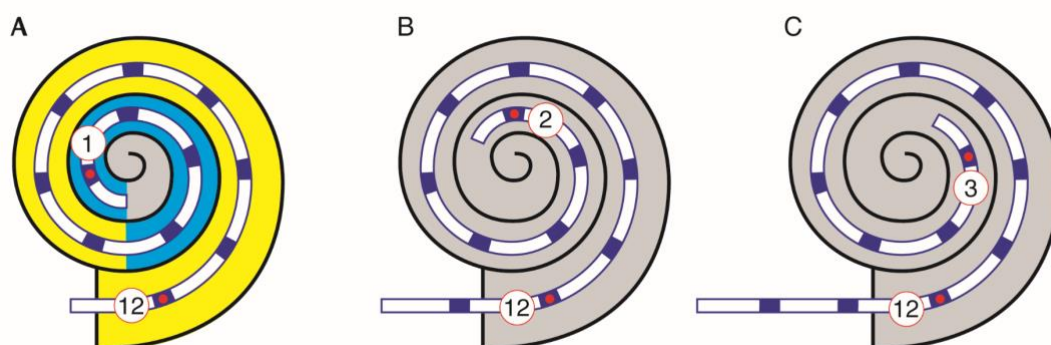


Figure 3-3: **Electrode number was corrected to account for extra-cochlear electrodes**

Schematic represents the MED-EL Standard electrode array showing that the basal-most electrode was corrected to 12, resulting in the effective number of electrodes being truncated A) Full insertion (720°). B) 1 extra-cochlear electrode. C) 2 extra-cochlear electrodes. In A, the three turns of the cochlea are indicated by colour: yellow, base; cyan, middle; grey, apex.

3.2.8 Statistical analysis

The software program MathWorks Matlab was used for data analysis. The adult and paediatric groups were analysed separately. Least-squares linear regression lines were fitted to the average impedance data (Matlab polyfit) (Figure 3-7).

Using Matlab, an outlier-labelling rule was applied to identify instances of raised EI (Figure 3-9, Figure 3-10)

$$T = Q_u + k(Q_u - Q_l)$$

(Hoaglin et al, 1986):

where Q_u and Q_l are the upper and lower quartiles, respectively and T is the threshold for an outlier. The constant k was fixed at 2.2, equivalent to a 5% probability of any given measurement being an outlier, for the adult and paediatric sample sizes tested (Hoaglin & Iglewicz, 1987). Cases were highlighted as statistically raised EI (SEI) when the EI was greater than T in ≥ 2 time bins within the first 2 years of CI use. Current methods of 'high impedance' detection are based on the upper limits of the stimulus delivery hardware for individual cases. Our new approach allows investigation of raised, but not extreme, levels of EI that would otherwise be considered sub-clinical.

Chapter 3

Highlighted cases of SEI are split into 'basal' (9 - 12) and 'non-basal' (1 – 8) depending on the position of the electrode showing raised EI. Basal electrodes, which are nearest to the insertion site, are expected to show significantly stronger immune-mediated tissue development: previous studies show significantly greater EI corresponding to this region. A judgement was made to categorise electrodes that are likely to be in the hook region as 'basal'. This is the straight region of the first cochlear turn, which extends 9 mm from the round window before it curves (Clark et al. 1990). The MED-EL Standard and Flex28 electrode arrays have contacts spaced at 2.2 mm and 1.9 mm respectively (Med-el, 2013). This means that the basal portion of the array (electrodes 9 – 12) spans 8.8 mm and 7.6 mm for Standard and Flex-28 electrodes respectively.

3.3 Results

3.3.1 Distribution of electrode impedance data varies with electrode

Data from 172 adults (176 adult ears) and 47 children (74 paediatric ears) were included in the main analysis of EI changes over time. Figure 3-4 shows subplots representing 12 separate electrodes. The magnitude of EI is plotted against time from initial CI activation to 5 years later. Each single dot represents the average EI level for a single patient over 3 months. Impedance data measured from actively stimulating electrodes are indicated by black dots whereas data measured at deactivated electrodes are indicated by red dots. The subplots both show a large number of deactivated electrodes, particularly at the most apical and basal electrodes (1 and 12 respectively), the reasons for which are analysed below. Figure 3-4a identifies a high number of deactivated basal electrodes for the adult population. Note that there are fewer dots at later time points, as not all patients had been using the device for the whole 5-year study period. The EI data were corrected to account for electrodes that were positioned outside the cochlea (see Figure 3-3). This was done to allow alignment of impedance data around an approximate physical position in the cochlea. The correction meant that plots for apical electrodes contain few data points, although this is not visible due to the high degree of overlay, especially for basal plots.

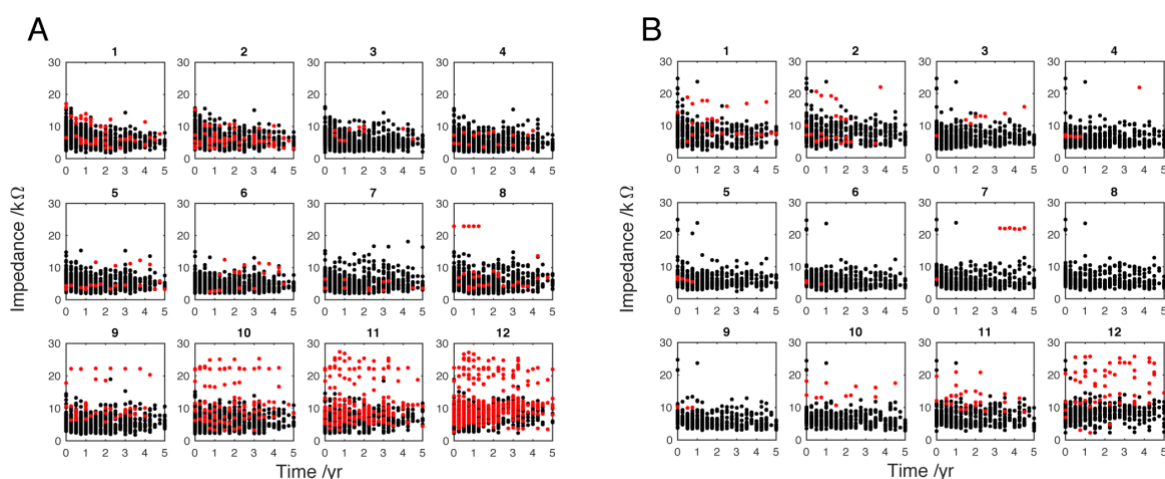


Figure 3-4: **Electrode impedance (kΩ) measured over 5 years from implantation**

A (adult, $n = 176$) and B (paediatric, $n = 66$) data are split into separate electrodes, from apical (1) to basal (12). Each dot represents the 3-month-average EI for one individual patient. The timeline for each patient begins with their respective device activation (time 0). Black dots, active electrodes; Red dots, deactivated electrodes. These data have been adjusted to correct for extra-cochlea position (see Figure 3-3)

3.3.2 Deactivation rate depends on electrode position

The percentage of active electrodes in the study population is shown in Figure 3-5. Deactivation is clearly most common in the most basal electrodes for both adults and children. The figure also shows an increasing number of deactivations over the first 1 to 2 years of CI use. The peak number of deactivations was higher in the adult group (Figure 3-5a) than the paediatric group (Figure 3-5b). Both groups had most deactivations at electrode 12, which can be seen as black at 2.25 years. At that epoch, only 60% of adult electrodes were active while 81% of paediatric electrodes were active. Electrode 11 showed the second highest number of deactivations for both groups. For example, 80% of adults had electrode 11 remaining active at 2.5, 3.25, 4 and 4.25 years. There was a slight increase in deactivations at the most apical electrodes compared to the mid-array for both adults and children. For example, adults had 88% of electrode 2 remaining active at 4 years. The children had 92% of electrode 1 remaining active at 4.5 years. A difference between the two groups was the mid-array electrodes were mostly active in the paediatric group, indicated by white area in Figure 3-5b. Although the adults were initially 100% active at electrodes 3 and 6, a few deactivations were made in the next 3-month epoch. In contrast, the children had 100% activation for the majority of the 5-year study period in electrodes 4, 5, 6 and 7.

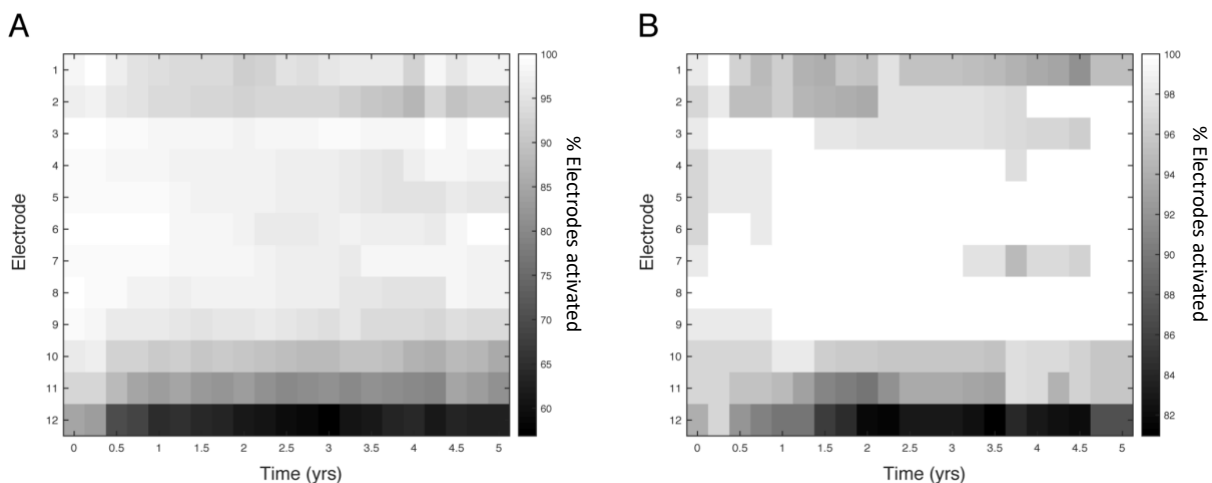


Figure 3-5: **Electrode deactivation was most common in basal electrodes, especially in adults** Percentage activation for 12 electrodes over 5 years. Each square represents a 3-month epoch for a given electrode. A (adult, n = 176) and B (paediatric, n = 66).

3.3.3 Clinical reasons for deactivation vary with electrode and age category

The patterns of deactivation seen above are better understood in light of the clinical reasons for deactivation shown in Figure 3-6. Electrodes in the most basal portion of the array were deactivated because they were outside the cochlea (extra-cochlear). In the basal electrodes (9 - 12), extra-cochlear position accounted for about one third of the adult reasons (Figure 3-6a), and about half of the paediatric reasons (Figure 3-6b). The majority of deactivations, however, in the adult group were informed by the patient reports of their subjective experience, such as ‘poor sound quality’ (See supplementary Figure B8-1 (page 221) for a complete list of deactivation reasons); there were relatively few deactivations owing to ‘Clinical Measures’ which offer objective information. The percentage of subjective ‘Patient Report’ reasons is highly likely to be biased by the age of the CI user; many of the children are very young and could not communicate their perception of sound. As shown in Figure 3-5, the children had significantly fewer deactivations overall.

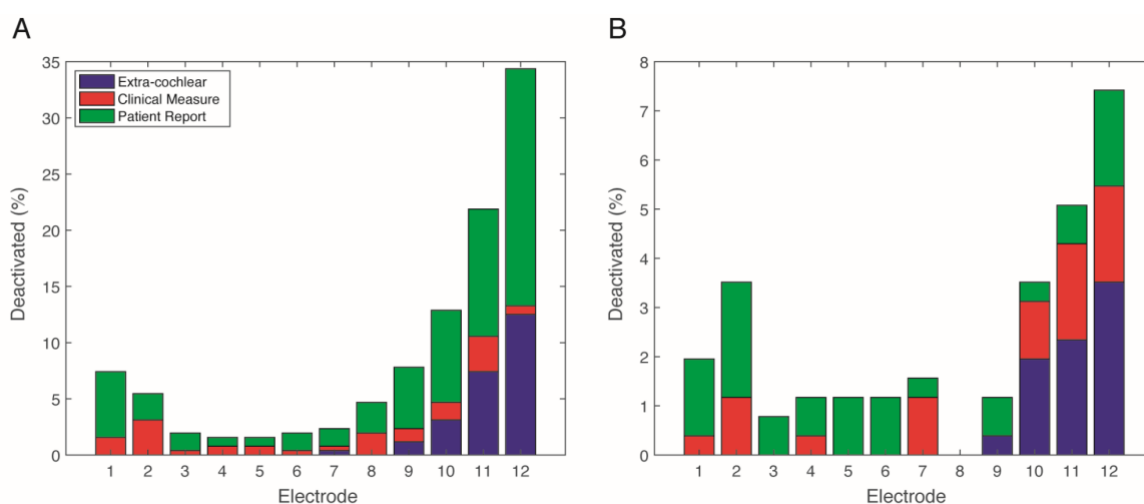


Figure 3-6: **Reasons for deactivation were proportionally different for adults and children**

Patient Report (e.g. poor sound quality), Clinical Measure (e.g. impedance telemetry). A (adult, n = 176) and B (paediatric, n = 66). Further breakdown of reason categories is shown in supplementary Figure B8-1 (page 221)

3.3.4 Long-term impedance trends vary with electrode position

Data points acquired at deactivated electrodes were removed at this stage of the analysis (red dots in Figure 3-4). Figure 3-7 shows the mean EI for the adults (Figure 3-7a) and the children

Chapter 3

(Figure 3-7b). Least-squares linear regression lines were fitted to the average impedance data (Matlab polyfit) for each electrode to show the trend of EI change over time. The adult group show a tendency for EI reduction at apical electrodes (negative slope), increase at basal electrodes (positive slope) and no change for mid electrodes. The paediatric group shows a different pattern of regression lines across the electrodes. All of the electrodes in this group, except electrode 1 show a positive slope. This suggests a difference in long-term EI evolution in children compared to adults, although the mean is more variable in this age group. This is probably caused by the lower overall sample size and fluctuation of sample size in each time window (i.e. by chance fewer individuals were seen in some 3-month epochs).

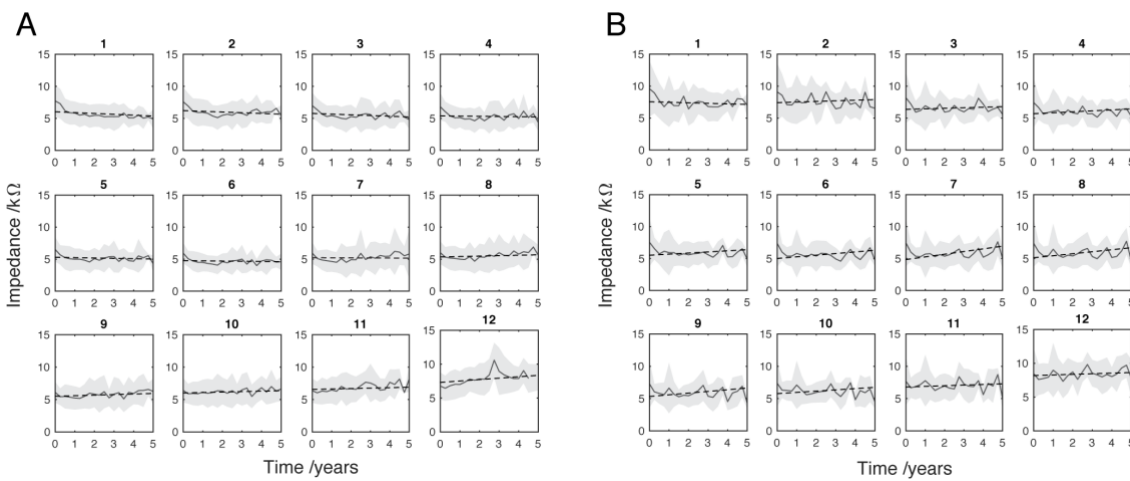


Figure 3-7: Mean EI for each electrode, over 5 years, for adults and children

Solid grey line = Mean EI, Light grey shading = Standard deviation, black dotted line = Regression line of least-squares. A (adult, $n = 176$) and B (paediatric, $n = 66$) data are split into separate electrodes from apical (1) to basal (12). At this stage of analysis data from deactivated electrodes was removed and electrode number was corrected to account for basal extra-cochlear electrodes. The timeline for each patient begins with their respective device activation (time 0) and subsequent points represent 3-month intervals.

3.3.5 Differences in adult and paediatric long-term impedance trends

The data above indicates that EI changes over time in a way that varies with electrode position. This is represented using a regression line for each electrode in Figure 3-7. The gradient of each line is plotted for each electrode in Figure 3-8. The adult group (Figure 3-8a) shows a positive relationship between gradient and electrode number. Each consecutive electrode shows a general

increase in gradient with electrode number. The largely monotonic relationship between gradient and electrode fits the consensus in the literature and highlights the phenomena quite simply. The crossover point from EI reduction (negative gradient) to increase (positive gradient) is at electrode 7, which is roughly the middle of the electrode array. This shows that EI evolution varies from base to apex in a continuous fashion. The relationship between fit-line gradient and electrode number in the paediatric group (Figure 3-8b) shows that EI largely increases over the 5-year period for all electrodes except number 1. The increase is steepest at electrode 7. The regression lines are an approximate linear fit and hence describe general trends. The paediatric sample shows a large degree of variability between timepoints because of the relatively low sample size and irregular frequency of clinical appointments. The peaks and troughs of mean EI cause some biasing of the fit lines, hence a conservative interpretation of differences between age groups.

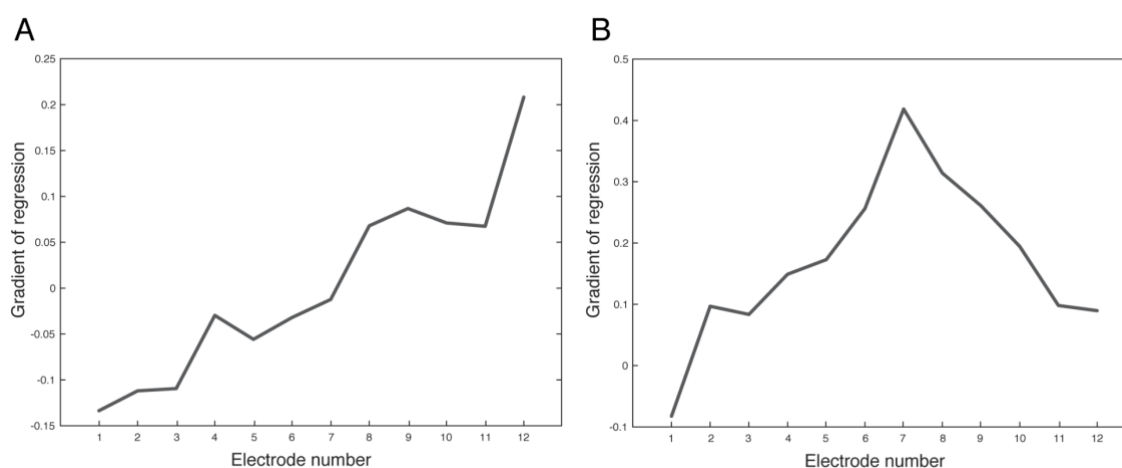


Figure 3-8: The 5-year trend of EI evolution for each electrode was different in adults and children

Grey line = Gradient of regression lines (Figure 3-7) for each electrode. A (adult, $n = 176$) and B (paediatric, $n = 66$). Positive gradient values represent a trend of EI increase over time and negative gradient values represent a trend of EI decrease over time.

3.3.6 Fourteen adult cases were identified with statistically high electrode impedance levels

An outlier labelling rule was used to highlight cases of statistically high EI levels (SEI). In the adult group, 14 patients met the SEI criteria (8%): one in basal electrodes, three in both basal and non-basal and 10 in non-basal electrodes only. The case shown in Figure 3-9a was implanted with a standard electrode array and the clinical record did not include the hearing-loss aetiology. The case shown in Figure 3-9b was implanted with a Flex28 electrode array and the clinical record

showed head injury as the cause of hearing loss. Figure 3-9a shows an EI increase at electrode 7 over the 5 years of CI use. This electrode is highlighted by (*) to indicate that EI level met the SEI criteria. A key observation is the difference in temporal development and absolute level of EI of this electrode compared to its immediate neighbours. This difference is unusual for non-basal electrodes where the EI is often mirrored in neighbouring electrodes. The absolute EI level shown in Figure 3-9b is lower than Figure 3-9a although the SEI criteria have been met at electrode 2. The figures corresponding to the other 12 individuals are shown in Appendix B8 (page 221).

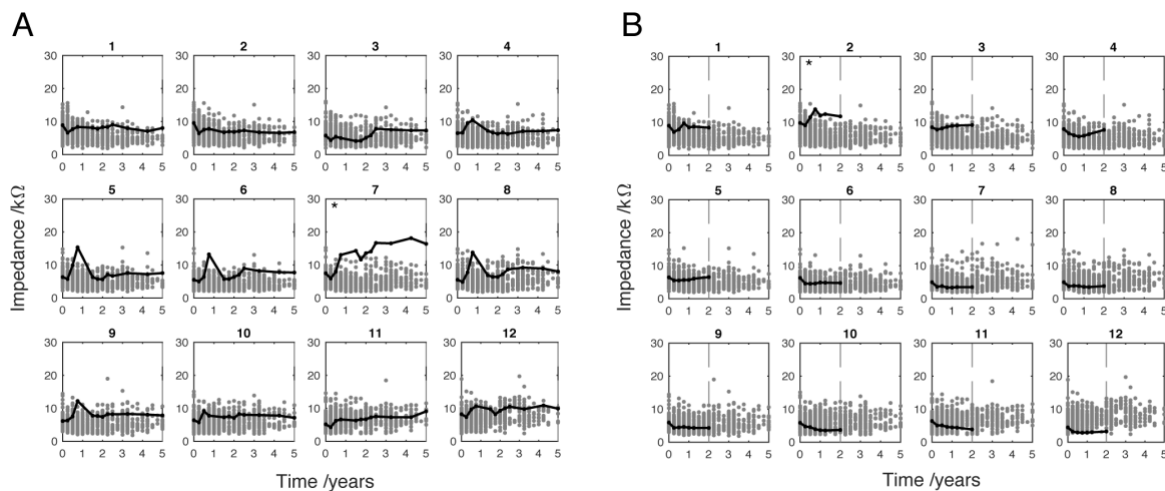


Figure 3-9: **Two individual adult cases showing EI at active electrodes only**

Case A shows 5 years CI use. Case B shows 2 years CI use indicated by vertical dotted line.

Electrode marked by * met the SEI criteria which indicates high EI compared to the sample distribution. These data have been adjusted to correct for extra-cochlea position (see Figure 3-3)

3.3.7 Three paediatric cases were identified with statistically high electrode impedance levels

In the paediatric group, three cases met the SEI criteria (5%): two in non-basal and one in both basal and non-basal electrodes. Figure 3-10 shows the EI measurements taken from two paediatric cases. Each was found to meet the SEI criteria in one of two implanted ears. The black line shows that EI is greater in these cases than the other cases in the sample (grey dots) which are mostly clustered around or below 10kΩ. The case shown in Figure 3-10a was implanted with a Flex-28 electrode. Clinical records show they were diagnosed with congenital hearing loss associated with Pendred syndrome. This case met the SEI criteria at electrode 5 (indicated by *). After the initial activation and tuning appointment, the EI increased relatively rapidly to peak

around one year of CI use. A similarly sharp reduction is shown in the following three-month period before EI plateau around 12k Ω . This case shows a general tendency for raised EI over the duration of observed CI use. This is especially marked in electrodes 2, 3 and 4, although the level did not meet the criterion for SEI. The case shown in Figure 3-10b was fitted with a Standard electrode array. The clinical record showed a diagnosis of genetic mutation of the gene GJB2 (connexin26). The case shown in Figure 3-10b met the SEI criteria at electrode 7, 8, 9 and 10. Unlike the pattern shown in Figure 3-10a, the EI tracked a stable level across the period of use. The figure for the remaining individual is shown in Appendix B8 (page 221).

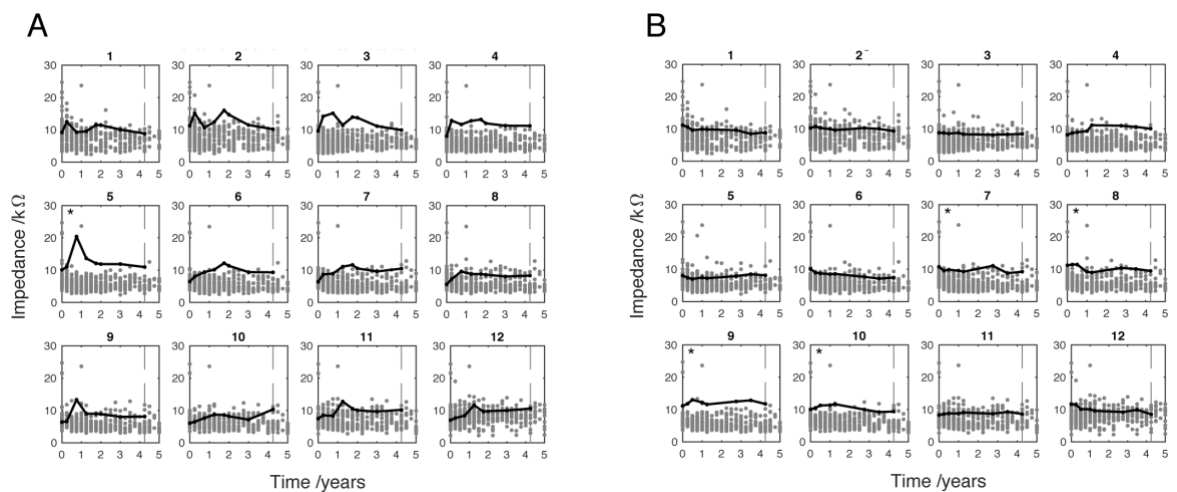


Figure 3-10: Two individual paediatric cases showing EI at active electrodes only

Case A shows 4.25 years CI use (indicated by vertical dotted line). Case B shows 4.25 years CI use (indicated by vertical dotted line). Electrode marked by * met the SEI criteria which indicates high EI compared to the sample distribution. These data have been adjusted to correct for extra-cochlea position (see Figure 3-3)

3.4 Discussion

3.4.1 Summary of main findings

This retrospective study of clinical data from a large sample of MED-EL CI users showed population-level trends in EI across time and between cochlear regions, and also yielded a potential new approach to define EI outliers for whom further clinical action may need to be taken. Research question 1 addressed the trend of impedance change over time for basal vs apical electrodes. The results showed that electrodes exhibit distinct trends of impedance evolution over 5 years. In the adult group growth in the basal electrodes contrasted with reduction for apical electrodes. The results also describe the range of the adult and paediatric dataset, which provides useful insights into individual variability. One reason for characterising the EI trends over time was to improve interpretation of any individual deviation from the normative range. Research question 2 asked how many individuals show statistically raised EI. The main analysis showed 8% of adults and 5% of children exhibited raised EI levels compared to the sample distribution. These cases were detected using a statistical outlier-labelling rule, which could be used to inform electrode deactivations with improved objectivity. Research question 3 queried the position of SEI electrodes. The adult group showed one in basal electrodes, three in both basal and non-basal and 10 in non-basal electrodes only. The paediatric group showed three cases met the SEI criteria (5%): two in non-basal and one in both basal and non-basal electrodes.

Research questions 4 and 5 focussed on the percentage of electrode deactivation and the reasons for them respectively. The analysis showed that most adult electrode deactivations were made because of reported subjective experiences rather than clinical measures such as neural-response telemetry or electrode-impedance telemetry. Adults also showed a greater proportion of electrode deactivations than children, which may be caused by differences in capacity and confidence for verbal communication. The method used here to detect raised impedance in individuals of a clinical population may offer an opportunity to activate or deactivate electrodes long before the current device-specific floor or ceiling levels are reached.

3.4.2 Electrode impedance changes associated with tissue development

This chapter presents the evolution of EI for adults and children at twelve electrodes along the MED-EL array. The measurement at the first (0 months) and second time points (3 months) identifies a drop in EI across all conditions. The drop is consistent with an increase in electrode surface area due to the electrolytic activity (Brummer & Turner, 1977), and/or clearance and reorganisation of organic molecules, cells, tissues on and around the electrode (Marsella et al,

2014). The main observation in the adult group is EI growth at basal electrodes and EI reduction at apical electrodes. Growth in basal-electrode EI is likely to be caused by fibrosis and osteogenesis based on its slow evolution over time. Previous findings from a post-mortem study of cochleae from CI users have shown the levels of fibrotic and bone tissue to be greatest in the basal turn of the cochlea (Fayad et al, 2009). The magnitude of fibrosis is also correlated with the level of trauma caused by surgery (Richard et al, 2012). It is also possible that there are differences in propensity for tissue response in different regions of the cochlea across individuals, e.g. due to anatomical variations such as vasculature, nerve innervation or scalae width.

It was observed that children show an increase in EI for all electrodes except electrode 1. This data shows more variability over time than the adults, possibly due to the lower number of cases analysed. If a difference exists, the likely explanation is a difference in the chronic tissue response to surgery in children and adults (i.e. developmental stage) or differences in aetiology among children vs. adults. Previous studies have shown increasing EI for basal, mid and apical electrodes in children compared to the adult group which only showed increase at the base (Hughes et al, 2001; Busby et al, 2002). The present findings appear to support this although no formal age-group comparison was made. There is some published evidence of differences in hearing preservation between adults and children. One study showed a small trend towards better residual hearing in children (Zanetti et al, 2015), although another found no effect of age (Skarzynski et al, 2013). The findings of the present study suggest an increased growth of intra-cochlear tissue around the base that is particularly clear in the adult group.

The fact that gradual increases in basal impedance were observed is indicative of a slow proliferation of tissue indicative of immune-mediated fibrosis. Studies have shown that such reactions lead to structurally organised fibrotic tissue and bone (Somdas et al, 2007; Li et al, 2007), which would begin to emerge within the same timeframe as the impedance increase shown here i.e. months to years. It should be noted that the exclusion of deactivated (mainly basal electrodes) would suggest that the findings under-estimate the extent of basal tissue growth. The data shows individual variability in EI, which may reflect surgical approach, age, aetiology, noise exposure or other factors. The cases included were implanted using either cochleostomy (approximately one third) or round window insertion (approximately two thirds). No formal assessment of surgical approach and its impact on EI was carried out. Evidence shows that this variable has no significant effect on EI or listening performance for phonemes or sentences (Cheng et al, 2018).

3.4.3 A novel method for early detection of increased electrode impedance

The population-based method of outlier detection applied in this study offers an objective insight into intra-cochlear tissue status. Ongoing challenges for neuroprostheses include biocompatibility and functional longevity (Adewole et al, 2017). Performance decrement, as contrasted with frank failure, is difficult to monitor and almost impossible to predict using current approaches. The consensus in the field of CI for clinical assessment of soft failure recommends a broad-spectrum approach. This includes patient interview, medical investigations such as X-ray imaging, audiological and hardware testing (Balkany et al, 2005). This relies on the CI user having well-established linguistic abilities. In children the consensus is that the clinician should record and interpret the user's behaviours, although this has limited reliability (Moberly et al, 2013). The methods presented here allow deeper enquiry into the telemetry data that is already routinely gathered. Results suggest that a minority of raised impedance cases can be detected in a population, which may aid triaging of patients, including those who can provide only limited verbal reports.

There is evidence to suggest the immune mediated tissue response to CI impacts long-term functionality. The influence of biological or soft factors at the interface are poorly understood and may well contribute to the wide performance variability that is still unaccounted for. It is possible to measure the tissue response using impedance telemetry, although the currently available tools are limited to detection of extreme high or low EI levels. In order to address this, statistical method of outlier labelling was performed to detect cases of raised impedance (SEI). This is distinct from the absolute threshold used by the MED-EL and other manufacturers, which serves to highlight high and low impedances that are extreme enough to prevent normal current delivery. These cases mostly indicate hardware faults and extra-cochlear electrode position. The cost of using high threshold methods for detecting raised impedance is the relative insensitivity to biological perturbations associated with EI changes below 20k Ω . The outlier labelling technique could be validated by measuring CI performance following customisation of processor maps where electrodes with SEI levels are deactivated. If validated, this would provide a quicker and more clinically useful method to guide electrode deactivation as compared with more challenging and time-consuming methods based on psychophysical measurements proposed in the literature: Mathew et al. (2017) and Zhou (2017). Further work to determine any correlation between the sorts of psychophysical methods proposed by these authors and outlier-EI values would help to further validate this approach.

3.4.4 Discretely localised electrode impedance increase may indicate insertion trauma

The long-term pattern of change of EI in those individuals identified as outliers may inform the underlying mechanism. Results show EI increase at discrete electrodes, some developing slowly over the 5-year study period. In several cases (13 of 14) the SEI criteria was met at non-basal electrodes, which is counter to the model that the tissue development driven by inflammation is most prevalent at the base near the site of array implantation (Bas et al, 2015; Richard et al, 2012). In some cases, gradual EI differences are specific to particular non-basal electrodes. For example, electrode 7 in Figure 7A shows a pronounced example of EI increase that develops slowly over many months. In most cases, this was limited to one, or at most, very few electrodes, which suggests the change is driven by spatially localised factors. It is noted that the relative position of electrodes is not standard across all participants. For example, electrode 1, which is most apical will be at a greater insertion angle for ‘Standard’ arrays compared to ‘Flex 28’. No hardware malfunctions were detected, and the electrode remained actively stimulated for the duration of the studied time period. One possible explanation is the presence of a spatially discrete trigger of inflammation such as mechanical trauma. This might have occurred during surgery as the electrode array tip passed through this region of the cochlear duct causing an abrasion, as lateral wall damage is known to elicit fibrotic changes (Li et al, 2007). To further understand the cause of raised but not “open-circuit” EI in particular electrode regions, the ability to cross-reference with newer and more sensitive imaging methods (Aschendorff, 2011) could also lead to a greater understanding of whether localised surgical trauma, cochlear anatomy, or other factors, predispose some individuals to showing higher EI values in apical or mid-cochlear regions.

3.4.5 Electro-chemical changes at the electrode surface may be reflected in electrode impedance

Electrical stimulation is known to affect the chemistry of the endo-cochlear environment. In the case of low charge density, the current flows via capacitive charge transfer where ions move along an electrochemical gradient back and forth in response to the biphasic stimulus. Examples of these ions are sodium and potassium in the perilymph. If the charge density is higher, due to high current flow or low electrode surface area, then charge is transferred by faradic means. One mechanism involves changes to molecules via oxidation and reduction (redox) that, assuming the biphasic current pulse is balanced, can oscillate between states with electrons being lost and gained in a process of electrolysis. In this case the electrode is oxidised to produce platinum oxide.



Another mechanism of faradaic charge transfer is hydrogen plating. In this case the electrode is plated with hydrogen atoms to produce platinum hydride.



In cases where the charge is above safe limits (Rose & Robblee, 1990) the chemical changes become permanent which gives rise to free oxygen and hydrogen gas which are toxic to biological tissues. The process can also lead to platinum dissolution, pH change, and protein-metal complexes (Brummer & Turner, 1977). These deleterious effects are largely avoided by careful design and implementation of CI device technology. Capacitors are used to block any direct current, electrodes are shorted between pulses and electrode size is carefully considered to avoid injection of high charge levels. However, it is not possible to avoid Faradaic charge transfer in all cases. Therefore, some CI users show performance fluctuations along with changes in EI due to platinum hydride formation (Hughes, 2013). In addition to the creation of toxic chemical species the process of hydrogen plating and oxidation can increase the electrode surface area which manifests as lowered impedance. This doesn't necessarily have a detrimental effect on CI function but may affect the interpretation of EI measurements.

These processes are safe and reversible when bi-phasic charge-balanced pulses are used. It has been suggested that such charge delivery mediates the process of protein adsorption onto platinum electrodes and can affect the organisation and density of the fibrotic capsule (Newbold et al, 2010). It is well documented that electrode deactivation contributes to EI increase, so ideally clinicians would utilise objective evidence before making electrode deactivations, which makes future reactivation more difficult. Neuburger (2009) presents further evidence of the effect of electrical stimulation on impedance. They observed cases of increasing EI in CI users with high rates of stimulation, which necessitate short pulse-width and high current to produce the desired perceived loudness. A therapeutic intervention involving increased pulse-width along with antibiotics and steroids proved effective at significantly reducing EI. The author suggests that the original EI increase could be caused by the occurrence of out-of-compliance charge delivery leading to slight asymmetries in bi-phasic pulses. Early detection of increasing impedance could therefore be clinically important. It might adjustment of stimulus parameters, which could result in lower EI, and reduce the likelihood of voltage compliance problems.

3.4.6 Electrode impedance as an objective guide to electrode deactivation

Analysis of the proportion of deactivated electrodes showed that electrode deactivation was primarily at basal electrodes for both age groups. However, the reasons for deactivations were overwhelmingly patient feedback from adults whereas the most common reason in children was

extra-cochlear position. In addition, deactivation was less common in children than in adults. One possible explanation for this was that clinical decisions about deactivations are more cautious with children, or, rather, that adult feedback to clinicians does lead to deactivation of electrodes with more fibrous tissue grown/higher EI (e.g. primarily basal). This begs the question of whether choice to deactivate electrodes is optimal, and in particular whether the smaller proportion of basal electrode deactivations among children in particular is clinically appropriate or whether deactivation of basal electrodes in adults is excessive. Cross-referencing with the outlier labelling method of EI analysis and other methods noted above could help to determine the answer to these questions. Alternatively, it may be that some differences in aetiology and /or anatomy predispose the child's cochlea to be more susceptible to other types of problem (e.g. non-auditory stimulation).

3.4.7 Future work

3.4.7.1 Proposed benefits of measuring impedance sub-components

The increase in total EI can be separated into two components; access resistance and polarization impedance. The former is known to reflect the bulk material around the electrode such as fluid, cells and tissue. The latter reflects the physical properties of the electrode surface and is therefore affected by protein adsorption, surface area increase and localised ionic changes (Tykocinski et al, 2005; Newbold et al, 2010). Most currently available telemetry systems, including the MED-EL system used here calculate EI using the methods shown in Figure 3-2 to capture total impedance only.

Evidence from clinical and in-vivo animal experiments show that the stimulation induced EI reduction is dominated by the capacitive reactance component i.e. the electrode surface micro-environment (Newbold et al, 2014). The slowly developing increase in impedance, which is observed in stimulated and non-stimulated electrodes (Figure 3-1c), represents the bulk tissue or media surrounding the electrode array. Because the polarization impedance produces a time-variable change in voltage, its effect can only be measured by sampling more than one voltage measurement during the current pulse (Swanson et al, 1995). Newbold et al (2014) was able to take advantage of the non-instantaneous voltage growth characteristic of polarization impedance to calculate the components of total impedance. Findings showed that the rapid (within 30 minutes) stimulation induced reduction in impedance was dominated by the polarization component, which localises the underlying mechanism to the electrode-electrolyte interface rather than the bulk tissue. The clinical study was supported by an animal model which allowed

for a percutaneous method of impedance measurement which greatly improves the resolution of the voltage waveform acquired.

Figure 3-11 shows the electrical behaviour of the interface as resistor-capacitor model. The media or bulk material surrounding the electrode array has resistive properties and can be modelled by a resistor. As discussed, current can flow across the interface by either ionic or Faradaic means, depending on the charge density. The ionic component is modelled by a capacitor, while the faradaic component is modelled by a resistor. The platinum electrode contacts, and the platinum-iridium wires carry current by electron flow so are modelled by another resistor. The capacitor (interface) creates a lag in voltage and therefore can only be measured by a system that allows multiple samples over time. Future extension to the work presented here would benefit from an adaptation to data acquisition that allows the two components to be isolated. At the time of writing CI manufacturers are introducing new telemetry systems that allow this measurement (personal correspondence with Barry Nevison, Cochlear Europe Ltd). This technology, which has been used in previous animal studies (Newbold et al, 2014) will be integrated into clinical systems to allow quick and easy calculation of access resistance, polarisation impedance and total impedance. The ability to separate the effect of the interface micro-environment from the bulk material will help distinguish between electrochemical changes on the electrode contact and immune mediated tissue growth such as FBR, fibrosis and osteogenesis.

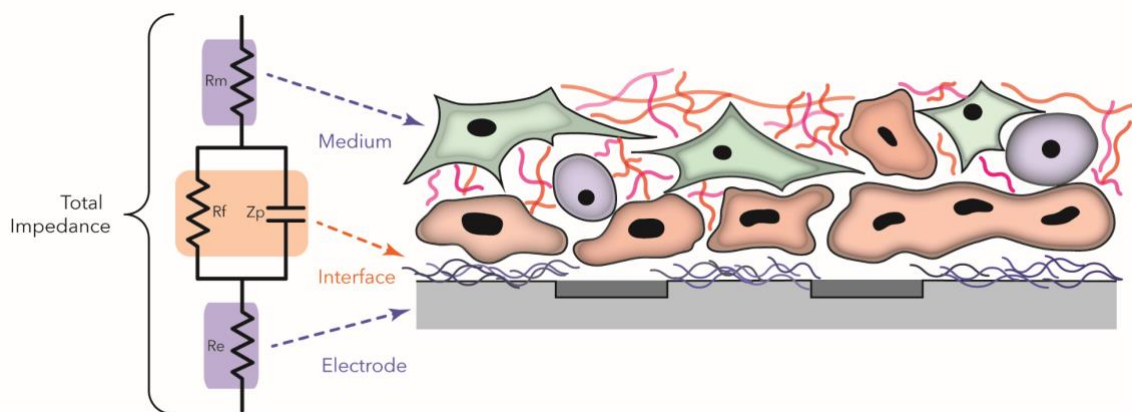


Figure 3-11: **The physical properties of the interface between electrode and tissue can be modelled by a resistor-capacitor circuit**

The electrode is shown enveloped by protein and cellular components of the fibrotic sheath. The medium (bulk material such as fibrosis) is modelled by a series resistor. The interface between the medium and the electrode is modelled by a parallel resistor and capacitor.

3.4.8 Conclusion

An important outcome of this work is the insight gained from applying a custom analysis protocol to existing clinical data. The approach was to characterise sample-wide trends and apply an outlier detection rule that could improve our early detection of sub-optimal performance. A key benefit of using this method alongside manufacturer-specific proprietary telemetry systems is the sensitivity to changes of lower magnitude that may be associated with performance. This offers clinicians and researchers a method for interrogating their existing population data to identify incremental changes in device behaviour, without extra financial, technical or ethical burden.

The immediate benefit of these methods and findings is to give clinicians fresh insight into their existing data. The increasing size and accessibility of clinical datasets presents an opportunity to professionals working with CI and other neuroprosthetics. Population-wide norms can be used to better interpret measurements from individual patients. The aim is to personalise clinical management to improve the function and biocompatibility of the implant interface over a user's lifetime.

Future work to explore the sensitivity of SEI method as a biomarker of CI performance decrement should combine EI measures with analysis of the physical tissue around the implanted electrode array. Chapter 2 presents histochemical analysis of human tissue following explant. In this case, EI was measured regularly over the 10 months period between device activation and explant. It would be revealing to see this data included in a large sample investigation. With some modifications the data extraction and analysis method could be applied to Cochlear devices. This may allow such cases to be detected or confirmed earlier. Such observational studies are limited by the large degree of variability across patients. Chapter 4 presents the development a mouse model that will allow control and manipulation of experimental variables including genetics and immune/inflammatory status. The model is being developed to allow electrical stimulation and EI measurement. By combining EI as an outcome measure with 3D X-ray histology, it will, in future, be possible to close the loop between the electrical properties and tissue status of the implanted cochlea.

Chapter 4 A mouse model of the cochlear wound healing response and resulting CI-tissue interface

4.1 Translation from a mouse model to human CI users

The aim of this project was to develop a mouse model for CI to allow investigation of the tissue response following surgical implantation and chronic stimulation. Due to time limitations, the work presented here describes the preliminary methodological development which will contribute to the continued creation of the mouse model for CI as part of other PhD studentships. A desirable attribute of such a model would be its generalisability to human CI users. The preceding chapters identified three key goals for this model. Firstly, the literature highlights a wide range of individual variability. The model system will therefore include controlled genetic and environmental variables so the effect of an independent variable such as surgical approach can be quantified with minimal within-group variance. Secondly, Chapter 3 shows the potential of impedance telemetry as an indicator of abnormal changes in intra-cochlea conditions and fibrosis. The model should allow replication of the clinical measurement regime to investigate the group statistics in a relatively controlled system i.e. genetically homogeneous, healthy and immunologically unchallenged. Thirdly, the model should allow detailed laboratory analysis of the intra and extra-cochlea tissue that developed following CI and chronic stimulation.

4.1.1 Selection of mouse as the model species for cochlear implantation

A model system for biomedical research should be selected depending on the goals and research questions. Previous research has shown some utility in investigating the CI-tissue interface, with regard to its electrical properties, in an in-vitro system (Newbold et al, 2011). However, the motivating research aims of this project are to directly compare to the human CI condition. The specification of the system must have considerable overlap with human CI, especially with regard to the natural wound-healing response in and around the cochlea. Non-human animals and especially mammals are therefore well suited, being closely related to humans. Rodents are the most common choice in auditory research as the cost, logistical challenges and availability of larger animals such as rabbits, cats and dogs can be prohibitive (Reis et al, 2017). The gerbil has been successfully used for in-vivo CI research. The advantages of the gerbil as a model including large auditory bulla and a frequency range similar to that of the human auditory system (DeMason et al, 2013). The disadvantages of the gerbil are that its husbandry requirements are quite specialist and it is less well established than the mouse with regard to genetic tractability.

Chapter 4

The scope of research performed in mice has been greater than other animals since early 2000s and since 2015 the number of studies using a mouse model has been greater than all other species put together. The various sub-strains of inbred mouse such as C57BL/6J, CBA/J and DBA/1J have become the clear choice for hearing and balance research in recent years (Ohlemiller et al, 2016).

The mouse was selected as a non-human animal model in the present study for its: 1) Genetic tractability. Laboratory strains exhibit near zero population variability and commercially available mutant inbred strains present myriad options for experimental modelling of human hearing loss aetiologies. The broad focus of this research is to better understand individual variability by A) characterising norms across a population and B) Identify and describe edge-cases where performance is reduced and/or device failure occurs. Therefore, the ability to control genetic and environmental variability are highly desirable in a model of CI. 2) Well described immunology in mice. In fact, mouse is the main model system used for immunological research (Mestas & Hughes, 2004), which means there is a wealth of knowledge to inform interpretation of findings. 3) The volume and scope of mouse immunological research over recent years has led to the development of an extremely wide range of reagents and products specifically targeted to mouse research. These off-the-shelf products, such as antibodies are well validated and relatively low cost.

4.1.2 The mouse model of CI is viable and shows development opportunity

Successful implantation of the mouse cochlea has been demonstrated. One study used two dummy array types: inert plastic filament and parylene coated platinum. Cone-beam CT was used to confirm successful placement of the array in the scala tympani. The spatial resolution of the images is adequate to confirm array position but relatively low. Histological staining (toluidine blue) showed tissue development surrounding the arrays suggestive of a fibrotic capsule, although no cell or molecule specific antibodies were used. Other structures of the organ of corti and SV were unharmed by the procedure (Mistry et al, 2014). The evidence presented by this study is encouraging as a proof of effective implantation of the mouse cochlea. The approach could be extended to address the challenges of understanding the CI-tissue interface in humans. This should include a functional electrode array that allows chronic stimulation. As discussed in Chapter 1 electrical stimulation has a measurable effect on EI which is attributed to the electrode surface micro-environment. There is some evidence that stimulation can contribute to platinum dissolution (Clark et al, 2014), although modern devices are designed to minimise this effect. The effect of chronic stimulation on the CI-tissue interface with regard to the immune mediated wound-healing response is not fully understood. More work is needed in this area.

A group at the University of Melbourne and the Bionic Ear Institute have developed a mouse model that allows chronic cochlear stimulation in free roaming animals via a current inducing cage system (Millard and Shepherd, 2007). Their device specification was designed to match human CI devices closely, stipulating: fully implantable, duration over 10 weeks, charge balanced biphasic pulse stimulus, variable pulse width, up to 5-volt compliance and capacitively coupled electrodes. (Millard & Shepherd, 2007) note that other fully implantable stimulator devices had previously been developed (Winter et al, 1998), but none small enough for mouse. The same group extended the work showing refinement of their surgical technique, proof of electrical cochlear stimulation using ABR and histological tissue analysis. Before this study, research had been limited by the lack of availability of a small enough electrode array and stimulator assembly. The findings of histology showed new bone formation and fibrosis of the scala tympani mainly in the basal turn of the cochlea, although animal numbers were too low for statistical analysis. These two studies demonstrated the potential for chronic stimulation in a mouse CI model (Irving et al, 2013).

Further refinements of CI surgical techniques and a platform for chronic stimulation in mouse have recently been published. A detailed open-access protocol has been established that demonstrates the mouse can be implanted safely and reliably, despite the size challenge and vulnerability of the stapedial artery (Navntoft et al, 2019). Progress has recently been made with chronic stimulation of the mouse cochlea. A study by (Claussen et al, 2019) investigated animals that were successfully implanted and chronically stimulated for around 20 days. The device was connected via a percutaneous commutator, which allowed delivery of the signal from the ambient sound in the laboratory. The receiver stimulator was manufactured by Cochlear, using technology developed for human CI devices. Nerve response telemetry (NRT) proved effective stimulation of the auditory nerve. They combined X-ray μ CT and histological imaging; a technique known as 3D X-ray histology, in a similar way to the methods proposed in this chapter.

4.1.3 Research aim and goals

The main objective of this project is to develop a mouse model to allow investigation of the CI-tissue interface while controlling genetic and environmental sources of variability. A key priority is to maximise the generalisability of the model to human clinical populations. To this end, the following two aims are defined.

1. Controlled genetic and environmental variables to model the human condition
2. Impedance telemetry measurement following chronic stimulation to verify human data

Chapter 4

Two benefits of the mouse are noted with regard to genetics. Firstly, the near homogenous genotype across a given colony of inbred strain. This means that a large source of human variability can be controlled. Secondly, the availability of mutant strains affords the ability to test the effect of specific factors that affect human hearing loss such as DFN mutations which cause permanent sensori-neural hearing loss in humans. The impact of such aetiological factors on the CI-tissue interface has not been investigated.

Assessment of such variables necessitates a high-resolution method of data collection. In order to characterise the wound-healing response at the CI-tissue interface in greater detail than the study discussed above, the following aim was defined.

3. Acquire and spatially align X-ray μ CT and immunohistochemical light microscopy

The initial development of the mouse model was done with the C57BL/6 mouse strain. While not completely identical, a colony of animals has minimal genetic variability. They were housed and treated identically with regards to food, water and housing. This regime will allow the desired level of homogeneity of genotype and environmental exposure so a reliable average wound-healing response can be characterised. The model will progress to chronic implantation and stimulation and allow testing of various factors which may influence CI performance but are poorly understood. This will include extrinsic factors such as immune challenge and intrinsic factors such as gene mutations associated with hearing loss. Using this approach, it will be possible to measure the effect of these variables and relate them to specific human aetiological profiles.

Chapter 3 proposes the valuable utility of EI as a measure of the status of fibrosis and FBR around the implanted electrode. A mouse model of CI with capabilities for stimulation and impedance measurement will allow the molecular and cellular wound healing response to be analysed following a detailed timeline of impedance measures. Thus, the approaches presented in Chapter 2 and Chapter 3, tissue analysis and EI respectively, can be triangulated.

The mouse model will employ a new method for identifying specific molecules, cells and tissues developing around the implanted electrode array. The approach combines the marker specificity of histological and immunohistochemical stains, with the high spatial resolution of X-ray μ CT imaging. This chapter outlines developments towards establishing this technique, 3D X-ray histology (Katsamenis et al, 2019) in the mouse model. Ultimately this will allow us to investigate the spatial position of the implanted electrode array and the associated molecular and cellular tissue response. At the time of writing, there was no published study with this level of molecular specificity and spatial resolution.

4.2 Methods

4.2.1 Workflow overview

The tissue analysis methods described here were carried out on tissue from animals housed and euthanised at University College London. The care and treatment of the animals met the UK Animals (Scientific Procedures) Act 1986 Home Office standards. Although no living animals were handled as part of this research Appendix C2 (page 233) shows a Home Office Personal License to demonstrate that the relevant training course was completed prior to beginning the development of the non-human animal model. The tissue was processed and analysed as shown in Figure 4-1.

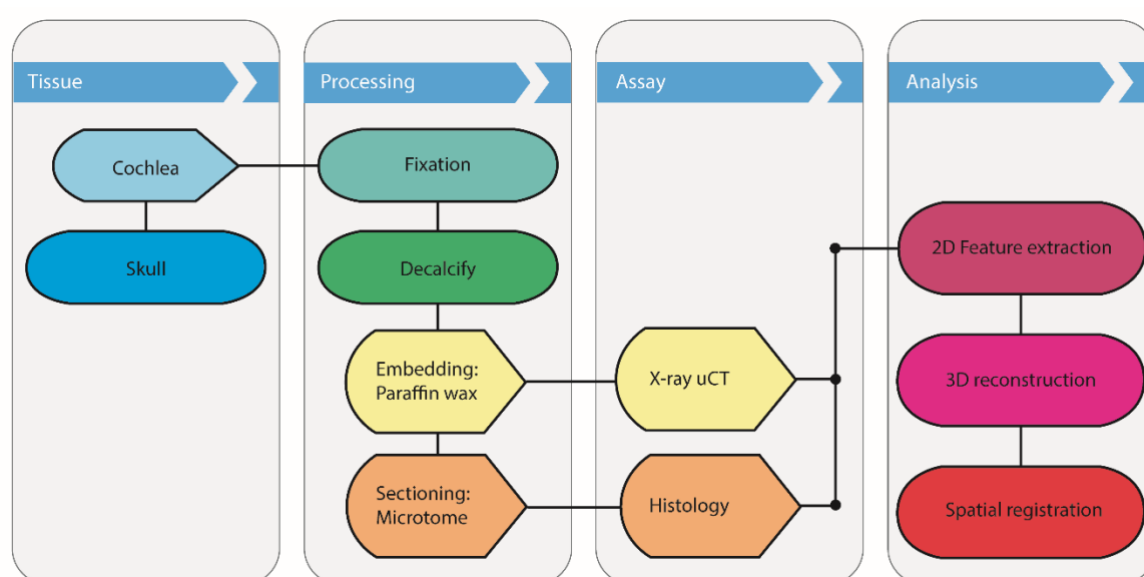


Figure 4-1: **Workflow for mouse cochlea tissue processing, testing and analysis**

4.2.2 Subjects

C57BL/6 mice, which were housed at the Ear Institute University College London (UCL) in pairs or small groups within a noise-controlled environment with free access to food, water, and environmental enrichment. Animals were examined daily for signs of stress, fighting with cage-mates or age-related illness. Following overdose with pentobarbital, mice were transcardially perfused with 4% paraformaldehyde (PFA) as per (Quraishe et al, 2019). Decapitated heads were transported in fixative (4% PFA) before transfer into 70% ethanol.

4.2.3 Mouse cochlea dissection

Cochleae were dissected from the mouse skull following an SOP shown in Appendix C3 (page 236). The dissection procedure was carried out on a black dissection plate with regular application

Chapter 4

of PBS to prevent drying. Tissue was kept moist by regularly applying PBS. An incision was made caudally from anterior to posterior along the midline. Blunt dissection of skin and soft tissue was performed using forceps to reveal skull. A pair of rongeurs was used to break the nasal bone anterior to the frontal bone. This opening into the skull was used to begin removing small pieces of bone, working through the frontal (Figure 4-2 Red), parietal (Yellow and Green) and occipital (Orange) bones to reveal the brain. Remaining bone was carefully removed from the dorsal aspect of squamosal bone to allow insertion of the spatula. The spatula was dipped in PBS and carefully scooped underneath olfactory bulbs to release from olfactory nerve. The spatula was then moved caudally in short increments to lift the brain from the skull base. The brain was released by severing the spinal cord or medulla while taking care to avoid damage to the ventral brainstem (cochlear nucleus), which may be used in other investigations. The brain was transferred to 70% ethanol for processing for histology. The remaining part of the skull was moistened with PBS and transferred to the stage of the light microscope. The styliiform process was targeted as the landmark to indicate the position of the otic capsule. The squamosal bone was broken anterior to the otic capsule (Figure 4-2 Blue) and soft tissue was cleared from the otic capsule using forceps. The cochlea was revealed using the following technique: a moderate pressure was applied to the otic capsule using forceps to hold it in position. A second set of forceps was used to apply a lateral force, away from the midline, to the tip of the styliiform process. This fractured the otic capsule from the bulla and revealed the apical aspect of cochlea. The excess skull bone and soft tissue was removed from the otic capsule, which was then immersed in 70% ethanol and stored at 4°C for further processing.

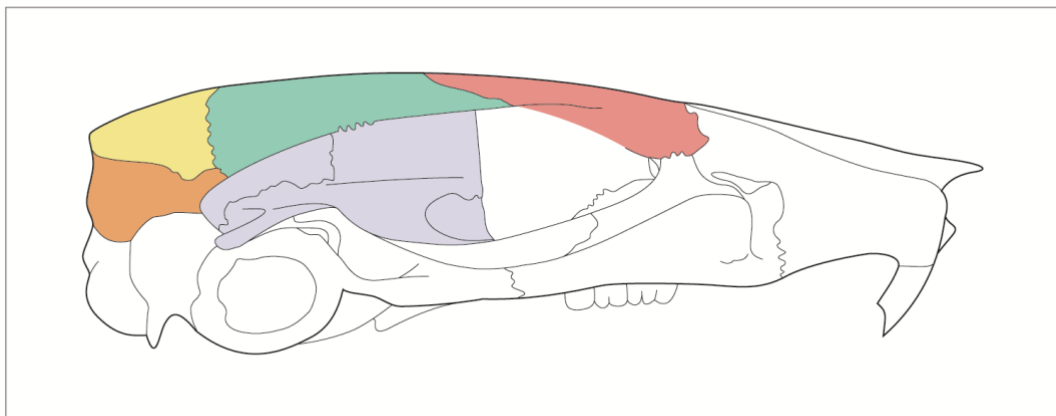


Figure 4-2: **The cochlea was dissected from the mouse skull after tissue fixation**
The frontal (red), parietal (green), interparietal (yellow) and occipital (orange) plates were removed. The squamosal bone (blue) was broken to provide access to the otic capsule.

4.2.4 Tissue processing

The isolated cochlea was decalcified by immersion in 0.125 M ethylenediaminetetraacetic acid (EDTA) with agitation, by placing on a rocker plate (40 revs/min) for 48 hours.

The tissue was prepared for embedding by automated stepwise dehydration and infiltration of molten paraffin wax under vacuum using an infiltration processor (Tissue-Tek VIP 5jr, Sakura). The cochlea was transferred to a pre-heated stainless-steel base mould. It was oriented in a small volume of molten wax using heated Dumont forceps and a hand-held magnifying glass. Orientation was performed so the cochlear modiolus laid in parallel to the cutting face of the wax block.

4.3 Histology and Immunohistochemistry methods

4.3.1 Sectioning mouse cochlea tissue

Tissue was sectioned using a Leica RM2135 microtome in preparation for mounting on glass slides. The microtome knife angle was set at 5° and section thickness to 10 µm. The face of the block was cooled on ice prior to sectioning. Sections were collected using forceps and transferred to a water bath (45 °C). The floating wax-tissue sections were collected onto 3-Aminopropyltriethoxysilane (APES) coated glass slides prior to drying at 37 °C overnight.

4.3.2 Immunohistochemical and histochemical staining

The tissue was labelled to identify macrophages using anti-Iba1 polyclonal antibody (Wako – Alpha labs, 1:1000). Chromagen 3,3'-Diaminobenzidine (DAB) and haematoxylin counterstain. The procedure was carried out according to the SOP shown in Appendix C5 (page 240).

4.3.3 Image acquisition and processing

The stained tissue was viewed using bright-field light microscopy. Images were captured using Q-imaging Q-Capture software via a Q-Imaging 2000R digital camera connected to a Nikon Eclipse E4000 microscope and Nikon HB-101004F light source. Various magnifications were achieved using 4x, 10x, 20x, 40x and 100x objectives. Brightness and contrast of the images were adjusted using Image-J software.

4.4 Computed tomography methods

4.4.1 Pilot X-ray μ CT investigation

An X-ray μ CT scan was performed as a pilot investigation of the mouse cochlea (Mu-Vis Job ID 1713). The cochlea had previously been dissected from a 22-month C57. The tissue had been fixed in 10% neutral buffered formalin solution. Decalcification of the tissue and embedding was performed as described. The scan was performed using Zeiss 160 kVp Versa 510, which is a conventional X-ray tube style scanner. The scan time was 13 hours, at a resolution of 4.16 μ m. Figure 4-3 shows an image reconstruction of the scan in three orthogonal planes (A-C) and three-dimensional reconstruction virtually sliced to reveal bony structures: modiolus, osseous spiral lamina and otic capsule (D).

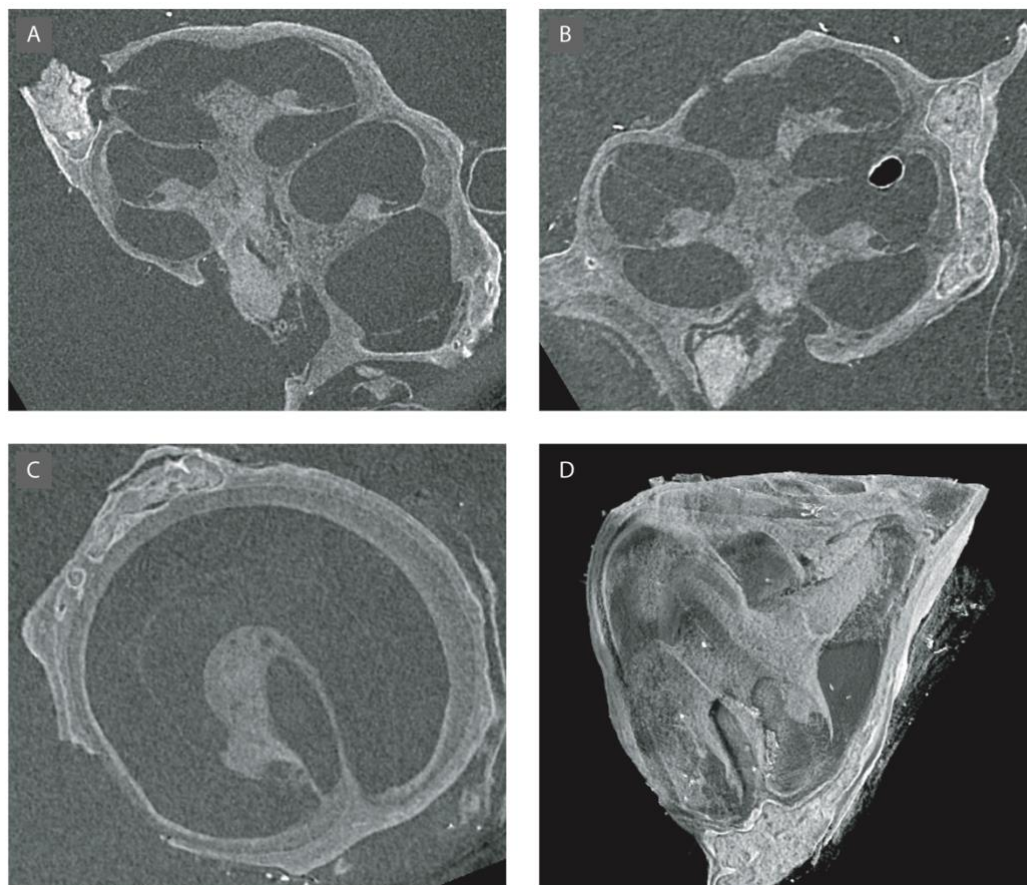


Figure 4-3: **X-ray μ CT Image reconstruction of a C57 mouse cochlea**

A) X-plane view B) Y-plane view C) Z-plane view D) 3-D digital reconstruction. Image processing was performed using VG Studio Max software.

4.4.2 Synchrotron X-ray μ CT investigation

An X-ray μ CT scan was performed to further the pilot investigation of the mouse cochlea (μ Vis Job ID 1747). The scans were performed at the Diamond Light Source Synchrotron facility in Oxford. All samples were scanned with a voxel size of $1.1 \mu\text{m}^3$. Seven cochleae were prepared for X-ray μ CT imaging, each with different attributes. This approach was chosen to determine the optimum parameters for future repeats.

Table 4-1: Processing details for cochleae included in X-ray SR μ CT session

| Number | Animal | Strain | Age | Fixative | Preparation | Treatment | Embedding |
|--------|--------|--------|-----------|--------------|-------------|----------------------------|-----------|
| 1 | Mouse | C57 | 4 Months | 10% Formalin | None | | PBS |
| 2 | Mouse | C57 | 4 Months | 10% Formalin | None | | PBS |
| 3 | Mouse | CBA | 4 Months | 10% Formalin | None | Noise exposure 3 months | PBS |
| 4 | Mouse | CBA | 4 Months | 10% Formalin | None | Sham exposure 3 months | PBS |
| 5 | Rat | | | Not Fixed | None | | PBS |
| 6 | Mouse | C57 | 22 Months | 10% Formalin | EDTA | | Paraffin |
| 7 | Mouse | C57 | 2 Months | 10% Formalin | EDTA | | Paraffin |

Following dissection, the tissue was either stored in 70% ethanol or embedded in paraffin wax. The cochleae and associated tissue were placed in sealed capsules made from Eppendorf tubes and pipette tips. These were adhered to an aluminium electron microscopy stubs to enable positioning in the scanner.



Figure 4-4: Dissected cochlea tissue preparations in sealed containers for scanning

Suspended in PBS (1-5) or embedded in paraffin wax (6&7). Labelled 1-7 correspond to details in Table 4-1

4.4.3 Synchrotron X-ray μ CT scanning

Scanning was carried out using synchrotron radiation-based μ CT (SR μ CT). The session was booked specifically for tissue samples belonging to other projects. There was an opportunity to scan the 7 cochlea samples during spare beam time. This meant that the scan settings were not optimised for rodent cochleae i.e. density, mass, embedding medium.

4.4.4 Image file details

Radiographs from the synchrotron scans were saved in RAW format. From these, an image stack was reconstructed in .tif format. The scanning was not optimised for analysis of the phase element of the radiograph. The analysis was performed using the attenuation data.

4.4.5 Image processing and feature extraction

The SVes, SM and ST were selected for segmentation. Sample 6 (Table 4-1) was chosen for image processing and analysis because its image quality was superior to other samples. This was determined by manual review of each image stack using Image-J software. All images from Samples 1-5 were very low contrast and blurred. The session notes show that the heat generated during the scan had caused evaporation of the PBS. Another general challenge was movement of the tissue during scanning (Appendix C4 page 239). The outcome of this trial of 7 different sample preparations was that paraffin embedded tissue is most robust in SR μ CT.

A semi-automated process was created to extract the main features of the cochlea to be modelled. Processing was performed using Image-J software. The tissue had been demineralised using EDTA and embedded in paraffin wax. Therefore, the contrast of the captured radiographs was low. The initial steps of processing shown in Figure 4-5 were designed to maximise contrast. The ultimate aim of this image processing was to create a binary mask which represents only the main feature to be modelled i.e. the cochlea scalae. This mask was manually edited in Avizo as shown in Figure 4-7.

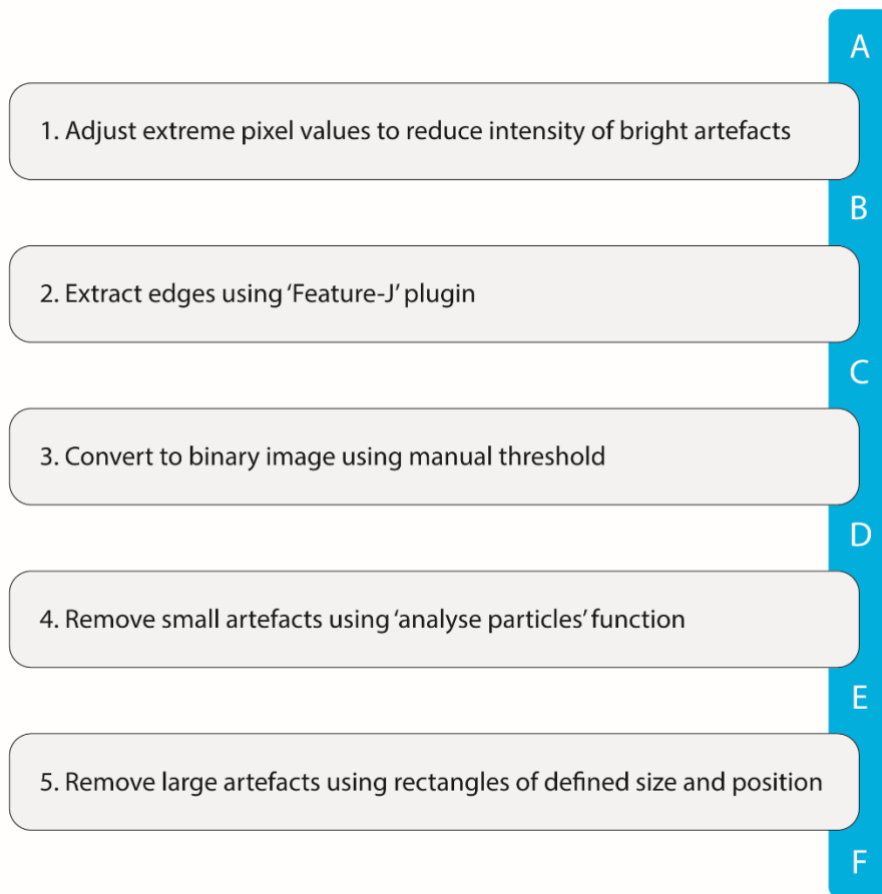


Figure 4-5: **Workflow for X-ray μ CT image processing using Image-J software**

A-F correspond to steps in Figure 4-6. Steps 1-5 correspond to sections of the macro script shown in Appendix C2 (page 233).

The processing shown Figure 4-6 was designed especially for this sample using an Image-J macro script designed to process the whole multi-image stack. Figure 4-6 shows a single image slice as an example. This dataset contained 1300 Image slices in .tif format. (pixel dimensions- 1700 x 2200 x 1300).

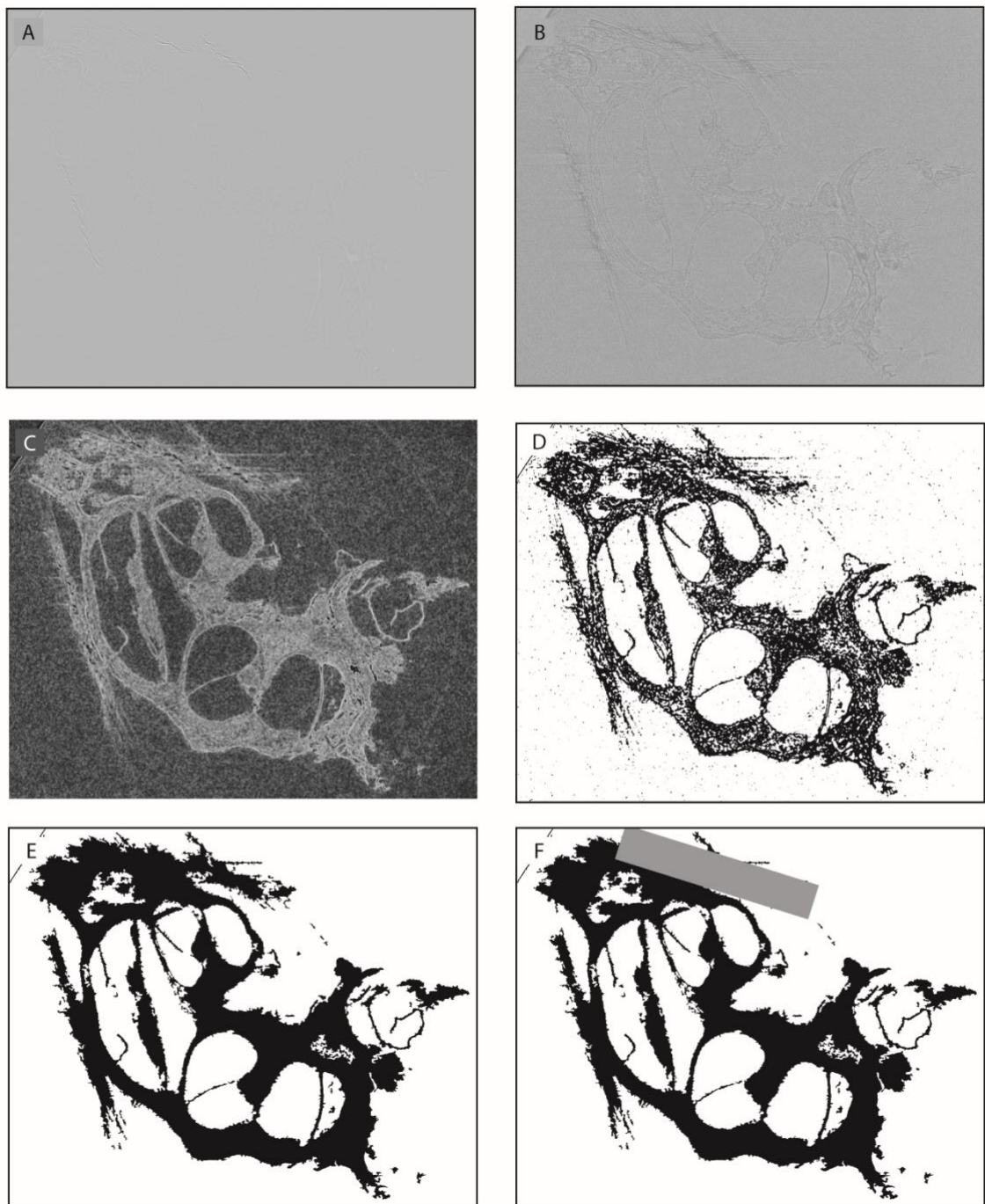


Figure 4-6: Image processing steps to extract a binary mask of the cochlea scalae in preparation for 3D reconstruction

Processing steps corresponds to the list in Figure 4-5. A) demonstrates the low contrast of the X-ray μ CT images (see Figure 4-7a for this image with manually adjusted brightness and contrast to enhance visibility of anatomical features). F = Grey rectangle is an example of the shapes used to remove large artefacts.

4.4.6 Feature segmentation

The cochlea scalae were virtually 'segmented' from other features of the cochlea. Segmentation was performed using Avizo software. The binary mask (Figure 4-7b) created using Image-J was placed over the raw μ CT Image (Figure 4-7a), which was used as a template. There were 1300 corresponding mask and image slices. Manual editing of the binary mask was necessary to identify the artefacts and imperfections generated through the semiautomatic Image-J macro script processing. The editing process was carried out using a Wacom Cintiq 13 graphics tablet connected to an Apple Macintosh Macbook Pro. The dataset consisting of 1300 image files was approximately 15 GB. Processing of the stack was carried out using Avizo on the University of Southampton remote supercomputer Iridis 5. Access to the Iridis environment was gained via a Linux remote machine running through a standard web browser. Approximately 40 hours was spent performing the manual segmentation editing.

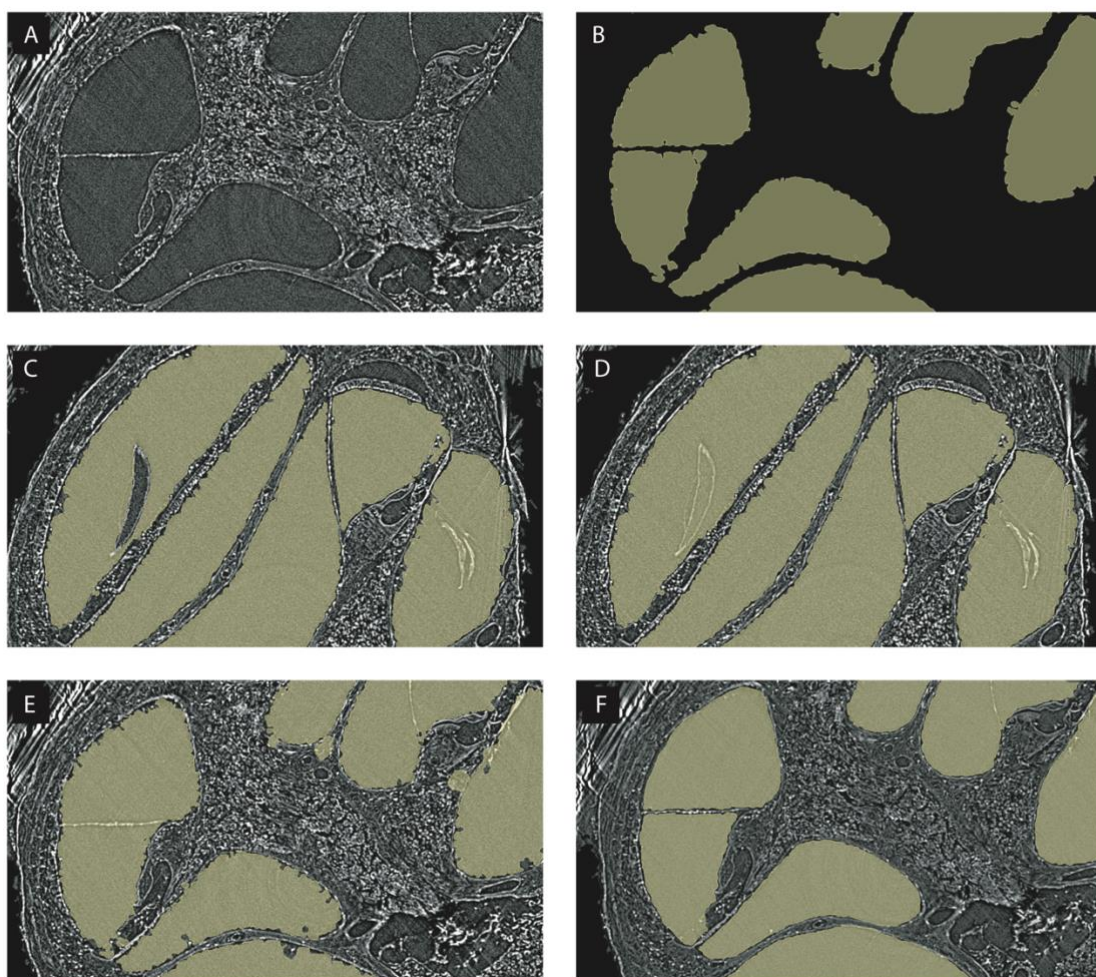


Figure 4-7: **Steps taken to manually edit and segment X-ray μ CT image slices**

A) Raw image used as a template. Brightness and contrast were manually edited to highlight anatomical features. B) Binary mask of scalae created from Image-J processing in Figure 4-6. C) Mask overlaid on image template showing example of artefact in the scala vestibuli. D) Artefact manually removed. E) Example of mask where Reisner's membrane was missed and edges were rough. F) Reisner's membrane manually defined and edges manually smoothed. Anatomical features are indicated in Figure 1-2.

4.5 Results

4.5.1 The mouse cochlea scalae were modelled by rendering the manually edited slices

A 3D model of the scalae of the mouse cochlea was rendered from the completed segmentation file using Avizo. The result is shown in Figure 4-8. An example of a single slice (number 465 of 1300) contributing to the volume is shown in Figure 4-8a. The virtual slice was performed using the orthoslice tool. The completed 3D volume rendered model is shown in Figure 4-8b. A bounding box is wrapped around the model to show the three orthogonal planes.

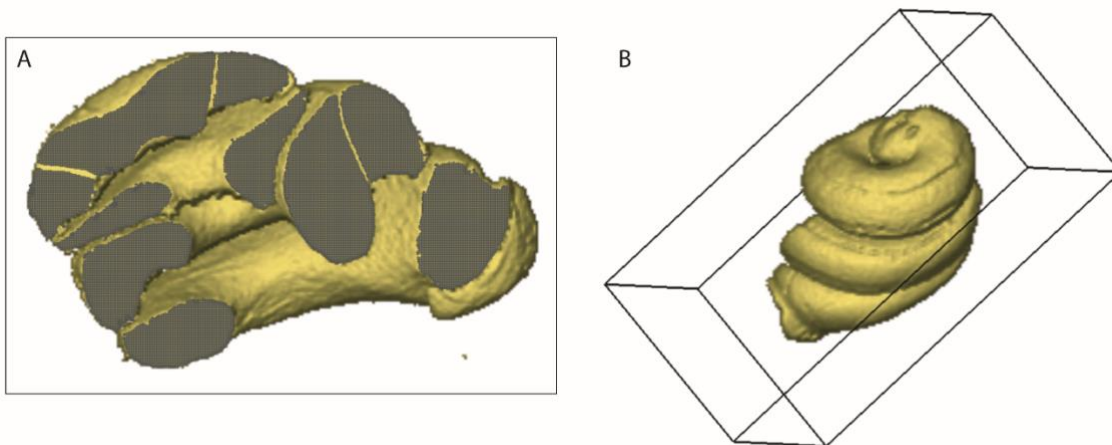


Figure 4-8: **A 3D reconstruction of the scalae of the mouse cochlea was created using Avizo**

A) 3D model virtually sectioned to show a single slice in green. The silhouette of each scalae: SM, ST and SVes are comparable to the schematic in Figure 1-2. B) Completed 3D model. 3 planes highlighted by surrounding bounding box.

4.5.2 Development of 3D X-ray histology of the mouse cochlea

A histological stain with haematoxylin showed the cellular organisation of the structures of the cochlea. Figure 4-9b shows a x20 magnification image showing the scala tympani, SM, SVes, SV, basilar membrane, Organ of Corti and SGNs, as labelled in Figure 1-2. The X-ray μ CT image in Figure 4-9a has been scaled to match the light microscopy; the same anatomical features can be seen. Using Avizo software the features in the microscopy image, such as the cells lining the underside of the basilar membrane can be spatially registered over the X-ray μ CT image. This has the benefit of correcting the distortions in the tissue created by sectioning and staining and is one of the strengths of the 3D X-ray histology technique. In future development of this work, X-ray μ CT images will be co-registered with immunohistochemical stains. By using a chromogen, or ideally a fluorophore, a semi-automated procedure will allow spatial co-registration of specific

cells from the light microscopy image into the 3D rendered model in Avizo software. Examples of such cells are Iba-1 positive macrophages and microglia indicated by brown stain (oxidised DAB) with colocalised purple stained nuclei (haematoxylin) in Figure 4-9d. The microglia and macrophages can be spatially registered into the X-ray μ CT virtual model. The position of such cells is shown by white asterisks and arrowheads in Figure 4-9c. Depending on the technique of tissue embedding and sectioning, the electrode or remaining electrode track could be incorporated into X-ray microscopy model. Although examples in Figure 4-9 are shown in two dimensions, the spatial co-registration would ultimately allow modelling in three dimensions as Figure 4-8. This will have the benefit of localising specific cells types, such as those associated with inflammation and proliferation described in Chapter 2, within a few microns.

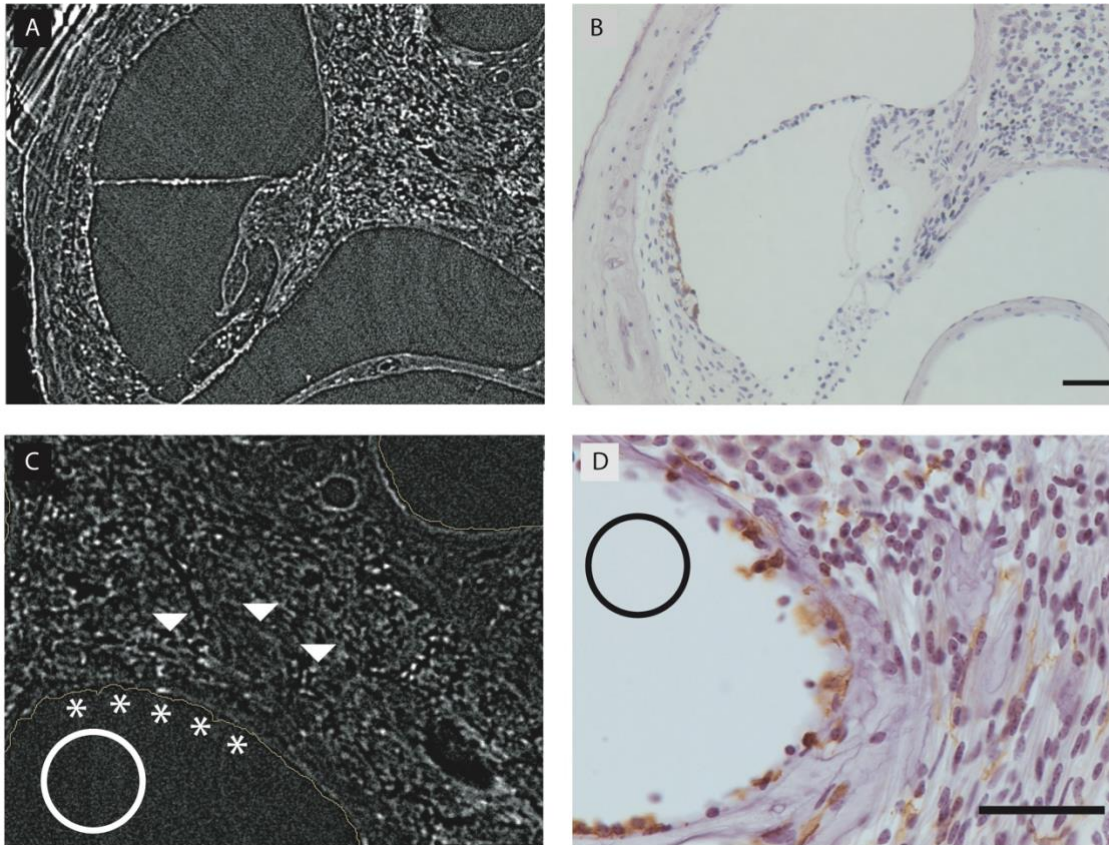


Figure 4-9: **Proposed spatial alignment of X-ray μ CT data and histology light microscopy imaging.**

A) μ CT slice of the 3 scalae, SGN and organ of corti. B) Light microscopy image stained with haematoxylin. Magnification x20. Scale bar 50 μ m. C) μ CT slice showing SGN region and medial wall of scala-tympani. Triangles indicate where positively stained macrophages and microglia could be co-registered from histology imaging. Asterisks indicate where macrophages within the scala could be co-registered. White circle shows where the implanted electrode or remaining electrode track would be in an implanted animal. D) Light microscopy image stained with anti-iba1 antibody with DAB and haematoxylin. Magnification x40. Scale bar 50 μ m. Black circle indicates where the electrode or electrode track would be in an implanted animal.

4.6 Discussion

4.6.1 Technical outcomes from histological and X-ray μ CT analysis of the C57BL/6 mouse cochlea

The main focus of the work covered in this chapter was analysis of the C57BL/6 mouse cochlea by immunohistochemical staining with microscopy and X-ray μ CT. Significant developments were made towards a robust and versatile mouse model of CI. Skills in mouse skull dissection were acquired and refined which now allows reliable removal of the cochlea with zero trauma to the tissue of interest. A trial of different tissue preparation and embedding methods revealed paraffin embedding is protective against heat during scanning although the density differential to decalcified bone is very low, which can lower the image contrast. Laboratory techniques for immunohistochemistry were developed and refined, which had transferable benefits to carrying out assays on both mouse (Chapter 4) and human (Chapter 2) tissue. A major point of method development in the present chapter was image processing for feature extraction and manual segmentation to create a 3D model of the mouse cochlea. This procedure can now be used in future iterations of this work when the implanted mouse is analysed.

4.6.2 Short-term planned application for the CI mouse model

The overarching theme of the work presented here is translation from basic research to clinical application. The work presented in this chapter creates the methodological foundation for a mouse model to allow testing of questions raised by the human investigations in Chapter 2 and Chapter 3. For example; are the cellular indicators of inflammation and proliferation observed in tissue from an explanted array the norm or unusual? Also, are the localised increased EI observed in 8% of adults and 5% of children indications of localised fibrosis or bony tissue growth around the electrode array? In order to test these questions, the following aims were defined for the mouse model.

1. Controlled genetic and environmental variables to model human condition.
2. Impedance telemetry measurement following chronic stimulation to verify human data.

The work presented in this chapter has met the goal of developing the pipeline for investigation of the mouse cochlea using X-ray μ CT imaging and immunohistochemistry with light microscopy. However, the long-term aim of implanting the animals to observe the immune response to CI was not met due to time and resource limitations. The processes outlined here will form an integral part of the wider research project investigating the wound-healing response to CI in a mouse

model under controlled experimental conditions. At the time of writing this project is transitioning into the prospective study of implanted and stimulated mouse cochleae. The multidisciplinary working group allows the project to span the range of methods necessary for an ambitious model of CI which will closely mirror the human condition. It will allow the development of a more complete model of the immune mediated tissue reaction to CI. Most importantly it will allow the effect of variables such as aetiology and health related factors such as infection and genetic variability to be tested. Such factors may contribute to the wide undescribed variability in patient performance and deserve scrutiny. In addition, the work is partly funded by Oticon Medical, who are developing low-impedance electrode materials. Testing the intra-cochlear tissue reaction to the new electrode materials is an important part their research and development prior to introduction to the market for human CI.

4.6.3 The protocol for dissection of the mouse cochlea was refined with experience

Imaging results from initial histological analysis showed that separation of the cochlea from the auditory bulla can damage the hook region of the cochlea. The cochlea dissection technique was therefore refined to avoid such damage, especially because of the importance of the hook region with regard to cochlear fibrosis and osteogenesis. It is important to preserve this region for analysis, especially in tissue samples from future implanted animals.

Tracking anatomical landmarks throughout the procedure proved essential. Following removal of the brain to reveal the skull base, a pair of rongeurs were used to fracture the squamosal bone. At this point it is difficult but highly important to gain sight of the apical turn of the cochlear as it is revealed. Experience with the tools; working under the light microscope was necessary to gain competence.

4.6.4 Future methodological planning for the mouse cochlea tissue processing

The ultimate aim of the project to create a mouse model of CI is to implant and stimulate healthy animals over long periods (several months) before harvesting the cochlear tissue. A major challenge to this is processing the tissue containing the electrode array made of platinum with a silicone carrier. On the one hand it is desirable to have the array in place when scanning and sectioning for histological analysis. On the other hand, the platinum and silicone create technical challenges making tissue processing more difficult. One method for preserving the tissue with the array in-situ is to embed using hard resin such as araldite. However, this method presents the risk of damaging the silicone carrier, which can allow the platinum electrode contacts and wires to dislodge. This disruption of the silicone carrier would prevent sectioning of mineralised tissue

(containing the platinum array) using a diamond knife. In addition, this method causes significant antigen masking which would limit capacity for detailed the immunohistochemical analysis. Embedding the implanted cochleae using paraffin wax maybe desirable considering the expertise developed using this method. However, the process of graded dehydration and penetration of molten wax takes time which can give opportunity for the electrode to move. Also, as demonstrated in this chapter, paraffin wax has a similar density to soft tissue and demineralised bone, which reduces contrast in μ CT scan images. Moreover, paraffin wax can cause some antigen masking which reduces the effectiveness of immunohistochemical stains depending on the chosen antibody. Therefore, future repeats may benefit from embedding using cryo-embedding in OCT as shown in Chapter 2. This will minimise the time between tissue fixation and the final stage of embedding when the tissue is stable and protected. Once embedded the electrode array will be removed leaving any newly formed fibrotic or bony tissue behind. The remaining tissue along with the cochlea will be cryo-sectioned ready for histological and immunohistochemical staining. Another benefit of using the OCT method is that thin sections as low as 1 μ m can be cut if required.

The methods developed here will allow efficient processing of the implanted mouse cochleae. The spatial resolution and cellular marker specificity of 3D X-ray histology is a powerful approach to tissue analysis. This technique applied to a mouse model of CI will allow significant Improvement in our knowledge of 'what' cells interact with the implanted cochlea, 'when' this happens following implantation, and 'where' the cells/molecules are relative to the array and electrode contacts. The ability to interrogate the system on this fine scale will allow experiments using pharmacological treatments, mutant strains and infection models to be carried out with some quantitative confidence.

Chapter 5 Discussion

5.1 Summary of outcomes

One of the main challenges for cochlear implantation is performance variation across CI users and the unpredictability of outcomes over a user's lifetime. Evidence suggests that a portion of outcome variability can be attributed to biological factors. The first touchpoint of the device with an individual's biology is the CI-tissue interface. Disturbances at this interface have been shown to impact performance but the mechanisms are not fully understood. This research presents three approaches to measuring and analysing the CI-tissue interface. The research has revealed new information about the cellular composition of the fibrotic sheath, which forms around the electrode array. It has characterised the temporal patterns of EI development over 5 years in a larger sample of CI users than previously studied. From these normative trends, it was possible to filter out cases of raised EI that met a statistical threshold. This takes the field a step closer to defining the point at which EI levels may serve as an early warning of abnormality. A limitation of human CI studies is the inaccessibility of the CI-tissue interface and the inability to manipulate the system experimentally. One of the outputs of this research is the development of a mouse model of CI, which is not constrained by these factors.

The case study presented in Chapter 2 includes immunohistochemical analysis of the fibrotic sheath removed from an explanted CI array following the device failure. The clinical findings shown in Figure 2-6 along with the surgeon's report confirm that this device had migrated to extrude four or five electrode contacts. The cellular composition of the tissue is informative on two levels: 1) to add a new detail to our understanding of the wound healing response to cochlear implantation. 2) to characterise biological correlates of migration related CI failure. Histochemical and immunohistochemical analyses showed that the fibrotic tissue is spatially heterogeneous. Interestingly, there was evidence of active inflammation alongside proliferation. For example, activated macrophages and the pro-inflammatory cytokine IL-1 β were observed distributed throughout the tissue in close proximity to proliferating tissue, indicated by the cell division marker Ki-67 and angiogenesis marker VEGF-R1. This shows that the wound-healing response to CI on the extra-cochlea portion of a migrating array is not moving through the phases of wound healing in a sequential manner. Rather, it is responding locally to signalling to switch cellular phenotypes between inflammation and proliferation. At the time of writing, this analysis is most detailed carried out on human CI fibrotic tissue. It appears to confirm the previously reported composition of the tissue while adding useful new depth of information. The profile of the wound-healing response shown matches that demonstrated by (Bas et al, 2015) in mouse and rat

Chapter 5

models. Importantly, the method development for tissue processing, sectioning and immunohistochemical staining have been established as a pipeline future investigation of explanted fibrotic tissue. This process, which involves collaboration between clinicians, academics and surgeons, will be repeated to allow comparison across individuals.

Chapter 3 presents a retrospective analysis of clinical data taken from 221 MED-EL CI users. The main analysis interrogated impedance telemetry data over a five-year study period. The findings confirmed other published studies showing stimulation induced impedance reduction and significantly greater impedance in basal electrodes compared to apical. The novel contribution of the research project is finding that a minority of cases (8% adults and 5% children) exhibit statistically high impedance levels when filtered using an outlier labelling technique. The majority of individuals detected showed high impedance at a single electrode, often in mid or apical electrodes. These cases have raised but not extreme impedance levels and therefore would not be detected using the manufacturer proprietary indicator of high impedance. This method may offer an early warning system to alert clinicians of unusual impedance so that clinical intervention such as adjustments to stimulation parameters can be made (Neuburger et al, 2009). It could be used by audiologists to inform decisions to activate or deactivate particular electrodes. The analysis showed that adults were more likely to have electrodes deactivated than children and the reasons for these were mostly due to subjective reports from the patient regarding poor sound quality or non-auditory sensations. Although several interpretations of this finding are discussed in Chapter 3, it seems clear that the outlier labelling approach to detection of raised impedance offers potential as an objective guide to clinician decision making. Data management and analysis was performed using a custom script in Matlab. The approach allows semi-automated processing, analysis and graphical presentation of data. This tool could be widely used in CI and other areas of medicine and will be discussed further.

The final project presented in Chapter 4 comprises the development of a mouse model of the wound healing response in CI. The long-term aim of this research is to create a mouse model of cochlear implantation that allows chronic implantation and electrical stimulation of the cochlea. The key motivation to developing this model is the need for an experimental system in which to test research questions from human CI users. The concept behind the design of experiments is discussed below. The main contribution of the work presented in Chapter 4 is the proof of concept for 3D X-ray histology to analyse tissue in the mouse cochlea. Although the technique has been used in other published work, the application of specific anti-body immunostaining was novel at the time of writing. This provides highly valuable cell marker specificity that is necessary to answer questions about the exact signalling mechanisms of wound healing in the cochlea following CI, as highlighted in the findings presented in Chapter 2.

5.2 The challenge of unpredictable and highly variable CI performance

Cochlear implant performance is highly variable across individual users, which means that the great potential benefits of the technology are not guaranteed for all. Previous efforts have been made to measure the effects of different pre, peri and post-implant factors on long-term performance. For example, the evidence shows a negative correlation between duration of severe-profound hearing loss and speech recognition scores (Kaandorp et al, 2017). Studies have found that factors influencing performance account for only 10% to 21% of the variability (Lazard et al, 2012). This suggests that there are other contributing factors that are currently not captured and included in analyses. Speech recognition is a high-level outcome in that it involves auditory processing and cognition. If we define outcomes at lower levels of physiological complexity, we can better understand the variability at each stage. The CI-tissue interface is the logical starting point. There is a limited understanding of the wound-healing response to CI, how this influences the long-term health of the interface and any downstream neurological impacts on the auditory pathway. Biological variability is an inevitable contributor to performance variability.

Not all variation in CI performance is necessarily bad or unwanted. One should consider that individual variability means different things to different healthcare stakeholders. We as researchers often aim to control variables so we can assess the effectiveness of treatments and estimate generalisability of findings to larger populations. This means we consider groups as a model described by variation around an average. A patient is concerned with the quality of the care they receive, and how it impacts their own clinical outcomes. The two perspectives differ in the questions they ask and necessitate different study designs to provide useful answers. Regression analysis is informative when investigating populations whereas longitudinal factorial designs are more appropriate for individuals (Neuhauser et al, 2011).

5.3 The challenge of monitoring the CI-tissue interface

As stated in Chapter 1, not only is performance highly variable but its definition is quite ambiguous. This may be due to the wide range of subjective and objective outcomes measures included in different studies. There is a need for reliable clinical measures that correlate with and/or predict wider user performance. The EI analysis tool presented and tested here may fulfil some aspects of this brief.

5.3.1 A novel and widely applicable method for filtering potential 'problem' cases

Chapter 3 presents the findings of a large retrospective clinical study of impedance telemetry. The data for a large sample of CI users was described over a five-year period to demonstrate EI mean, range and its regression. The novel approach to graphical reconstruction of the data provides a transparent insight into the data without unnecessary parsing. An outlier labelling technique was applied to allow filtering of high impedance cases. This approach allowed individual cases to be earmarked as outliers relative to the local population. Considering the current standard technique used in the CI programming software highlights extreme cases only, the approach applied here can be used to differentiate normal from raised and extreme.

There is currently a lack of clinical indicators of tissue change associated with poor performance. The EI analysis tool presented in Chapter 3 has potential to address this problem. Using an outlier labelling technique, a small number of individuals (both adults and children) exhibited raised EI levels that would not have detected using the manufacturers software tool. This finding could be validated through an investigation of performance to test correlation with the SEI measure.

5.3.2 Clinical impedance telemetry findings can be explored in a mouse model

The cases showing raised levels in the mid and apical electrodes are especially interesting because this represents an area of the cochlea which shows much less fibrotic and bony tissue. If the impedance increases in these cases do not correlate with the typical growth of tissue in the basal turn, then what local factors are influencing the impedance change? Combining impedance telemetry with the tissue analysis planned for the mouse model of CI described in Chapter 4 could provide valuable information to answer this question. The 3D X-Ray histology technique would provide a window into the localised cellular conditions to reveal the physical correlates of the EI increase.

5.3.3 Wider applications of the automated analysis of electrode impedance data

The algorithmic design of the data processing makes it easily applicable to other datasets in an automated fashion. At the time of writing, a multicentre research study was at this stage of ethics application to be carried out over the coming year.

The automated method of analysis used in this project could be integrated into manufacturers software to allow a real-time big data approach to telemetry monitoring. This would place each individual patient within a normative range with the local population for any given time point. This could allow fluctuations in the device performance to be highlighted prior to gross subjective

indicators of poor performance and failure. This approach could be integrated into a remote care regime, which has been shown to offer significant benefits to CI users (Cullington et al, 2018).

5.4 Experimental investigation of individual differences and their effect on CI performance

5.4.1 Experimental approach to modelling human CI in a mouse model

Chapter 2 highlights an extreme case of the problem of poor performance. Chapter 3 offers a description of variation in a population over time and a method for identifying individuals with abnormal EI that would be undetected using existing clinical tools. Clinical monitoring using EI shows promise as a biomarker, especially if the tissue analysis techniques in human and mouse can be used to validate the cellular correlates of impedance fluctuation. There is a clear need for a model of the human condition that better captures the intrinsic (e.g. genetic hearing loss aetiology) and extrinsic (e.g. bacterial infection) factors that influence variability over long periods of time. The model should aim to investigate the complex relationship between cellular events at the CI-tissue interface and the wider physiology of the animal. This will necessitate the ongoing capture of various biomarkers. For example, audiological measures like EI, NRT and ABR should be correlated with systemic markers like inflammatory cytokines and leukocytes.

If the systemic inflammatory markers are associated with cochlear health, either as cause or effect, they must do so through physical interactions. This signalling, through small molecules such as cytokines and cells such as circulating non-resident macrophages would pass between the compartments shown in Figure 5-1.

This model offers a framework for designing experiments for the mouse model which test various aspects of the human condition. Immune challenges from viral and bacterial infections of the upper respiratory tract are a common occurrence in humans and currently have an unknown effect on the performance variability of CI users. Poor diet and sedentary lifestyle, which have been shown to increase blood markers of inflammation may also have an impact on CI performance variability. It is possible to test such a hypothesis in a mouse model of CI given careful selection of independent variables such as immune challenge and dependent variables such as EI and cellular markers of inflammation and proliferation at the CI-tissue interface. This approach to testing wider influences on CI outcomes using an animal model has not been applied in published studies to date.

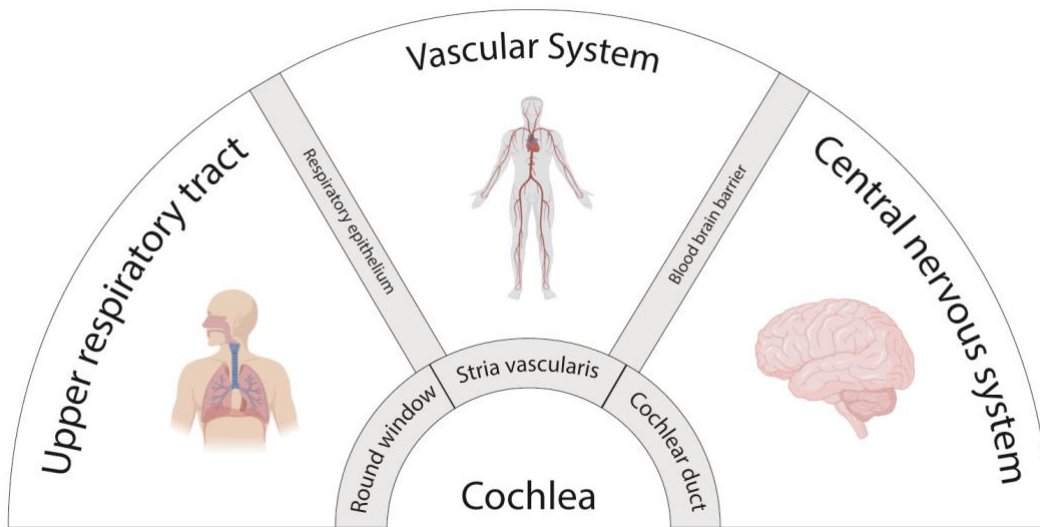


Figure 5-1: Cochlea health can be influenced by pathogens and immune mediators from distal parts of the body

Schematic representation of body compartments that communicate with the cochlea. Grey barriers represent the membranes and epi/endothelia through which cells and molecules such as leukocytes and cytokines can transfer. Each compartment and corresponding barrier have a different permeability which may create a variable influence on cochlea inflammation.

Figure 5-1 shows the concept of how the cells and molecules may transfer between compartments to carry immune signalling to promote or dampen aspects of the wound healing response in the cochlea. Figure 5-2 shows the same compartments with longitudinal timescale extending into the past and future from the CI surgery (indicated by 0 on the time axis).

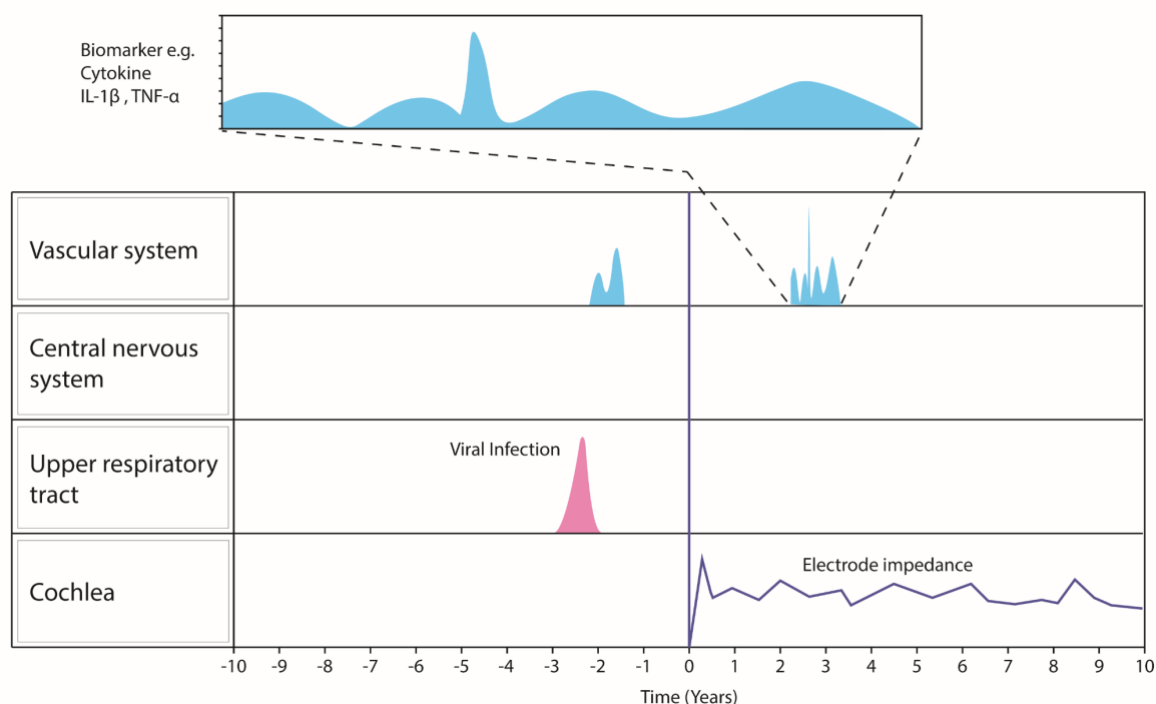


Figure 5-2: **Conceptual timeline of bio-marker fluctuations in the human body that may affect cochlea health**

Interdependence of bio-marker fluctuations depends on their physical connection shown in Figure 5-1. The 0 time-point represents cochlear implantation surgery. Examples show past events as a spike in inflammation with viral infection (magenta). Fluctuations in blood markers of inflammation can be monitored over time (cyan). Electrode impedance (blue).

The example of a human timeline shown in Figure 5-2 could be condensed and recreated experimentally in the mouse model with the benefits of genetic tractability, control over environmental exposure and time-specific access to harvested tissue for histochemical analysis.

5.5 Improving outcomes for existing CI users

5.5.1 Anti-inflammatory intervention to modulate cochlear wound healing

Recent work has identified improved preservation of spiral ganglion neurones after dexamethasone elution in chronically stimulated animals (Scheper et al, 2017). Another study of dexamethasone eluting CI electrodes in guinea pigs showed significant reductions in fibrotic tissue and EI compared to no-steroid controls (Wilk et al, 2016). A complementary result was shown in humans where the cochlea was perfused with the steroid triamcinolone; long-term EI levels were

significantly lower in the treatment group compared to controls (De Ceulaer et al, 2003). Systemic delivery of the steroid methylprednisolone in another study did not reduce EI spikes (Choi et al, 2017), which suggests the anti-inflammatory action of steroids is most effective when topically administered. It would be interesting to study the benefit of steroid based intervention in the mouse model, guided by the EI outlier-labelling tool.

5.6 Conclusion

Understanding variability in CI outcomes, poor performance and soft failure can be improved by enhanced measurement and analysis of the CI-tissue interface. Refinements in technology and surgical procedures over time has meant the biological or soft factors are becoming the priority for research enquiry. Several past studies have investigated the CI-tissue interface in post-mortem analyses. There remains a need for improved measurement of the CI-tissue interface with a view to improving CI outcomes to reduce the undesirable variability. To this end, this research presents three approaches to investigation of the CI-tissue interface that translates between basic research clinical application.

A case study of a CI migration related failure is presented in Chapter 2. A detailed immunohistochemical analysis was performed on the tissue from the explanted array. The findings show clear evidence of unresolved inflammation and active tissue proliferation. This profile of wound-healing in human CI represents a novel finding among other post-mortem temporal bone studies. This research, which is ongoing, will determine whether the findings represent the average or an outlier in the population.

There is a lack of clinical tools for monitoring the CI-tissue interface. Evidence suggests that EI reflects the type and volume of tissue which develops around the CI electrode array. A study was carried out to describe and analyse EI norms for a large sample of CI users over five years. The study revealed a minority of individuals with raised EI levels in electrodes that were not deactivated. 8% of adults and 5% of children reached the threshold of SEI, often in mid and apical electrodes, which may be explained by localised fibrotic or bony tissue growth. This outlier detection tool may represent an objective indicator of abnormality at the electrode-tissue interface that could guide clinicians to deactivate electrodes or change stimulation parameters.

Unanswered questions such as the effect of specific aetiologies on the CI-tissue interface could be tested using a mouse model. The methods developed here allow tissue analysis using a combination of immunohistochemistry and X-ray μ CT imaging. This technique, known as 3D X-ray histology, offers the benefits of high spatial resolution and cell-marker specificity. This will be a

valuable tool answering research questions regarding the molecular and cellular mechanisms of wound healing that influence the CI-tissue interface.

Future development of the model will allow controlled investigation of factors that influence human CI outcomes such as aetiological differences and health status. The algorithmic approach to data processing applied in Chapter 3 could be used to improve monitoring of the CI-tissue interface with minimal cost and could guide pre-emptive anti-inflammatory treatment. This would be further optimised by improved knowledge of the human wound healing response from ongoing work using the mouse model and explanted human fibrotic tissue.

Appendix A

A.1 Appendix A1

OCT Embedding SOP

To embed tissue in OCT to freeze, OCT was poured on top of tissue on blue roll and left to let it form a matrix over the tissue.

OCT was poured into small cylinder of foil and the tissue was placed in the small cylinder before placing the whole cylinder into a slurry of isopentane to freeze the OCT matrix.

Risk (Isopentane): Extremely flammable liquid and vapour. If inhaled, may cause drowsiness or dizziness. Keep container away from heat and open flames. Wear goggles, gloves and lab coat. If inhaled, remove person to fresh air and keep comfortable for breathing.

Risk (Dry ice): The very low temperature can cause severe burn damage to skin. In contact, skin can freeze and adhere to liquid cooled surfaces, causing tearing on removal. The vapour can cause damage to softer tissue e.g eyes and lungs.

Wear gloves, lab coat and goggles. Always use dry ice in a well-ventilated area. never dispose of large amounts of dry ice by tipping into water – can cause CO₂ toxicity.

If tissue comes into contact with the solid, cooled liquid or gas, it is important to restore that tissue to normal body temperature as rapidly as possible. This should be done by immersing the affected area in warm (40°C) water (NOT hot water), followed by protection of the injured tissue from further trauma or infection. A First Aider trained in frostbite treatment should be summoned and, if severe, the casualty taken immediately to hospital.

The block of OCT was stored at – 20 °C until sectioning.

Prior to commencing sectioning, the OCT block was placed in a cyro-chamber before sequential 10 µm sections were cut and collected on APES or superfrost plus glass slides. The slides were dried for 1 hour at room temperature then stored at – 20 °C.

A.2 Appendix A2

Cutting frozen sections

Method:

Remove specimens to be cut from cryostorage and place in cryo-chamber to come up to temperature

Risk (Biohazard): Risk of contamination with biological material. Wear goggles, gloves and lab coat. If contaminated, rinse with water and anti-bacterial cleaner.

Ensure handwheel on the cryostat is locked and anti-roll plate is lowered, covering the blade.

The cryostat temp should be -20°C . Check the knife angle is set to 5° and correct section thickness is selected.

To mount specimens for cutting, place a pea sized drop of OCT on to a chuck, place prepared specimen on OCT and allow to freeze in the quick freeze shelf/bit.

Place chuck into holder, move the knife block toward the specimen head, then use the advance button until close enough to trim in to block.

Risk (sharp blade): Cut finger tips. Wear two pairs of gloves and be cautious. If have an accident, seek a trained first aider.

When cutting a full-face, raise anti-roll plate and slowly cut a few sections. Lower the anti-roll plate and start to cut. Carefully pick-up sections on labelled, coated slides (APES or superfrost plus).

Dry sections for at least 1 hour at room temp, then stain immediately or wrap in aluminium foil and store at -20°C and use within two weeks.

When finished, brush debris into the waste tray, remove and empty into an orange bin.

Summary of risks:

Biological: All fresh tissue must be treated as potentially harmful.

Physical: risk of cuts/lacerations from microtome blade and glass slides

A.3 Appendix A3

Haematoxylin and Eosin Staining - OCT

Coshh form for DPX/ PERTEX and Xylene must be read and signed before staining is commenced

OCT Embedded Tissue

Warm tissue at 37⁰C for 15 mins

If tissue is unfixed- fix in 100% Ethanol for 5 mins at 4⁰C

Risk (Ethanol): Flammable and acutely toxic. Wear protective lab coat, goggles and gloves. Dispose down sink with copious water.

Place tissue sections into water for 2 mins

Tap off excess water and place sections into Haematoxylin solution in fume hood for 5 mins- USE TIMER

Risk (Haematoxylin): Irritant. Avoid contact and inhalation. Wear lab coat, gloves and goggles. If contacted, seek immediate medical attention. To dispose – pour down sink with running water.

Tap off excess Haematoxylin and place sections into clean tap water to wash off excess Haematoxylin

Replace the tap water until it remains clear

Place sections into 1% Acid 70% Ethanol for two dips

Place section back into tap water

Differentiate the Haematoxylin stain by allowing clean tap water to flow over the sections PINK to BLUE ~2mins.

[If staining with Eosin place into Eosin for 1-3 mins]

[Wash off excess Eosin with tap water washes]

Once Haematoxylin stain has turned blue place into 70% Ethanol~5 mins

Continue dehydration by placing sections through Ethanol Concentration gradient

Risk (Ethanol): See above

70% Ethanol ~5 mins

80% Ethanol~ 5 mins

95% Ethanol ~5 mins

100% Ethanol I ~5 mins

Appendix

100% Ethanol II [CLEAN] ~5mins

Place into xylene I ~10 mins

Risk (Xylene): Harmful if inhaled or contact with skin. Wear protective lab coat, goggles and gloves. If contact with skin – rinse under running water. Do not wash down sink; collect in non-chlorinated liquids waste container.

Place into xylene II [CLEAN] ~10mins

Clover slip with DPX or PERTEX

Risk (DPX): Harmful if inhaled or contact with skin. Wear protective lab coat, goggles and gloves. Do not wash down sink; collect in non-chlorinated liquids waste container.

Leave to dry in fume hood

A.4 Appendix A4

MSB Trichrome

Dewax sections in clearene 2 x 5 minutes

Risk (Clearene): Harmful if inhaled or contact with skin. Wear protective lab coat, goggles and gloves. If contact with skin – rinse under running water. Do not wash down sink; collect in non-chlorinated liquids waste container.

2. Hydrate through decreasing grades of alcohol to water 3 x 1 minute

Risk (Ethanol): Flammable and acutely toxic. Wear protective lab coat, goggles and gloves. Dispose down sink with copious water.

Stain with Weigert's haematoxylin 5 minutes

Risk (Haematoxylin): Irritant. Avoid contact and inhalation. Wear lab coat, gloves and goggles. If contacted, seek immediate medical attention. To dispose – pour down sink with running water.

4. Blue in running tap water 5 minutes

5. Rinse in 95% alcohol

Risk (Ethanol): Flammable and acutely toxic. Wear protective lab coat, goggles and gloves. Dispose down sink with copious water.

6. Stain with Martius Yellow 2 minutes

Risk (Martius Yellow): Irritant! Irritating to eyes, respiratory system and skin. Wear protective lab coat, goggles and gloves. If contact with skin or eyes – wash with lots of water.

7. Wash briefly in water.

8. Stain with Crystal Ponceau 10 minutes

Risk (Crystal Ponceau): Avoid contact with skin and eyes. Wear protective lab coat, goggles and gloves. If contact with skin or eyes - wash with lots of water.

9. Wash in water

10. Treat with Phosphotungstic acid solution 5-10 minutes

Appendix

Risk (Phosphotungstic acid solution): Irritant corrosive. Causes severe skin burns and eye damage. Wear protective lab coat, goggles and gloves. If contact with skin or eyes - wash immediately with lots of water.

11. Stain with aniline blue 5-10 minutes

Risk (aniline blue): Irritant. Causes severe skin, eye and respiratory irritation. Wear protective lab coat, goggles and gloves. Use in a well-ventilated area. if contact with skin or eye – wash immediately with water.

12. Wash and blot dry

13. Dehydrate clear and mount

Results

| | |
|-----------------|------------|
| Fibrin | red |
| Muscle | paler red |
| Nuclei | blue-black |
| Collagen | blue |
| Red blood cells | yellow |

A.5 Appendix A5

OCT Embedded Tissue

1. Warm at 37°C for 5 mins
2. Place into PBS ~5 mins
3. Block activity of endogenous peroxidase- incubation with 1% H₂O₂ in Methanol for 15 mins

Risk (Hydrogen peroxide): Irritant and corrosive. Avoid contact with skin and eyes. Wear protective lab coat, goggles and gloves. If contact with skin – rinse under running water.

Risk (Methanol): Flammable, toxic. Avoid contact with skin and eyes. Wear protective lab coat, goggles and gloves. If contact with skin – rinse under running water.

4. Wash in PBS Tween [0.05%] 2x 5 mins

Risk (Tween): Avoid inhalation and contact with skin. Work with low concentrations (0.05-0.5%) and small volumes (~1ml). Wear protective lab coat, goggles and gloves. If contact with skin – rinse under running water.

5. Antigen retrieval-
 - i. microwave sections in citrate buffer 3 mins
 - ii. Cool sections by placing them into tap water 5 mins
 - iii. Re-microwave in citrate buffer 3 mins [check every 30 seconds for overflowing]
 - iv. Cool in tap water for 5 mins

Risk (Sodium citrate buffer): Avoid inhalation and contact with skin. Wear protective lab coat, goggles and gloves. To dispose – pour down sink with running water.

Risk (Boiling liquid): Boiling liquid can burn skin. Wear heat-proof protective gloves, as well as lab coat, goggles and gloves. In the incident of a burn – run under cold water. If severe- seek medical attention.

Appendix

6. Wash off citrate buffer PBS Tween[0.05%] 2 x 5 mins

Risk (Tween): See above

7. Block sections in 5% BSA or Serum
8. Incubate in primary Antibody Overnight at 4°C
- i. Make Primary antibody solution in 0.25% BSA and 0.01% Tx100
9. Wash PBS Tween[0.05%] 2x 5 mins

Risk (Tween): See above

10. Incubate in Secondary Antibody 1 hour at room temperature—BIOTIN SECONDARY
- i. Make Secondary Antibody solution in 0.25% BSA and 0.01% Tx100
11. Make ABC solution
- i. 1 drop A (Avidin Solution)
- ii. 1 drop B (Biotyl enzyme)
- iii. In 5 ml PBS

Allow to mix on shaker for 15 mins

12. Wash section in PBS Tween [0.05%] 2 x 5 mins

Risk (Tween): See above

13. Put on ABC solution—30 mins room temperature
14. Wash sections PBS Tween[0.05%] 2x 5mins

Risk (Tween): See above

15. Put in DAB solution
- i. 250ml 0.1M Phosphate Buffer, 5ml DAB solution, 125µl H2O2

Risk: (DAB): Carcinogenic. Avoid any contact. Wear lab coat, gloves and goggles. If contacted, seek immediate medical attention. Ensure there is no cross contamination across the lab. To dispose – add bleach in sink and leave the water running to rinse.

Risk (Hydrogen peroxide): See above

16. Check for staining after 30 seconds—USE TIMER
 - i. Then in 10 second intervals
17. Put into PBS to stop reaction- rinse 2 x 5mins in PBS
18. Counter stain with Haematoxylin—5 mins in haematoxylin
 - a. Follow Haematoxylin staining protocol

Risk (Haematoxylin): Irritant. Avoid contact and inhalation. Wear lab coat, gloves and goggles. If contacted, seek immediate medical attention. To dispose – pour down sink with running water.

Appendix B

B.1 Appendix B1



Protocol

Study Title: Investigation of cochlear implant electrode impedance as a biomarker for hearing performance outcomes: A retrospective study

Researcher(s) Alan Sanderson (Main researcher, PhD student), Dr Carl Verschuur (PhD supervisor), Dr Tracey Newman (PhD supervisor)

Funder: EPSRC

Background

Cochlear implants (CI) are prosthetic hearing devices that can provide significant benefit for people with severe to profound hearing loss. Despite thorough pre-implant assessment, some CI users experience much lower performance than predicted. This sub-optimal performance manifests itself in various ways including poor speech recognition and undesirable auditory sensations. Emerging evidence suggests the underlying cause for this is multifactorial and likely to have an inflammatory component. This is supported by reports that anti-inflammatory treatment using steroids improves speech recognition performance and reduces undesirable symptoms. Evidence from in-vitro and in-vivo investigations shows that CI electrode impedance measurements reflect tissue changes around the implanted electrode. Although impedance measurements are used in CI assessment clinics, their application is currently limited to gross checks of the status of the electrical circuit.

Appendix

This study will investigate electrode impedance to establish a model of the normal status of the measure over time. Additional aims are to investigate the relationship between electrode impedance and hearing threshold levels, speech recognition scores and hearing loss aetiology. These measures are included as an indicator of cochlear health and the function of the CI and its interface with the auditory system. The retrospective design will include analyses of measurements spanning the initial pre-implant audiological assessment through to the most recent clinical assessment. By investigating the relationship between cochlear electrophysiology, functionality and pathology we aim to investigate the predictive power of electrode impedance as a biomarker for future CI performance.

The study has the following aims and objectives:

Objective 1) Extract electrode impedance data from patient records in order to describe the variation between values recorded at different time points.

Objective 2) Extract pure tone and speech audiometry data from patient records in order to calculate hearing preservation scores and describe the variation between values recorded at different time points. The following data will be extracted: unaided hearing threshold levels, aided hearing threshold levels, aided speech recognition scores (BKB Sentence Test or McCormick Toy Test depending on patient age). Data spanning complete care pathway for the individual to date will be extracted where possible

Objective 3) Extract patient aetiology information from patient records in order to investigate the relationship between causes/types of deafness with electrode impedance.

Aim 1)

a) Describe the electrode impedance at each recorded time-point corresponding to previous clinical sessions. This will include electrode impedance levels at each electrode. To summarise, the analysis will include two variables; time point and electrode number.

b) Describe the differences between electrode impedance levels taken from two sub-sample groups; patients implanted with a Med-el device and those implanted with an Advanced Bionics device.

Aim 2)

a) Analyse the relationship between electrode impedance levels and low frequency hearing preservation (LFHP: standardised measure calculated using pre and post implantation

hearing threshold levels). This analysis will be performed within the aforementioned sub-sample groups; Med-el and Advanced Bionics.

b) Electrode impedance fluctuation over time VS Speech recognition score (BKB or Toy Test) (each comparison will be time matched i.e. corresponding to a given clinical session). This analysis will be performed within the aforementioned sub-sample groups; Med-el and Advanced Bionics.

c) Electrode impedance fluctuation over time VS unaided hearing threshold levels over time (each comparison will be time matched i.e. corresponding to a given clinical session). This analysis will be performed within the aforementioned sub-sample groups; Med-el and Advanced Bionics.

d) Electrode impedance fluctuation over time VS unaided hearing threshold levels over time (each comparison will be time matched i.e. corresponding to a given clinical session). This analysis will be performed within the aforementioned sub-sample groups; Med-el and Advanced Bionics. This is because of the different method applied by the two manufacturers in their clinical software/hardware system to measure impedance.

Aim 3) Analyse the relationship between electrode impedance magnitude and hearing loss aetiology. For example, the preliminary analysis from Aim 1 shows a small subset of the sample exhibits significantly great magnitude of impedance than the majority of the sample. One might hypothesise that the minority patients are distinct from the remainder of the sample in a way that is predicted by the hearing loss aetiology.

Hypothesis A: Electrode impedance levels, at one or several electrodes (after the expected acute fluctuation following implantation) will be negatively correlated with low frequency hearing preservation (LFHP).

Hypothesis B: Electrode impedance levels, at one or several electrodes (after the expected acute fluctuation following implantation) will be significantly different between aetiology groups.

Method

Data collection

This study will consist of a retrospective analysis of patient data. The data will be collected from patient records of measurements of electrode impedance, hearing threshold levels (aided and unaided), speech recognition scores (BKB or Toy Test) and hearing loss aetiology. The electrode impedance, hearing threshold and speech recognition score data will be extracted by a clinically qualified employee of the University of Southampton Auditory Implant Service (USAIS).

Electrode impedance

Appendix

The impedance measurement produces a single value in Ohms for each electrode. Values are stored in a manufacturer specific database at every clinical session. The values will be manually or batch transferred from the software database to the data collection sheet. The data will be organised into the following levels: time point (relative to implantation date, electrode number. See data collection Excel document.

Hearing threshold level

This measurement is made using pure tone audiometry (PTA). The test yields a value in dB HL which defines the hearing threshold level at a given time point for a specific frequency. The data is stored in a secure USAIS database. Hearing threshold values will be manually transferred to the data collection sheet. The data will be organised into the following levels: aided/unaided, time point, stimulus frequency, ear (left/right/binaural). See data collection Excel document.

Speech recognition score

This measurement is made using speech audiometry. The specific style of testing depends on the developmental age of the patient. Paediatric patients (define range) are assessed using the McCormick toy test which yields a single value in dB (A) representing the stimulus intensity required for the patient to correctly identify 80% of the words (check this detail). The data will be organised into the following levels for paediatric patients: time point.

Adult patients are assessed using the Bamford-Kowal-Bench (BKB) sentence test which yields a percentage score of speech recognition performance. If a patient scores highly when listening to the stimulus is quiet, they will be tested using additional noise. Therefore a patient may have a percentage score as well as a value representing the signal to noise ratio at which the maximum score was achieved. The data will be organised into the following levels for adult patients: time point, signal to noise ratio (SNR is more like a category than a variable)

Hearing loss aetiology

This information is gathered by the clinical team at USAIS and stored in a secure USAIS database. The detail of the information can be variable depending on its source. For example, not all patients undergo aetiological investigations such as genetic testing. Although this may limit the resolution of the variable, it will be possible to split the sample by gross categories such as congenitally and acquired hearing loss.

Testing the hypotheses

The main hypothesis will be tested using linear regression analysis. The electrode impedance variable will be treated as the predictor or independent variable. The LFHP variable will be the dependent variable.

Additional data

The following details will be collected to be used as categorical data.

- Age of implant: Evidence shows that some people experience age related hearing loss earlier than others. Also, outcomes have been shown to be different in adult and paediatric cases. We aim to test whether age is a factor in the above analysis.
- Gender: This will allow for a test of differences between male and female CI users in the above hypothesis test. Anecdotal clinical evidence suggests that there may be a gender effect.
- Hearing loss aetiology: Knowledge of aetiology may provide insight into the underlying mechanism associated with high electrode impedance and/or poor outcomes on hearing threshold and speech recognition outcomes.
- Duration of deafness: Evidence shows that CI performance outcomes are lower in cases of long term auditory deprivation. Including this data will allow this factor to be controlled.
- Electrode array type: Recent evidence from CI manufacturers suggests that hearing preservation is affected by the shape, size and length of the electrode array. Inclusion of this data will allow this factor to be included as a category in the hypothesis testing.

Materials

- Computer connected to the University of Southampton Auditory Implant Service (USAIS) local network.
- Microsoft Excel data collection sheet (see additional document)

Participants

The retrospective data will be collected from the notes of CI users under the care of USAIS. Each user has previously been implanted with either a Med-el or advanced bionics device. They have undergone pre and post implant audiological assessment and monitoring which has yielded the aforementioned clinical outcome measures.

Adult CI users

Users that were implanted at or above the age of 18, classified as adult, will be included in the study. As there is no evidence to suggest a gender effect both male and female users will be included. Data will be collected from approximately 100 CI MED-EL CI users and approximately 100 Advanced Bionics CI users. This group have provided consent for their data to be used anonymously.

Paediatric CI users

Users that were implanted below the age of 18, classified as paediatric, will be included in the study. As there is no evidence to suggest a gender effect both male and female users will be included. Data will be collected from approximately 100 CI MED-EL CI users and

Appendix

approximately 100 Advanced Bionics CI users. The parents or guardians of CI users in this group have provided consent on the child's behalf.

The sample population will be split according to the manufacturer of the device used by the patient (Med-el or Advanced bionics). This is because of the different method applied by the two manufacturers in their clinical software/hardware system to measure impedance.

Procedure

This study has a retrospective design. The electrode impedance, hearing threshold level and speech recognition score data will be extracted by a clinically qualified employee of USAIS. This clinician will transfer the anonymised data into a pre-designed spreadsheet (see additional document) using only a unique identifier code for each patient. The clinician will have no other stake in the research project. The spreadsheet containing the raw data will be sent electronically to the main researcher via a password secured email client hosted by the University of Southampton. The data will be analysed using a University of Southampton workstation with Microsoft Excel, IBM SPSS and GraphPad Prism.

Statistical analysis

Descriptive statistical analysis will be used to show the mean and standard error of the mean. The raw data will be plotted in figure showing electrode impedance over time.

ANOVA will be used to test the differences between electrode impedance levels taken from two sub-sample groups; users implanted with a Med-el device and those implanted with an Advanced Bionics device. Further post-hoc tests may be used to investigate gender, time point and electrode number as contributing factors.

Linear regression analysis will be used to establish the strength of the covariance of the variables. A t-test will be used to establish the significance of the correlation. The four relationships outlined in Aim 2a, b, c, d will be plotted in scatterplots.

Ethical issues

The anonymity of all CI users will be protected by severing the link between data extraction and data analysis. An employee of USAIS with clinical qualification and experience will perform data extraction. They will transfer the aforementioned data into a predesigned spreadsheet using a number to label each CI user. This will be transferred to

the main researcher with no identifying information outside of those detailed. The main research has no personal or professional relationship with any USAIS CI users.

Anonymity of patient details:

Collected data will be compiled using a password secured Microsoft Excel spreadsheet and saved in a directory within a password protected profile on the University of Southampton computer network. Following compilation of the dataset the key which links the data to individual CI users will be destroyed.

The data will be coded with an identifier to allow alignment of each variable in the raw dataset. The key for the identification codes will be destroyed immediately following collation of the dataset providing unlinked anonymity. The USAIS clinician who undertakes the data extraction will have no other stake in the research project.

Informed consent:

All USAIS CI users are given the choice to sign an agreement that their anonymised data can be used in groups analysis without the need for further consent. Only users that signed such an agreement will be included in the analysis proposed here.

Data Protection:

Collected data will be compiled in one password secured Microsoft Excel spreadsheet. This will be saved in a password protected secure directory on the local hard drive of the computer used by the main researcher. This directory is mirrored by the University of Southampton server which is also password protected. There will be no link between the spread sheet and the original CI user information. The data will not be transferred to anyone outside of the University of Southampton. Data storage and handling will adhere to the University of Southampton Data Protection Policy (2008).

B.2 Appendix B2

ERGO Ethics approval

Your Ethics Submission (Ethics ID:17430) has been reviewed and approved



○ ERGO <ergo@soton.ac.uk>

Wednesday, 3 February 2016 at 12:04

○ Sanderson A.P.

[Show Details](#)

Submission Number: 17430

Submission Name: Investigation of cochlear implant electrode impedance as a biomarker for hearing performance outcomes: A retrospective study

This is email is to let you know your submission was approved by the Ethics Committee.

You can begin your research unless you are still awaiting specific Health and Safety approval (e.g. for a Genetic or Biological Materials Risk Assessment)

Comments

1.A well-constructed, detailed and clear application. Submission approved.

2.Approved on behalf of the third reviewer to expedite review. ERGO Administrator

[Click here to view your submission](#)

ERGO : Ethics and Research Governance Online

<http://www.ergo.soton.ac.uk>

DO NOT REPLY TO THIS EMAIL

B.3 Appendix B3

Surgery consent form

Patients Name: _____

Surgeon: _____

Side of implantation: RIGHT LEFT

WE SUGGEST YOU USE A PEN TICKING EACH SECTION AS YOU READ IT AND JOTTING DOWN ANY QUESTIONS.

PATIENT INFORMATION ABOUT THE COCHLEAR IMPLANT OPERATION

Cochlear Implant Surgery

A cochlear implant takes over the function of the cochlear which is no longer working effectively. The internal part of the implant has two main parts. The 'receiver stimulator' part and the 'electrode array' part. The 'receiver stimulator' part is placed on the surface of the skull bone under the skin behind the ear. A bed is drilled into the skull bone to accommodate the receiver- stimulator and it is fixed to the skull with stitches. The other part of the implant is the 'electrode array', which is like a wire, that runs from the receiver stimulator package down through the mastoid bone, into the middle ear space under the ear drum and into the cochlea. In order for the electrode array to reach the cochlear a passageway needs to be created by drilling through the bone of the mastoid into the middle ear space where the outer surface of the cochlea can be seen. Getting into the middle ear space means drilling a slot in the bone between the facial nerve and the ear drum. The facial nerve supplies the muscles on one side of the face and is responsible for facial movement. Once the cochlea is exposed a hole needs to be drilled through the bony wall of the cochlea. The cochlea (the organ of hearing) is intimately related to the balance system.

Cochlear implantation is a safe operation. Complications are very uncommon. However there are risks associated with any operation and those related to cochlear implantation are listed below.

Anaesthesia

The operation typically takes 3-4 hours and is performed under general anaesthesia. There is some risk associated with any anaesthetic of this length, but this risk is very small. The anaesthetist will see you just before the operation to discuss any concerns you may have.

I have read and understood the above paragraph *please tick*

Questions _____

Facial Nerve Damage.

In order to gain access to the cochlea the surgeon needs to drill very close to the facial nerve. During this procedure it is possible that the nerve could be damaged. The damage would result in a weakness or paralysis of one side of the face. This could be temporary or permanent. It is an extremely uncommon complication (less than 1%). The nerve is monitored throughout the operation.

I have read and understood the above paragraph *please tick*

Questions _____

Wound Infection.

If the wound becomes infected during the healing process it will often settle with antibiotic treatment. However sometimes antibiotic treatment alone may not be sufficient and it may be necessary to remove the implant. If the implant needs to be removed then any hearing which was present in that ear before the operation is likely to be lost. Although this is a very uncommon problem it is an important consideration in patients with some hearing before surgery when deciding which ear

to implant as the small amount of hearing they have could be lost. Sometimes it may be possible to re-implant the ear at a later date.

I have read and understood the above paragraph *please tick*

Questions _____

Device Failure

An implant is a man made device and inevitably, however good a company's quality control, the device may stop working or malfunction. There is about a 2% risk of this happening. If it does the device can usually be successfully replaced but this will require another operation.

I have read and understood the above paragraph *please tick*

Questions _____

Meningitis.

The fluid inside the cochlea may sometimes be in communication with the fluid around the brain (the cerebro-spinal fluid or CSF). There is a risk that infection could enter the cochlea and then the CSF causing meningitis. The risk of this happening around the time of surgery is extremely small – around 1 in 4000 cases. This risk is slightly higher in patients who have an abnormally formed cochlea. As a precaution we recommend that any one undergoing cochlear implant surgery should have a 'pneumococcal' vaccination before the surgery. We also recommend that if the patient develops an ear infection in the months and years after the surgery that they receive early treatment with antibiotics from their GP.

I have read and understood the above paragraph *please tick*

Questions _____

Outcome not predictable

Unfortunately, even with our sophisticated tests, it is not possible to accurately predict the outcome of the procedure. The degree of benefit can range from only hearing environmental sounds (door bells, telephones, microwave), to gaining help with lip reading, to being able to understand someone talking behind you, to using the telephone. Most patients are delighted with the benefit they gain from their implant. Unfortunately it is possible that you/your child may gain no benefit from the implant. **Ensuring that you/your child have realistic expectations is a very important part of the assessment process.**

I have read and understood the above paragraph *please tick*

Questions _____

Implant Damage

A blow to the head at the site of the implant may result in damage of the implant causing it to stop working. If this happens the device can usually be successfully replaced but this will require another operation. We would not recommend taking part in activities where there is a high risk of injury to the implant site.

I have read and understood the above paragraph *please tick*

Questions _____

Replacement of implant

It is unlikely that the implant will last forever and inevitably children and some adults may need to have the implant replaced at some time in the future.

I have read and understood the above paragraph *please tick*

Questions _____

Dizziness

As the balance system is so closely related to the cochlea interference with this system during surgery or from infection is a possibility. This could result in balance problems which could be temporary or permanent. Dizziness and balance problems are surprisingly uncommon after cochlear implantation

I have read and understood the above paragraph *please tick*

Questions _____

Tinnitus

Tinnitus is a noise which is heard by the patient but is not actually present in the environment. It is an internally generated noise due to a problem somewhere in the hearing pathway. In other words it may be generated from a problem inside the cochlea, in the hearing nerve or in the hearing pathways in the brain. Cochlear implantation may have no effect on any tinnitus that you or your child already have; alternatively it may cause tinnitus, worsen tinnitus or improve or abolish tinnitus.

I have read and understood the above paragraph *please tick*

Questions _____

Electrical stimulation

The implant causes a tiny electric current to be produced in the cochlea. It is this current that stimulates the hearing nerve. Occasionally the electrical current can stimulate other nerves such as the facial nerve causing facial twitching or discomfort. This can usually be avoided by re-tuning or turning off the offending electrode(s). The long-term effect of the electrical current put out by the implant on the nervous tissue, or any other tissue is unknown. There is no reason to expect any detrimental effect. Many patients report an improvement in their sound quality over years following the operation. We will not fully understand the results of this stimulation by electric currents until many patients have used these devices for many years.

I have read and understood the above paragraph *please tick*

Questions _____

This information sheet is not intended to be an exclusive list of all possible complications.

After the Operation

After the operation you will have a bandage around the head which should stay on for at least 24 hours.

Behind the ear there will be some plasters (Steristrips) covering the wound. These should be left in place for at least a week.

The ear canal will be packed with a dressing which will be removed at the first out patients visit.

A piece of cotton wool will be in place covering the ear hole. This may become moist and should be changed carefully.

The stitches used will dissolve themselves and so do not need to be removed.

Antibiotics will be given intravenously while in hospital and antibiotics will be given to take at home for about 5 days.

An Xray will be performed before leaving the hospital.

You will be seen for a first post operative visit in the cochlear implant clinic 1 – 2 weeks after the operation.

You should keep the ear and the wound dry until you are seen.

In the first two weeks keep away from crowds of other people to minimise the risk of picking up an infection

Avoid any strenuous exercise for a month.

Motivation

Cochlear implantation is a significant undertaking and a major step in anyone’s life. The process is a PARTNERSHIP between the implant team and the patient or parents. It involves serious responsibilities on both sides and a successful outcome requires active participation by the patient/parents and a commitment of time and effort. The members of the implant team will do everything in our power to achieve as good an outcome as is possible.

Developments in Cochlear Implants

The implanted device and the external speech processor device are under constant development and improvement. In the future it may or may not be possible to update the external device. Any cochlear implant will become out of date, meaning that for new patients a different device will be used.

The cochlear implant programme may be stopped without your consent under various possible conditions including lack of funding, or failure to follow instructions.

Is There an Alternative to Surgery?

Yes. The alternative to surgery is to persevere with hearing aids or to learn sign language or a combination of both.

Manufacturer

The intended implant manufacturer to be used is:

Advanced Bionics / Cochlear / Med-el (*please delete the manufacturers not going to be used*).

Confidentiality

All patient information will be treated as confidential. Only those persons involved with the programme and its evaluation will have access to the records. Any data published in scientific journals will be pooled summary data without patient identification. Specific data on an individual patient will be published only with the specific written permission of that patient.

Other physicians, scientists, and technicians may be in the operating theatre for educational purposes.

I have read and understand the contents of this information sheet. I have been given adequate time to consider it and have discussed the above material with those whom I feel may be of benefit in my understanding of the above,

Signature of Patient:_____

or

Signature of Patient’s Parent or Guardian:_____

Date:_____

B.4 Appendix B4

Anonymised data consent form

CONSENT FORM

Patient name _____

CI number _____

The University of Southampton Auditory Implant Service is committed to research to improve patient outcomes and the service our patients receive. As such we would like to be able to use information collected from our patients in research projects, service evaluations or audits. These projects could occur at the University of Southampton, at other cochlear implant centres or Universities, at the cochlear implant companies, or at other external agencies. Your data would be anonymised; this means that you would not be able to be recognised from the data used.

By signing below you agree that you are happy for anonymised data from you (or your child if the patient here is a child) to be used for these purposes.

Please note, if you choose not to allow your data to be used for research, service evaluation or audit this will not affect your treatment at the University of Southampton Auditory Implant Service in any way.

Name of person signing Date Signature

Relation to patient _____

Name of person taking consent (Staff member) Date Signature

When completed, 1 for patient; 1 for patient file

B.5 Appendix B5

Process Impedance Data

```

function [figure_path, data_path] = process_impedance_data(patient_type,
load_xls, save_formats, save_figures, save_data, plot_outliers)
%% configuration
channels = 1:12;
if nargin == 0
    patient_type = 'paed'; % 'adult' or 'paed'
    load_xls = false;

    save_formats = {'fig', 'png', 'eps'};
    save_figures = true;
    save_data = false;
    plot_outliers = false;
    use_median = false;
end

%% load data
if load_xls
    filename = ['input_data' filesep 'Sorting data with new ID into
seperate channels 2 corrected age_v2(remove compress split).xlsx'];

    dob_file = ['input_data' filesep 'Export from access with all fields
and new ID corrected Age_2.xlsx'];
    activation_file = ['input_data' filesep 'Deactivations_sorting into
channels_v3.xlsx'];

    reason_file = ['input_data' filesep 'Query Deactivations_export from
Access_(reason)_v8.xlsx'];

    for ii = channels

        [ID, timepoint_yr, data(ii, :, :)] = import_hearing_data(filename,
['Ch' num2str(ii)]);

        end

        [PatientId_dob, Birthday] =
import_dob_data(dob_file, 'Query__impedance_with_rel_time1');
        % load activation data
        [PatientId_active, Time_active, Channel_active, Activation] =
import_activation_data(activation_file);
        [PatientId_reason, Year_reason, reason_array_local,
reason_array_global] = import_reason_data(reason_file);
        save('xls_cache')
    else
        varlist = who; %Find the variables that already exist
        varlist = strjoin(varlist, '$|'); %Join into string, separating vars
by '|'
        load('xls_cache', '-regexp', ['^(?!' varlist ')\w']);
    end

    %% clean activation data
    % replace NaN with last activation state
    Activation = clean_activation_data(Activation);

    %% shift data along if reason for deactivation is extra-cochlear

```

Appendix

```
data_inc_extra_cochlear = data;
[data, Activation, any_reason_ec] = extra_coclear_shift(data, ID,
Activation, PatientId_active, PatientId_reason, reason_array_local,
reason_array_global);
%%

split = find(cellfun(@(x) strcmp(x, 'child'), ID));

roi_ad = 1:split-1;
roi_ch = split+1:length(ID);
ad_data = data(:,roi_ad,:);
ch_data = data(:,roi_ch,:);
ad_data_inc_extra_cochlear = data_inc_extra_cochlear(:,roi_ad,:);
ch_data_inc_extra_cochlear = data_inc_extra_cochlear(:,roi_ch,:);

ad_ID = ID(roi_ad);
ch_ID = ID(roi_ch);
save('adult_and_child_ids', 'ad_ID', 'ch_ID');

switch patient_type
    case 'adult'
        all_impedance_data = ad_data;
        all_ID = ad_ID;
        type = 'Adult';
        figure_path = 'adult figures';
        data_path = 'adult data';
        data_inc_extra_cochlear = ad_data_inc_extra_cochlear;
    case 'paed'
        all_impedance_data = ch_data;
        all_ID = ch_ID;
        type = 'Paediatric';
        figure_path = 'child figures';
        data_path = 'child data';
        data_inc_extra_cochlear = ch_data_inc_extra_cochlear;
    otherwise
        error ('Impedance:Unexpected_patient_type', 'Unexpected patient
type')
end
if ~exist(figure_path, 'dir')
    mkdir(figure_path)
end
if ~exist(data_path, 'dir')
    mkdir(data_path)
end

%%

ad_mean = squeeze(nanmean(ad_data, 2));
ch_mean = squeeze(nanmean(ch_data, 2));
ad_count = squeeze(sum(~isnan(all_impedance_data),2));
ch_count = squeeze(sum(~isnan(ch_data),2));

%% Activation plotting
[pc_active, pc_deactive, is_electrode_active] =
calculate_pc_active(all_ID, all_impedance_data, PatientId_active,
Activation);

figure(300)
imagesc(timepoint_yr(timepoint_yr<=5), channels,
pc_active(:,timepoint_yr<=5))
colorbar
ylabel('Electrode')
```

```

xlabel('Time (yrs)')
set(gca, 'YTick', channels)
colormap gray

if save_figures
    set(300, 'Renderer', 'painters');
    saveallformats(300, [figure_path, filesep, type,
'_activation_heatmap'], save_formats);
end
%%
impedance_of_active_electrodes = all_impedance_data;
impedance_of_active_electrodes(is_electrode_active == 0) = NaN;
impedance_of_deactive_electrodes = all_impedance_data;
impedance_of_deactive_electrodes(is_electrode_active == 1) = NaN;
% Remove unknown from _deactive. This is not done for active. Is this
wrong?
% I know only one place where _deactive is used, so this doesn't break
% anything. I haven't checked _active
all_data_deactive(isnan(is_electrode_active)) = NaN;
%note unknown are in both matrices but usually these should have no
%impedance
mean_active = zeros(length(channels), length(timepoint_yr));
timepoint_yr_arr = repmat(timepoint_yr, [size(all_impedance_data, 2),
1]);
gradient_of_fits_to_mean = zeros(size(channels));
trendline = zeros(length(channels), length(timepoint_yr));
for curr_ch = 1:length(channels)
    curr_ch_active =
squeeze(impedance_of_active_electrodes(curr_ch, :, :));
    curr_ch_deactive =
squeeze(impedance_of_deactive_electrodes(curr_ch, :, :));
    figure(7)
    subplot(3,4,curr_ch)
    plot (timepoint_yr_arr(:), curr_ch_active(:)/1000, '.', 'MarkerSize',
10, 'Color', 'k');
    hold on
    plot (timepoint_yr_arr(:), curr_ch_deactive(:)/1000, '.',
'MarkerSize', 10, 'Color', 'r');
    hold off
    title(num2str(curr_ch), 'Color', 'k')
    set(gca, 'XTick', 0:5)

    xlim([0, 5])
    ylim([0, 30])

    if curr_ch == 12
        supAxes = [.08 .1 .84 .84];
        suplabel('Impedance /k\Omega{}', 'y', supAxes);
        suplabel('Time /yr', 'x', supAxes);

        if save_figures
            set(7, 'Renderer', 'painters');
            saveallformats(7, [figure_path, filesep, type,
'_all_data_active_deactive'], save_formats);
        end
    end

    figure(9)
    subplot(3,4,curr_ch)
    plot (timepoint_yr_arr(:), curr_ch_active(:)/1000, '.', 'MarkerSize',
10, 'Color', 'k');
    title(num2str(curr_ch), 'Color', 'k')
    set(gca, 'XTick', 0:5)

```

Appendix

```
xlim([0, 5])
ylim([0, 30])

if curr_ch == 12
    supAxes = [.08 .1 .84 .84];
    suplabel('Impedance /k\Omega{}','y', supAxes);
    suplabel('Time /yr', 'x', supAxes);

    if save_figures
        set(9, 'Renderer', 'painters');
        saveallformats(9, [figure_path, filesep, type,
'_all_data_active'], save_formats);
    end
end

if use_median
    average_active(curr_ch,:) = nanmedian(curr_ch_active,1)/1000;
    range_active = iqr(curr_ch_active,1)/1000;
else
    average_active(curr_ch,:) = nanmean(curr_ch_active,1)/1000;
    range_active = nanstd(curr_ch_active,1)/1000;
end

average_deactive = nanmean(curr_ch_deactive,1)/1000;
range_deactive = nanstd(curr_ch_deactive,1)/1000;

plot_inds_active = ~isnan(average_active(curr_ch,:)) &
~isnan(range_active);
plot_inds_deactive = ~isnan(average_deactive) &
~isnan(range_deactive);
fit = polyfit(timepoint_yr(plot_inds_active),
average_active(curr_ch,plot_inds_active), 1);
gradient_of_fits_to_mean(curr_ch) = fit(1);
trendline(curr_ch,:) = polyval(fit, timepoint_yr);
figure(8)
subplot(3,4,curr_ch)
plot (timepoint_yr, average_active(curr_ch,:), '-', 'MarkerSize', 10,
'Color', 'k');
hold on
plot(timepoint_yr, trendline(curr_ch,:), 'k:')
jbbfill (timepoint_yr(plot_inds_active), ...
average_active(curr_ch,
plot_inds_active)+range_active(plot_inds_active), ...
average_active(curr_ch,plot_inds_active)-
range_active(plot_inds_active), ...
'k',[1,1,1]*0.5,false,
0.2);%(xpoints,upper,lower,color,edge,add,transparency));
hold off
title(num2str(curr_ch), 'Color', 'k')
set(gca,'XTick',0:5)

xlim([0, 5])
ylim([0, 15])

if curr_ch == 12
    supAxes = [.08 .1 .84 .84];
    suplabel('Impedance /k\Omega{}','y', supAxes);
    suplabel('Time /yr', 'x', supAxes);

    if save_figures
        set(8, 'Renderer', 'painters');
```



```

        saveallformats(8, [figure_path, filesep, type,
'_all_data_mean_active'], save_formats);
    end
end
end

change_in_impedance = gradient(mean_active);
figure(10)
plot(timepoint_yr, change_in_impedance);
xlabel('Time /yr');
ylabel('Change in impedance /k\Omega{}');
legend(num2str(channels.))
xlim([0,5])
if save_figures
    set(10, 'Renderer', 'painters');
    saveallformats(10, [figure_path, filesep, type, '_gradient_vs_time'],
save_formats);
end

figure(11)
plot(channels, gradient_of_fits_to_mean);
xlabel('Channel');
ylabel('Gradient of fit');
if save_figures
    set(11, 'Renderer', 'painters');
    saveallformats(11, [figure_path, filesep, type,
'_gradient_of_fit_vs_channel'], save_formats);
end

figure(12)
plot(timepoint_yr, trendline-trendline(:,1));
xlabel('Time /yr');
ylabel('Arb normalised units');
legend(num2str(channels.))
xlim([0,5])
if save_figures
    set(12, 'Renderer', 'painters');
    saveallformats(12, [figure_path, filesep, type,
'_fan_fit_over_time'], save_formats);
end

%% ***** New section for outlier plotting
outlier_limit = 8;

% section below is calculating outlier for all (active and inactive) data
thresh = quantile(all_impedance_data(:, :, 1:outlier_limit), 0.75, 2) + 2.2 *
iqr(all_impedance_data(:, :, 1:outlier_limit), 2);
thresh = squeeze(thresh);
outlier_indx = false(12, size(all_impedance_data, 2));
for curr_ch = channels
    outlier_indx(curr_ch, :) =
sum(squeeze(all_impedance_data(curr_ch, :, 1:outlier_limit)) > (ones(size(all
_impedance_data, 2), 1) * thresh(curr_ch, :)), 2) >= 2;
end

% section below is calculating outlier for only active data
thresh_active =
quantile(impedance_of_active_electrodes(:, :, 1:outlier_limit), 0.75, 2) +
2.2 * iqr(impedance_of_active_electrodes(:, :, 1:outlier_limit), 2);
thresh_active = squeeze(thresh_active);
outlier_indx_active = false(12, size(impedance_of_active_electrodes, 2));
for curr_ch = channels

```

Appendix

```
    outlier_indx_active(curr_ch,:) =
sum(squeeze(impedance_of_active_electrodes(curr_ch,:,1:outlier_limit))>(o
nes(size(impedance_of_active_electrodes,2),1)*thresh_active(curr_ch,:)),2
) >= 2;
end

for curr_ch = channels %loop over channels

    impedance_curr_ch=squeeze(all_impedance_data(curr_ch,:,:));
    active_ch = squeeze(impedance_of_active_electrodes(curr_ch,:,:));

    figure(6)
    subplot(3,4,curr_ch)
    plot (timepoint_yr_arr(:), impedance_curr_ch(:)/1000, '.',
'MarkerSize', 10, 'Color', 'k');
    title(num2str(curr_ch), 'Color', 'k')
    xlim([0, 5])
    set(gca,'XTick',0:5)
    ylim([0, 30])

    if curr_ch == 12
        tt = sprintf('%s', type);
        supAxes = [.08 .1 .84 .84];
        suplabel(tt,'t', supAxes);
        suplabel('Impedance /k\Omega{}','y', supAxes);
        suplabel('Time /yr', 'x', supAxes);

        if save_figures
            set(6, 'Renderer', 'painters');
            saveallformats(6, [figure_path, filesep, type, '_all_data'],
save_formats);
        end
    end
    if plot_outliers
        for ii = 1:length(outlier_indx_active) %loop over patients
            if any(outlier_indx_active(:,ii))
                current_ID_str = all_ID{ii};

                activation_patient_index = find(cellfun(@(x) strcmp(x,
current_ID_str), PatientId_active));

                figure(ii+100)
                subplot(3,4,curr_ch)

                activation_plot = squeeze(Activation(curr_ch,
activation_patient_index,:));
                last_good_ind = find(~isnan(impedance_curr_ch(ii,:)),1,
'last');
                if isempty(last_good_ind)
                    last_good_ind = 0;
                end
                invalid_inds = 1:length(activation_plot) > last_good_ind;
                activation_plot(invalid_inds) = NaN;
                plot (timepoint_yr_arr(:), active_ch(:)/1000, '.',
'MarkerSize', 10, 'Color', [1 1 1]*0.5);
                if last_good_ind > 0
                    line([1 1]*timepoint_yr(last_good_ind), [0, 1000],
'LineStyle', '--', 'Color', [1 1 1]*0.5)
                end
                hold on
                impedance_plot =impedance_curr_ch(ii,:);
                deactivate_impedance_plot =
squeeze(impedance_of_deactive_electrodes(curr_ch, ii,:));
```

```

        time_plot = timepoint_yr;
        good_inds = ~isnan(impedance_plot);
        impedance_plot = impedance_plot(good_inds);
        time_plot = time_plot(good_inds);
        deactivate_impedance_plot =
deactivate_impedance_plot(good_inds);

        plot(time_plot, impedance_plot/1000, '-k', 'LineWidth',
1, 'MarkerSize', 10)
        plot(time_plot, deactivate_impedance_plot/1000, '.r',
'LineWidth', 1, 'MarkerSize', 10)

        hold off
        xl = xlim;
        title(num2str(curr_ch), 'Color', 'k')
        xlim([0, 5])
        set(gca, 'XTick', 0:5)
        ylim([0, 30])

        r_pos = strfind(current_ID_str, 'r');
        if isempty(r_pos)
            ear_string = current_ID_str(end-3:end);
            assert(strcmp(ear_string, 'left'));
            ID_str = current_ID_str(1:end-4);
        else
            ear_string = current_ID_str(end-4:end);
            assert(strcmp(ear_string, 'right'));
            ID_str = current_ID_str(1:end-5);
        end
        ID_num = str2double(ID_str);
        assert(~isnan(ID_num));

        dob_ind = find(ID_num == PatientId_dob, 1, 'first');
        curr_dob = Birthday(dob_ind);

        if outlier_indx_active(curr_ch, ii)
            text(0.05, 0.9, '*', 'Units', 'Normalized', 'FontSize',
18)
        end
        if curr_ch == 12
            tt = sprintf('ID: %d, Ear: %s, DOB: %s, %s', ID_num,
ear_string, datestr(curr_dob, 'dd/mm/yyyy'), type);
            supAxes = [.08 .1 .84 .84];
            suplabel(tt, 't', supAxes);
            suplabel('Impedance /k\Omega{}', 'y', supAxes);
            suplabel('Time /yr', 'x', supAxes);

            if save_figures
                set(gcf, 'Renderer', 'painters');
                saveallformats(ii+100, [figure_path, filesep,
current_ID_str], save_formats);
            end
        end
    end
end % end loop over patients
end % end if plot_outliers
end % end loop over channels

%%
if save_data
    xl_cell_array = cell(length(all_ID)+1, 14);
    xl_cell_array{1,1} = 'ID';

```

Appendix

```
xl_cell_array{1,2} = 'Overall Outlier';
xl_cell_array(2:end,1) = all_ID;
xl_cell_array(2:end,2) = num2cell(double(any(outlier_indx)));
xl_cell_array(2:end,3:14) = num2cell(double(outlier_indx).');

for ii = channels
    xl_cell_array{1,ii+2} = num2str(ii);
end
outlier_fname = [type '_outlier_info.csv'];
pad_and_write_to_csv(fullfile(data_path, outlier_fname),
xl_cell_array);

%% writing out only active impedances

for curr_ch = channels
    xl_cell_array = cell(length(all_ID)+1,length(timepoint_yr)+1);
    xl_cell_array{1,1} = 'ID';
    xl_cell_array(2:end,1) = all_ID;
    xl_cell_array(1,2:length(timepoint_yr)+1) =
num2cell(timepoint_yr);
    xl_cell_array(2:end,2:length(timepoint_yr)+1) =
num2cell(squeeze(impedance_of_active_electrodes(curr_ch, :, :)));
    pad_and_write_to_csv(fullfile(data_path, [type
'_active_impedances_Ch_' num2str(curr_ch) '.csv']), xl_cell_array);
end

%%
xl_cell_array = cell(length(all_ID)+1,14);
xl_cell_array{1,1} = 'ID';
xl_cell_array{1,2} = 'Overall Outlier';
xl_cell_array(2:end,1) = all_ID;
xl_cell_array(2:end,2) = num2cell(double(any(outlier_indx_active)));
xl_cell_array(2:end,3:14) = num2cell(double(outlier_indx_active).');

for ii = channels
    xl_cell_array{1,ii+2} = num2str(ii);
end
pad_and_write_to_csv(fullfile(data_path, [type
'_outlier_info_active.csv']), xl_cell_array);

%% write out impedance data from ONLY extra-cochlear electrodes

ec_data = data_inc_extra_cochlear;

[~, index_reason, index_id] = intersect(PatientId_reason, all_ID);
assert(length(index_id) == length(all_ID), 'Reason data not found for
at least one ID');

ec_ind_array = repmat(any_reason_ec(:,index_reason), 1,1,
length(timepoint_yr));
ec_data(~ec_ind_array) = NaN;%set non-ec data to NaN;

patient_indices_not_ec = all(all(isnan(ec_data),1),3);
ec_data(:,patient_indices_not_ec,:) = []; %remove all patient that
are all NaN;
ec_ID = all_ID(~patient_indices_not_ec); %subset of patients who
have ec electrodes;

chan_indices_not_ec = all(all(isnan(ec_data),2),3);
ec_data(chan_indices_not_ec, :, :) = []; %remove channels that are all
NaN;
```

```
ec_chan = channels(~chan_indices_not_ec);%note which channels have
been removed

for ii = 1:length(ec_chan)
    xl_cell_array = cell(length(ec_ID)+1,length(timepoint_yr)+1);
    xl_cell_array{1,1} = 'ID';
    xl_cell_array(2:end,1) = ec_ID;
    xl_cell_array(1,2:length(timepoint_yr)+1) =
num2cell(timepoint_yr);
    xl_cell_array(2:end,2:length(timepoint_yr)+1) =
num2cell(squeeze(ec_data(ii, :, :)));
    pad_and_write_to_csv(fullfile(data_path, [type
'_extra_cochlear_data_Ch_' num2str(ec_chan(ii)) '.csv']), xl_cell_array);
end

end
```

B.6 Appendix B6

Process Deactivation Reason Data

```

function [figure_path, data_path] = process_reason_data(patient_type, ~,
save_formats, save_figures, save_data, ~)
%% configuration
if nargin == 0
    patient_type = 'adult'; % 'adult' or 'paed'
    % load_xls = false;

    save_formats = {'fig', 'png', 'eps'};
    save_figures = true;
    save_data = true;
end
%% Import the data
[ID_axis, year_axis, channel_axis, Reason_array_local,
Reason_array_global] = import_reason_data(['input_data' filesep 'Query
Deactivations_export from Access_(reason)_v8.xlsx']);

%% separate adults and children
load('adult_and_child_ids', 'ad_ID', 'ch_ID');

switch patient_type
    case 'adult'
        ID_of_interest = ad_ID;
        figure_path = 'adult figures';
        data_path = 'adult data';
    case 'paed'
        ID_of_interest = ch_ID;
        figure_path = 'child figures';
        data_path = 'child data';
    otherwise
        error('Impedance:Unexpected_patient_type', 'Unexpected patient
type')
end

if ~exist(figure_path, 'dir')
    mkdir(figure_path)
end
if ~exist(data_path, 'dir')
    mkdir(data_path)
end

%% Write to CSV file
if save_data
    for curr_ch = 1:12
        xl_cell_array = cell(length(ID_axis)+1,length(year_axis)+1);
        xl_cell_array{1,1} = 'ID';
        xl_cell_array(2:end,1) = ID_axis;
        xl_cell_array(1,2:length(year_axis)+1) = num2cell(year_axis);

        xl_cell_local = xl_cell_array;
        xl_cell_local(2:end,2:length(year_axis)+1) =
squeeze(Reason_array_local(curr_ch, :, :));
        pad_and_write_to_csv(['Reason_for_disabling_local_Ch_',
num2str(curr_ch), '.csv'], xl_cell_local);

        xl_cell_global = xl_cell_array;
        xl_cell_global(2:end,2:length(year_axis)+1) =
squeeze(Reason_array_global(curr_ch, :, :));

```

```

        pad_and_write_to_csv(['Reason_for_disabling_global_Ch_',
num2str(curr_ch), '.csv'], xl_cell_global);
    end
end

inds_of_interest = cellfun(@(x) ismember(x, ID_of_interest), ID_axis);

total_electrodes_per_channel = sum(inds_of_interest);

Reason_array_global = Reason_array_global(:,inds_of_interest,:);
Reason_array_local = Reason_array_local(:,inds_of_interest,:);
%% allow replacement of similar terms

Reason_array_local = regexp(Reason_array_local, '^r$', '');
Reason_array_local = regexp(Reason_array_local, '^research$', ''); %
delete research ones.
Reason_array_local = regexp(Reason_array_local, '^pct$', ''); % delete
pct ones.

Reason_array_local = strrep(Reason_array_local, 'Might be out of
cochlear', 'Disabled because of extra-cochlear');
Reason_array_global = strrep(Reason_array_global, 'Might be out of
cochlear', 'Disabled because of extra-cochlear');
Reason_array_local = strrep(Reason_array_local, 'to see if whistling
goes', 'other');
Reason_array_local = strrep(Reason_array_local, 'small dynamic range',
'other');
Reason_array_local = strrep(Reason_array_local, 'poor loudness growth on
ART', 'other');
Reason_array_local = strrep(Reason_array_local, 'pitch mismatch',
'Disabled because not tonotopic');
Reason_array_local = strrep(Reason_array_local, 'not hearing at 28.86
level, switch off at It1', 'Disabled because no auditory percept');
Reason_array_local = strrep(Reason_array_local, 'not hearing and pain',
'Disabled because of non auditory side effect: pain');
Reason_array_local = strrep(Reason_array_local, 'may be out of cochlea',
'Disabled because of extra-cochlear');
Reason_array_local = strrep(Reason_array_local, 'incase it is not in the
cochlea', 'Disabled because of extra-cochlear');
Reason_array_local = strrep(Reason_array_local, 'discomfort to high pitch
curtains', 'Disabled because of poor sound quality');
Reason_array_local = strrep(Reason_array_local, 'disabled', 'other');
Reason_array_local = strrep(Reason_array_local, 'Mixed of sound and
feeling', 'Disabled because of non auditory side effect: discomfort');
Reason_array_local = strrep(Reason_array_local, 'Disabled to increase
rate', 'other');
Reason_array_local = strrep(Reason_array_local, 'Disabled to increase
channel separation', 'other');
Reason_array_local = strrep(Reason_array_local, 'Disabled in the imported
CIStudio+ Map', 'other');

Reason_array_local = strrep(Reason_array_local, 'Disabled because of ',
'');
Reason_array_global = strrep(Reason_array_global, 'Disabled because of ',
'');
Reason_array_local = strrep(Reason_array_local, 'Disabled because ', '');
Reason_array_global = strrep(Reason_array_global, 'Disabled because ',
'');
Reason_array_local = strtrim(Reason_array_local);
Reason_array_global = strtrim(Reason_array_global);

```

Appendix

```
Reason_array_local = regexprep(Reason_array_local, '^non auditory side
effect:.*$', 'non auditory side effect'); % delete pct ones.
Reason_array_global = regexprep(Reason_array_global, '^non auditory side
effect:.*$', 'non auditory side effect'); % delete pct ones.

Reason_array_local = cellfun(@upper_first_char, Reason_array_local,
'UniformOutput', false);
Reason_array_global = cellfun(@upper_first_char, Reason_array_global,
'UniformOutput', false);

%% collapse reasons down to 3 categories; EC, Subjective, Objective

% Reason_array_local = strrep(Reason_array_local, 'Other', 'Subjective');
% Reason_array_global = strrep(Reason_array_global, 'Other',
'Subjective');
% Reason_array_local = strrep(Reason_array_local, 'Disturbs overall sound
impression', 'Subjective');
% Reason_array_global = strrep(Reason_array_global, 'Disturbs overall
sound impression', 'Subjective');
% Reason_array_local = strrep(Reason_array_local, 'Excessive noise',
'Subjective');
% Reason_array_global = strrep(Reason_array_global, 'Excessive noise',
'Subjective');
% Reason_array_local = strrep(Reason_array_local, 'No auditory percept',
'Subjective');
% Reason_array_global = strrep(Reason_array_global, 'No auditory percept',
'Subjective');
% Reason_array_local = strrep(Reason_array_local, 'Non auditory side
effect', 'Subjective');
% Reason_array_global = strrep(Reason_array_global, 'Non auditory side
effect', 'Subjective');
% Reason_array_local = strrep(Reason_array_local, 'Not tonotopic',
'Subjective');
% Reason_array_global = strrep(Reason_array_global, 'Not tonotopic',
'Subjective');
% Reason_array_local = strrep(Reason_array_local, 'Poor sound quality',
'Subjective');
% Reason_array_global = strrep(Reason_array_global, 'Poor sound quality',
'Subjective');
% Reason_array_local = strrep(Reason_array_local, 'Stimulation level too
high compared to neighbors', 'Subjective');
% Reason_array_global = strrep(Reason_array_global, 'Stimulation level too
high compared to neighbors', 'Subjective');
% Reason_array_local = strrep(Reason_array_local, 'ART shows no nerve
response', 'Objective');
% Reason_array_global = strrep(Reason_array_global, 'ART shows no nerve
response', 'Objective');
% Reason_array_local = strrep(Reason_array_local, 'HI impedance',
'Objective');
% Reason_array_global = strrep(Reason_array_global, 'HI impedance',
'Objective');
% Reason_array_local = strrep(Reason_array_local, 'Short circuit',
'Objective');
% Reason_array_global = strrep(Reason_array_global, 'Short circuit',
'Objective');

poss_reasons = unique([unique(Reason_array_local);
unique(Reason_array_global)]);

counts_local = zeros(length(channel_axis), length(poss_reasons));
counts_global = zeros(length(channel_axis), length(poss_reasons));
for ii = 1:length(channel_axis)
    for jj = 1:length(ID_of_interest)
```



```

        curr_ID_chan_reason = squeeze(Reason_array_local(ii,jj,:));
        curr_ID_chan_reason = unique(curr_ID_chan_reason);
        found_reason = cellfun(@(x) ismember(x, curr_ID_chan_reason),
poss_reasons);
        counts_local(ii,:) = counts_local(ii, :)+found_reason.';
        curr_ID_chan_reason = squeeze(Reason_array_global(ii,jj,:));
        curr_ID_chan_reason = unique(curr_ID_chan_reason);
        found_reason = cellfun(@(x) ismember(x, curr_ID_chan_reason),
poss_reasons);
        counts_global(ii,:) = counts_global(ii, :)+found_reason.';
    end
end

assert isempty(poss_reasons{1}) % check blank is first
counts_local = counts_local(:,2:end); %delete blank
counts_global = counts_global(:,2:end); %delete blank
poss_reasons = poss_reasons(2:end);
counts = counts_local+counts_global;
figure(1)
h = bar(100*counts/total_electrodes_per_channel, 'stacked');
number_of_reasons = length(h);
colours = distinguishable_colors(number_of_reasons);
for ii = 1:number_of_reasons
    h(ii).FaceColor = colours(ii,:);
end
xlabel('Electrode','FontSize',14)
ylabel('Deactivated (%)', 'FontSize',14)
ylim ([0 55])
legend(poss_reasons, 'Location', 'NorthWest','FontSize',12)
set(gca, 'FontSize',14)
if save_figures
    saveallformats(1, [figure_path filesep patient_type '_reason_stack'],
save_formats)
end
% colormap('colorcube')

```


B.7 Appendix B7

Research paper

Published in Frontiers in Neuroscience 2019

“Exploiting Routine Clinical Measures to Inform Strategies for Better Hearing Performance in Cochlear Implant Users”

Alan P. Sanderson¹, Edward T. F. Rogers, Carl A. Verschuur and Tracey A. Newman



Exploiting Routine Clinical Measures to Inform Strategies for Better Hearing Performance in Cochlear Implant Users

Alan P. Sanderson^{1*}, Edward T. F. Rogers², Carl A. Verschuur^{3†} and Tracey A. Newman^{4†}

¹ Institute of Sound and Vibration Research, Faculty of Engineering and the Environment, University of Southampton, Southampton, United Kingdom, ² Institute for Life Sciences and Optoelectronics Research Centre, University of Southampton, Southampton, United Kingdom, ³ Auditory Implant Service, Faculty of Engineering and the Environment, University of Southampton, Southampton, United Kingdom, ⁴ Clinical Neurosciences, Institute for Life Sciences, Faculty of Medicine, University of Southampton, Southampton, United Kingdom

OPEN ACCESS

Edited by:

Mikhail Lebedev,
Duke University, United States

Reviewed by:

Etienne Gaudrain,
Center for the National Scientific
Research (CNRS), France
Kazutaka Takahashi,
University of Chicago, United States

*Correspondence:

Alan P. Sanderson
a.sanderson@soton.ac.uk

†These authors have contributed
equally to this work

Specialty section:

This article was submitted to
Neuroprosthetics,
a section of the journal
Frontiers in Neuroscience

Received: 03 September 2018

Accepted: 24 December 2018

Published: 15 January 2019

Citation:

Sanderson AP, Rogers ETF,
Verschuur CA and Newman TA (2019)
Exploiting Routine Clinical Measures
to Inform Strategies for Better Hearing
Performance in Cochlear Implant
Users. *Front. Neurosci.* 12:1048.
doi: 10.3389/fnins.2018.01048

Neuroprostheses designed to interface with the nervous system to replace injured or missing senses can significantly improve a patient's quality of life. The challenge remains to provide implants that operate optimally over several decades. Changes in the implant-tissue interface may precede performance problems. Tools to identify and characterize such changes using existing clinical measures would be highly valuable. Modern cochlear implant (CI) systems allow easy and regular measurements of electrode impedance (EI). This measure is routinely performed as a hardware integrity test, but it also allows a level of insight into the immune-mediated response to the implant, which is associated with performance outcomes. This study is a 5-year retrospective investigation of MED-EL CI users at the University of Southampton Auditory Implant Service including 176 adult ears (18–91) and 74 pediatric ears (1–17). The trend in EI in adults showed a decrease at apical electrodes. An increase was seen at the basal electrodes which are closest to the surgery site. The trend in the pediatric cohort was increasing EI over time for nearly all electrode positions, although this group showed greater variability and had a smaller sample size. We applied an outlier-labeling rule to statistically identify individuals that exhibit raised impedance. This highlighted 14 adult ears (8%) and 3 pediatric ears (5%) with impedance levels that deviated from the group distribution. The slow development of EI suggests intra-cochlear fibrosis and/or osteogenesis as the underlying mechanism. The usual clinical intervention for extreme impedance readings is to deactivate the relevant electrode. Our findings highlight some interesting clinical contradictions: some cases with raised (but not extreme) impedance had not prompted an electrode deactivation; and many cases of electrode deactivation had been informed by subjective patient reports. This emphasizes the need for improved objective evidence to inform electrode deactivations in borderline cases, for which our outlier-labeling approach is a promising candidate. A data extraction and analysis

protocol that allows ongoing and automated statistical analysis of routinely collected data could benefit both the CI and wider neuroprosthetics communities. Our approach provides new tools to inform practice and to improve the function and longevity of neuroprosthetic devices.

Keywords: cochlear implant – neuroprosthesis, clinical monitoring and alerting, foreign body response, cochlear implant – impedance telemetry, hearing impairment

INTRODUCTION

Neuroprosthetics is a rapidly developing and profoundly important area of medical science and engineering. Substantial progress in this field, owing to improvements in biomaterials, electronics and computer science, presents opportunities to manage sensory and motor deficits that were previously untreatable. Neuroprosthetic interfaces of the central or peripheral nervous system share three common design objectives; selectivity of stimulation/recording to supplement function, biocompatibility, and long-term reliability. Despite their differences in target tissue, size and function they all face the same challenges of longevity. Device wear and tear and the biological response to the device such as fibrosis are currently major limiting factors of efficacy in neuroprosthetics (Adewole et al., 2017). Although the micro-environments of the central and peripheral nervous system exhibit specific chemical and cellular profiles, the broad challenges are universal and are driving the need for improved understanding of the tissue-implant interactions.

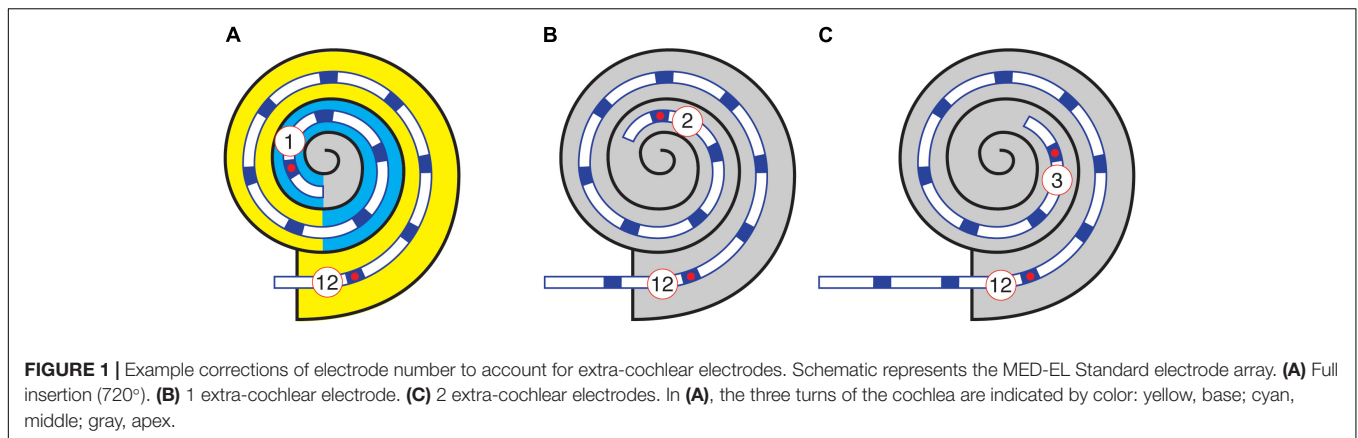
Cochlear implants (CIs) are the most common and successful sensory neuroprosthetic device with almost 600,000 recipients worldwide (Ear Foundation, 2016). They enable people with severe and profound deafness to hear speech, music and environmental sound (Wilson and Dorman, 2008). They make ideal models for neuroprosthetic research because their performance can be measured both subjectively and objectively: CI users can describe their hearing experience to clinicians and researchers who can then remotely measure hardware performance *in-situ*. The most common cause of deafness is loss or damage to the hair cells in the cochlea, meaning that they cannot convert vibrations in the air into electrical signals for the brain to process. CIs collect sound through an external microphone, convert it to electrical signals, and directly stimulate the auditory nerve with these signals, bypassing the normal hearing mechanism within the outer, middle and inner ear. The device delivers a sequence of current pulses, similar to those generated by the biological hearing apparatus, through a platinum multi-electrode array positioned in the cochlea. The signals from the auditory nerve are then interpreted as for normal biological hearing, by processing in the central auditory pathways of the brain. In many cases this affords 100% speech recognition for the implant user when listening in favorable acoustic conditions (Gifford et al., 2008).

The cochlea consists of a bone encased membranous spiral containing the sensory apparatus of hearing and its supporting structures, which are essential for sensory transduction and homeostasis. The scalae of the cochlea are three tube-like chambers projecting through the spiral: the scala tympani, the

scala media and scala vestibuli. The electrode is usually surgically inserted into the scala tympani, in close proximity to the spiral ganglion neurons (SGNs). The average total length of the cochlear spiral is 42 mm and the total length of the first complete turn is 22.6 mm (Rask-Andersen et al., 2011). The majority of human cochleae have between 2.5 and 2.75 turns (Biedron et al., 2009). For ease of reference, these turns are conventionally denoted base, middle and apex, from the largest to the smallest (Rask-Andersen et al., 2012) (**Figure 1A**).

Since the widespread introduction of CIs in the 1980s, there have been several refinements to the technology and related health policy. Improvements in hardware manufacture, signal processing strategies, surgical techniques and the relaxation of CI candidacy criteria have all contributed to better clinical outcomes, including preservation of residual hearing (Nguyen et al., 2016), improved speech recognition (Wilson and Dorman, 2008) and fewer device related adverse events (Causon et al., 2013). Despite these improvements, however, some users still experience poor or declining speech recognition, poor sound quality and stimulation of non-auditory sensations. In around 2% of cases, additional surgery is needed to explant and replace the CI. The explanted device is tested, and if hardware failure and surgical complications are excluded, a “soft failure” is diagnosed (Balkany et al., 2005). As hardware has improved, these soft failures, or idiopathic cases, have become relatively more common (Causon et al., 2013), and research is clearly needed to better understand how individual biology, and in particular the immune system, interacts with the neuroprosthesis to drive these adverse events. Conventional counts of soft failures only record those devices which perform badly enough to need surgical removal and not those that underperform, and so will necessarily under-estimate the influence of these biological factors.

Cochlear implants, like any bio-implant, stimulate an inflammatory response, which culminates in the encapsulation of the prostheses, in a sheath of fibrotic or scar tissue (Anderson et al., 2008). Currently, CIs are constructed from a silicone carrier and platinum electrodes. A common type of medical grade silicone, polydimethylsiloxane (PDMS) is quite well understood and is used in many bio-implants including breast implants (Hillard et al., 2017), cardiac pacemakers and spinal cord stimulators which help patients with chronic pain and to manage incontinence (Hassler et al., 2011). As well as the materials themselves, though, the tissue response is modulated by electrode microscopic surface topography and chemical composition (Christo et al., 2015). It seems that tissue growth in response to CI is inevitable (Li et al., 2007) although the nature and extent of the response is somewhat variable across individuals (Fayad et al., 2009).



Although fibrosis can foul the implant and impair its function, it is also beneficial in mechanically fixing the array within the cochlea. This helps create a seal to prevent both loss of perilymph and infiltration of bacteria from the middle ear (Stöver and Lenarz, 2009). A healthy inflammatory response to an injury comprises successive waves of pro- and anti-inflammatory chemokines and cytokines, controlled cellular migration to the wound site, with eventual resolution of inflammation and controlled apoptosis of recruited cells accompanied by wound repair and remodeling. In the case of implanted biodevices, the immune system reacts to the acute surgical trauma as well as the protracted exposure to the implanted biomaterials. Initially, the inflammatory response is characterized by exudation of fluid and plasma proteins from the circulation together with active infiltration of neutrophils to the surgical wound site. Proteins including fibrin are rapidly adsorbed onto the implanted biomaterial to form a provisional matrix that attracts macrophages, which can fuse to form multi-nucleated giant cells. Macrophages contribute to the fibrotic capsule by releasing cytokines that attract fibroblasts and stimulate them to secrete collagen.

The inflammatory process leads to the commonly described tissue reaction to a CI: a tightly packed layer of fibroblasts and collagen with occasional macrophages surrounding the electrode array (Grill and Thomas Mortimer, 1994). In the majority of cases, this tissue state remains stable over time. However, in some instances there is tissue hypertrophy, or extensive fibrosis and bone formation, which hinders the function of the electrode. Lim et al. (2011) found that pathological foreign body reactions (FBR) requiring revision surgery are rare. However, evidence from post-mortem temporal bones suggests that the characteristic indicators of FBR such as foreign body giant cells are more common than expected (Nadol et al., 2014; Seyyedi and Nadol, 2014). This highlights the potential for sub-clinical FBR, which does not reach soft-failure but is clearly detectable to post-mortem histological analysis. The complex reaction to CI often also includes new bone formation (osteogenesis) (Somdas et al., 2007). Osteogenesis appears more detrimental to implant performance than fibrosis and is associated with reduced speech discrimination scores, (Kamakura and Nadol, 2016) and an effective reduction in

dynamic range of stimulus current (Kawano et al., 1998). It is therefore crucial to understand the transition from a healthy short-lived tissue response to a chronic or spontaneous over-exuberant response.

Studies of donated temporal bones from CI users have shown that intra-cochlear location can significantly affect tissue development after CI implantation. The basal, high-frequency region of the cochlea exhibits significantly greater fibrosis and osteogenesis, and poorer survival of both hair cells and peripheral projections of SGNs (Fayad et al., 2009). Histological analysis identifies greater numbers of giant cells and lymphocytes at the cochleostomy site than at the mid and apical regions of the cochlea (Seyyedi and Nadol, 2014). In addition to the consistent pattern of basal tissue hypertrophy, some individuals also exhibit fibrosis that extends along the full length of the electrode array and beyond (Somdas et al., 2007). There is evidence that the volume of new tissue correlates with the level of damage to the lateral wall (Li et al., 2007) and other structures including the basilar membrane (Kamakura and Nadol, 2016). While this data is intriguing, and clearly points to the importance of the biological response to the implant, it is limited to post-mortem studies, meaning that the majority of the data is collected after long-term implantation. This means it cannot be used to interpret performance fluctuations, and does not give us the early warning of soft failure that would be so useful in the clinic.

A readily available, non-invasive, clinical measure from a CI is electrode impedance (EI) telemetry (Hughes et al., 2001). EI describes the ease with which electrical current flows through and between implanted electrodes. The CI stimulator delivers a current pulse that flows through the platinum electrodes of the CI and into the ionic environment of the cochlear tissue. This pulse must be calibrated so that it delivers sufficient of charge to stimulate the SGN, without damaging the tissue. High EI means the implant must deliver a higher voltage to maintain the delivered charge. This has two undesirable effects: it drains the battery of the device faster and, more importantly, it spreads the excitation across more SGN reducing frequency resolution, and in turn the quality of the perceived sound. In general, therefore, low EI makes it more likely that an implant performs well.

The EI is determined by delivering a low-level current pulse through the relevant electrode inputs on the CI and

measuring the resulting voltage across the associated electrodes. It can be performed quickly in the clinic using a hardware interface that connects the implant to a computer via a transcutaneous link. In the clinic, EI telemetry is primarily used as an electrode integrity test. Open or short circuit faults (very high or very low impedances, respectively) can easily be diagnosed, which is useful to clinicians in deciding whether a given electrode should be activated. These faults are relatively common: Carlson et al. (2010) showed a 9% chance of either at least one open- or short-circuit fault in an implanted device.

Despite its primary role as an integrity check, EI is a continuous measure, which can provide much more information on the biology around the implant. A major factor in determining EI is the volume and composition of bulk tissue surrounding the implanted electrode array (Tykocinski et al., 2001). Clark (2003) recommends that EI levels should be monitored routinely as an indicator of cochlear tissue changes such as fibrosis and electrode surface roughening. In a study of chronic high-rate stimulation using cats, Xu et al. (1997) demonstrated that levels of fibrosis and presence of inflammatory cells were greatest in the cochleae that exhibited the greatest EI levels. Clark et al. (1995) found that EI was significantly correlated with the amount of tissue around the electrode contacts and cases where inflammatory cells were found in the tissue showed particularly high levels of EI.

The studies above show the value of EI as an indicator of tissue status, but initial studies also show that it may be useful for predicting patient outcomes. Electrodes that exhibit high impedance levels are associated with raised thresholds of auditory sensation and reduced dynamic range (Busby et al., 2002) which can be associated with poorer performance outcomes (Wolfe et al., 2013). EI increase and/or fluctuation are recognized as clinical indicators of soft-failure (Balkany et al., 2005). The onset of sudden changes in EI over time are correlated with marked loss of residual hearing in CI users (Choi et al., 2017).

Considering the potential value of monitoring and interpreting EI fluctuations, there is a surprising lack of consensus guidance on clinical utility of impedance telemetry, especially in light of its proven association with the immune-mediated tissue response. A number of authors have shown greater EI levels in the basal region of the cochlea compared to more apical locations. Jia et al. (2011) analyzed EI from 20 adult CI users and found higher levels at the basal position after 3 months that were maintained for the 36-month study duration. The pattern of raised EI at basal electrodes has been observed in other clinical CI studies (Hughes et al., 2001; Busby et al., 2002; Leone et al., 2017) and supports the temporal bone histology studies showing greater tissue growth in this region. These studies, which draw from cohort sizes ranging from 19 to 35 individuals, have generated useful preliminary evidence. However, a lack of larger study groups—ideally complete clinical caseloads—combined with the known inter-patient variability, is a major factor in the lack of clinical consensus. To date there is no published evidence of a clinical platform for systematic analysis of EI to

produce normative models, against which individuals can be compared.

There is evidence that change in EI over time can serve as an indicator of the immune-mediated tissue response. Following surgical implantation of the CI electrode array, the tissue undergoes rapid changes attributable to the acute inflammatory response (Shepherd et al., 1994). This change manifests in a measurable increase in EI between implantation and the date of activation (Busby et al., 2002; Saunders et al., 2002). Several studies report a significant reduction in EI following commencement of electrical stimulation, which often plateaus over 1–3 months (Hughes et al., 2001; Henkin et al., 2006; Jia et al., 2011). After the initial stimulation-induced reduction, EI usually remains at a stable level in actively stimulated electrodes for several months (Henkin et al., 2003, 2006), while inactive electrodes show a steady increase over time (Dorman et al., 1992; Hughes et al., 2001).

The present study is a retrospective investigation of clinical data from an auditory implant service and demonstrates the untapped value in clinical recordings taken from neuroprostheses—in our case, CIs. As shown above, there is a pressing need to reduce the wide variance of outcomes and improve implant longevity, which will be substantially helped by improving observations of the CI-tissue interface. We describe sample-wide variability over 5 years. This view is not available through the clinical software, which prevents clinicians from easily identifying deviations from normal. We asked the question: what is the general trend of impedance change over time for different electrode positions? Based on previous evidence of tissue proliferation around the round window and hook region we predicted that the electrodes furthest from the base would show lower impedance with a downward trend over time. Next, we applied an upper threshold to identify individuals with raised impedance, statistically outside the main distribution but below the manufacturer's "high impedance" warning level. We asked the questions: how many individuals exhibit significantly raised impedance levels? Of these, how many were identified with raised impedance at electrodes away from the base? These are particularly interesting cases to consider because no mechanism has been proposed for localized tissue proliferation away from the site of array insertion, i.e., cochleostomy or round window. This information could be used as early detection of unwanted inflammatory responses caused by the implant and its function rather than the surgery, which may go on to affect the CI interface and therefore longer-term performance. Clinical data review, like that proposed here, incurs a negligible burden on the CI user and minimal cost in both money and time.

MATERIALS AND METHODS

Ethics Statement

This study was carried out in accordance with the recommendations of the University of Southampton Ethics Committee (UEC) and Faculty of Engineering and the Environment Ethics Committee (FEC). The protocol was

approved by the FEC. All subjects gave written informed consent in accordance with the Declaration of Helsinki. [UEC Ethics ID: 17430].

Participants

The study included 172 adult (176 adult ears) and 47 children (74 ears). Mean adult age was 58 years (18–91) and mean child age was 4.5 years (1–17). The patients included were implanted using either cochleostomy (approximately one third) or round window insertion (approximately two thirds). Data were collected from two sources within the University of Southampton Auditory Implant Service (USAIS); the clinical software database MED-EL Maestro and the local patient database.

Electrode Characteristics

Study participants had previously received MED-EL Standard ($n = 131$), Flex-28 (96), Flex-24 (7), Flex-Soft (2), or Form24 (1) CI arrays. These are relatively long arrays enabling EI measures to be taken at a wide range of physical positions in the cochlea. For example, the Standard array has an active stimulation range of 26.4 mm, which is equivalent to two turns of the cochlea or an insertion angle of 720° . Each array carries 12 electrodes, each of which has either one or two exposed electrical contacts, depending on the array model. The effective electrode surface area for these MED-EL electrodes is $0.13\text{--}0.14\text{ mm}^2$.

EI Data Acquisition

The main study aims were to describe the trends of EI in a large sample and highlight individuals who deviate from this. A single manufacturer and limited number of arrays were chosen to minimize the hardware variability with a view to focusing primarily on the soft or biological mechanisms for impedance evolution. Importantly, the method of voltage acquisition and impedance calculation varies significantly between manufacturers. The method used by the MED-EL telemetry system is shown in **Supplementary Figure S1**. The change in EI can be separated into two components; access resistance and polarization impedance. The latter reflects the physical properties of the electrode surface and is therefore affected by protein adsorption, surface area increase and localized ionic changes (Tykocinski et al., 2005; Newbold et al., 2010). The stimulation-induced EI reduction, which occurs rapidly following device activation, is dominated by this component (Newbold et al., 2014). Access resistance is known to reflect the bulk material around the electrode such as fluid, cells and tissue and is likely to change over longer time scales. Clinically available impedance telemetry does not allow the two components to be measured separately; however, using the MED-EL system allows both impedance components to be captured. Therefore, changes occurring over different time scales give some indication of the relative contribution of the two components. The impedance measurement is performed using monopolar, low-amplitude bi-phasic current pulses, similar to those used for stimulation via the device. Total impedance (Z_t) can be calculated using total voltage which is measured at the

end of the current pulse (See **Supplementary Figure S1**). Total impedance comprises the developing polarization component (Z_p) and the access resistance component (R_a). EI is calculated as: $Z_t = V_t/I$.

EI Data Management

Data were exported from MED-EL Maestro in Microsoft Access format. A custom database query was then used to return anonymized individual patients with their age at implant, implanted ear, date of birth, electrode activation status, electrode specific EI and corresponding date stamp. The difference between the date of implant and date stamp for each EI measurement was used to normalize data to a 0 date (day 0 is date of implantation) for each patient. Subsequent EI measurements were split according to the 12 individual electrodes and then averaged into 3-month time bins. All query results were exported in Microsoft spreadsheet format. MathWorks MATLAB (R2018a) was used to read data from excel spreadsheets and plot **Figures 2–8**.

Deactivated Electrode Data Filtering

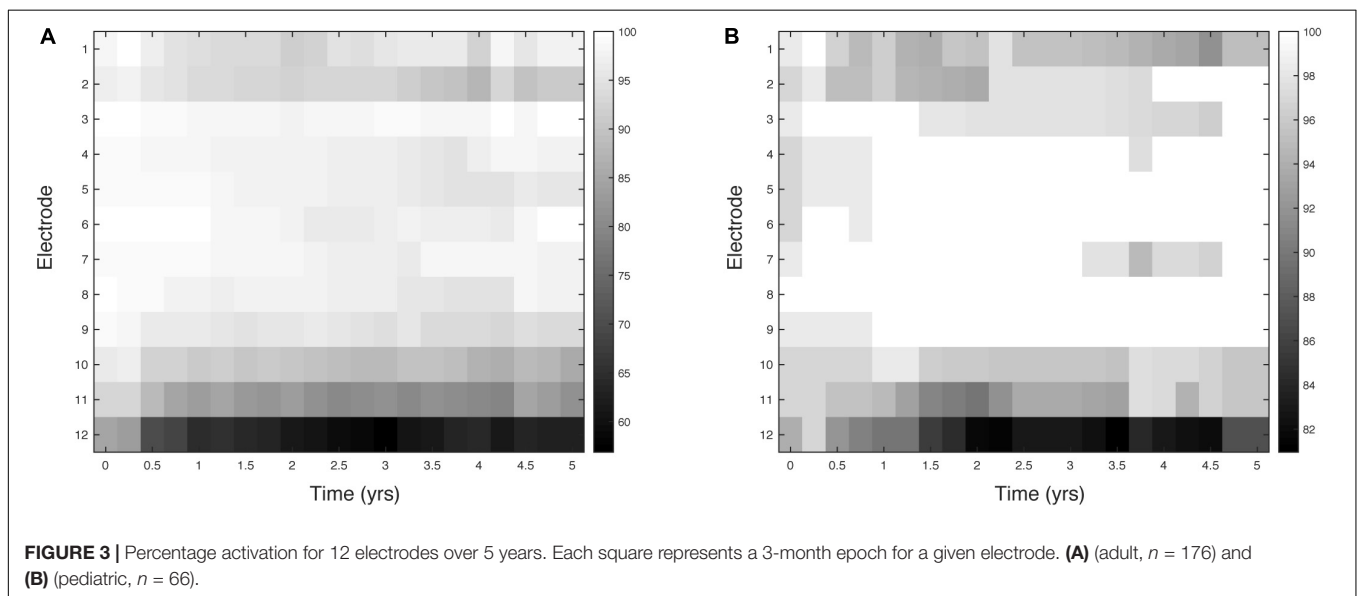
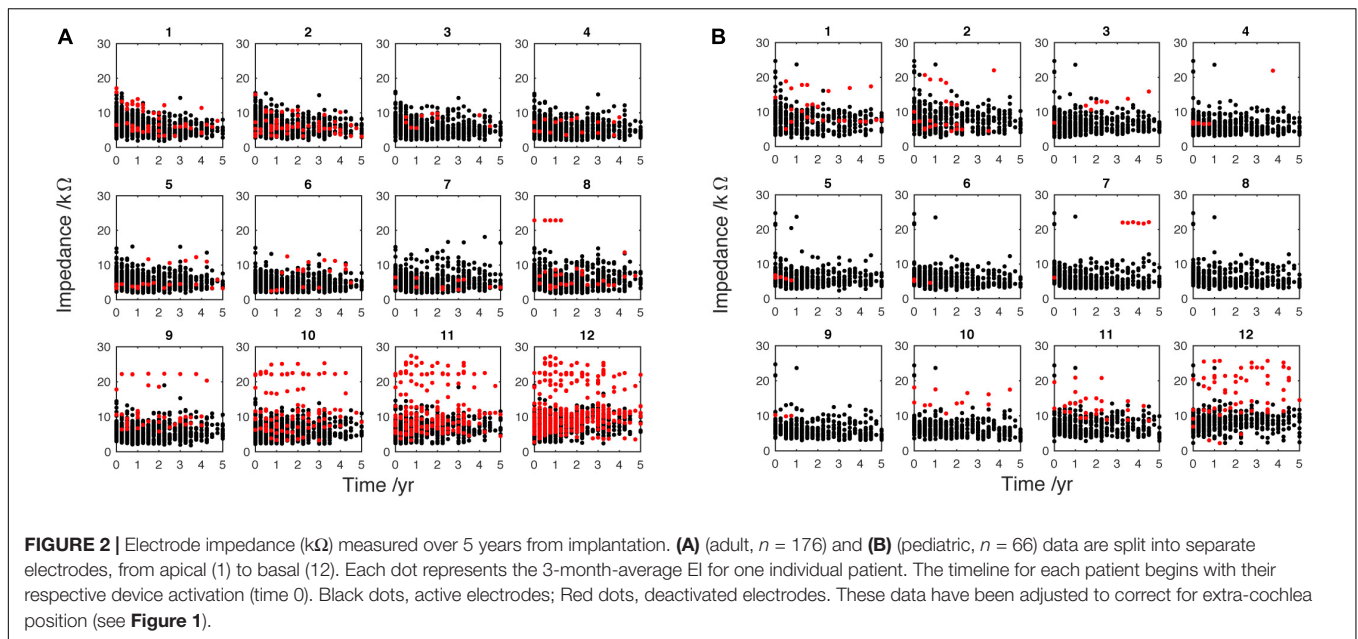
It is very common for CI users to have electrodes deactivated by clinicians. As discussed, several studies show an increasing EI in the absence of electrical stimulation. Therefore, to minimize the effect of this upward bias on the analysis, only data from actively stimulating electrodes (black dots in **Figure 2**) were included in analyses from **Figure 5** onward; deactivated electrodes (red dots in **Figure 2**) were automatically removed from the analysis using a custom MATLAB script.

Electrode Numbers Were Corrected for Extra-Cochlea Position

During surgery, it is common for the electrode array not to be fully inserted in the cochlea, meaning that electrodes (referred to by position along the array) may be shifted relative to the cochlear anatomy. We corrected for this effect to allow meaningful comparison of electrode positions between patients. Surgical records were interrogated to determine presence/number of extra-cochlear electrodes. The following correction was applied: correct electrode number = [original electrode number + number of extra cochlear electrodes; maximum of 12]. **Figure 1** shows how this results in new electrode numbers being assigned to intra-cochlear electrodes. This does not allow for an estimation of insertion depth, but it does enable analysis of electrodes from “most basal” onward. This correction is applied to all data in **Figures 2, 3, 5–8**. The correction is not applied to **Figure 4** (analysis of reasons for deactivation) as it would mask extra-cochlear deactivations.

Statistical Analysis

The software program MathWorks MATLAB was used for data analysis. The adult and pediatric groups were analyzed separately. Least-squares linear regression lines were fitted to the average impedance data (Matlab polyfit) (**Figure 5**).



Using MATLAB, an outlier-labeling rule was applied to identify instances of raised EI (**Figures 7, 8** and **Supplementary Material**)

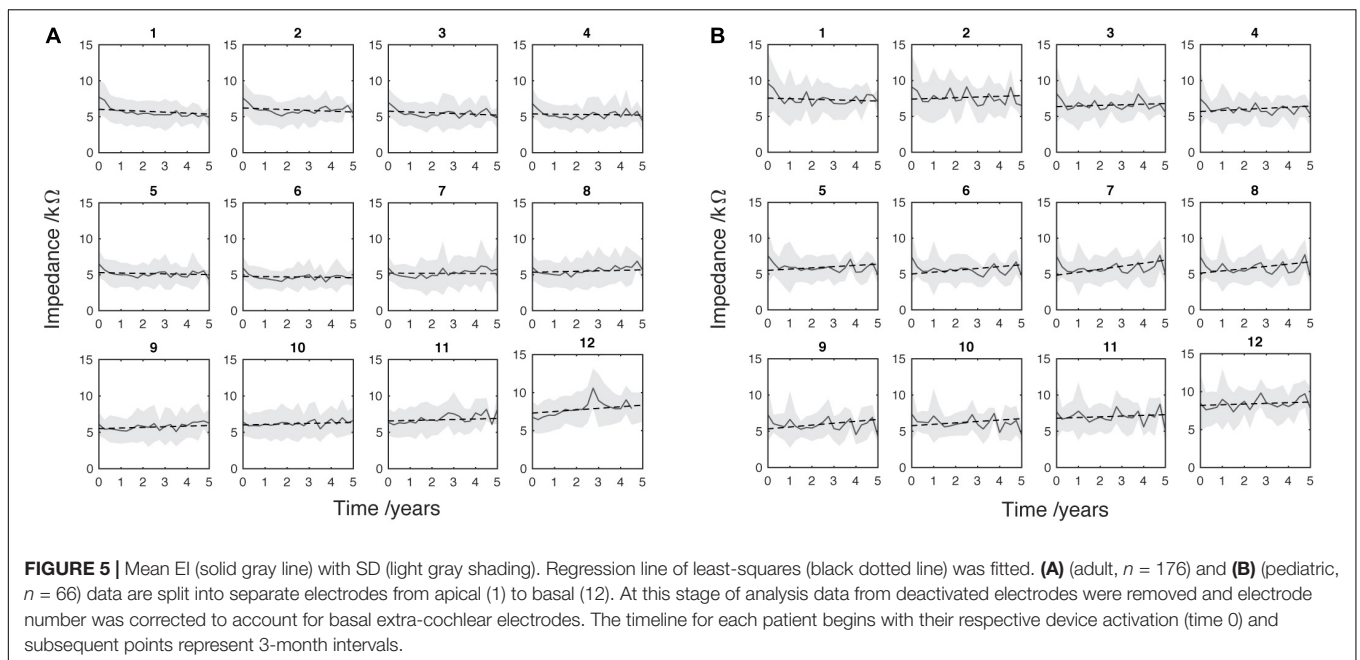
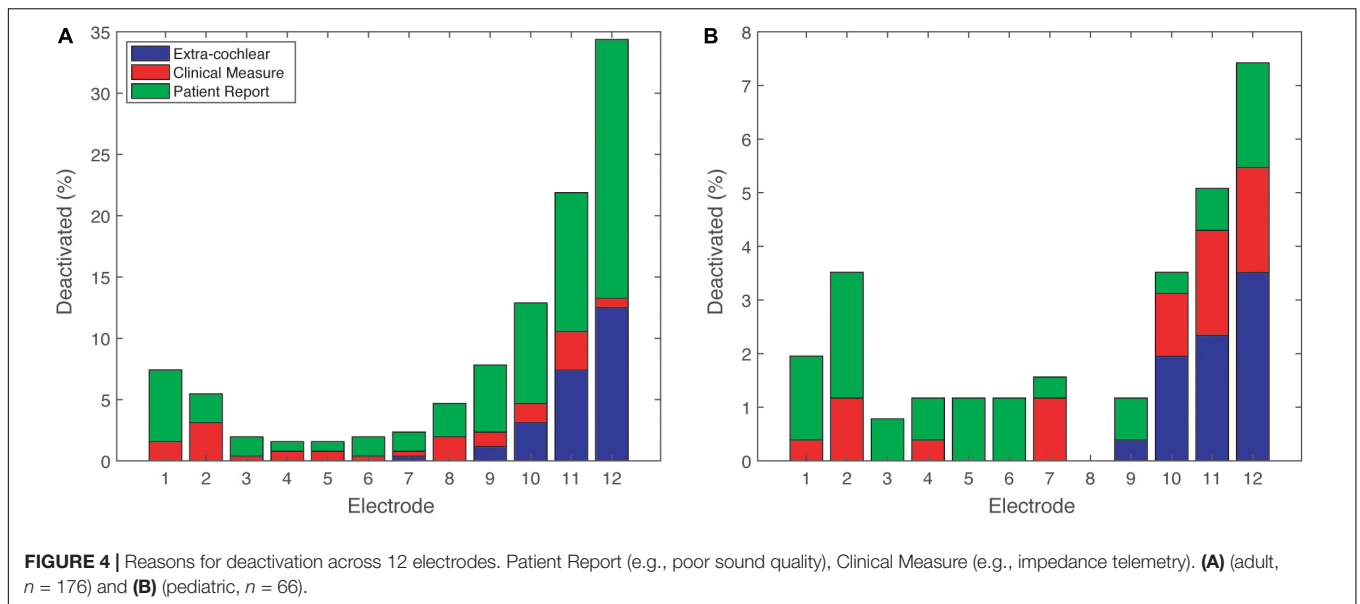
$$T = Q_u + k(Q_u - Q_l)$$

(Hoaglin et al., 1986):

where Q_u and Q_l are the upper and lower quartiles, respectively, and T is the threshold for an outlier. The constant k was fixed at 2.2, equivalent to a 5% probability of any given measurement being an outlier, for the adult and pediatric sample sizes tested (Hoaglin and Iglewicz, 1987). Cases were highlighted as statistically raised EI (SEI) when the EI was greater than T in ≥ 2 time bins within the first 2 years of CI use. Current methods of “high impedance” detection are based on the upper limits of

the stimulus delivery hardware for individual cases. Our new approach allows investigation of raised, but not extreme, levels of EI that would otherwise be considered sub-clinical.

Highlighted cases of SEI are split into “basal” (9–12) and “non-basal” (1–8) depending on the position of the electrode showing raised EI. Basal electrodes, which are nearest to the insertion site, are expected to show significantly stronger immune-mediated tissue development: previous studies show significantly greater EI corresponding to this region. A judgment was made to categorize electrodes that are likely to be in the hook region as “basal.” This is the straight region of the first cochlear turn, which extends 9 mm from the round window before it curves (Clark et al., 1990). The MED-EL Standard and Flex28 electrode arrays have contacts spaced at 2.2 and 1.9 mm,

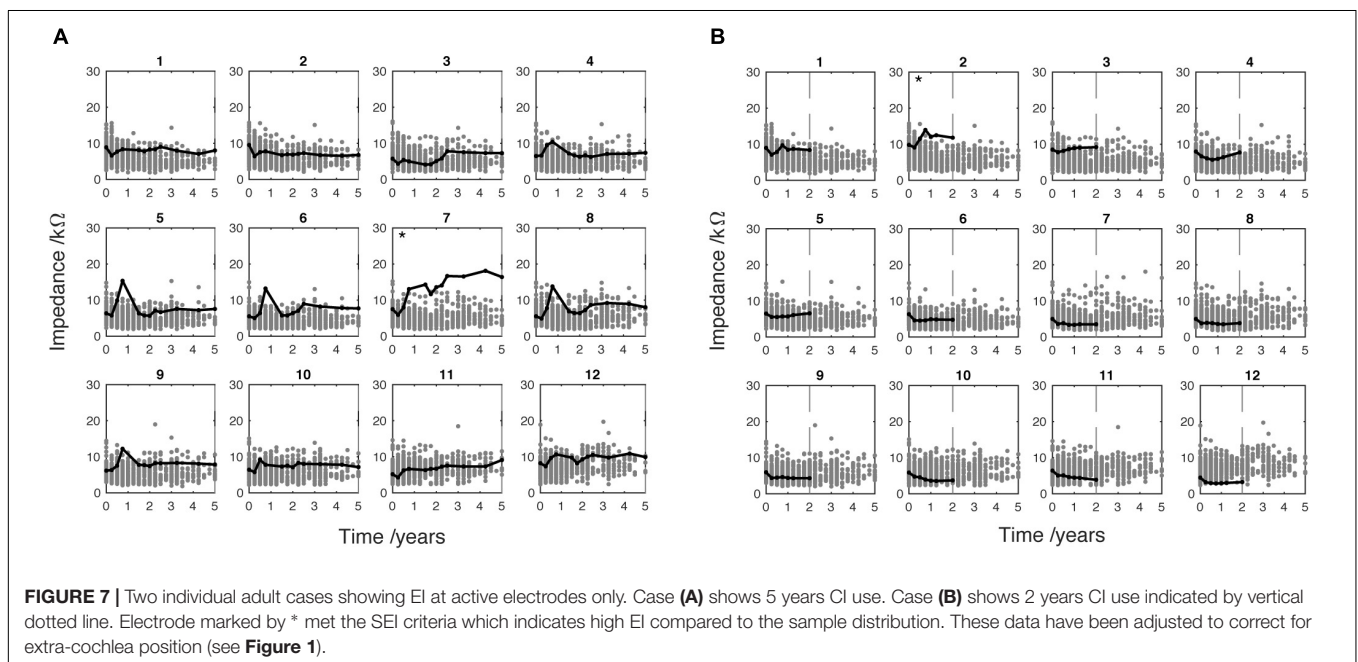
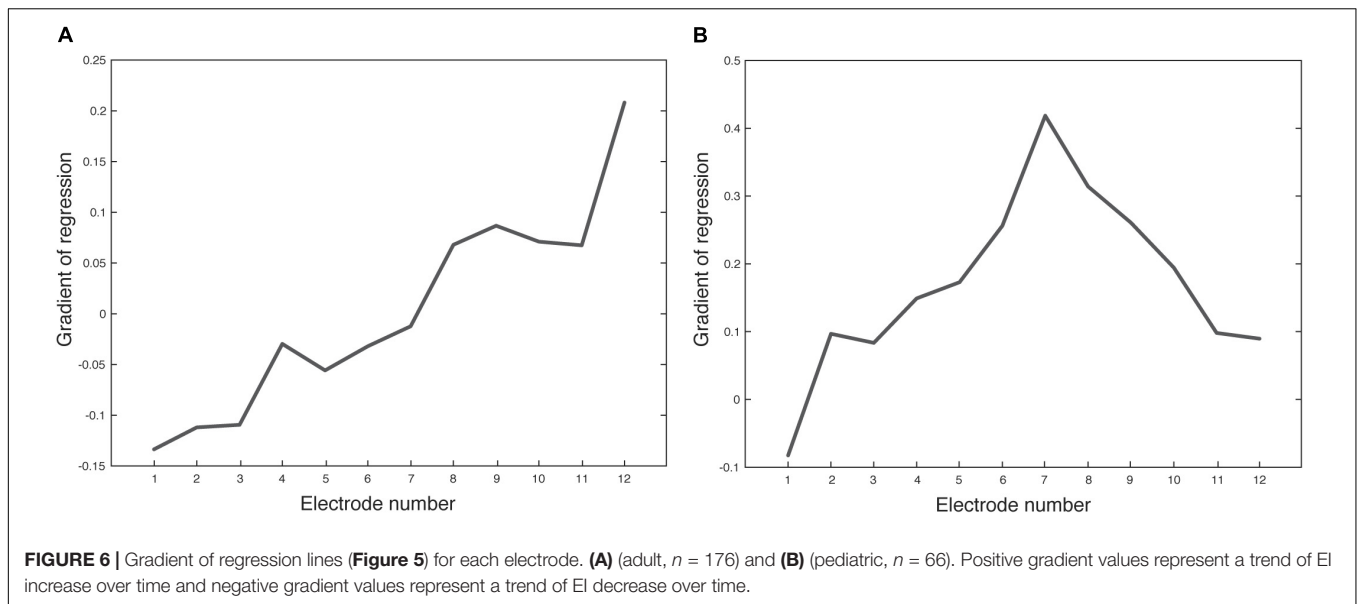


respectively (Med-El, 2013). This means that the basal portion of the array (electrodes 9–12) spans 8.8 and 7.6 mm for Standard and Flex-28 electrodes, respectively.

RESULTS

Data from 242 ears (176 adult and 66 pediatric) were included in the main analysis of EI changes over time. **Figure 2** shows subplots representing 12 separate electrodes. The magnitude of EI is plotted against time from initial CI activation to 5 years later. Each single dot represents the average EI level for a single patient over 3 months. Impedance data measured

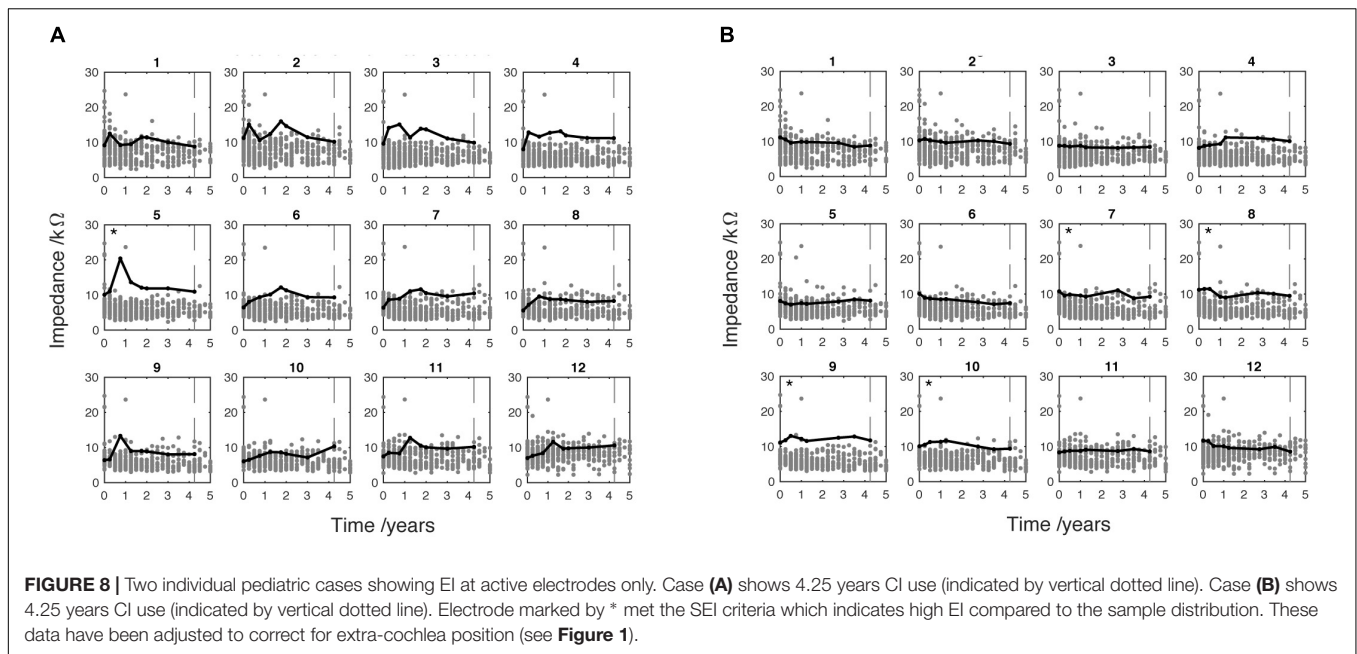
from actively stimulating electrodes are indicated by black dots whereas data measured at deactivated electrodes are indicated by red dots. The subplots both show a large number of deactivated electrodes, particularly at the most apical and basal electrodes (1 and 12, respectively), the reasons for which are analyzed below. **Figure 2A** identifies a high number of deactivated basal electrodes for the adult population. Note that there are fewer dots at later time points, as not all patients had been using the device for the whole 5-year study period. The EI data were corrected to account for electrodes that were positioned outside the cochlea (see Section “Materials and Methods” and **Figure 1**). This was done to allow alignment of impedance data around an approximate physical position in the cochlea.



The proportion of deactivated electrodes in the population is shown in Figure 3. Deactivation is clearly most common in the most basal electrodes for both adults and children. The figure also shows an increasing number of deactivations over the first 1–2 years of CI use. The peak number of deactivations was higher in the adult group (Figure 3A) than the pediatric group (Figure 3B). Both groups had most deactivations at electrode 12, which can be seen as black at 2.25 years. At that epoch, only 60% of adult electrodes were active while 81% of pediatric electrodes were active. Electrode 11 showed the second highest number of deactivations for both groups. For example, 80% of adults had electrode 11 remaining active at 2.5, 3.25, 4 and 4.25 years. There was a slight increase in deactivations at the most

apical electrodes compared to the mid-array for both adults and children. For example, adults had 88% of electrode 2 remaining active at 4 years. The children had 92% of electrode 1 remaining active at 4.5 years. A difference between the two groups was the mid-array electrodes were mostly active in the pediatric group, indicated by white area in Figure 3B. Although the adults were initially 100% active at electrodes 3 and 6, a few deactivations were made in the next 3-month epoch. In contrast, the children had 100% activation for the majority of the 5-year study period in electrodes 4, 5, 6 and 7.

The patterns of deactivation seen above are better understood in light of the clinical reasons for deactivation shown in Figure 4. Electrodes in the most basal portion of the array were deactivated



because they were outside the cochlea (extra-cochlear). In the basal electrodes (9–12), extra-cochlear position accounted for about one third of the adult reasons (**Figure 4A**), and about half of the pediatric reasons (**Figure 4B**). The majority of deactivations, however, in the adult group were informed by the patient reports of their subjective experience, such as “poor sound quality” (See **Supplementary Figure S2** for a complete list of deactivation reasons); there were relatively few deactivations owing to “Clinical Measures” which offer objective information. The percentage of subjective “Patient Report” reasons is highly likely to be biased by the age of the CI user: many of the children are very young and could not communicate their perception of sound. As shown in **Figure 3**, the children had significantly fewer deactivations overall.

Data points acquired at deactivated electrodes were removed at this stage of the analysis (red dots in **Figure 2**). **Figure 5** shows the mean EI for the adults (**Figure 5A**) and the children (**Figure 5B**). Least-squares linear regression lines were fitted to the average impedance data (Matlab polyfit) for each electrode to show the trend of EI change over time. The adult group show a tendency for EI reduction at apical electrodes (negative slope), increase at basal electrodes (positive slope) and no change for mid electrodes. The pediatric group shows a different pattern of regression lines across the electrodes. All of the electrodes in this group, except electrode 1 show a positive slope. This suggests a difference in long-term EI evolution in children compared to adults, although the mean is more variable in this age group. This is probably caused by the lower overall sample size and fluctuation of sample size in each time window (i.e., by chance fewer individuals were seen in some 3-month epochs).

The data above indicates that EI changes over time in a way that varies with electrode position. We describe this EI change over time using a regression line for each electrode in **Figure 5**. The gradient of each line is plotted for each

electrode in **Figure 6**. The adult group (**Figure 6A**) shows a positive relationship between gradient and electrode number. Each consecutive electrode shows a general increase in gradient with electrode number. The largely monotonic relationship between gradient and electrode fits the consensus in the literature and highlights the phenomena quite simply. Another observation is that the crossover point from EI reduction (negative gradient) to increase (positive gradient) is at electrode 7, which is roughly the middle of the electrode array. This shows that EI evolution varies from base to apex in a continuous fashion. The relationship between fit-line gradient and electrode number in the pediatric group (**Figure 6B**) shows that EI largely increases over the 5-year period for all electrodes except number 1. The increase is steepest at electrode 7. We note that the regression lines are an approximate linear fit and hence describe general trends. The pediatric sample shows a large degree of variability between timepoints because of the relatively low sample size and irregular frequency of clinical appointments. The peaks and troughs of mean EI cause some biasing of the fit lines so we have been conservative in our interpretation of differences between age groups.

In the adult group, 14 patients met the SEI criteria (8%): one in basal electrodes, three in both basal and non-basal and 10 in non-basal electrodes only. The case shown in **Figure 7A** was implanted with a standard electrode array and the clinical record did not include the hearing-loss etiology. The case shown in **Figure 7B** was implanted with a Flex28 electrode array and the clinical record showed head injury as the cause of hearing loss. **Figure 7A** shows an EI increase at electrode 7 over the 5 years of CI use. This electrode is highlighted by (*) to indicate that EI level met the SEI criteria. A key observation is the difference in temporal development and absolute level of EI of this electrode compared to its immediate neighbors. This difference is unusual for non-basal electrodes where the EI is often mirrored in

neighboring electrodes. The absolute EI level shown in **Figure 7B** is lower than **Figure 7A** although the SEI criteria have been met at electrode 2.

In the pediatric group, three cases met the SEI criteria (5%): two in non-basal and one in both basal and non-basal electrodes. **Figure 8** shows the EI measurements taken from two pediatric cases. Each was found to meet the SEI criteria in one of two implanted ears. The black line shows that EI is greater in these cases than the other cases in the sample (gray dots) which are mostly clustered around or below 10 k Ω . The case shown in **Figure 8A** was implanted with a Flex-28 electrode. Clinical records show they were diagnosed with congenital hearing loss associated with Pendred syndrome. This case met the SEI criteria at electrode 5 (indicated by *). After the initial activation and tuning appointment, the EI increased relatively rapidly to peak around 1 year of CI use. A similarly sharp reduction is shown in the following 3-month period before EI plateau around 12 k Ω . This case shows a general tendency for raised EI over the duration of observed CI use. This is especially marked in electrodes 2, 3 and 4, although the level did not meet the criterion for SEI. The case shown in **Figure 8B** was fitted with a Standard electrode array. The clinical record showed a diagnosis of genetic mutation of the gene GJB2 (connexin26). The case shown in **Figure 8B** met the SEI criteria at electrode 7, 8, 9 and 10. Unlike the pattern shown in **Figure 8A**, the EI tracked a stable level across the period of use.

DISCUSSION

This retrospective study of clinical data from a large sample of MED-EL CI users showed population-level trends in EI across time and between cochlear regions, and also yielded a potential new approach to define EI outliers for whom further clinical action may need to be taken. The analysis showed that most adult electrode deactivations were made because of reported experiences rather than clinical measures such as neural-response telemetry or electrode-impedance telemetry. The population-based method of outlier detection used here offers an objective insight into intra-cochlear tissue status to inform decisions to deactivate electrodes. Ongoing challenges for neuroprostheses include biocompatibility and functional longevity (Adewole et al., 2017). Performance decrement, as contrasted with frank failure, is difficult to monitor and almost impossible to predict using current approaches. The consensus in the field of CI for clinical assessment of soft failure recommends a broad-spectrum approach. This includes patient interview, medical investigations such as X-ray imaging, audiological and hardware testing (Balkany et al., 2005). This relies on the CI user having well-established linguistic abilities. In children the consensus is that the clinician should record and interpret the user's behaviors, although this has limited reliability (Moberly et al., 2013). The methods presented here allow deeper enquiry into the telemetry data that is already routinely gathered. Our results suggest that a minority of raised impedance cases can be detected in a population, which may aid triaging of patients, including those who can provide only limited verbal reports.

We describe the evolution of EI for adults and children at 12 electrodes along the MED-EL array. The measurement at the first (0 months) and second time points (3 months) identifies a drop in EI across all conditions. The drop is consistent with an increase in electrode surface area due to the electrolytic activity (Brummer and Turner, 1977), and/or clearance and reorganization of organic molecules, cells, tissues on and around the electrode (Marsella et al., 2014). The main observation in the adult group is EI growth at basal electrodes and EI reduction at apical electrodes. Growth in basal-electrode EI is likely to be caused by fibrosis and osteogenesis based on its slow evolution over time. Previous findings from a post-mortem study of cochleae from CI users have shown the levels of fibrotic and bone tissue to be greatest in the basal turn of the cochlea (Fayad et al., 2009). The magnitude of fibrosis is also correlated with the level of trauma caused by surgery (Richard et al., 2012). It is also possible that there are differences in capacity for inflammatory response in different regions of the cochlea, e.g., due to anatomical variations such as vasculature, nerve supply or cochlear-duct width.

We observed the trend that children show an increase in EI for all electrodes except electrode 1. This data shows more variability over time than the adults, possibly due to the lower number of cases analyzed. If a difference exists, the likely explanation is a difference in the chronic tissue response to surgery in children and adults (i.e., developmental stage) or differences in etiology among children vs. adults. Previous studies have shown increasing EI for basal, mid and apical electrodes in children compared to the adult group which only showed increase at the base (Hughes et al., 2001; Busby et al., 2002). Our data appear to support this although no formal age-group comparison was made. There is some published evidence of differences in hearing preservation between adults and children. One study showed a small trend toward better residual hearing in children (Zanetti et al., 2015), although another found no effect of age (Skarzynski et al., 2013). The findings of the present study suggest an increased growth of intra-cochlear tissue around the base that is particularly clear in the adult group.

The fact that gradual increases in basal impedance were observed is indicative of a slow proliferation of tissue indicative of immune-mediated fibrosis. Studies have shown that such reactions lead to structurally organized fibrotic tissue and bone (Li et al., 2007; Somdas et al., 2007), which would begin to emerge within the same timeframe as the impedance increase shown here, i.e., months to years. It should be noted that the exclusion of deactivated (mainly basal electrodes) would suggest that our findings under-estimate the extent of basal tissue growth. The data shows individual variability in EI, which may reflect surgical approach, age, etiology, noise exposure or other factors. The cases included were implanted using either cochleostomy (approximately one third) or round window insertion (approximately two thirds). No formal assessment of surgical approach and its impact on EI was carried out. Evidence shows that this variable has no significant effect on EI or listening performance for phonemes or sentences (Cheng et al., 2018).

We have limited understanding of the wide variability in performance and outcomes for CI users. A wealth of evidence suggests that the biological response to the implant

is pivotal to its long-term functionality. It is possible to measure the response using impedance telemetry, although the currently available tools are limited to detection of extreme high or low EI levels. In order to address this, we applied a statistical method of outlier-labeling to detect cases of raised impedance (SEI). This is distinct from the absolute threshold used by the MED-EL and other manufacturers, which serves to highlight high and low impedances that are extreme enough to prevent normal current delivery. These cases mostly indicate hardware faults and extra-cochlear electrode position. The cost of using high threshold methods for detecting raised impedance is the relative insensitivity to biological perturbations associated with EI changes below 20 k Ω . Our technique could be validated by measuring CI performance following customization of processor maps where electrodes with SEI levels are deactivated. If validated, this would provide a quicker and more clinically useful method to guide electrode deactivation as compared with more challenging and time-consuming methods based on psychophysical measurements proposed in the literature: Mathew et al. (2017) and Zhou (2017). Further work to determine any correlation between the sorts of psychophysical methods proposed by these authors and the proposed outlier-EI values would help to further validate this approach.

The long-term pattern of change of EI in those individuals identified as outliers may inform the underlying mechanism. Results show EI increase at discrete electrodes, some developing slowly over the 5-year study period. In several cases (13 of 14) the SEI criteria was met at non-basal electrodes, which is counter to the model that the tissue development driven by inflammation is most prevalent at the base near the site of array implantation (Richard et al., 2012; Bas et al., 2015). In some cases, gradual EI differences are specific to particular non-basal electrodes. For example, electrode 7 in **Figure 7A** shows a pronounced example of EI increase that develops slowly over many months. In most cases, this was limited to one, or at most, very few electrodes, which suggests the change is driven by spatially localized factors. No hardware malfunctions were detected, and the electrode remained actively stimulated for the duration of the studied time period. One possible explanation is the presence of a spatially discrete trigger of inflammation such as mechanical trauma. This might have occurred during surgery as the electrode array tip passed through this region of the cochlear duct causing an abrasion, as lateral wall damage is known to elicit fibrotic changes (Li et al., 2007). To further understand the cause of raised but not “open-circuit” EI in particular electrode regions, the ability to cross-reference with newer and more sensitive imaging methods (Aschendorff, 2011) could also lead to a greater understanding of whether localized surgical trauma, cochlear anatomy, or other factors, predispose some individuals to showing higher EI values in apical or mid-cochlear regions.

Electrical stimulation is known to electro-chemically effect the endo-cochlear environment. When charge is delivered within safe tolerances the predominant mechanisms are ionic transfer and platinum hydrogen plating (Brummer and Turner, 1977). These processes are safe and reversible when bi-phasic

charge-balanced pulses are used. It has been suggested that such charge delivery mediates the process of protein adsorption onto platinum electrodes and can affect the organization and density of the fibrotic capsule (Newbold et al., 2010). It is well documented that electrode deactivation contributes to EI increase, so ideally clinicians would access objective evidence before making electrode deactivations that make future reactivation more difficult. Neuburger et al. (2009) presents further evidence of the effect of electrical stimulation on impedance. They observed cases of increasing EI in CI users with high rates of stimulation, which necessitate short pulse-width and high current to produce the desired perceived loudness. A therapeutic intervention involving increased pulse-width along with antibiotics and steroids proved effective at significantly reducing EI. The author suggests that the original EI increase could be caused by the occurrence of out-of-compliance charge delivery leading to slight asymmetries in bi-phasic pulses. Early detection of increasing impedance could therefore be clinically important: it will inform stimulus parameter adjustments, which could lower impedance levels before they cause voltage compliance problems.

Recent work has identified improved preservation of spiral ganglion neurones after dexamethasone elution in chronically stimulated animals (Scheper et al., 2017). Another study of dexamethasone eluting CI electrodes in guinea pigs showed significant reductions in fibrotic tissue and EI compared to no-steroid controls (Wilk et al., 2016). A complementary result was shown in humans where the cochlea was perfused with the steroid triamcinolone; long-term EI levels were significantly lower in the treatment group compared to controls (De Ceulaer et al., 2003). Systemic delivery of the steroid methylprednisolone in another study did not reduce EI spikes (Choi et al., 2017), which suggests the anti-inflammatory action of steroids is most effective when topically administered. It would be interesting to study the benefit of steroid based intervention that is directed by the outlier-labeling rule used here.

Our analysis of the proportion of deactivated electrodes in children and adults was quite telling. Generally, both age groups showed a pattern of electrode deactivation primarily at basal electrodes. However, the reasons for deactivations were overwhelmingly patient feedback from adults whereas the most common reason in children was extra-cochlear position. In addition, deactivation was less common in children than in adults. One possible explanation for this was that clinical decisions about deactivations are more cautious with children, or, rather, that adult feedback to clinicians does lead to choice of deactivation of electrodes with more fibrous tissue grown/higher EI (e.g., primarily basal). This begs the question of whether choice to deactivate electrodes is optimal, and in particular whether the smaller proportion of basal electrode deactivations among children in particular is clinically appropriate or whether deactivation of basal electrodes in adults is excessive. Cross-referencing with the outlier method of EI analysis and other methods noted above could help to determine the answer to these questions. Alternatively, it may be that some differences in etiology and/or anatomy pre-dispose the child's cochlea to be more susceptible to other types of problem (e.g., non-auditory stimulation).

CONCLUSION

An important outcome of this work is the insight gained from applying a custom analysis protocol to existing clinical data. Our approach was to characterize sample-wide trends and apply an outlier detection rule that could improve our early detection of sub-optimal performance. A key benefit of using this method alongside manufacturer-specific proprietary telemetry systems is the sensitivity to changes of lower magnitude that may be associated with performance. This offers clinicians and researchers working in neuroprosthetics a method for interrogating their existing population data to identify incremental changes in device behavior, without extra financial, technical or ethical burden.

Our first question addressed the trend of impedance change over time for different electrode positions. The results showed that electrodes exhibit distinct trends of impedance evolution over 5 years. In the adult group growth in the basal electrodes contrasted with reduction for apical electrodes. The results also describe the range of the adult and pediatric dataset, which provides useful insights into individual variability. One reason for characterizing the EI trends over time was to improve interpretation of any individual deviation from the normative range. We asked how many individuals show statistically raised EI. The main analysis showed 8% of adults and 5% of children exhibited raised EI levels compared to the sample distribution. These cases were detected using a statistical outlier-labeling rule, which could be used to inform electrode deactivations with improved objectivity. Indeed, our findings show that clinical decisions to deactivate electrodes for adults were most commonly informed by patient subjective reports. The fact that adults had proportionally more electrodes deactivated than children may be caused by differences in capacity and confidence for verbal communication. The method used here to detect raised impedance in individuals of a clinical population may offer an opportunity to activate or deactivate electrodes long before the current device-specific floor or ceiling levels are reached. We determine that the information extracted from populations of users can be used alongside subjective reports to inform clinical management of individual patients. More work is needed to explore the sensitivity of this method as a biomarker of CI performance decrement.

The immediate benefit of these methods and findings is to give clinicians fresh insight into their existing data. The increasing

size and accessibility of clinical datasets presents an opportunity to professionals working with neuroprosthetics. Population-wide norms can be used to better interpret measurements from individual patients. The aim is to personalize clinical management to improve the function and biocompatibility of the implant interface over a user's lifetime.

AUTHOR CONTRIBUTIONS

AS conceived the research idea in conversation with TN and CV (academic supervisory team), performed the data collection, design of analysis, and literature review, and wrote the manuscript with guidance from TN and CV. ER wrote the custom MathWorks MATLAB code used for main analyses (as detailed in section “Materials and Methods”) and automated generation of **Figures 2–4, 5, 7, 8** with contribution from AS. AS, ER, TN, and CV performed the final manuscript editing and proofreading process with equal contribution.

ACKNOWLEDGMENTS

We thank K. Hough (Institute of Sound and Vibration Research, Faculty of Engineering and the Environment, University of Southampton) for manuscript proofreading and supporting discussions of biological responses to CI. We also thank M. Grasmeder for data extraction (MED-EL Maestro) and supporting discussions of clinical implications of findings, S. Cross for the management of clinical data (MED-EL Maestro and local patient database), and all patients of the Auditory Implant Service (Auditory Implant Service, Faculty of Engineering and the Environment, University of Southampton). We would like to acknowledge that the lead author's contributions to this work were made as part of a Ph.D. studentship funded by the Engineering and Physical Sciences Research Council (EPSRC Grant Code is 513830136) via a Doctoral Training Partnership with the University of Southampton, United Kingdom.

SUPPLEMENTARY MATERIAL

The Supplementary Material for this article can be found online at: <https://www.frontiersin.org/articles/10.3389/fnins.2018.01048/full#supplementary-material>

REFERENCES

- Adeyemi, D. O., Serruya, M. D., Harris, J. P., Burrell, J. C., Chen, H. I., Wolf, J. A., et al. (2017). The evolution of neuroprosthetic interfaces. *Crit. Rev. Biomed. Eng.* 44, 123–152. doi: 10.1615/CritRevBiomedEng.2016017198
- Anderson, J. M., Rodriguez, A., and Chang, D. T. (2008). Foreign body reaction to biomaterials. *Semin. Immunol.* 20, 86–100. doi: 10.1016/j.smim.2007.11.004
- Aschendorff, A. (2011). Imaging in cochlear implant patients. *GMS Curr. Top. Otorhinolaryngol. – Head Neck Surg.* 90, S16–S21. doi: 10.1055/s-0030-1270448
- Balkany, T. J., Hodges, A. V., Buchman, C. A., Luxford, W. M., Pillsbury, C. H., Roland, P. S., et al. (2005). Cochlear implant soft failures consensus development conference statement. *Cochlear Implants Int.* 6, 105–122. doi: 10.1179/cim.2005.6.3.105
- Bas, E., Goncalves, S., Adams, M., Dinh, C. T., Bas, J. M., Van De Water, T. R., et al. (2015). Spiral ganglion cells and macrophages initiate neuro-inflammation and scarring following cochlear implantation. *Front. Cell. Neurosci.* 9:303. doi: 10.3389/fncel.2015.00303
- Biedron, S., Westhofen, M., and Ilgner, J. (2009). On the number of turns in human cochleae. *Otol. Neurotol.* 30, 414–417. doi: 10.1097/MAO.0b013e3181977b8d

- Brummer, S. B., and Turner, M. J. (1977). Electrochemical considerations for safe electrical stimulation of the nervous system with platinum electrodes. *IEEE Trans. Biomed. Eng.* 24, 59–63. doi: 10.1109/TBME.1977.326218
- Busby, P. A., Plant, K. L., and Whitford, L. A. (2002). Electrode impedance in adults and children using the Nucleus 24 cochlear implant system. *Cochlear Implants Int.* 3, 87–103. doi: 10.1002/cii.55
- Carlson, M. L., Archibald, D. J., Dabade, T. S., Gifford, R. H., Neff, B. A., Beatty, C. W., et al. (2010). Prevalence and timing of individual cochlear implant electrode failures. *Otol. Neurotol.* 31, 893–898. doi: 10.1097/MAO.0b013e318d2d697
- Causon, A., Verschuur, C. A., and Newman, T. A. (2013). Trends in cochlear implant complications: implications for improving long-term outcomes. *Otol. Neurotol.* 34, 259–265. doi: 10.1097/MAO.0b013e31827d0943
- Cheng, X., Wang, B., Liu, Y., Yuan, Y., Shu, Y., and Chen, B. (2018). Comparable electrode impedance and speech perception at 12 months after cochlear implantation using round window versus cochleostomy: an analysis of 40 patients. *Orl* 200031, 1–11. doi: 10.1159/000490764
- Choi, J., Payne, M. R., Campbell, L. J., Bester, C. W., Newbold, C., Eastwood, H., et al. (2017). Electrode impedance fluctuations as a biomarker for inner ear pathology after cochlear implantation. *Otol. Neurotol.* 38, 1433–1439. doi: 10.1097/MAO.0000000000001589
- Christo, S. N., Diener, K. R., Bachhuka, A., Vasilev, K., and Hayball, J. D. (2015). Innate immunity and biomaterials at the nexus: friends or foes? *Biomed Res. Int.* 2015:342304. doi: 10.1155/2015/342304
- Clark, G. M., Tong, C. T., and Patrick, J. F. (1990). *Cochlear Prostheses*. 1st Edn, ed. G. M. Clark, C. T. Tong, and J. F. Patrick (London: Longman Group UK Limited).
- Clark, G. M., Shute, S. A., Shepherd, R. K., and Carter, T. D. (1995). Cochlear implantation: osteoneogenesis, electrode-tissue impedance, and residual hearing. *Ann. Otol. Rhinol. Laryngol.* 166, 40–42.
- Clark, G. M. (2003). *Cochlear Implants: Fundamentals and Applications*, ed. Robert T. Beyer (New York: Springer-Verlag New York, Inc.). doi: 10.1007/b97263
- De Ceulaer, G., Johnson, S., Yperman, M., Daemers, K., Offeciers, F. E., O'Donoghue, G. M., et al. (2003). Long-term evaluation of the effect of intracochlear steroid deposition on electrode impedance in cochlear implant patients. *Otol. Neurotol.* 24, 769–774. doi: 10.1097/00129492-200309000-00014
- Dorman, M. F., Smith, L. M., Dankowski, K., McCandless, G., and Parkin, J. L. (1992). Long-term measures of electrode impedance and auditory thresholds for the Ineraid cochlear implant. *J. Speech Hear. Res.* 35, 1126–1130. doi: 10.1044/jshr.3505.1126
- Ear Foundation (2016). *Cochlear Implants Information Sheet*. Available at: <http://www.earfoundation.org.uk/files/download/1221>
- Fayad, J. N., Makarem, A. O., and Lintinich, F. H. (2009). Histopathologic assessment of fibrosis and new bone formation in implanted human temporal bones using 3D reconstruction. *Otolaryngol. - Head Neck Surg.* 141, 247–252. doi: 10.1016/j.otohns.2009.03.031
- Gifford, R. H., Shallop, J. K., and Peterson, A. M. (2008). Speech recognition materials and ceiling effects: considerations for cochlear implant programs. *Audiol. Neurotol.* 13, 193–205. doi: 10.1159/000113510
- Grill, W. M., and Thomas Mortimer, J. (1994). Electrical properties of implant encapsulation tissue. *Ann. Biomed. Eng.* 22, 23–33. doi: 10.1007/BF02368219
- Hassler, C., Boretius, T., and Stieglitz, T. (2011). Polymers for neural implants. *J. Polym. Sci. Part B Polym. Phys.* 49, 18–33. doi: 10.1002/polb.22169
- Henkin, Y., Kaplan-Neeman, R., Kronenberg, J., Migirov, L., Hildesheimer, M., and Muchnik, C. (2006). A longitudinal study of electrical stimulation levels and electrode impedance in children using the Clarion cochlear implant. *Acta Otolaryngol.* 126, 581–586. doi: 10.1080/00016480500443391
- Henkin, Y., Kaplan-Neeman, R., Muchnik, C., Kronenberg, J., and Hildesheimer, M. (2003). Changes over time in electrical stimulation levels and electrode impedance values in children using the Nucleus 24M cochlear implant. *Int. J. Pediatr. Otorhinolaryngol.* 67, 873–880. doi: 10.1016/S0165-5876(03)00131-9
- Hillard, C., Fowler, J. D., Barta, R., and Cunningham, B. (2017). Silicone breast implant rupture: a review. *Gland Surg.* 6, 163–168. doi: 10.21037/gls.2016.09.12
- Hoaglin, D. C., and Iglewicz, B. (1987). Fine-tuning some resistant rules for outlier labeling. *J. Am. Stat. Assoc.* 82, 1147–1149. doi: 10.1080/01621459.1987.10478551
- Hoaglin, D. C., Iglewicz, B., and Tukey, J. W. (1986). Performance of some resistant rules for outlier labeling. *J. Am. Stat. Assoc.* 81, 991–999. doi: 10.1080/01621459.1986.10478363
- Hughes, M. L., Vander Werff, K. R., Brown, C. J., Abbas, P. J., Kelsay, D. M., Teagle, H. F., et al. (2001). A longitudinal study of electrode impedance, the electrically evoked compound action potential, and behavioral measures in nucleus 24 cochlear implant users. *Ear. Hear.* 22, 471–486. doi: 10.1097/00003446-200112000-00004
- Jia, H., Venail, F., Piron, J. P., Batrel, C., Pelliccia, P., Artierles, F., et al. (2011). Effect of surgical technique on electrode impedance after cochlear implantation. *Ann. Otol. Rhinol. Laryngol.* 120, 529–534. doi: 10.1177/00034894111200807
- Kamakura, T., and Nadol, J. B. (2016). Correlation between word recognition score and intracochlear new bone and fibrous tissue after cochlear implantation in the human. *Hear. Res.* 339, 132–141. doi: 10.1016/j.heares.2016.06.015
- Kawano, A., Seldon, H. L., Clark, G. M., Msden, R. T., and Raine, C. H. (1998). Intracochlear factors contributing to psychophysical percepts following cochlear implantation: a case study. *Acta Otolaryngol.* 104, 54–57. doi: 10.1080/00016489850183386
- Leone, C. A., Mosca, F., Grassia, R., and Hospital, M. (2017). Temporal changes in impedance of implanted adults for various cochlear segments. *Acta Otorhinolaryngol. Ital.* 37, 312–319. doi: 10.14639/0392-100X-1471
- Li, P. M., Somdas, M. A., Eddington, D. K., and Nadol, J. B. (2007). Analysis of intracochlear new bone and fibrous tissue formation in human subjects with cochlear implants. *Ann. Otol. Rhinol. Laryngol.* 116, 731–738. doi: 10.1177/000348940711601004
- Lim, H. J., Lee, E. S., Park, H. Y., Park, K., and Choong, Y. H. (2011). Foreign body reaction after cochlear implantation. *Int. J. Pediatr. Otorhinolaryngol.* 75, 1455–1458. doi: 10.1016/j.ijporl.2011.08.004
- Marsella, P., Scorpecci, A., Pacifico, C., Resca, A., Vallarino, M. V., Ingrosso, A., et al. (2014). Safety and functional results of early cochlear implant switch-on in children. *Otol. Neurotol.* 35, 277–282. doi: 10.1097/MAO.00000000000000259
- Mathew, R., Undurraga, J., Li, G., Meerton, L., Boyle, P., Shaida, A., et al. (2017). Objective assessment of electrode discrimination with the auditory change complex in adult cochlear implant users. *Hear. Res.* 354, 86–101. doi: 10.1016/j.heares.2017.07.008
- Med-El (2013). *Electrode Arrays: Designed for Atraumatic Implantation Providing Superior Hearing Performance*. Available at: <http://www.medel.com/data/pdf/21617.pdf>
- Moberly, A., Welling, B., and Nittrouer, S. (2013). Detecting soft failures in pediatric cochlear implants: relating behavior to language outcomes. *Otol. Neurotol.* 34, 1648–1655. doi: 10.1016/j.pmrj.2014.02.014
- Lumbar
- Nadol, J. B., O'Malley, J. T., Burgess, B. J., and Galler, D. (2014). Cellular immunologic responses to cochlear implantation in the human. *Hear. Res.* 318, 11–17. doi: 10.1016/j.heares.2014.09.007
- Neuburger, J., Lenarz, T., Lesinski-Schiedat, A., and Büchner, A. (2009). Spontaneous increases in impedance following cochlear implantation: suspected causes and management. *Int. J. Audiol.* 48, 233–239.
- Newbold, C., Mergen, S., Richardson, R., Seligman, P., Millard, R., Cowan, R., et al. (2014). Impedance changes in chronically implanted and stimulated cochlear implant electrodes. *Cochlear Implants Int.* 15, 191–199. doi: 10.1179/1754762813Y.00000000050
- Newbold, C., Richardson, R., Millard, R., Huang, C., Milojevic, D., Shepherd, R., et al. (2010). Changes in biphasic electrode impedance with protein adsorption and cell growth. *J. Neural Eng.* 7:056011. doi: 10.1088/1741-2560/7/5/056011
- Nguyen, S., Cloutier, F., Philippon, D., Côté, M., Bussièrès, R., and Backous, D. D. (2016). Outcomes review of modern hearing preservation technique in cochlear implant. *Auris Nasus Larynx* 43, 485–488. doi: 10.1016/j.anl.2016.02.014

- Rask-Andersen, H., Erixon, E., Kinnefors, A., Löwenheim, H., Schrott-Fischer, A., and Liu, W. (2011). Anatomy of the human cochlea – implications for cochlear implantation. *Cochlear Implants Int.* 12(Suppl. 1), S8–S13. doi: 10.1179/146701011X13001035752174
- Rask-Andersen, H., Liu, W., Erixon, E., Kinnefors, A., Pfaller, K., Schrott-Fischer, A., et al. (2012). Human cochlea: anatomical characteristics and their relevance for cochlear implantation. *Anat. Rec.* 295, 1791–1811. doi: 10.1002/ar.22599
- Richard, C., Fayad, J. N., Doherty, J., and Linthicum, F. H. (2012). Round window versus cochleostomy technique in cochlear implantation: histologic findings. *Otol. Neurotol.* 33, 1181–1187. doi: 10.1097/MAO.0b013e318263d56d
- Saunders, E., Cohen, L., Aschendorff, A., Shapiro, W., Knight, M., Stecker, M., et al. (2002). Threshold, comfortable level and impedance changes as a function of electrode-modiolar distance. *Ear Hear.* 23, 28S–40S. doi: 10.1097/00003446-200202001-00004
- Scheper, V., Hessler, R., Hu, M., Wilk, M., Jolly, C., Lenarz, T., et al. (2017). Local inner ear application of dexamethasone in cochlear implant models is safe for auditory neurons and increases the neuroprotective effect of chronic electrical stimulation. *PLoS ONE* 12:e0183820. doi: 10.1371/journal.pone.0183820
- Seyyedi, M., and Nadol, J. B. Jr. (2014). Intracochlear inflammatory response to cochlear implant electrodes in humans. *Otol. Neurotol.* 35, 1545–1551. doi: 10.1097/MAO.0000000000000540
- Shepherd, R. K., Matsushima, J., Martin, R. L., and Clark, G. M. (1994). Cochlear pathology following chronic electrical stimulation of the auditory nerve: II deafened kittens. *Hear. Res.* 81, 150–166. doi: 10.1016/0378-5955(94)90162-7
- Skarzynski, H., van de Heyning, P., Agrawal, S., and Arauz, S. L. (2013). Towards a consensus on a hearing preservation classification system. *Acta Otolaryngol. Suppl.* 133, 3–13. doi: 10.3109/00016489.2013.869059
- Somdas, M. A., Li, P. M., Whiten, D. M., Eddington, D. K., and Nadol, J. B. (2007). Quantitative evaluation of new bone and fibrous tissue in the cochlea following cochlear implantation in the human. *Audiol. Neurotol.* 12, 277–284. doi: 10.1159/000103208
- Stöver, T., and Lenarz, T. (2009). Biomaterials in cochlear implants. *Laryngorhinootologie* 88, S12–S31. doi: 10.3205/cto000062
- Tykocinski, M., Cohen, L. T., and Cowan, R. S. (2005). Measurement and analysis of access resistance and polarization impedance in cochlear implant recipients. *Otol. Neurotol.* 26, 948–956. doi: 10.1097/01.mao.0000185056.99888.f3
- Tykocinski, M., Duan, Y., Tabor, B., and Cowan, R. S. (2001). Chronic electrical stimulation of the auditory nerve using high surface area (HiQ) platinum electrodes. *Hear. Res.* 159, 53–68. doi: 10.1016/S0378-5955(01)00320-3
- Wilk, M., Hessler, R., Mugridge, K., Jolly, C., Fehr, M., Lenarz, T., et al. (2016). Impedance changes and fibrous tissue growth after cochlear implantation are correlated and can be reduced using a dexamethasone eluting electrode. *PLoS One* 11:e0147552. doi: 10.1371/journal.pone.0147552
- Wilson, B. S., and Dorman, M. F. (2008). Cochlear implants: a remarkable past and a brilliant future. *Hear. Res.* 242, 3–21. doi: 10.1016/j.heares.2008.06.005
- Wolfe, J., Baker, R., and Wood, M. (2013). Clinical case study review: steroid-responsive change in electrode impedance. *Otol. Neurotol.* 34, 227–232. doi: 10.1097/MAO.0b013e31827b4bba
- Xu, J., Shepherd, R. K., Millard, R. E., and Clark, G. M. (1997). Chronic electrical stimulation of the auditory nerve at high stimulus rates: a physiological and histopathological study. *Hear. Res.* 105, 1–29. doi: 10.1016/S0378-5955(96)00193-1
- Zanetti, D., Nassif, N., Redaelli De Zinis, L. O., and Civili, S. (2015). Factors affecting residual hearing preservation in cochlear implantation. *Acta Otorhinolaryngol. Ital.* 35, 433–441. doi: 10.14639/0392-100X-619
- Zhou, N. (2017). Deactivating stimulation sites based on low-rate thresholds improves spectral ripple and speech reception thresholds in cochlear implant users. *J. Acoust. Soc. Am.* 141, EL243–EL248. doi: 10.1121/1.4977235

Conflict of Interest Statement: The authors declare that the research was conducted in the absence of any commercial or financial relationships that could be construed as a potential conflict of interest.

Copyright © 2019 Sanderson, Rogers, Verschuur and Newman. This is an open-access article distributed under the terms of the Creative Commons Attribution License (CC BY). The use, distribution or reproduction in other forums is permitted, provided the original author(s) and the copyright owner(s) are credited and that the original publication in this journal is cited, in accordance with accepted academic practice. No use, distribution or reproduction is permitted which does not comply with these terms.

B.8 Appendix B8

Chapter 3 Supplementary Figures

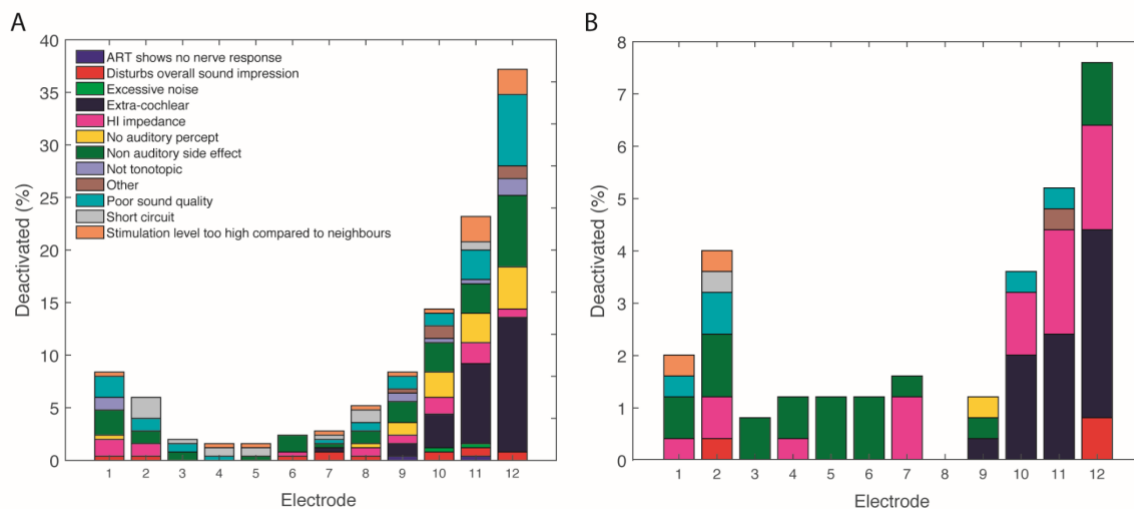


Figure B8-1: Count of reasons for deactivation (problem in MATLAB. Other= 'to see if whistling goes', 'small dynamic range', 'poor loudness growth on ART', 'disabled', 'Disabled to increase rate', 'Disabled to increase channel separation', 'Disabled in the imported CIStudio+ Map')

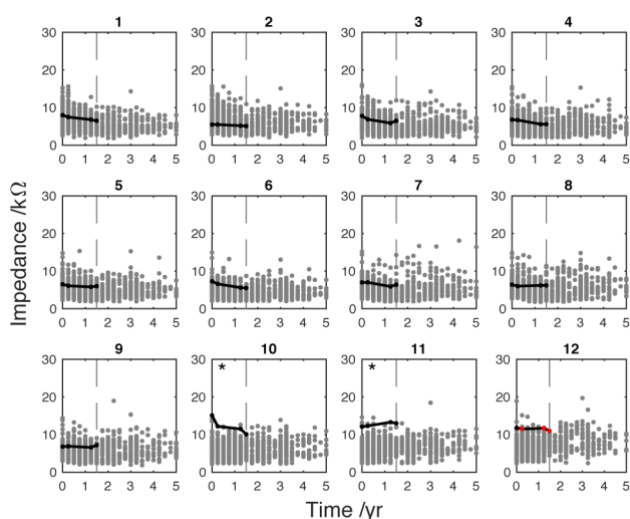


Figure B8-2: A individual adult case showing EI. Case shows 1.5 years CI use indicated by vertical dotted line. Electrode marked by * met the SEI criteria which indicates high EI compared to the sample distribution. Red dots indicate EI data points measured at deactivated electrodes (not included in SEI detection).

Appendix

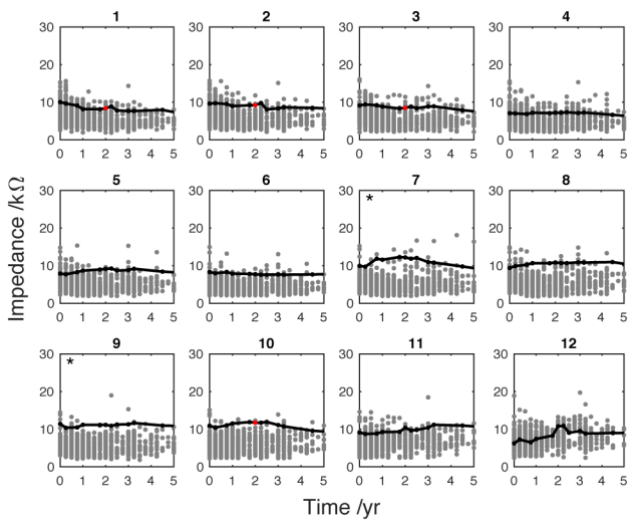


Figure B8-3: A individual adult case showing EI. Case shows 5 years CI use indicated by vertical dotted line. Electrode marked by * met the SEI criteria which indicates high EI compared to the sample distribution. Red dots indicate EI data points measured at deactivated electrodes (not included in SEI detection).

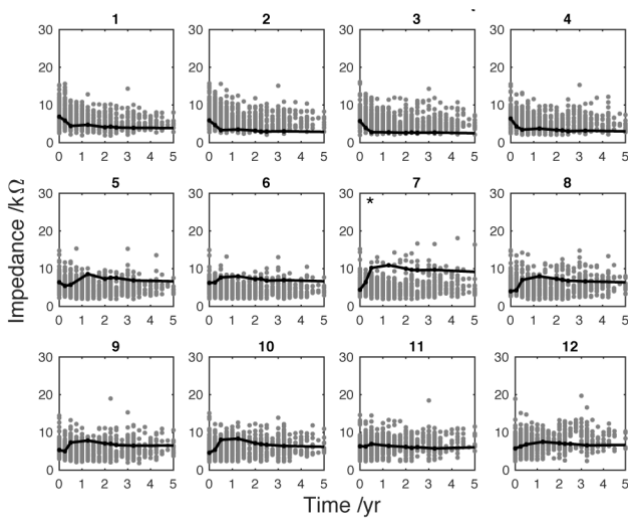


Figure B8-4: A individual adult case showing EI. Case shows 5 years CI use indicated by vertical dotted line. Electrode marked by * met the SEI criteria which indicates high EI compared to the sample distribution.

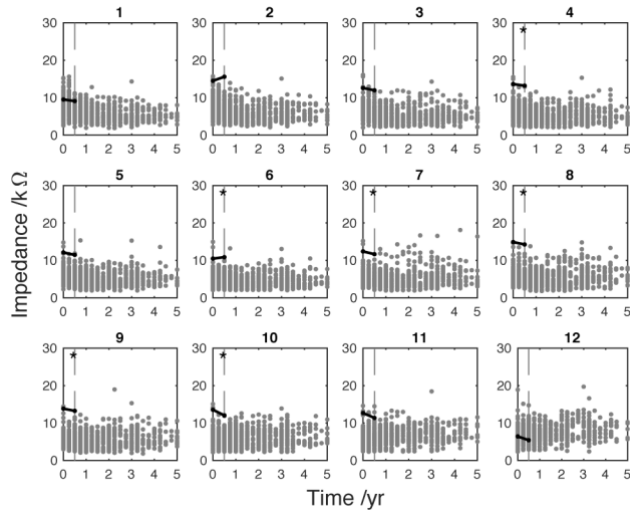


Figure B8-5: A individual adult case showing EI. Case shows 0.5 years CI use indicated by vertical dotted line. Electrode marked by * met the SEI criteria which indicates high EI compared to the sample distribution.

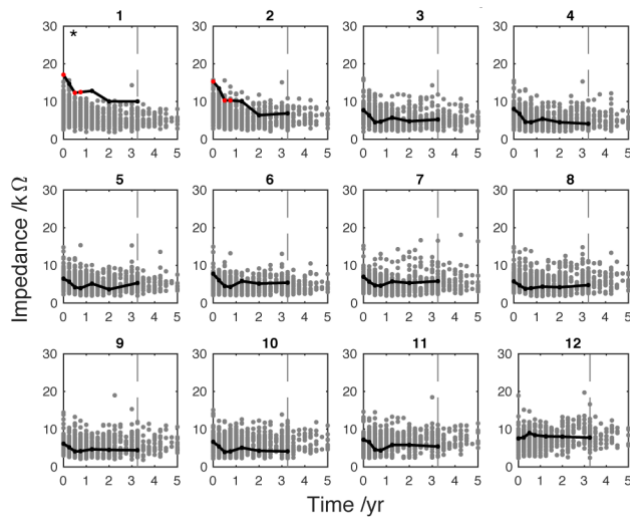


Figure B8-6: A individual adult case showing EI. Case shows 3.25 years CI use indicated by vertical dotted line. Electrode marked by * met the SEI criteria which indicates high EI compared to the sample distribution. Red dots indicate EI data points measured at deactivated electrodes (not included in SEI detection).

Appendix

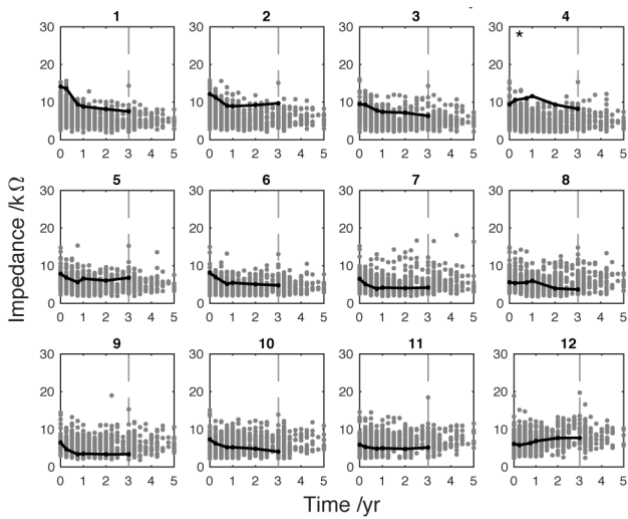


Figure B8-7: A individual adult case showing EI. Case shows 3 years CI use indicated by vertical dotted line. Electrode marked by * met the SEI criteria which indicates high EI compared to the sample distribution.

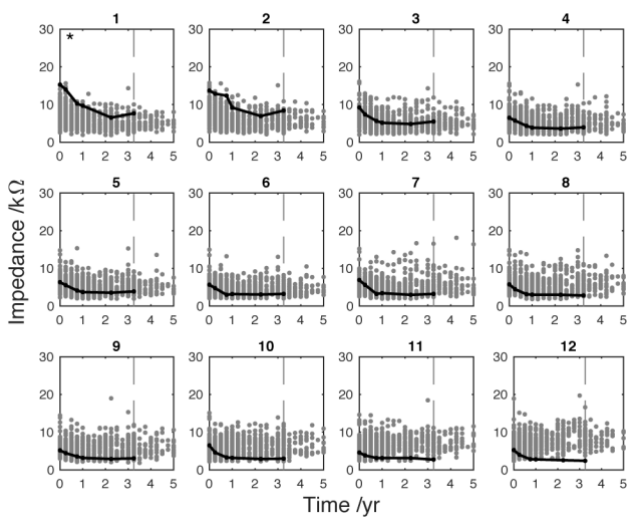


Figure B8-8: A individual adult case showing EI. Case shows 3.25 years CI use indicated by vertical dotted line. Electrode marked by * met the SEI criteria which indicates high EI compared to the sample distribution.

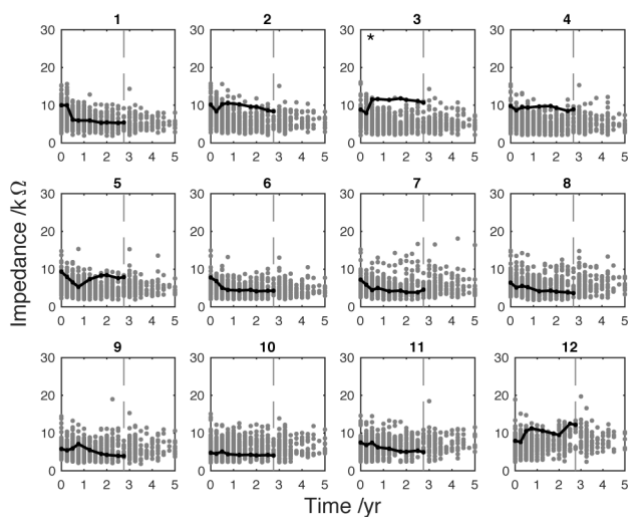


Figure B8-9: A individual adult case showing EI. Case shows 2.75 years CI use indicated by vertical dotted line. Electrode marked by * met the SEI criteria which indicates high EI compared to the sample distribution.

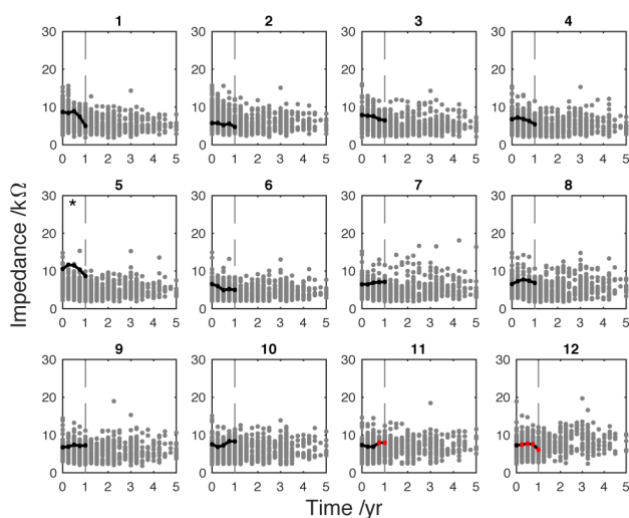


Figure B8-10: A individual adult case showing EI. Case shows 1 years CI use indicated by vertical dotted line. Electrode marked by * met the SEI criteria which indicates high EI compared to the sample distribution. Red dots indicate EI data points measured at deactivated electrodes (not included in SEI detection).

Appendix

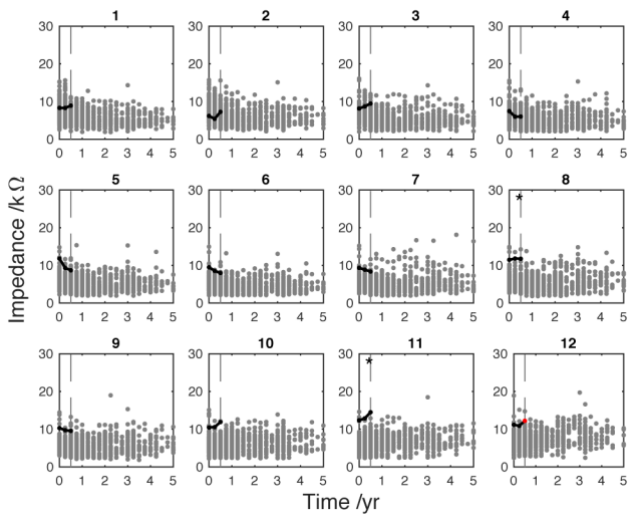


Figure B8-11: A individual adult case showing EI. Case shows 0.5 years CI use indicated by vertical dotted line. Electrode marked by * met the SEI criteria which indicates high EI compared to the sample distribution. Red dots indicate EI data points measured at deactivated electrodes (not included in SEI detection).

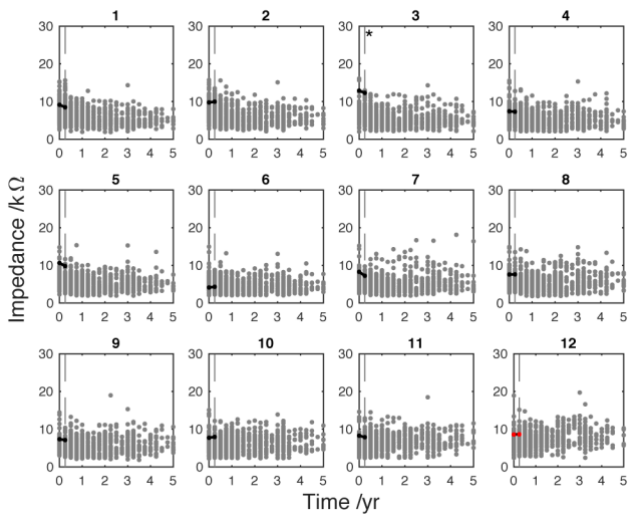


Figure B8-12: A individual adult case showing EI. Case shows 0.25 years CI use indicated by vertical dotted line. Electrode marked by * met the SEI criteria which indicates high EI compared to the sample distribution. Red dots indicate EI data points measured at deactivated electrodes (not included in SEI detection).

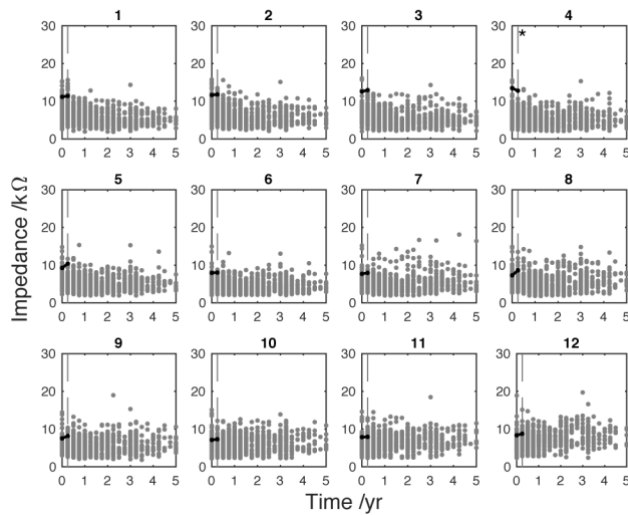


Figure B8-13: A individual adult case showing EI. Case shows 0.25 years CI use indicated by vertical dotted line. Electrode marked by * met the SEI criteria which indicates high EI compared to the sample distribution.

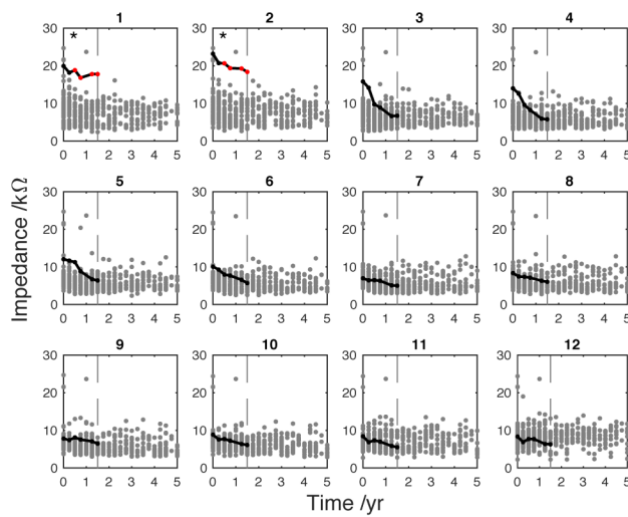


Figure B8-14: A individual paediatric case showing EI. Case shows 1.5 years CI use indicated by vertical dotted line. Electrode marked by * met the SEI criteria which indicates high EI compared to the sample distribution. Red dots indicate EI data points measured at deactivated electrodes (not included in SEI detection).

Appendix C

C.1 Appendix C1

Home Office Personal License (ANIMALS (SCIENTIFIC PROCEDURES) ACT 1986)



Home Office

Animals in Science Regulation Unit
Home Office Science
Mail Point A11/12,
1st Floor, Peel Building NE
2 Marsham Street, London, SW1P 4DF

www.gov.uk/research-and-testing-using-animals

Mr Alan Sanderson
University of Southampton
Office of the Vice-Chancellor, Building 37, Highfield
Campus, Southampton SO17 1BJ

Our Reference: I022E3686
Date: 10 May 2017

Dear Mr Sanderson

ANIMALS (SCIENTIFIC PROCEDURES) ACT 1986

Please find attached your personal licence.

You should check through your licence carefully for any endorsements on this licence in relation to animal types, licence category and the conditions attached to it. A personal licence on its own does not authorise you to perform regulated procedures on protected animals. You may perform only the procedures of the category specified by it if the procedure is applied as part of a programme of work specified in a project licence authorising the application, as part of that programme, of a regulated procedure of that description to an animal of that description. The application of unauthorised regulated procedures is a contravention of the Act and may result in prosecution and/or variation, suspension or revocation of your licence.

You are required to keep a record of all regulated procedures that you have carried out. This information must be made readily available to the Inspector or Secretary of State when required. If you cease to carry out work requiring a licence (for example leaving the UK to work abroad) you must return your licence to the Home Office.

As soon as you cease to work at the establishment given as the primary availability on your licence, or it ceases to be the place where you wish your licence to be primarily available, you must notify the Home Office, as this change will affect the fees charged. No other person may perform, either in whole or in part, any procedure authorised by your licence. The only exceptions are certain specific tasks of a non-technical nature. No other delegation is permitted (see Guidance on the Operation of the Act).

Should you wish any part of this licence to be amended, you must apply to the Home Office via your Home Office Liaison Contact giving details of the changes requested.

Yours sincerely

ASRU Licensing Team

The Home Office, in line with the rest of HMG, has implemented the Government Security Classification (GSC). Details of the GSC can be found at <https://www.gov.uk/government/publications/government-security-classifications>. Please note that documents and emails you receive may contain specific handling instructions.

Handling Instructions: Contains personal sensitive information, subject to confidentiality requirements under the Data Protection Act. This should only be circulated in accordance with ASPA Guidance and stored in a locked secure location. All government information may be subject to an FOI request and subsequent assessment.

C.2 Appendix C2

Macro script for Image-J (FIJI)

```

titleStack = getTitle();
NameStack = File.nameWithoutExtension;
dir = getDirectory("image");

run("Duplicate...", "title=OriginalDuplicate duplicate");
titleStackDupli = getTitle();

//change pixel value of artifact to values closer to background
for(i=1; i<=nSlices; i++){
    setSlice(i);
    changeValues(0,87,118);
    changeValues(168,255,118);
}

// reduce background and enhance contrast
run("Subtract Background...", "rolling=50 stack");
run("Enhance Contrast...", "saturated=0.3 process_all");

// extract edges with FeatureJ
setSlice(1);
run("Duplicate...", "title=newStackEdge");
run("FeatureJ Options", "close progress");
run("FeatureJ Edges", "compute smoothing=2 lower=[] higher=[]");
rename("newStackEdge");

selectWindow(titleStackDupli);
for(i=2; i<=nSlices; i++){

    setSlice(i);

    run("Duplicate...", "title="+i);
    run("FeatureJ Options", "close progress");
    run("FeatureJ Edges", "compute smoothing=2 lower=[] higher=[]");

    run("Concatenate...", "title=newStackEdge open image1=[newStackEdge] image2=["+i+"
edges] image3=[-- None --]");

    selectWindow(titleStackDupli);
}
selectWindow(titleStackDupli);
close();

selectWindow("newStackEdge");
//run("Brightness/Contrast...");
run("Enhance Contrast", "saturated=0.35");
run("Median...", "radius=4 stack");
run("8-bit");

```

Appendix

```
setAutoThreshold("Huang dark");
run("Threshold...");
waitForUser("Threshold the sample (try different slices), then press OK");
getThreshold(lower, upper);
resetThreshold;

setBatchMode(true);

setThreshold(lower, 255);
setOption("BlackBackground", false);
run("Convert to Mask", "method=Huang background=Dark");
rename("Binary");
selectWindow("Threshold");
run("Close");

run("Invert", "stack");
run("Analyze Particles...", "size=2000-Infinity show=Masks stack");

selectWindow("Binary");
close();

selectWindow("Mask of Binary");
rename("MaskBinary");
run("Analyze Particles...", "size=0-9000 show=Masks stack");

selectWindow("MaskBinary");
run("Invert", "stack");
imageCalculator("Add create stack", "MaskBinary", "Mask of MaskBinary");
selectWindow("MaskBinary");
close();
selectWindow("Mask of MaskBinary");
close();

selectWindow("Result of MaskBinary");
run("Analyze Particles...", "size=200-Infinity show=Masks stack");
selectWindow("Result of MaskBinary");
close();
selectWindow("Mask of Result of MaskBinary");

run("Line Width...", "line=100");
run("Colors...", "foreground=white background=black selection=yellow");
//setTool("line");
makeLine(1344, 0, 1695, 372);
setForegroundColor(255, 255, 255);
run("Fill", "stack");
makeLine(0, 2370, 213, 2595);
run("Fill", "stack");
//setTool("rectangle");
makeRectangle(1578, 2487, 122, 113);
run("Fill", "stack");
run("Select None");

saveAs("Tiff", dir+NameStack+"_Binary.tif");
titleBinary = getTitle();
```



```
run("Fill Holes", "stack");
run("Colors...", "foreground=black background=black selection=yellow");

for(i=1; i<=nSlices; i++){
    setSlice(i);
    run("Create Selection");
    selectWindow(titleStack);
    setSlice(i);
    run("Restore Selection");
    setBackgroundColor(0, 0, 0);
    run("Clear Outside", "slice");
    run("Select None");
    selectWindow(titleBinary);
}
selectWindow(titleStack);
saveAs("Tiff", dir+NameStack+"_ClearOutside.tif");
run("Close All");
exit("END OF MACRO");
```

C.3 Appendix C3

Step by Step dissection – Brain and Cochlea

Set up all equipment next to dissecting microscope – blue roll, black dissection plate, instruments, beaker with PBS, bijoux containers, marker pen, 70% ethanol in squeeze dispenser and 50ml centrifuge tube.

Risk (Ethanol): Flammable and acutely toxic. Dispose down sink with copious water.

Risk (Biohazard): Risk of contamination with biological material. Wear goggles, gloves and lab coat. If contaminated, rinse with water and anti-bacterial cleaner.

Label bijoux containers with date, sample code/description (brain or cochlea)

Place head on dissection plate and squirt with PBS

Using scalpel, cut through skin caudally (from anterior to posterior) from snout along midline. Apply enough pressure to feel the resistance of the underlying bone.

Risk (Sharp scalpel): Could cut yourself. Wear gloves. If have an accident, seek a trained first aider.

Blunt dissection of skin and soft tissue to reveal skull.

Using rongeur, crush bone on top of snout. Use this opening to work caudally removing frontal, parietal, interparietal and occipital skull sections to reveal the brain.

Carefully lift away any bone from dorsal aspect of squamosal bone to allow entry of spatula.

Wet spatula in PBS and carefully scoop underneath olfactory bulbs to release from olfactory nerve.

Move caudally, lifting the brain from skull-base.

Release brain by severing spinal cord or medulla, being careful of the ventral brainstem (cochlear nucleus). Place in bijoux container of 70% ethanol.

Risk (Ethanol): See above

Transfer head to microscope – Moisten tissue using PBS

Should be able to see the stylohyoid process which indicates the position of the otic capsule

Use rongeur to break squamosal bone anterior to otic capsule.

Clear soft tissue from stylohyoid process/ otic capsule.

Using a pair of forceps, hold down auditory bulla. Using a second set in the other hand apply lateral force (away from midline) to the tip of the stylohyoid process. This will fracture the otic capsule from the bulla and reveal the cochlea underneath.

Remove excess skull bone and soft tissue from otic capsule

Place in labelled bijoux container with 70% ethanol

Risk (Ethanol): See above

Fixation

Place tissue in 10% formalin if fresh.

Risk (Formalin): Harmful if ingested, inhaled or absorbed. Wear glove, lab coat and goggles. Use small volumes and do not handle outside class 2 cabinet or fume hood. Wash with copious water if in contact with skin/eyes and get medical attention.

Decalcification

Cochleae

Individual cochlea placed in 3.5 ml glass vials containing excess 0.125 M EDTA, on a rocker plate set at 40 rev/min, for 48 - 55 hours.

Risk (EDTA): Irritant if contact with skin. Wear gloves and lab coat. Use small volumes and concentrations. If contact with skin, rinse under cold water with soap.

The cochleae were then placed under the microscope and checked to see if they were transparent and soft to touch.

Appendix

If not, the EDTA was replaced and the cochleae were left for another 24 hours to complete decalcification.

Skulls

Skull were placed in a large volume of D.F.B decalcifying agent (H.K. Kristenson) for 3-4 days – until the tissue is soft and cuts easily with a scalpel.

Risk (D.F.B): Causes severe burns and eye damage. Wear lab coat, goggles and gloves. If contact with skin or eye – rinse with plenty of cold water.

Risk (Sharp scalpel): Could cut yourself. Wear gloves. If have an accident, seek a trained first aider.

How to remove cochlea from bulla

If a dissection has been carried out and the cochlea is still attached to the bulla:

For L sides

Place right side of forcep into hole of bulla to grab a hold of the bulla then use right hand forceps to push the pointy out bit away and downwards. There should be a joint like flexibility and a break where the cochlea is on the right bit of tissue and the bulla is the left bit of tissue.

C.4 Appendix C4

Synchrotron X-ray μ CT scan session log

| Extra - log | | | | | |
|-------------|-----------------|----------|----------|---|---------|
| Owner | Sample | Scans | Y pos | Notes | Checked |
| SLP | T4_4 TEFa | 99168.vv | 266.11 | 99169 new raw.vv 99170 higher | |
| SLP | T5_3 | 99171 | 265.11 | | |
| Owner | Sample | Scans | Y pos | Notes | Checked |
| OLK | Bug 1752 AL | 99178 | 266.7530 | 0.7 sec, 4.5 iser (40 proc) → floor (exposed) | X |
| OLK | Bug 1752 AL | 99179 | - | - " - " Sub-opt samples | ✓ |
| OLK | Bug 1752 AL | 99180 | - | 0.7 sec 0.5 step | ✓ |
| OLK | Bug 1752 AL | 99181 | - | 0.7 sec - " Det at 80mm | ✓ |
| OLK | - | 99182 | - | - " - " re-scanned | ✓ |
| OLK | Bug 1752 AL | 99183 | 266.7530 | 0.05 sec / 4x / 0.5 step | ✓ |
| OLK | Bug 1747 4 | 99184 | 248 | 0.2 sec / 4x / 0.5 step / alcohol | ✓ |
| OLK | Bug 1747 2 | 99185 | 250.39 | - " - " decalcified (?) | X |
| OLK | Bug 1747 1 | 99186 | 258.39 | - " - " No. of issue | X |
| OLK | Bug 1747 4 | 99187 | 249.6 | repeat of 99184 - No liquid / over exposure | ✓ |
| OLK | Bug 1747 6 | 99188 | 261.94 | exposed in situ | ✓ |
| OLK | Bug 1743 1. b7a | 99189 | 261.34 | 0.2 sec / 0.5 step / 10x FAILED → 140mm | ✓ |
| OLK | - | 99190 | - | - " - " repeat of 99189 FAILED | ✓ |
| OLK | - | 99191 | - | repeat of 99189 | ✓ |
| OLK | - | 99194 | 261.161 | 0.2 sec / 0.5 sec / 10x / 40mm Pet 105 | ✓ |
| OLK | - | 99195 | - | - " - " / 10x / 20mm Pet 105 | ✓ |
| OLK | - | 99196 | FAILED | - " - " / 10x / 80mm Pet 105 | ✓ |
| OLK | - | 99197 | - | - " - " - " - " | ✓ |
| OLK | Bug 1752 AL | 99200 | - | 0.15 step / 0.5 sec / 40mm Pet | ✓ |
| OLK | Bug 1752 CL | 99201 | - | - " - " - " - " | ✓ |
| OLK | Bug 1752 51 | 99202 | - | - " - " - " - " | ✓ |
| OLK | Bug 1747 1 | 99203 | - | Not scanned | ✓ |
| OLK | Bug 1747 6 | 99203 | - | 0.07 sec / 40mm | ✓ |

Handwritten notes on the right side of the log:
 - Repeat scans for
 - Pet 0.45mm
 - Pet at 250mm
 - Pet 1.1mm
 - Pet 1.1mm
 - out of Pet
 - MOVED bottles in liquid
 - w/ Guinif scan

C.5 Appendix C5

Paraffin wax embedded tissue – Haematoxylin and DAB Staining Anti Iba1 (Wako)

Read COSHH forms for DAB staining before commencing staining

Dewax – incubate sections at 60 °C for 30 mins. (Check incubator is switched on before hand)

Rinse in Xylene I ~ 10 mins

Risk (Xylene): Harmful if inhaled or contact with skin. Wear protective lab coat, goggles and gloves. If contact with skin – rinse under running water. Do not wash down sink; collect in non-chlorinated liquids waste container.

Rinse in Xylene II [CLEAN] ~ 10 mins

Risk (Xylene): See above

Rehydrate sections

100% Ethanol I ~ 5 mins

100% Ethanol II [CLEAN] ~ 5 mins

95% Ethanol I ~ 5 mins

80% Ethanol I ~ 5 mins

70% Ethanol I ~ 5 mins

PBS ~ 2 mins

Risk (Ethanol): Flammable and acutely toxic. Wear protective lab coat, goggles and gloves. Dispose down sink with copious water.

Draw wax circles around the tissue – wipe of excess liquid on slide first then draw wax circle.

Block activity of endogenous peroxidase – QUENCH – incubate with 1% H₂O₂ in Methanol for 15 mins

100µl 30% H₂O₂ in 2900µl Methanol. Make in small bijou with white lid.

Risk (Hydrogen peroxide): Irritant and corrosive. Avoid contact with skin and eyes. Wear protective lab coat, goggles and gloves. If contact with skin – rinse under running water.

Risk (Methanol): Flammable, toxic. Avoid contact with skin and eyes. Wear protective lab coat, goggles and gloves. If contact with skin – rinse under running water.

Wash in PBS Tween [0.05%] 2x 5 mins – pipette a small bit of PBS Tween onto slide to wash.

Prevent drying out before putting in rack in PBS. Change PBS between wash (take rack out when pour off PBS)

Risk (Tween): Avoid inhalation and contact with skin. Work with low concentrations (0.05-0.5%) and small volumes (~1ml). Wear protective lab coat, goggles and gloves. If contact with skin – rinse under running water.

Antigen retrieval

Microwave sections in sodium citrate buffer 3 mins – in black plastic rack – TAKE CARE WITH BOILING BUFFER

Cool sections by placing them into tap water 5 mins

Risk (Sodium citrate buffer): Avoid inhalation and contact with skin. Wear protective lab coat, goggles and gloves. To dispose – pour down sink with running water.

Risk (Boiling liquid): Boiling liquid can burn skin. Wear heat-proof protective gloves, as well as lab coat, goggles and gloves. In the incident of a burn – run under cold water. If severe- seek medical attention.

Wash off citrate buffer PBS [0.05%] 2 x 5 mins

Block sections in 1.5% normal goat serum in PBS for 45 mins – drop onto slides

3ml total = 45 ul NGS + 2955ul PBS

6 ml total = 90 ul NGS, 5890 ul PBS

DON'T FORGET: For negative control – wipe off liquid with cotton bud then draw a line with wax pen. Add PBS instead of primary

Tap off block and add primary

Incubate in primary antibody Anti Iba1 Antibody at for 1 hour 4 °C or overnight use 1:1000 dilution. Make in white bijou.

If leaving overnight – put some blue paper towel and distilled water in the plastic box to retain moisture overnight.

3ul of pAb, 3ml PBS

Wash PBS Tween [0.05%] 2x 5 mins – Dunk slides in rack

Incubate in secondary antibody 1 hour at RT – Biotin secondary e.g. Biotinylated anti-rabbit IgG Antibody 1:200

3000 ul / 200 = 15 ul of secondary

3000 – 15 = 2985 ul PBS

Make ABC solution

1 drop A (Avidin Solution)

1 drop B (Biotyl enzyme)

in 5 ml PBS

Invert to mix and leave for half an hour on the bench

Wash sections in PBS 2 x 5 mins

Put on ABC solution – 30 mins at room temp

Wash sections in PBS Tween [0.05%] 2 x 5 mins

Put in DAB solution (get out of freezer a bit before)

250ml 0.1M phosphate buffer, 5ml DAB solution, 125ul H₂O₂

Risk: (DAB): Carcinogenic. Avoid any contact. Wear lab coat, gloves and goggles. If contacted, seek immediate medical attention. Ensure there is no cross contamination across the lab. To dispose – add bleach in sink and leave the water running to rinse.

Risk (Hydrogen peroxide): See above

Check for staining after 30 seconds – USE TIMER

then in 10 secondary intervals (about 1 min 10s)

Put in PBS to stop reaction – rinse 2 x 5 mins in PBS

Appendix

Put in Haematoxylin for 5 minutes

Risk (Haematoxylin): Irritant. Avoid contact and inhalation. Wear lab coat, gloves and goggles. If contacted, seek immediate medical attention. To dispose – pour down sink with running water.

Tap off excess haematoxylin and place sections into clean tap water to wash off excess haematoxylin

Replace tap water until clear

Place sections into 1% acid 70% ethanol for two dips

Place back into tap water

Differentiate the haematoxylin stain by allowing clean tap water to flow over the sections for 2mins

Once haematoxylin stain has turned blue, place into 70% ethanol for ~5mins

Dehydrate sections

70% Ethanol ~5mins

80% Ethanol ~5mins

95% Ethanol ~5mins

100% Ethanol I ~ 5mins

100% Ethanol II [CLEAN] ~5mins

Risk (Ethanol): See above

Place into xylene I ~10mins

Place into xylene II [CLEAN] ~10mins

Risk: (Xylene) See above

Cover slip with DPX – add some xylene to DPX to change viscosity. Be careful when mixing to not introduce air bubbles.

Risk (DPX): Harmful if inhaled or contact with skin. Do not wash down sink; collect in non-chlorinated liquids waste container.

Leave to dry in fume hood

Ethanol

If the bottle is completely empty, make up 400 ml.

If there is a bit in the bottle, make up 200 ml.

| Ethanol | To make 200 ml | | To make 400 ml | |
|---------|------------------|--------|------------------|--------|
| 70 % | EtOH | 140 ml | EtOH | 280 ml |
| | H ₂ O | 60 ml | H ₂ O | 120 ml |
| 80 % | EtOH | 160 ml | EtOH | 320 ml |
| | H ₂ O | 40 ml | H ₂ O | 80 ml |
| 95 % | EtOH | 190 ml | EtOH | 380 ml |
| | H ₂ O | 10 ml | H ₂ O | 20 ml |

| | | | | |
|------------|------------------|--------|------------------|--------|
| 100 % (I) | EtOH | 200 ml | EtOH | 400 ml |
| | H ₂ O | 0 ml | H ₂ O | 0 ml |
| 100 % (II) | EtOH | 200 ml | EtOH | 400 ml |
| | H ₂ O | 0 ml | H ₂ O | 0 ml |
| | | | | |

1 % Acid 70 % Ethanol - Make in glass bottle

| | | |
|-----------------------------------|-------------------|--------|
| 1 % Acid 70 % Ethanol | To make up 400 ml | |
| | EtOH | 280 ml |
| | H ₂ O | 120 ml |
| Then add 4 ml of Concentrated HCl | | |

QUENCH – make in small white bijou

| | |
|------------------------------------|---------|
| 30 % H ₂ O ₂ | 100 ul |
| MethOH | 2900 ul |

Block for Iba1 Protocol – make in white bijou

| | | |
|--------------------|-------------------|---------|
| Block | Normal goat serum | PBS |
| To make 3 ml total | 45 ul | 2955 ul |
| To make 6 ml total | 90 ul | 5890 ul |

Primary Antibody – 1:1000 dilution – Make in small white bijou

| | |
|--------------------|------|
| Anti Iba1 Antibody | |
| PBS | 3 ml |
| Antibody | 3 ul |

Secondary antibody – 1:200 dilution - Make in small white bijou

| | |
|---------------------------------------|---------|
| Biotinylated anti-Rabbit IgG Antibody | |
| PBS | 2985 ul |
| Secondary Antibody | 15 ul |

Citrate buffer – Make in glass bottle, to be kept in fridge

| | |
|--------------------------|--------------------------------|
| Citrate buffer | |
| 10 mM Citric acid pH 6.0 | 1.92 g citric acid (anhydrous) |
| Distilled water | 1000 ml |
| Get to pH 6.0 | |

0.1M Phosphate Buffer pH 7.4 – Kept at room temperature

| |
|------------------------------|
| 0.1M Phosphate Buffer pH 7.4 |
|------------------------------|

Appendix

| | |
|--|---------------------|
| Sodium phosphate monobasic NaH_2PO_4 | 2.4g |
| Sodium phosphate dibasic Na_2HPO_4 | 11.36 g |
| H_2O | Add to 400 ml water |
| When dissolved – add the rest of the water (up to 1L) and continue stirring for 5 mins. pH to 7.4 | |

PBS To make 900 ml = one large glass bottle

| |
|---------------------------------------|
| 9 PBS Tablets |
| 900 ml distilled H_2O |

PBS Tween (0.05 %)

| |
|--|
| PBS Tablets |
| 1000 ml distilled H_2O |
| 1 ml of 50 % Tween |

C.6 Appendix C6

Paraffin embedding and sectioning of mouse cochlea

Embedding Cochleae

The apex of the cochlea should be opened to allow full infiltration of the paraffin wax. Use the tip of a scalpel or sharp forceps to apply gentle pressure to apical turn of the cochlea. The bony wall of the capsule will fracture to open the scalae.

Risk (Sharp scalpel): Could cut yourself. Wear gloves. If have an accident, seek a trained first aider.

Place the dissected cochlea in plastic cassette, sandwiched between two layers of thin foam. Leave in 70 % ethanol until it goes into the processor. Put into processor - Tissue-Tek VIP 5 jnr, Sakura.

Risk (Ethanol): Flammable and acutely toxic. Dispose down sink with copious water.

Risk (Hot wax 60°C): Burn the skin. Wear goggle and lab coat and be cautious. Rinse immediately under cold water if in contact with skin.

Make sure the shallow-to-medium square metal trays are on the heat to warm up
 Add a small volume of wax to the tray to give the cochlea some adhesion and stability
 Place the cochlea so the modiolus is parallel with the bed of the tray
 Place on ice cold part so the cochlea doesn't move but don't let it set too much on there – fine balance
 Then add cassette and add more wax to fill
 Then place on ice side for 45 minutes to set

Sectioning Cochleae

Risk (Sharp blade): Cut fingertips. Be cautious. If have an accident, seek a trained first aider.

Align block – 10 um sections

Label 20 slides

Start cutting into the tissue when aligned and put one section on slide and hold up to the light to check for signs of internal features of scalae

Once an indication of the turns of the cochlea are visible, check every few sections (looking for features of the Organ of Corti and the modiolus)

The mid-modiolar portion is only 5-10 sections thick. Take care to preserve these.

Appendix D

D.1 Appendix D1

Conference talks and posters

| Title | Description | Location | Date |
|--|---|---------------------------------|--------|
| Communicating in the modern world | Pint of Science Public Engagement | Southampton | May-19 |
| Investigation of fibrotic tissue from an explanted CI array following migration-related failure | British Cochlear Implant Group Annual Conference | Southampton Solent University | Apr-19 |
| Clinical and Laboratory Approaches to Assessing the Cochlear Implant-Tissue Interface | Meeting to establish collaboration for multi-centre study | Addenbrookes Hospital Cambridge | Jan-19 |
| Can innate immune memory hinder cochlear implant performance? | Southampton Neuroscience Group weekly seminar | University of Southampton | Nov-18 |
| The immense benefits of cochlear implants are not enjoyed by everyone. What can we learn from immune reactions in the ear? | Three-minute thesis competition | University of Southampton | May-18 |
| Cochlear Implant Electrode Impedance: A biomarker of localised tissue changes | Southampton Neuroscience Group weekly seminar | University of Southampton | Oct-17 |
| Cochlear Implant Electrode Impedance: A biomarker of localised tissue changes | OverHear Workshop: Evotion 'BIG DATA SUPPORTING PUBLIC HEARING HEALTH POLICIES' | University College London | Sep-17 |
| Electrode impedance: Defining the norm | Annual cochlear performance meeting | University College London | Jul-17 |
| Cochlear implant electrode impedance: A potential biomarker for clinical outcomes? | British Academy of Audiology Annual Conference | Glasgow | Nov-16 |
| Cochlear implant electrode impedance: A retrospective study of MED-EL CI users | University of Southampton Auditory Implant Service | University of Southampton | Jul-16 |
| Cochlear implant electrode impedance: A retrospective study of MED-EL CI users | Annual cochlear performance meeting | University College London | Jul-16 |

D.2 Appendix D2

Training Record

| Organised By | Location | Type of Course | Short Description | Date |
|---|--------------------------------|---|---|------------|
| Mark Willet | B85 L3 | Fluorescence microscopy | Practical training session on procedures for capturing digital images using a fluorescence microscope. Issues of best practice and theory were covered. | 21/01/2019 |
| The Lancet (Journal) | Barcelona | International conference on Neuroinflammation | 3 Day meeting of international researchers from the field of Neuroinflammation. 'Inflammation and immunity in disorders of the brain and mind' | 15/11/2018 |
| University of Southampton, Doctoral College | Highfield Campus, B7 | 3-minute thesis competition. University Final | Internationally organised initiative for students to present their PhD research in within 3 minutes and meet the criteria: communications skills, need for research, findings and impact. Outcome: Second place. | 17/05/2018 |
| British Neuroscience Association | Kings College, London | Annual Christmas national conference for Neuroscientists | One day conference of talk and networking with academic and clinical professionals working in various fields within Neuroscience. Opportunity to branch out from hearing research and audiology | 17/12/2018 |
| British Neuroscience Association | Canary Wharf, London | Annual Christmas national conference for Neuroscientists | One day conference of talk and networking with academic and clinical professionals working in various fields within Neuroscience. Opportunity to branch out from hearing research and audiology | 18/12/2017 |
| University of Southampton, Doctoral College | Highfield Campus, B7 | 3-minute thesis competition. Faculty Heat | Internationally organised initiative for students to present their PhD research in within 3 minutes and meet the criteria: communications skills, need for research, findings and impact. Outcome: First place. | 19/03/2018 |
| Tracey Newman | B85 L3 Labs | Mouse cochlea dissection training | Practical training on the procedures for removing cochleae from sacrificed mice. Issues of competency and safety were covered | 20/01/2018 |
| Alzheimer's Research UK | Solent University, Southampton | Workshop on hearing and cognition at an annual layperson conference | Developed and delivered a workshop on the associations between hearing loss and cognition/dementia. Annual conference for local population to hear updates on the latest developments in the field of Alzheimer's research. | 15/01/2018 |
| Orestis Katsamenis | UoS Muvis | X-ray μ CT training | Informal practical session. Orestis performed the scanning but kindly offered his time to explain the processes involved and guide our decision making around tissue preparation and image analysis. | 04/12/2017 |

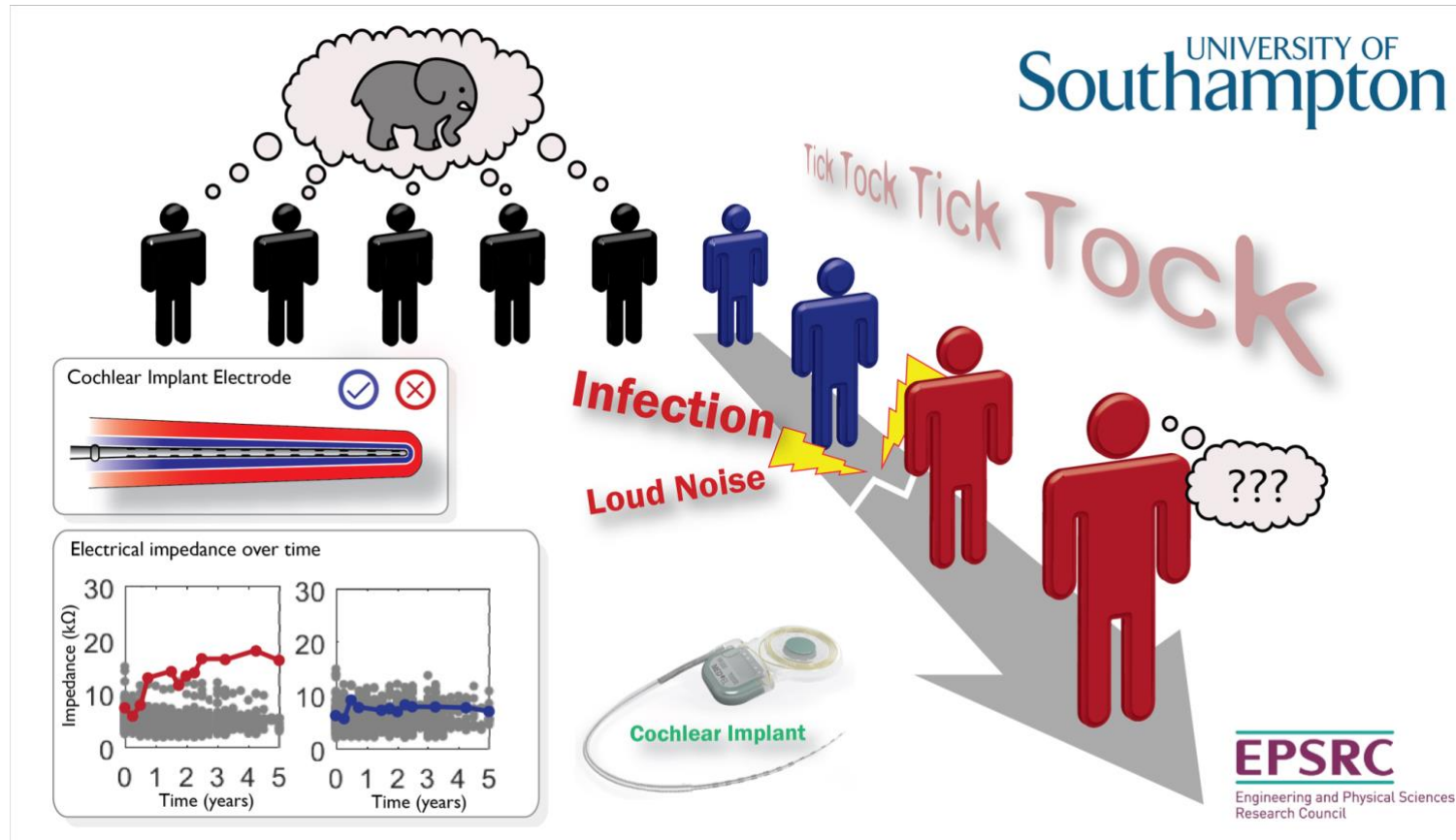
Appendix

| Organised By | Location | Type of Course | Short Description | Date |
|------------------------------|---------------------------|--|---|------------|
| Mark Willet | B85 L3 | Light Microscopy Training | Practical training session on procedures for capturing digital images using a light microscope. Issues of best practice and theory were covered. | 29/11/2017 |
| Tracey Newman | B85 L3 Labs | Immunohistochemistry | Practical training session on protocol steps to stain sectioned tissue with antibody and visualise with DAB and Haematoxylin counterstain | 20/11/2017 |
| Jenny Norman | SGH Histology | Microtome tissue sectioning at SGH Histology | Practical training to section paraffin wax embedded tissue and mount on glass slides. | 25/01/2018 |
| British Academy of Audiology | Bournemouth | National conference on Audiology | Poster presentation at a national UK conference for clinicians, researchers, academics and students in the field of Audiology. | 16/11/2017 |
| Edward Rogers | B85 L3 | Light Microscopy training | Edward was teaching an undergraduate course on microscopy; Tracey Newman suggested this would be a good opportunity to cover some microscopy basics with the group. | 19/09/2017 |
| Lucy Anderson | University College London | Animal dissection and surgery training session | I observed surgical dissection and cochlear implantation of gerbil and mouse. I also carried out the procedure with supervision. The training involved dead animals only. | 02/05/2017 |
| BRF/Home Office | SGH BRF | Animal handling training course | A three-day training course on animal husbandry, welfare, anesthesia, surgery and monitoring. Written examination. Practical examination of handling small rodents. | 22/11/2016 |
| Carl Verschuur | USIAS | Clinical meetings | Attend the monthly meeting of the 'adverse events' special interest group where specific clinical cases and emerging scientific evidence are discussed. | Ongoing |
| Edward Rogers | Highfield B85 L3 | MATLAB software training | Data management requires use of MATLAB. Training from a post-doctoral researcher Edward Rogers who will be cited as an author of the paper to be submitted. | 15/01/2017 |

| Organised By | Location | Type of Course | Short Description | Date |
|--|---------------------------|--|--|------------|
| British Academy of Audiology | Glasgow | National conference on Audiology | Poster presentation at a national UK conference for clinicians, researchers, academics and students in the field of Audiology. | 10/11/2016 |
| Carl Verschuur | USAIS | MED-EL CI user clinics | The research project focuses on patients fitted with MED-EL devices. To improve my vision of the broader clinical implications of my work, I attended three clinical sessions. These covered assessment and CI tuning. | 07/11/2016 |
| Self-directed | Personal computer | Database training using www.Lynda.com | Data handling in the current project requires knowledge and experience of MS Access databases. I followed the Lynda course to develop the necessary skills to design custom queries, add new data tables and create functions. | 09/10/2016 |
| British Academy of Audiology | Glasgow conference | Conference poster session | I presented the design and preliminary findings of my work to the delegates of the BAA annual conference in Glasgow. | 09/11/2016 |
| Deborah Vickers | University College London | Group seminar of scientists and clinicians | 4th Improving Cochlear Implant Performance Meeting at UCL | 21/04/2015 |
| Carl Verschuur | USAIS | Observed two clinical assessment sessions | A clinical scientist from USAIS and engineer from the device manufacturer performed various tests to explore the nature of a patients CI functionality problems. | 07/09/2015 |
| Faculty of Engineering and the Environment | Personal computer | Online Health & Safety e-learning course | | 16/10/2014 |
| Faculty of Engineering and the Environment | Highfield B7 R3009 | General course induction | Welcome talk, Course overview, Health & Safety, Plagiarism | 22/09/2014 |

D.3 Appendix D3

Three-minute Thesis slide (YouTube <https://www.youtube.com/watch?v=Z-28OulP-9w&t=77s>)



List of References

- Addams-Williams, J., Munaweera, L., Coleman, B., Shepherd, R., Backhouse, S., 2011. Cochlear implant electrode insertion: in defence of cochleostomy and factors against the round window membrane approach. *Cochlear Implants Int.*, 12 Suppl 2.
- Adewole, D.O., Serruya, M.D., Harris, J.P., Burrell, J.C., Chen, H.I., et al, 2017. The Evolution of Neuroprosthetic Interfaces. *Crit Rev Biomed Eng*, 44, p.123–152.
- Anderson, J.M., Rodriguez, A., Chang, D.T., 2008. Foreign body reaction to biomaterials. *Semin. Immunol.*, 20(2), p.86–100.
- Archbold, S., Lamb, B., O' Neill, C., Atkins, J., 2014. The real cost of adult hearing loss: Reducing its impact by increasing access to the latest hearing technologies. *Ear Found.*, p.1–6. Available at: <http://www.earfoundation.org.uk/files/download/869>.
- Arenberg Bierer, J., 2010. Probing the Electrode-Neuron Interface With Focused Cochlear Implant Stimulation. *Trends Amplif.*, 14(2), p.84–95.
- Arlinger, S., Gatehouse, S., Bentler, R.A., Byrne, D., Cox, R.M., et al, 1996. Eriksholm workshop on auditory deprivation. *Ear Hear.*, p.87–98.
- Aschendorff, A., 2011. Imaging in cochlear implant patients. *GMS Curr. Top. Otorhinolaryngol. - Head Neck Surg.*, 90(Suppl 1), p.S16-21. Available at: <http://www.ncbi.nlm.nih.gov/pubmed/21523630>.
- Balkany, T.J., Connell, S.S., Hodges, A. V., Payne, S.L., Telischi, F.F., et al, 2006. Conservation of residual acoustic hearing after cochlear implantation. *Otol. Neurotol.*, 27(8), p.1083–1088.
- Balkany, T.J., Hodges, A. V, Buchman, C.A., Luxford, W.M., Pillsbury, C.H., et al, 2005. Cochlear implant soft failures consensus development conference statement. *Cochlear Implants Int.*, 6(3), p.105–22. Available at: <http://www.ncbi.nlm.nih.gov/pubmed/18792329>.
- Bas, E., Goncalves, S., Adams, M., Dinh, C.T., Bas, J.M., et al, 2015. Spiral ganglion cells and macrophages initiate neuro-inflammation and scarring following cochlear implantation. *Front. Cell. Neurosci.*, 9(303), p.1–16. Available at: <http://journal.frontiersin.org/Article/10.3389/fncel.2015.00303/abstract>.
- Blamey, P., Arndt, P., Brimacombe, J., Staller, S., Bergeron, F., et al, 1996. Factors affecting auditory performance of postlinguistically deaf adults using cochlear implants. *Audiol.*

References

- Neuro-Otology*, 1(5), p.293–306.
- Blamey, P., Artieres, F., Başkent, D., Bergeron, F., Beynon, A., et al, 2012. Factors affecting auditory performance of postlinguistically deaf adults using cochlear implants: An update with 2251 patients. *Audiol. Neurotol.*, 18(1), p.36–47.
- Bruce, I., Cooper, H., Waltzman, S., Schramm, D., Graham, J., 2015. Maximising research value in the field of hearing implantation: A call for ‘big data.’ *Cochlear Implants Int.*, 16(6), p.301.
- Brummer, S.B., Turner, M.J., 1977. Electrochemical considerations for safe electrical stimulation of the nervous system with platinum electrodes. *IEEE Trans. Biomed. Eng.*, 24(1), p.59–63. Available at: <http://www.ncbi.nlm.nih.gov/pubmed/851475>.
- Bui, J.M., Perry, T., Ren, C.D., Nofrey, B., Teitelbaum, S., et al, 2015. Histological Characterization of Human Breast Implant Capsules. *Aesthetic Plast. Surg.*, 39(3), p.306–315. Available at: <http://link.springer.com/10.1007/s00266-014-0439-7>.
- Bullen, A., Anderson, L., Bakay, W., Forge, A., 2019. Localized disorganization of the cochlear inner hair cell synaptic region after noise exposure. *Biol. Open*, 8(1).
- Busby, P.A., Plant, K.L., Whitford, L.A., 2002. Electrode impedance in adults and children using the Nucleus 24 cochlear implant system. *Cochlear Implants Int.*, 3(2), p.87–103. Available at: <https://www.ncbi.nlm.nih.gov/pubmed/18792117>.
- Carlson, M.L., 2015. Prospective Randomized Controlled Double-blinded Study Comparing Cochlear Implantation Through a Round Window Versus Cochleostomy Approach. *ClinicalTrials.gov*. Available at: <https://clinicaltrials.gov/ct2/show/NCT02466763> [Accessed June 10, 2020].
- Carlson, M.L., Archibald, D.J., Dabade, T.S., Gifford, R.H., Neff, B.A., et al, 2010. Prevalence and timing of individual cochlear implant electrode failures. *Otol. Neurotol.*, 31(6), p.893–898.
- Causon, A., Verschuur, C.A., Newman, T.A., 2013. Trends in cochlear implant complications: implications for improving long-term outcomes. *Otol. Neurotol.*, 34(2), p.259–65.
- De Ceulaer, G., Johnson, S., Yperman, M., Daemers, K., Offeciers, F.E., et al, 2003. Long-term evaluation of the effect of intracochlear steroid deposition on electrode impedance in cochlear implant patients. *Otol. Neurotol.*, 24(5), p.769–774.
- Chang, A., Eastwood, H., Sly, D., James, D., Richardson, R., et al, 2009. Factors influencing the efficacy of round window dexamethasone protection of residual hearing post-cochlear

- implant surgery. *Hear. Res.*, 255(1–2), p.67–72. Available at:
<http://dx.doi.org/10.1016/j.heares.2009.05.010>.
- Cheng, X., Wang, B., Liu, Y., Yuan, Y., Shu, Y., et al, 2018. Comparable electrode impedance and speech perception at 12 months after cochlear implantation using round window versus cochleostomy: An analysis of 40 patients. *Orl*, p.1–11. Available at:
<https://www.karger.com/Article/FullText/490764>.
- Cherny, S.S., Livshits, G., Wells, H.R.R., Freidin, M.B., Malkin, I., et al, 2020. Self-reported hearing loss questions provide a good measure for genetic studies: a polygenic risk score analysis from UK Biobank. *Eur. J. Hum. Genet.*, 28(8), p.1056–1065. Available at:
<http://dx.doi.org/10.1038/s41431-020-0603-2>.
- Choi, J., Payne, M.R., Campbell, L.J., Bester, C.W., Newbold, C., et al, 2017. Electrode impedance fluctuations as a biomarker for inner ear pathology after cochlear implantation. *Otol. Neurotol.*, 38(10), p.1433–1439.
- Christo, S.N., Diener, K.R., Bachhuka, A., Vasilev, K., Hayball, J.D., 2015. Innate immunity and biomaterials at the nexus: friends or foes? *Biomed Res. Int.*, p.2–23.
- Chung, D., Kim, A.H., Parisier, S., Linstrom, C., Alexiades, G., et al, 2010. Revision cochlear implant surgery in patients with suspected soft failures. *Otol. Neurotol.*, 31(8), p.1194–8. Available at: <http://www.ncbi.nlm.nih.gov/pubmed/20729777>.
- Ciuman, R.R., 2010. The efferent system or olivocochlear function bundle - fine regulator and protector of hearing perception. *Int. J. Biomed. Sci.*, 6(4), p.276–288.
- Clark, G. M., Tong, C. T., Patrick, J.F., 1990. *Cochlear Protheses* 1st ed., London: Longman Group UK Limited.
- Clark, G. M.; Shute, S. A.; Shepherd, R. K.; Carter, T.D., 1995. Cochlear implantation: osteoneogenesis, electrode-tissue impedance, and residual hearing. *Ann. Otol. Rhinol. Laryngol.*, 166, p.40–2.
- Clark, G.M., 2003. *Cochlear Implants: Fundamentals and Applications* Robert T. Beyer, ed., East Melbourne, Victoria, Australia: Springer-Verlag New York, Inc.
- Clark, G.M., Clark, J., Cardamone, T., Clarke, M., Nielsen, P., et al, 2014. Biomedical studies on temporal bones of the first multi-channel cochlear implant patient at the University of Melbourne. *Cochlear Implants Int.*, 15, p.1–15. Available at:
<http://www.ncbi.nlm.nih.gov/pubmed/24915284>.

References

- Clark, G.M., Shepherd, R.K., Franz, B.K.H., Dowell, R.C., Tong, Y.C., et al, 1988. The histopathology of the human temporal bone and auditory central nervous system following cochlear implantation in a patient: Correlation with psychophysics and speech perception results. *Acta Otolaryngol.*, 105(S448), p.1–65.
- Claussen, A.D., Quevedo, R.V., Mostaert, B., Kirk, J.R., Dueck, W.F., et al, 2019. A mouse model of cochlear implantation with chronic electric stimulation. *PLoS One*, 14(4), p.1–23.
- Cohen, B.E., Durstenfeld, A., Roehm, P.C., 2014. Viral causes of hearing loss: A review for hearing health professionals. *Trends Hear.*, 18, p.1–17.
- Connell, S.S., Balkany, T.J., Hodges, A. V., Telischi, F.F., Angeli, S.I., et al, 2008. Electrode migration after cochlear implantation. *Otol. Neurotol.*, 29(2), p.156–159.
- Cosetti, M.K., Waltzman, S.B., 2012. Outcomes in cochlear implantation: Variables affecting performance in adults and children. *Otolaryngol. Clin. North Am.*, 45(1), p.155–171.
- Cullington, H., Kitterick, P., Weal, M., Margol-Gromada, M., 2018. Feasibility of personalised remote long-term follow-up of people with cochlear implants: A randomised controlled trial. *BMJ Open*, 8(4), p.e019640.
- Dawson, P.W., Blamey, P.J., Rowland, L.C., Dettman, S.J., Clark, G.M., et al, 1992. Cochlear implants in children, adolescents, and prelinguistically deafened adults: Speech perception. *J. Speech Hear. Res.*, 35(2), p.401–417.
- DeMason, C., Choudhury, B., Ahmad, F., Fitzpatrick, D.C., Buchman, C. a, et al, 2013. Electrophysiological properties of cochlear implantation in the gerbil using a flexible array. *Ear Hear.*, 33(4), p.534–542. Available at: <https://www.ncbi.nlm.nih.gov/pubmed/22436408>.
- Dhanasingh, A., Jolly, C., 2017. An overview of cochlear implant electrode array designs. *Hear. Res.*, 356, p.93–103. Available at: <https://doi.org/10.1016/j.heares.2017.10.005>.
- Dietz, A., Wennström, M., Lehtimäki, A., Löppönen, H., Valtonen, H., 2016. Electrode migration after cochlear implant surgery: more common than expected? *Eur. Arch. Oto-Rhino-Laryngology*, 273(6), p.1411–1418.
- Dorman, M.F., Smith, L.M., Dankowski, K., McCandless, G., Parkin, J.L., 1992. Long-term measures of electrode impedance and auditory thresholds for the Ineraid cochlear implant. *J. Speech Hear. Res.*, 35(5), p.1126–30.
- Eppsteiner, R.W., Shearer, A.E., Hildebrand, M.S., DeLuca, A.P., Ji, H., et al, 2012. Prediction of

- cochlear implant performance by genetic mutation: The spiral ganglion hypothesis. *Hear. Res.*, 292(1–2), p.51–58. Available at: <http://www.pubmedcentral.nih.gov/articlerender.fcgi?artid=3461332&tool=pmcentrez&rendertype=abstract> [Accessed August 4, 2014].
- Erixon, E., Högstorp, H., Wadin, K., Rask-Andersen, H., 2009. Variational anatomy of the human cochlea: Implications for cochlear implantation. *Otol. Neurotol.*, 30(1), p.14–22.
- Eshraghi, A.A., Yang, N.W., Balkany, T.J., 2003. Comparative study of cochlear damage with three perimodiolar electrode designs. *Laryngoscope*, 113(3), p.415–419.
- Fayad, J.N., Linthicum, F.H., 2006. Multichannel cochlear implants: relation of histopathology to performance. *Laryngoscope*, 116(8), p.1310–20. Available at: <http://www.ncbi.nlm.nih.gov/pubmed/16885730> [Accessed August 21, 2014].
- Fayad, J.N., Makarem, A.O., Linthicum, F.H., 2009. Histopathologic assessment of fibrosis and new bone formation in implanted human temporal bones using 3D reconstruction. *Otolaryngol. - Head Neck Surg.*, 141(2), p.247–252. Available at: <http://dx.doi.org/10.1016/j.otohns.2009.03.031>.
- Finley, C.C., Skinner, M.W., 2009. Role of electrode placement as a contributor to variability in cochlear implant outcomes. *Otol Neurotol*, 29(7), p.920–928.
- Friedland, D.R., Runge-Samuels, C., 2009. Soft cochlear implantation: Rationale for the surgical approach. *Trends Amplif.*, 13(2), p.124–138.
- Fujioka, M., Kanzaki, S., Okano, H.J., Masuda, M., Ogawa, K., et al, 2006. Proinflammatory Cytokines Expression in Noise-Induced Damaged Cochlea. *J. Neurosci. Res.*, 83(January), p.575–583.
- Gassner, H.G., Shallop, J.K., Driscoll, C.L.W., 2005. Long-term clinical course and temporal bone histology after cochlear implantation. *Cochlear Implants Int.*, 6(2), p.67–76.
- Gaurav, V., Sharma, S., Singh, S., 2020. Effects of Age at Cochlear Implantation on Auditory Outcomes in Cochlear Implant Recipient Children. *Indian J. Otolaryngol. Head Neck Surg.*, 72(1), p.79–85. Available at: <https://doi.org/10.1007/s12070-019-01753-4>.
- Gautschi-Mills, K., Khoza-Shangase, K., Pillay, D., 2019. Preservation of residual hearing after cochlear implant surgery: an exploration of residual hearing function in a group of recipients at cochlear implant units. *Braz. J. Otorhinolaryngol.*, 85(3), p.310–318. Available at: <https://doi.org/10.1016/j.bjorl.2018.02.006>.

References

- Gifford, R.H., Dorman, M.F., Skarzynski, H., Lorens, A., Polak, M., et al, 2013. Cochlear implantation with hearing preservation yields significant benefit for speech recognition in complex listening environments. *Ear Hear.*, 34(4), p.413–425.
- Green, K.M.J., Bhatt, Y.M., Mawman, D.J., O’Driscoll, M.P., Saeed, S.R., et al, 2007. Predictors of audiological outcome following cochlear implantation in adults. *Cochlear Implants Int.*, 8(1), p.1–11.
- Havenith, S., Lammers, M.J.W., Tange, R.A., Trabalzini, F., Della Volpe, A., et al, 2013. Hearing preservation surgery: Cochleostomy or round window approach? A systematic review. *Otol. Neurotol.*, 34(4), p.667–674.
- Henkin, Y., Kaplan-Neeman, R., Kronenberg, J., Migirov, L., Hildesheimer, M., et al, 2006. A longitudinal study of electrical stimulation levels and electrode impedance in children using the Clarion cochlear implant. *Acta Otolaryngol.*, 126(6), p.581–586.
- Henkin, Y., Kaplan-Neeman, R., Muchnik, C., Kronenberg, J., Hildesheimer, M., 2003. Changes over time in electrical stimulation levels and electrode impedance values in children using the Nucleus 24M cochlear implant. *Int. J. Pediatr. Otorhinolaryngol.*, 67(8), p.873–880.
- Hirose, K., Liberman, M.C., 2003. Lateral wall histopathology and endocochlear potential in the noise-damaged mouse cochlea. *JARO - J. Assoc. Res. Otolaryngol.*, 4(3), p.339–352.
- Hoaglin, D.C., Iglewicz, B., 1987. Fine-tuning some resistant rules for outlier labeling. *J. Am. Stat. Assoc.*, 82(400), p.1147–1149. Available at: <http://www.tandfonline.com/doi/abs/10.1080/01621459.1987.10478551> [Accessed December 12, 2016].
- Hoaglin, D.C., Iglewicz, B., Tukey, J.W., 1986. Performance of some resistant rules for outlier labeling. *J. Am. Stat. Assoc.*, 81(396), p.991–999. Available at: <http://www.tandfonline.com/doi/abs/10.1080/01621459.1986.10478363> [Accessed December 12, 2016].
- Holden, L.K., Firszt, J.B., Reeder, R.M., Uchanski, R.M., Dwyer, N.Y., et al, 2016. Factors affecting outcomes in cochlear implant recipients implanted with a perimodiolar electrode array located in scala tympani. *Otol. Neurotol.*, 37(10), p.1662–1668.
- Hoppe, U., Hocke, T., Hast, A., Iro, H., 2019. Maximum preimplantation monosyllabic score as predictor of cochlear implant outcome. *HNO*, 67, p.62–68.
- Hughes, M., 2013. *Objective Measures in Cochlear Implants*, Abingdon, Oxfordshire, UK, OX14

- 1EA: Plural Publishing Inc. Available at:
https://www.pluralpublishing.com/publication_omci.htm.
- Hughes, M.L., Vander Werff, K.R., Brown, C.J., Abbas, P.J., Kelsay, D.M., et al, 2001. A longitudinal study of electrode impedance, the electrically evoked compound action potential, and behavioral measures in nucleus 24 cochlear implant users. *Ear Hear.*, 22(6), p.471–486.
- Irving, S., Trotter, M.I., Fallon, J.B., Millard, R.E., Shepherd, R.K., et al, 2013. Cochlear implantation for chronic electrical stimulation in the mouse. *Hear. Res.*, 306, p.37–45. Available at:
<http://dx.doi.org/10.1016/j.heares.2013.09.005>.
- Ishai, R., Herrmann, B.S., Nadol, J.B., Quesnel, A.M., 2017. The pattern and degree of capsular fibrous sheaths surrounding cochlear electrode arrays. *Hear. Res.*, 348, p.44–53. Available at:
<http://dx.doi.org/10.1016/j.heares.2017.02.012>.
- James, C., Albegger, K., Battmer, R., Burdo, S., Deggouj, N., et al, 2005. Preservation of residual hearing with cochlear implantation: How and why. *Acta Otolaryngol.*, 125(5), p.481–491.
- Jia, H., Venail, F., Piron, J.P., Batrel, C., Pelliccia, P., et al, 2011. Effect of surgical technique on electrode impedance after cochlear implantation. *Ann. Otol. Rhinol. Laryngol.*, 120(8), p.529–534.
- Kaandorp, M.W., Smits, C., Merkus, P., Festen, J.M., Goverts, S.T., 2017. Lexical-access ability and cognitive predictors of speech recognition in noise in adult cochlear implant users. *Trends Hear.*, 21, p.1–15.
- Kamakura, T., Nadol, J.B., 2016. Correlation between word recognition score and intracochlear new bone and fibrous tissue after cochlear implantation in the human. *Hear. Res.*, 339, p.132–141. Available at: <http://dx.doi.org/10.1016/j.heares.2016.06.015>.
- Kamel, M., Protzner, K., Fornasier, V., Peters, W., Smith, D., et al, 2001. The peri-implant breast capsule: An immunophenotypic study of capsules taken at explantation surgery. *J. Biomed. Mater. Res.*, 58(1), p.88–96.
- Karosi, T., Kónya, J., Szabó, L.Z., Pytel, J., Jóri, J., et al, 2005. Codetection of measles virus and tumor necrosis factor-alpha mRNA in otosclerotic stapes footplates. *Laryngoscope*, 115(7), p.1291–1297.
- Katsamenis, O.L., Olding, M., Warner, J.A., Chatelet, D.S., Jones, M.G., et al, 2019. X-ray Micro-Computed Tomography for Nondestructive Three-Dimensional (3D) X-ray Histology. *Am. J. Pathol.*, 189(8), p.1608–1620. Available at: <http://dx.doi.org/10.1016/j.ajpath.2019.05.004>.

References

- Kawano, A., Seldon, H.L., Clark, G.M., Ramsden, R.T., Raine, C.H., 1998. Intracochlear factors contributing to psychophysical percepts following cochlear implantation. *Acta Otolaryngol.*, 118(3), p.313–326.
- Kendall, R.T., Feghali-Bostwick, C.A., 2014. Fibroblasts in fibrosis: Novel roles and mediators. *Front. Pharmacol.*, 5(May), p.1–13.
- Kollmannsberger, P., Bidan, C.M., Dunlop, J.W.C., Fratzl, P., Vogel, V., 2018. Tensile forces drive a reversible fibroblast-to-myofibroblast transition during tissue growth in engineered clefts. *Sci. Adv.*, 4(1).
- Krashenl, S.D., 1967. Lateralization, Language Learning and the Critical Period: Some New Evidence. *Language (Baltim.)*, p.63–74.
- Kunda, L.D., Stidham, K.R., Inserra, M.M., Roland, P.S., Franklin, D., et al, 2006. Silicone allergy: A new cause for cochlear implant extrusion and its management. *Otol. Neurotol.*, 27(8), p.1078–1082.
- Kurabi, A., Keithley, E.M., Housley, G.D., Ryan, A.F., Wong, A.C.Y., 2017. Cellular mechanisms of noise-induced hearing loss. *Hear. Res.*, 349, p.129–137. Available at: <http://dx.doi.org/10.1016/j.heares.2016.11.013>.
- Kuthubutheen, J., Smith, L., Hwang, E., Lin, V., 2016. Preoperative steroids for hearing preservation cochlear implantation: A review. *Cochlear Implants Int.*, 17(2), p.63–74.
- Lambriks, L.J.G., Van Hoof, M., Debruyne, J.A., Janssen, M., Chalupper, J., et al, 2020. Evaluating hearing performance with cochlear implants within the same patient using daily randomization and imaging-based fitting - The ELEPHANT study. *Trials*, 21(1), p.1–14.
- Di Laora, A., Mosnier, I., Ciorba, A., Pelucchi, S., Sterkers, O., et al, 2019. Cochlear implant electrode migration due to cholesterol granuloma: Cues from a case. *J. Int. Adv. Otol.*
- Lazard, D.S., Vincent, C., Venail, F., van de Heyning, P., Truy, E., et al, 2012. Pre-, per- and postoperative factors affecting performance of postlinguistically deaf adults using cochlear implants: A new conceptual model over time. *PLoS One*, 7(11), p.1–11.
- Lehnhardt, E., 1993. Intracochlear placement of cochlear implant electrodes in soft surgery technique. *HNO*, 41(7), p.356–359.
- Leone, C.A., Mosca, F., Grassia, R., Hospital, M., 2017. Temporal changes in impedance of implanted adults for various cochlear segments. , p.312–319.

- Leung, J., Yeagle, J.D., Chinnici, J., Bowditch, S., Francis, H.W., et al, 2005. Predictive models for cochlear implantation in elderly candidates. *Arch. Otolaryngol. - Head Neck Surg.*, 131(12), p.1049–1054.
- Li, P.M.M.C., Somdas, M.A., Eddington, D.K., Nadol, J.B., 2007. Analysis of intracochlear new bone and fibrous tissue formation in human subjects with cochlear implants. *Ann. Otol. Rhinol. Laryngol.*, 116(10), p.731–738. Available at: <http://aor.sagepub.com/lookup/doi/10.1177/000348940711601004>.
- Lim, H.J., Lee, E.S., Park, H.Y., Park, K., Choung, Y.H., 2011. Foreign body reaction after cochlear implantation. *Int. J. Pediatr. Otorhinolaryngol.*, 75(11), p.1455–1458.
- Linthicum, F.H., Fayad, J.N., 2009. Spiral Ganglion Cell Loss is Unrelated to Segmental Cochlear Sensory System Degeneration in Humans. *Otol Neurotol.*, 30(3), p.418–422.
- Liu, C.-M., Lee, C.T.-C., 2019. Association of Hearing Loss With Dementia. *JAMA Netw. Open*, 2(7), p.e198112.
- Livingston, G., Sommerlad, A., Orgeta, V., Costafreda, S.G., Huntley, J., et al, 2017. Dementia prevention, intervention, and care. *Lancet*, 390(10113), p.2673–2734.
- Lo, J., Campbell, L., Sale, P., Chambers, S., Hampson, A., et al, 2017. The role of preoperative steroids in atraumatic cochlear implantation surgery. *Otol. Neurotol.*, 38(8), p.1118–1124.
- Lyu, A.R., Kim, D.H., Lee, S.H., Shin, D.S., Shin, S.A., et al, 2018. Effects of dexamethasone on intracochlear inflammation and residual hearing after cochleostomy: A comparison of administration routes. *PLoS One*, 13(3), p.1–15.
- Mangus, B., Rivas, A., Tsai, B.S., Haynes, D.S., Roland, J.T., 2012. Surgical techniques in cochlear implants. *Otolaryngol. Clin. North Am.*, 45(1), p.69–80. Available at: <http://dx.doi.org/10.1016/j.otc.2011.08.017>.
- Van Der Marel, K.S., Verbist, B.M., Briaire, J.J., Joemai, R.M.S., Frijns, J.H.M., 2012. Electrode migration in cochlear implant patients: Not an exception. *Audiol. Neurotol.*, 17, p.275–281.
- Marsella, P., Scorpecci, A., Pacifico, C., Resca, A., Vallarino, M.V., et al, 2014. Safety and functional results of early cochlear implant switch-on in children. *Otol. Neurotol.*, 35(2), p.277–282.
- Mathew, R., Undurraga, J., Li, G., Meerton, L., Boyle, P., et al, 2017. Objective assessment of electrode discrimination with the auditory change complex in adult cochlear implant users. *Hear. Res.*, 354, p.86–101. Available at: <https://doi.org/10.1016/j.heares.2017.07.008>.

References

- Mathur, P., Yang, J., 2015. Usher syndrome: Hearing loss, retinal degeneration and associated abnormalities. *Biochim. Biophys. Acta - Mol. Basis Dis.*, 1852(3), p.406–420. Available at: <http://dx.doi.org/10.1016/j.bbadis.2014.11.020>.
- Med-el, 2013. Electrode arrays: designed for atraumatic implantation providing superior hearing performance. , p.Online. Available at: <http://www.medel.com/data/pdf/21617.pdf>.
- Mei, X., Atturo, F., Wadin, K., Larsson, S., Agrawal, S., et al, 2018. Human inner ear blood supply revisited: the Uppsala collection of temporal bone—an international resource of education and collaboration. *Ups. J. Med. Sci.*, 123(3), p.131–142. Available at: <https://doi.org/10.1080/03009734.2018.1492654>.
- Mener, D.J., Betz, J., Genther, D.J., Chen, D.S., Lin, F.R., 2013. Hearing loss and depression in older adults. *J Am Geriatr Soc*, 61(9), p.1627–1629.
- Mestas, J., Hughes, C.C.W., 2004. Of mice and not men: Differences between mouse and human immunology. *J. Immunol.*, 172(5), p.2731–2738.
- Mesure, L., de Visscher, G., Vranken, I., Lebacqz, A., Flameng, W., 2010. Gene expression study of monocytes/macrophages during early foreign body reaction and identification of potential precursors of myofibroblasts. *PLoS One*, 5(9).
- Micallef, L., Vedrenne, N., Billet, F., Coulomb, B., Darby, I.A., et al, 2012. The myofibroblast, multiple origins for major roles in normal and pathological tissue repair. *Fibrogenesis Tissue Repair*, 5(Suppl 1:55), p.1–5.
- Millard, R.E., Shepherd, R.K., 2007. A fully implantable stimulator for use in small laboratory animals. *J Neurosci Methods*, 166(2), p.168–177.
- Miranda, P.C., Luiz, A., Sampaio, L., Aquino, R., Lopes, F., et al, 2014. Hearing Preservation in Cochlear Implant Surgery. *Int. J. Otolaryngol.*, p.1–6.
- Misrahy, G.A., Spradley, J.F., Beran, A. V., Garwood, V.P., 1960. Permeability of cochlear partitions: Comparison with blood-brain barrier. *Acta Otolaryngol.*, 52(1–6), p.525–534.
- Mistry, N., Nolan, L.S., Saeed, S.R., Forge, A., Taylor, R.R., 2014. Cochlear implantation in the mouse via the round window: Effects of array insertion. *Hear. Res.*, 312, p.81–90. Available at: <http://dx.doi.org/10.1016/j.heares.2014.03.005>.
- Moberly, A., Welling, B., Nittrouer, S., 2013. Detecting soft failures in pediatric cochlear implants: relating behavior to language outcomes. *Otol. Neurotol.*, 34(9), p.1–15.

- Morais, J.M., Papadimitrakopoulos, F., Burgess, D.J., 2010. Biomaterials/tissue interactions: Possible solutions to overcome foreign body response. *AAPS J.*, 12(2), p.188–196.
- Munro, K.J., 2008. Reorganization of the adult auditory system: Perceptual and physiological evidence from monaural fitting of hearing aids. *Trends Amplif.*, 12(2), p.85–102. Available at: <http://www.scopus.com/inward/record.url?eid=2-s2.0-45749143209&partnerID=40&md5=8386904f5fe0fefff00e557d4b7349bb>.
- Nadol, J.B., Eddington, D.K., Burgess, B.J., 2008. Foreign body or hypersensitivity granuloma of the inner ear after cochlear implantation: one possible cause of a soft failure? *Otol. Neurotol.*, 29(8), p.1076–1084. Available at: <http://www.ncbi.nlm.nih.gov/pubmed/18997635>.
- Nadol, J.B., Ketten, D.R., Burgess, B.J., 1994. Otopathology in a case of multichannel cochlear implantation. *Laryngoscope*, 104(3 Pt 1), p.299–303. Available at: <http://www.ncbi.nlm.nih.gov/pubmed/8127186>.
- Nadol, J.B., O'Malley, J.T., Burgess, B.J., Galler, D., 2014. Cellular immunologic responses to cochlear implantation in the human. *Hear. Res.*, 318, p.11–17.
- Navntoft, C.A., Marozeau, J., Barkat, T.R., 2019. Cochlear implant surgery and electrically-evoked auditory brainstem response recordings in C57BL/6 mice. *J. Vis. Exp.*, 2019(143), p.1–9.
- Neilan, R.E., Pawlowski, K., Isaacson, B., Roland, P.S., 2012. Cochlear implant device failure secondary to cholesterol granuloma-mediated cochlear erosion. *Otol. Neurotol.*, 33(5), p.733–735.
- Neuburger, J., Lenarz, T., Lesinski-Schiedat, A., Büchner, A., 2009. Spontaneous increases in impedance following cochlear implantation: suspected causes and management. *Int. J. Audiol.*, 48(5), p.233–239.
- Neuhauser, D., Provost, L., Bergman, B., Blanchard, C.E., 2011. The meaning of variation to healthcare managers, clinical and health-services researchers, and individual patients. *BMJ Qual. Saf.*, 20, p.36–40.
- Newbold, C., Mergen, S., Richardson, R., Seligman, P., Millard, R., et al, 2014. Impedance changes in chronically implanted and stimulated cochlear implant electrodes. *Cochlear Implants Int.*, 15(4), p.191–9. Available at: <http://www.ncbi.nlm.nih.gov/pubmed/23998484>.
- Newbold, C., Richardson, R., Millard, R., Huang, C., Milojevic, D., et al, 2010. Changes in biphasic electrode impedance with protein adsorption and cell growth. *J. Neural Eng.*, 7(5), p.056011. Available at: <http://www.ncbi.nlm.nih.gov/pubmed/20841637> [Accessed August 18, 2016].

References

- Newbold, C., Richardson, R., Millard, R., Seligman, P., Cowan, R., et al, 2011. Electrical stimulation causes rapid changes in electrode impedance of cell-covered electrodes. *J. Neural Eng.*, 8(3), p.36029. Available at: <http://www.ncbi.nlm.nih.gov/pubmed/21572219>.
- NICE, 2019. Cochlear implants for children and adults with severe to profound deafness. *NICE Technol. Apprais. Guid.*, p.1–41. Available at: <https://www.nice.org.uk/guidance/ta566>.
- Nomura, Y., 1977. Vascular supply to the organ of Corti in man. *Arch. Otorhinolaryngol.*, 214(3), p.213–220.
- Nyberg, S., Joan Abbott, N., Shi, X., Steyger, P.S., Dabdoub, A., 2019. Delivery of therapeutics to the inner ear: The challenge of the blood-labyrinth barrier. *Sci. Transl. Med.*, 11(482), p.1–12.
- O’Leary, S.J., Monksfield, P., Kel, G., Connolly, T., Souter, M.A., et al, 2013. Relations between cochlear histopathology and hearing loss in experimental cochlear implantation. *Hear. Res.*, 298, p.27–35.
- Ohlemiller, K.K., Jones, S.M., Johnson, K.R., 2016. Application of Mouse Models to Research in Hearing and Balance. *JARO - J. Assoc. Res. Otolaryngol.*, 17(6), p.493–523.
- Okano, T., Nakagawa, T., Kita, T., Kada, S., Yoshimoto, M., et al, 2008. Bone marrow-derived cells expressing Iba1 are constitutively present as resident tissue macrophages in the mouse cochlea. *J. Neurosci. Res.*, 86(8), p.1758–1767.
- Pelliccia, P., Venail, F., Bonafé, A., Makeieff, M., Iannetti, G., et al, 2014. Cochlea size variability and implications in clinical practice. *Acta Otorhinolaryngol. Ital.*, 34(1), p.42–9. Available at: <http://www.ncbi.nlm.nih.gov/pubmed/24711682><http://www.pubmedcentral.nih.gov/articlerender.fcgi?artid=PMC3970226>.
- Perreau, A., Tyler, R.S., Witt, S.A., 2010. The effect of reducing the number of electrodes on spatial hearing tasks for bilateral cochlear implant recipients. *J. Am. Acad. Audiol.*, 21(2), p.110–120.
- Philippon, D., Bergeron, F., Ferron, P., Bussièrès, R., 2010. Cochlear implantation in postmeningitic deafness. *Otol. Neurotol.*, 31(1), p.83–7. Available at: <http://www.ncbi.nlm.nih.gov/pubmed/20050267>.
- Quraishe, S., Newman, T., Anderson, L., 2019. Auditory temporal acuity improves with age in the male mouse auditory thalamus: A role for perineuronal nets? *J. Neurosci. Res.*, p.1–20.

- Rader, T., Baumann, U., Stover, T., Weissgerber, T., Adel, Y., et al, 2016. Management of cochlear implant electrode migration. *Otol. Neurotol.*, 37(9), p.e341–e348.
- Rajput, K., Brown, T., Bamiou, D.E., 2003. Aetiology of hearing loss and other related factors versus language outcome after cochlear implantation in children. *Int. J. Pediatr. Otorhinolaryngol.*, 67(5), p.497–504.
- Reis, A. dos, Dalmolin, S.P., Dallegrave, E., 2017. Animal models for hearing evaluations: a literature review. *Rev. CEFAC*, 19(3), p.417–428.
- Richard, C., Fayad, J.N., Doherty, J., Linthicum, F.H., 2012. Round window versus cochleostomy technique in cochlear implantation: histologic findings. *Otol. Neurotol.*, 33(7), p.1181–7. Available at: <http://www.ncbi.nlm.nih.gov/pubmed/?term=22892806>.
- Rolfe, B., 2011. The fibrotic response to implanted biomaterials: implications for tissue engineering. *Regen. Med. Tissue Eng. - Cells Biomater.*, p.552–568. Available at: http://www.intechopen.com/source/pdfs/19012/InTech-The_fibrotic_response_to_implanted_biomaterials_implications_for_tissue_engineering.pdf.
- Rose, T.L., Robblee, L.S., 1990. Electrical stimulation with Pt electrodes. VIII. Electrochemically safe charge injection limits with 0.2 ms pulses. *IEEE Trans. Biomed. Eng.*, 37(11), p.1118–1120.
- Rousset, A.M., 2017. *Outcomes and predictive factors with cochlear implants for adults with a significant, early-onset hearing loss.*
- Saunders, E., Cohen, L., Aschendorff, A., Shapiro, W., Knight, M., et al, 2002. Threshold, comfortable level and impedance changes as a function of electrode-modiolar distance. *Ear Hear.*, 23(1 Suppl), p.28S-40S.
- Schaefer, S., Henderson, L., Graham, J., Broomfield, S., Cullington, H., et al, 2017. Review of outcomes and measurement instruments in cochlear implantation studies. *Cochlear Implants Int.*, 18(5), p.237–239.
- Scheper, V., Hessler, R., Hu, M., Wilk, M., Jolly, C., et al, 2017. Local inner ear application of dexamethasone in cochlear implant models is safe for auditory neurons and increases the neuroprotective effect of chronic electrical stimulation. , p.1–22.
- Schuknecht, H., 1953. Techniques for study of cochlear function and pathology in experimental animals. *AMA. Arch. Otolaryngol.*, 58(4), p.377–397.

References

- Seyyedi, M., Nadol Jr, J.B., 2014. Intracochlear inflammatory response to cochlear implant electrodes in humans. *Otol. Neurotol.*, 35(9), p.1545–1551.
- Shepherd, R.K., Matsushima, J., Martin, R.L., Clark, G.M., 1994. Cochlear pathology following chronic electrical stimulation of the auditory nerve: II deafened kittens. *Hear. Res.*, 81(1–2), p.150–166.
- Skarzynski, H., van de Heyning, P., Agrawal, S., Arauz, S.L., 2013. Towards a consensus on a hearing preservation classification system. , 133(Suppl 564), p.3–13.
- Smith, R.J.H., Hildebrand, M., 1998. Nonsyndromic Hearing Loss and Deafness, DFNB1. *GeneReviews [Internet]*, p.1–14. Available at: <https://www.ncbi.nlm.nih.gov/books/NBK1272/>.
- Snels, C., Inthout, J., Mylanus, E., Huinck, W., Dhooge, I., 2019. Hearing Preservation in Cochlear Implant Surgery: A Meta-Analysis. *Otol. Neurotol.*, 40(2), p.145–153.
- Snow, R.B., Kossovsky, N., 1989. Hypersensitivity reaction associated with sterile ventriculoperitoneal shunt malfunction. *Surg. Neurol.*, 31(3), p.209–214.
- Somdas, M.A., Li, P.M.M.C., Whiten, D.M., Eddington, D.K., Nadol, J.B., 2007. Quantitative evaluation of new bone and fibrous tissue in the cochlea following cochlear implantation in the human. *Audiol. Neurotol.*, 12(5), p.277–284.
- Sorrentino, T., Côté, M., Eter, E., Laborde, M.L., Cochard, N., et al, 2009. Cochlear reimplantations: Technical and surgical failures. *Acta Otolaryngol.*, 129(4), p.380–384.
- Spiers, K., Cardamone, T., Furness, J.B., Clark, J.C.M., Patrick, J.F., et al, 2016. An X-ray fluorescence microscopic analysis of the tissue surrounding the multi-channel cochlear implant electrode array. , 17(3), p.129–131.
- Swanson, B., Seligman, P., Carter, P., 1995. Impedance measurement of the nucleus 22-electrode array in patients. *Ann. Otol. Rhinol. Laryngol.*, 104(9 II SUPPL.), p.141–144.
- Tanamai, N., Mulder, J.J.S., Verhaegen, V.J.O., Kunst, H.P.M., Mylanus, E.A., et al, 2018. Postoperative systemic corticosteroids and hearing preservation in cochlear implantation. *Ann. Otolaryngol.*, 2(1), p.2–7.
- Timm, M.E., Majdani, O., Weller, T., Windeler, M., Lenarz, T., et al, 2018. Patient specific selection of lateral wall cochlear implant electrodes based on anatomical indication ranges. *PLoS One*, 13(10), p.1–14.

- Todt, I., Mittmann, P., Ernst, A., 2014. Intracochlear fluid pressure changes related to the insertional speed of a CI electrode. *Biomed Res. Int.*, 2014.
- Tykocinski, M., Cohen, L.T., Cowan, R.S., 2005. Measurement and Analysis of Access Resistance and Polarization Impedance in Cochlear Implant Recipients. *Otol. Neurotol.*, 26(5), p.948–956. Available at: <http://content.wkhealth.com/linkback/openurl?sid=WKPTLP:landingpage&an=00129492-200509000-00021>.
- Tykocinski, M., Duan, Y., Tabor, B., Cowan, R.S., 2001. Chronic electrical stimulation of the auditory nerve using high surface area (HiQ) platinum electrodes. *Hear. Res.*, 159(1–2), p.53–68. Available at: <http://www.sciencedirect.com/science/article/pii/S0378595501003203> [Accessed February 18, 2016].
- Vargas, J.L., Sainz, M., Roldan, C., Alvarez, I., de la Torre, A., 2012. Long-term evolution of the electrical stimulation levels for cochlear implant patients. *Clin. Exp. Otorhinolaryngol.*, 5(4), p.194–200.
- Venail, F., Sicard, M., Piron, J.P., Levi, J., Artieres, F., et al, 2008. Reliability and complications of 500 consecutive cochlear implantations. *Arch. Otolaryngol. - Head Neck Surg.*, 134(12), p.1276–1281. Available at: <http://www.embase.com/search/results?subaction=viewrecord&from=export&id=L354042297%0Ahttp://archotol.ama-assn.org/cgi/reprint/134/12/1276%0Ahttp://dx.doi.org/10.1001/archoto.2008.504>.
- Wilk, M., Hessler, R., Mugridge, K., Jolly, C., Fehr, M., et al, 2016. Impedance changes and fibrous tissue growth after cochlear implantation are correlated and can be reduced using a dexamethasone eluting electrode. *PLoS One*, 11(2), p.1–19.
- Wilson, B.S., Dorman, M.F., 2008. Cochlear implants: current designs and future possibilities. *J. Rehabil. Res. Dev.*, 45(5), p.695–730.
- Wingard, J.C., Zhao, H.B., 2015. Cellular and deafness mechanisms underlying connexin mutation-induced hearing loss – A common hereditary deafness. *Front. Cell. Neurosci.*, 9(MAY), p.1–13.
- Winter, K.F., Hartmann, R., Klinke, R., 1998. A stimulator with wireless power and signal transmission for implantation in animal experiments and other applications. *J. Neurosci. Methods*, 79(1), p.79–85.

References

- Wolfe, J., Baker, R., Wood, M., 2013. Clinical case study review: steroid-responsive change in electrode impedance. *Otol. Neurotol.*, 34, p.227–232.
- Wong, K., Kozin, E.D., Kanumuri, V. V., Vachicouras, N., Miller, J., et al, 2019. Auditory brainstem implants: Recent progress and future perspectives. *Front. Neurosci.*, 13(JAN), p.1–8.
- Xin, Y., Yuan, Y.S., Chi, F.L., Wang, J., Yang, J.M., 2015. Foreign body reaction after cochlear implantation: A case report. *Chin. Med. J. (Engl.)*, 128(15), p.2124–2125.
- Xu, J., Shepherd, R.K., Millard, R.E., Clark, G.M., 1997. Chronic electrical stimulation of the auditory nerve at high stimulus rates: a physiological and histopathological study. *Hear. Res.*, 105(1–2), p.1–29.
- Zanetti, D., Nassif, N., Redaelli De Zinis, L.O., Civili, S., 2015. Factors affecting residual hearing preservation in cochlear implantation. , p.433–441.
- Zeng, F.-G., 2017. Challenges in Improving Cochlear Implant Performance and Accessibility. *IEEE Trans Biomed Eng*, 64(8), p.1662–1664.
- Zhang, K.D., Coate, T.M., 2016. Ganglion Neurons in the Mammalian Inner Ear. *Semin. Cell Dev. Biol.*, p.1–8. Available at: <http://dx.doi.org/10.1016/j.semcdb.2016.09.017>.
- Zhang, W., Dai, M., Fridberger, A., Hassan, A., Degagne, J., et al, 2012. Perivascular-resident macrophage-like melanocytes in the inner ear are essential for the integrity of the intrastrial fluid-blood barrier. *Proc. Natl. Acad. Sci. U. S. A.*, 109(26), p.10388–93. Available at: <http://www.pnas.org/content/109/26/10388.long%5Cnhttp://www.pubmedcentral.nih.gov/articlerender.fcgi?artid=3387119&tool=pmcentrez&rendertype=abstract>.
- Zhou, N., 2017. Deactivating stimulation sites based on low-rate thresholds improves spectral ripple and speech reception thresholds in cochlear implant users. *J. Acoust. Soc. Am.*, 141(3), p.EL243–EL248. Available at: <http://aip.scitation.org/doi/10.1121/1.4977235>.